

**STUDIES TOWARD THE TOTAL SYNTHESIS OF
STAGONOLIDE B AND JASPINE B & SYNTHESIS OF NOVEL
FURANO β -AMINO ACIDS (β -FAA) AND THEIR HOMO-
OLIGOMERS**

**BY
AWADUT GAJENDRA GIRI**

**Dr. C. V. RAMANA
(RESEARCH GUIDE)**

**ORGANIC CHEMISTRY DIVISION
NATIONAL CHEMICAL LABORATORY
PUNE-411008 (India)**

MARCH-2010

**STUDIES TOWARD THE TOTAL SYNTHESIS OF STAGONOLIDE B AND
JASPINE B & SYNTHESIS OF NOVEL FURANO β -AMINO ACIDS (β -FAA)
AND THEIR HOMO-OLIGOMERS**

A THESIS
SUBMITTED FOR THE DEGREE OF
DOCTOR OF PHILOSOPHY
(IN CHEMISTRY)

TO
UNIVERSITY OF PUNE

BY
Mr. Awadut Gajendra Giri

Dr. C. V. Ramana
(Research Guide)

ORGANIC CHEMISTRY DIVISION
NATIONAL CHEMICAL LABORATORY
PUNE-411008 (India)

MARCH-2010

*DEDICATED
TO
MY FAMILY*

DECLARATION

The research work embodied in this thesis has been carried out at National Chemical Laboratory, Pune under the supervision of **Dr. C. V. Ramana**, Organic Chemistry Division, National Chemical Laboratory, Pune – 411008. This work is original and has not been submitted in part or full, for any degree or diploma of this or any other University.

Organic Chemistry Division
National Chemical Laboratory
Pune – 411008
March–2010

(Awadut Gajendra Giri)

Dr. C. V. Ramana

Phone: +91-20-25902577

+91-20-25902455

E-mail: vr.chepuri@ncl.res.in

CERTIFICATE

The research work presented in thesis entitled “**Studies Toward the Total Synthesis of Stagonolide B and Jaspine B & Synthesis of Novel Furano β -Amino Acids (β -FAA) and their Homo-oligomers**” has been carried out under my supervision and is a bonafide work of **Mr. Awadut Gajendra Giri**. This work is original and has not been submitted for any other degree or diploma of this or any other University.

Pune – 411008

March –2010

Dr. C. V. Ramana

(Research Guide)

Acknowledgements

It gives me immense pleasure to express my deep sense of gratitude to my teacher and research guide **Dr. C. V. Ramana**, who has helped me a lot to learn and think more about chemistry. I thank him for an excellent and inspiring guidance, constant encouragement, sincere advice and unstinted support during all the times of my Ph.D. work. Working with him was a great pleasure and learning experience.

I would like to thank Dr. P. R. Rajamohanan for guidance and help in undertaking the 2D NMR studies which was of great help for the completion of my thesis work.

I would like to thank Dr. S. Hotha, Dr. B. L. V. Prasad, Dr. H.V. Thulasiram, Dr. M. N. Deshmukh, Dr. S. P. Chavan, Dr. H. B. Borate, Dr. U. R. Kalkote, Dr. R. A. Joshi, Dr. R. R. Joshi, Mr. I. Shivakumar and Dr. Gajbhiye throughout my stay at NCL. I am thankful to my mentors at my school, college and University for their inspirational teaching, ethics and discipline. I am highly thankful to Dr. B. M. Bhawal and Dr. V. H. Deshpande for their sincere efforts and patience in guiding me in my early days of research career. My sincere thanks to Ganesh Jogdand from NMR facility for helping me with the NMR analysis.

I gratefully acknowledge the training and support extended by my senior colleagues Dr. N. Raghupathi, Dr. Soumitra, Dr. Ramdas, Dr. Bhargava, Dr. Nageswar, Dr. Sumantha, Dr. Srinivas, Dr. Induvadna, Dr. Anuj, Dr. Tushar, and Dr. Bagawat, during the tenure of my Ph.D life. I would like to thank all my colleagues Rahul, Pitambar, Dr. Sharad, Pandeyji, Atul, Mondal, Rosy, paresh, yogesh, Mangesh, shyam, Chandrababu, Sachin, Jitu, Ajay, Suneel, Vilas, Sridhar, Yadagiri and Senthil for their cooperation and friendly attitude.

I am also thankful to my friends Nagendra, Vinod, Rameshwar, Shriram, Amol, Laxman, Namdev, Pandurang and Kulbhushan for their continuous encouragement, help and whose companionship always kept my mood cheerful and with whom I shared golden moments. My sincere thanks to all other friends from NCL and SA for their co-operation specially Sharad.

A special thanks all "NCL-Chemistry" members for their cheerful company. Help from the spectroscopy, mass and X-ray crystallographic groups is gratefully acknowledged. I sincerely thank Dr. Gonnade and Mrs. Shanthakumari their helpful discussions and cooperation. My sincere thanks to Dr. G. Pandey, Head, Division of Organic Chemistry for his cooperation and support.

It is impossible to express my sense of gratitude for my parents in mere words. Whatever I am and whatever I will be in future is because of their enormous blessings, commitments to my ambitions and their selfless sacrifices. I am thankful to my wife, Kalpana for her care, encouragement, support and sacrifice. Words fall short to thank my daughter Aastha, uncle Gangagir Giri, Bhagwan Giri, brother Digumber and Sisters Indu, Chandrakala for their love and support at tough time.

Finally I thank Director, National Chemical Laboratory, Pune for providing infrastructural facilities to complete my work successfully. Financial assistance from UGC New Delhi in the form of fellowship is gratefully acknowledged.

Awadut Gajendra Giri

DEFINATIONS AND ABBREVIATIONS

Ac	–	Acetyl
Ac ₂ O	–	Acetic anhydride
aq.	–	Aqueous
Bn	–	Benzyl
BnBr	–	Benzyl bromide
NaIO ₄	–	Sodium periodate
DCM	–	Dichloro methane
DCE	–	1,2-Dichloro ethane
<i>n</i> -BuLi	–	<i>n</i> -Butyl lithium
NaBH ₄	–	Sodium borohydride
Cat.	–	Catalytic/catalyst
TsCl	–	Tosyl chloride
Conc.	–	Concentrated
MCPBA	–	<i>Meta</i> -Chloroperbenzoic acid
DMF	–	<i>N,N</i> -Dimethylformamide
DMAP	–	<i>N,N'</i> -Dimethylaminopyridine
DMSO	–	Dimethyl sulfoxide
Tf ₂ O	–	Triflic unhydride
Et ₂ O	–	Diethyl ether
EtOAc	–	Ethyl acetate
Et ₃ N	–	Triethylamine
HMPA	–	Hexamethylphosphoramide
Im	–	Imidazole
LAH	–	Lithium aluminium hydride
LiN ₃	–	Lithium azide
Ms/Mesyl	–	Methanesulfonyl
Me	–	Methyl
MTPA	–	α -Methoxytrifluorophenylacetic acid
NOESY	–	Nuclear overhauser effect spectroscopy
ORTEP	–	Oak Ridge Thermal Ellipsoid Plot
Pd/C	–	Palladium on Carbon

TMSI	–	Trimethyl Sulphonium iodide
TBSCl	–	<i>tert</i> -Butyldimethylsilyl chloride
TBAF	–	<i>Tetra-n</i> -butylammonium fluoride
NaClO ₂	–	Sodium chlorite
NaH ₂ PO ₄	–	Sodium dihydrogen phosphate
PMBCl	–	<i>Para</i> -Methoxy benzyl chloride
(COCl) ₂	–	Oxalyl chloride
CH ₃ PPh ₃ Br	–	Methyltripheyposphonium bromide
<i>t</i> -BuOK	–	Potassium tertiary butoxide
EtMgBr	–	Ethyl magnesium bromide
CuCN	–	Copper cyanide
DCC	–	N,N'-Dicyclohexylcarbodiimide
EDCI	–	1-(3-Dimethylaminopropyl)-3-ethylcarbodiimide hydrochloride
DDQ	–	2,3-Dichloro-5,6-dicyanobenzoquinone
TFA	–	Trifluoroacetic acid
NH ₄ Cl	–	Ammonium chloride
DIPEA	–	Diisopropylethyl amine
CD	–	Circular dichroism
COSY	–	Correlation spectroscopy
HSQC	–	Heteronuclear Single Quantum Coherence
HMBC	–	Heteronuclear Multiple Bond Coherence
HOBT	–	1-Hydroxybenzotriazole

GENERAL REMARKS

- ^1H NMR spectra were recorded on AV-200 MHz, AV-400 MHz, and DRX-500 MHz spectrometer using tetramethylsilane (TMS) as an internal standard. Chemical shifts have been expressed in ppm units downfield from TMS.
- ^{13}C NMR spectra were recorded on AV-50 MHz, AV-100 MHz, and DRX-125 MHz spectrometer.
- EI Mass spectra were recorded on Finnigan MAT-1020 spectrometer at 70 eV using a direct inlet system.
- The X-Ray Crystal data were collected on *Bruker SMART APEX* CCD diffractometer using Mo K_α radiation with fine focus tube with 50 kV and 30 mA.
- Infrared spectra were scanned on Shimadzu IR 470 and Perkin-Elmer 683 or 1310 spectrometers with sodium chloride optics and are measured in cm^{-1} .
- Optical rotations were measured with a JASCO DIP 370 digital polarimeter.
- All reactions are monitored by Thin Layer Chromatography (TLC) carried out on 0.25 mm E-Merck silica gel plates (60F-254) with UV light, I_2 , and anisaldehyde in ethanol as developing agents.
- All reactions were carried out under nitrogen or argon atmosphere with dry, freshly distilled solvents under anhydrous conditions unless otherwise specified. Yields refer to chromatographically and spectroscopically homogeneous materials unless otherwise stated.
- All evaporations were carried out under reduced pressure on Buchi rotary evaporator below 45 °C unless otherwise specified.
- Silica gel (60-120), (100-200), and (230-400) mesh were used for column chromatography.

CONTENTS

	Page No.
Abstract	i–xv
Chapter I:	
Section I: The total synthesis of stagonolide B and 4-<i>epi</i>-stagonolide B	
Introduction	1
Present work	11
Experimental	26
Spectra	39
References	58
Section II: Total synthesis of Jaspine B (Pachastrissamine) from D-glucose	
Introduction	64
Present work	71
Experimental	77
Spectra	82
References	89
Chapter II:	
Synthesis of novel furano β-amino acids from D-xylose and their homo-oligomers	
Introduction	91
Present Work	103
Secondary Structural Analysis by 2D NMR	115
Experimental	140
Spectra	150
References	165
List of Publications	169

ABSTRACT

ABSTRACT

The thesis entitled “**Studies Toward the Total Synthesis of Stagonolide B and Jaspine B & Synthesis of Novel Furano β -Amino Acids (β -FAA) and their Homo-oligomers**” consist of two chapters. The first chapter is divided in two sections. The first section describes the total synthesis of Stagonolide B. Second section describes the total synthesis of Jaspine B (pachastrissamine) from D-glucose. The second chapter deals with the synthesis of novel furano β -amino acids from D-xylose and their homo-oligomers.

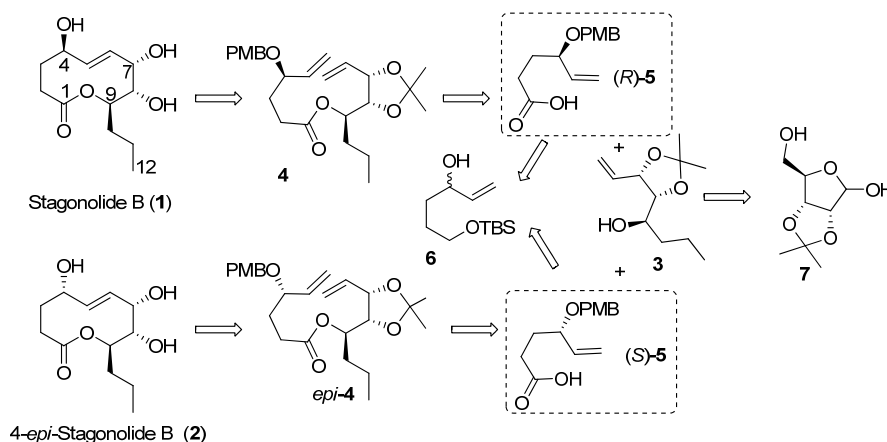
Chapter I: Section-I

The total synthesis of stagonolide B and 4-*epi*-stagonolide B

Stagonolide **A**, was isolated in 2007 from the pathogenic fungus *Stagonospora cirsii*. Later, the bioassay guided extraction of solid culture of *Stagonospora cirsii* led to the isolation of phytotoxic secondary metabolites stagonolides B–F. Considering their similarity in the ^1H and ^{13}C NMR with the stagonolide **A**, these new metabolites were considered as the family members of **A** and were named as stagonolide B–F. Stagonolide B (**1**) presents a 2*E*-ene-1,4-*trans*-diol unit which has been realized as one of the tough task to construct by employing ring closing metathesis based upon ours as well as the others earlier observations. The 4-*epi*-stagonolide (**2**) has also been selected as a target for the total synthesis considering the fact that RCM of the substrates leading to a 1,4-*cis*-diol configured nonenolides seems to be facile.

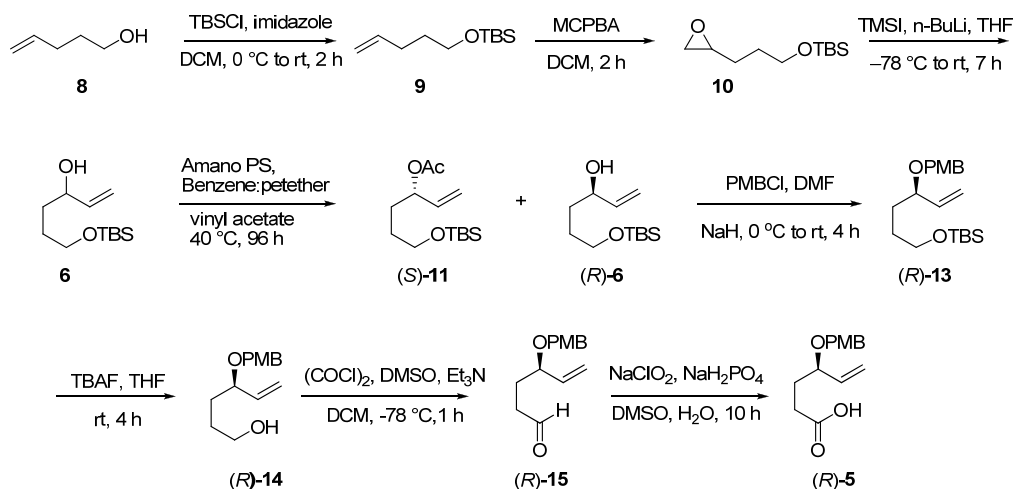
A detailed retrosynthetic planning for stagonolide B and 4-*epi*-stagonolide B (**2**) is given in the (Figure 1). After the application of the RCM transform, the enantiomeric acids (*R*)-**5** and (*S*)-**5**, and the alcohol **3** were identified as the key coupling partners for the synthesis of stagonolide B (**1**) and its 4-epimer (**2**). Easily available D-ribose has been selected as a starting point for the chiral pool synthesis of the known alcohol fragment **3**. The synthesis of the enantiomeric acids **5** was planned through the enzymatic resolution of the TBS protected diol **6**.

Figure 1: Retrosynthetic analysis for stagonolide B and 4-*epi*-stagonolide B



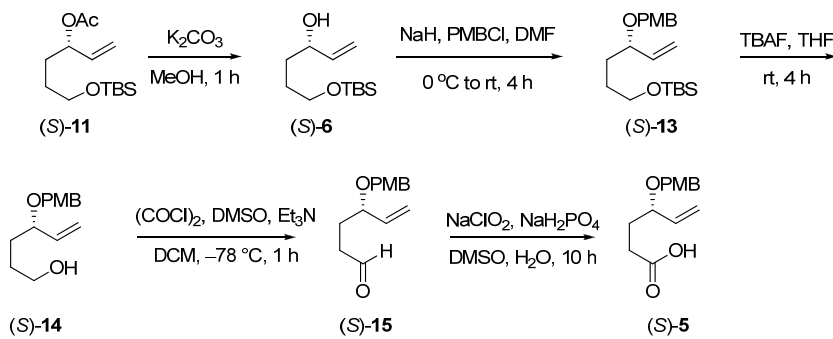
Our synthesis of stagonolide B started with the preparation of the acid (*R*)-**5** (Scheme 1). Readily available 4-pentene-1-ol was converted to the racemic epoxide **10**. The one carbon extension of the epoxide was carried out using TMSI, *n*-BuLi in THF to afford the key allyl alcohol **6**. Alcohol **6** on treatment with enzyme *Amano PS* afforded alcohol (*R*)-**6** and acetate (*S*)-**11**. The absolute configuration of the alcohol (*R*)-**6** was established by using Mosher method. Protection of the hydroxyl group of (*R*)-**6** as its PMB ether followed by silyl deprotection using TBAF gave (*R*)-**14**. Oxidation of alcohol (*R*)-**14** to the aldehyde under Swern conditions followed by further oxidation of intermediate aldehyde employing sodium hypochlorite under buffered conditions completed the synthesis of the acid fragment (*R*)-**5**.

Scheme 1: Synthesis of acid (*R*)-**5**



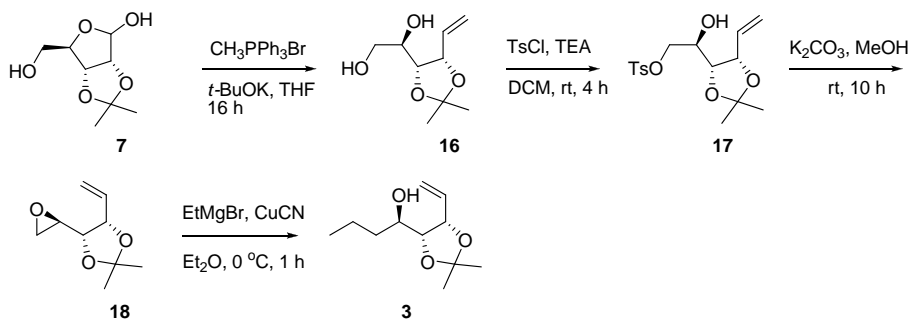
The acetate (*S*)-**11** was subjected for deacetylation using potassium carbonate and methanol and resulting (*S*)-**6** was used for the synthesis of acid (*S*)-**5** employing the same sequence of reaction as used for its enantiomer synthesis (*R*)-**5** (Scheme 2).

Scheme 2: Synthesis of acid (*S*)-5



The alcohol fragment **3** was synthesized from D-ribose. The known 2,3-acetonide of ribose **7** was prepared according to the reported procedure and subjected for one carbon Wittig homologation to afford the 1,2-diol **16**. Selective 1°-OH tosylation of **16** followed by base treatment furnished the epoxide **18**. Opening of the oxirane by using EtMgBr needed some experimentation and under the optimized conditions, we could isolate requisite coupling partner **3** in good yields (Scheme 3).

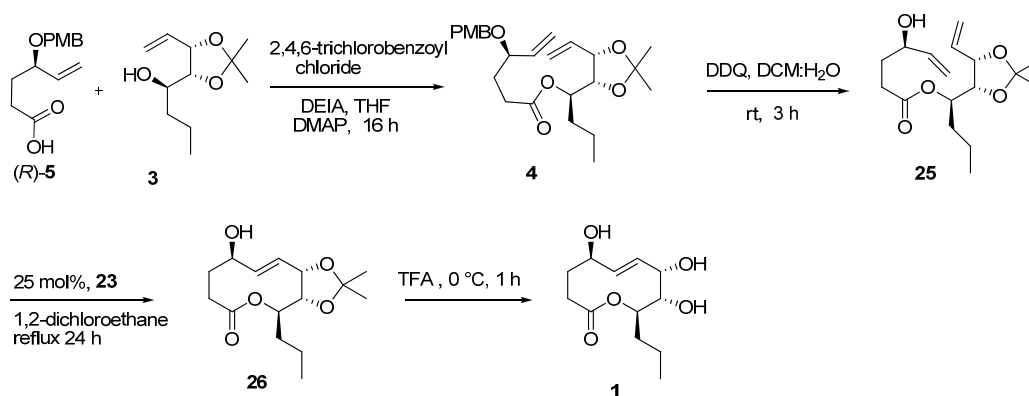
Scheme 3: Synthesis of alcohol 3



The RCM precursor **4** was obtained by coupling of acid (*R*)-**5** and alcohol **3** using Yamaguchi reagent. Various catalysts prescribed for the metathesis have been explored with this substrate **4**, RCM of which turned to be a difficult proposition. In this context, we have opted for the PMB deprotection which indeed was selected in priority as a safe

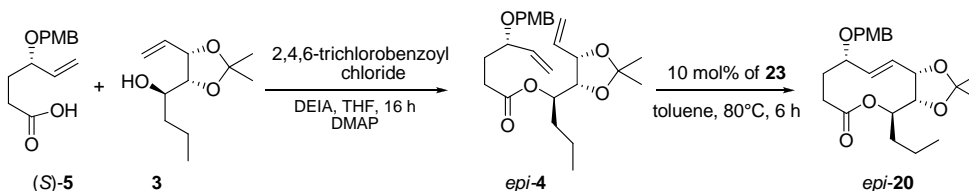
handle to change the nature of the adjacent functional groups around the olefins that participate in RCM. The PMB deprotection was carried out with DDQ to afford the diene ester **25**. The attempted RCM of **25** was found to yield mainly the oligomeric products with both the 1st and 2nd generation catalysts of Grubbs' and Hoyeda in solvents such as dichloromethane, benzene and toluene either at rt or at reflux temperatures. When we switched to dichloroethane as a solvent, and with the 2nd gen. Grubbs/Hoyeda catalysts we could notice the molecular ion peaks corresponding to the product in the LCMS.

Scheme 4: Total synthesis of stagonolide B



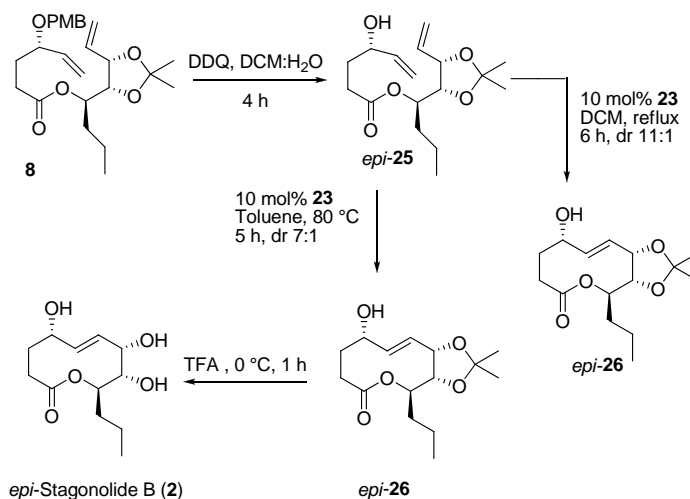
After examining the various reaction parameters, the RCM of **25** could be conducted successfully using 25 mol% of Grubbs' 2nd gen. catalyst in dichloroethane at reflux temperatures. However, the separation of the resulting lactone was found to be tedious so, crude metathesis reaction mixture used directly for the acetonide deprotection with TFA at 0 °C for 1h to obtain the Stagonolide B (**1**) in moderate yields. The analytical and spectral data of **1** were in agreement with the data reported for the natural product (Scheme 4).

Scheme 5: Synthesis of epi-20



The RCM of *epi-4* was found to be facile with Grubbs' 2nd generation catalyst in toluene at 80 °C and gave the desired *E*-isomer *epi-20* exclusively (Scheme 5). Next we synthesized *epi-25*. The synthesis started with the coupling of alcohol **3** with acid (*S*)-**5**. The resulting ester *epi-4* (the RCM of which was executed by my colleague at 80 °C in toluene) was subjected for selective PMB deprotection to afford *epi-25*. The RCM of *epi-25* could be carried out smoothly in dichloromethane at reflux temperature and *E/Z* noneolides *epi-26* were obtained in a 11:1 ratio.

Scheme 6: Synthesis of 4-*epi*-Stagonolide B (2**)**



Carrying the reaction under conditions similar those for *epi-25* (toluene, 80 °C) resulted in an increase of *Z*-isomer 7:1 (Scheme 6). To achieve the synthesis of 4-*epi*-stagonolide B (**2**), the compound *epi-26* was treated with neat TFA for 1 h at 0 °C and compound **2** was obtained as crystalline solid in 85% isolated yield. The spectral data of compound **2** was in good agreement with the data reported earlier by my colleague.

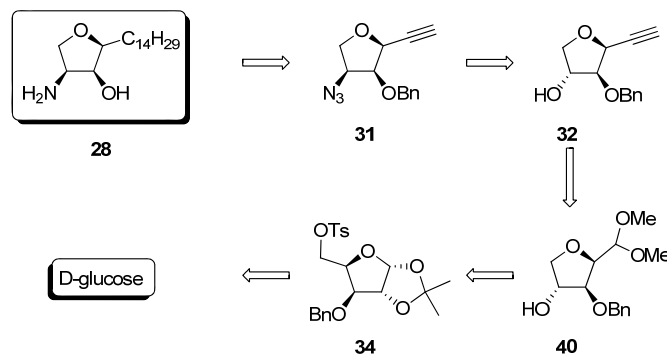
In conclusion first total synthesis of stagonolide B (**1**) confirming its absolute stereochemistry has been documented. A combination of the chiral pool approach and enzymatic resolution has been adopted to synthesize the key coupling partners. The 4-*epi*-stagonolide B (**2**) has also been synthesized to check the influence of the relative stereochemistry of allylic hydroxy groups and their protecting groups on the efficiency of the RCM and on the rate acceleration by the catalyst.

Chapter I: Section-II

Total synthesis of Jaspine B (pachastrissamine) from D-glucose

Jaspine B (**28**), isolated and characterized by Higa and co-workers in 2002 from the Okinawa marine sponge *Pachastrissa sp.* (family Calthropellidae) is a novel anhydrophytosphingosine with promising anti-cancer activity. Considering its simple structure and important biological activity, we have started a program to develop enantio-divergent strategy for the synthesis of jaspine B enantiomers with a provision of flexibility to modify the side chain for analogues synthesis. A retrosynthetic strategy for the synthesis of jaspine B is depicted below (Figure 2).

Figure 2: Retrosynthetic strategy of jaspine B

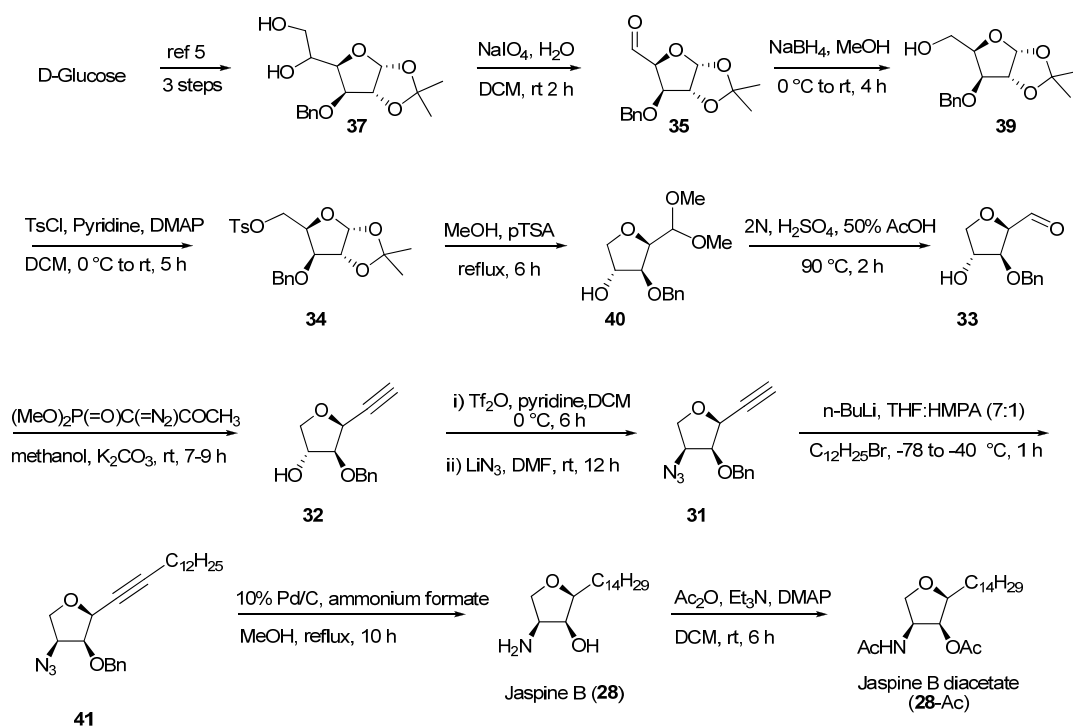


The synthesis of jaspine B was started from D-glucose. Reduction of aldehyde **35** (prepared from D-glucose following the literature procedure, Scheme 7) with NaBH₄ gave alcohol **39**. Tosylation of **39** using *p*-TsCl in pyridine followed by acid mediated acetonide deprotection with concomitant 2,5-ring closure gave the dimethylacetal **40** in a good yields. The following acetal hydrolysis reaction proceeded with 2N sulfuric acid in acetic acid and the resulting aldehyde **33** was subjected to Ohira-Bestmann alkylation under standard conditions, to afford alkyne **32**.

The alkyne **32** was transformed to the corresponding azidoalkyne **31** by treatment with Tf₂O in pyridine followed by reaction of the intermediate triflate with LiN₃ in DMF. The alkylation of azidoalkyne **31** with 1-bromododecane was facile using

n-BuLi in THF, HMPA and the alkylate product **41** was obtained in 61% yield. Hydrogenolysis of **41** was effected by refluxing in methanol in the presence of ammonium formate and cat. 10% Pd/C. The spectral and analytical data of the **28** and its diacetate **28**-Ac were in agreement with the reported values and the structure of **28**-Ac was further established by the single crystal X-ray analysis.

Scheme 7: Synthesis of Jaspine B



In conclusion, a simple chiral pool strategy for the total synthesis of jaspine B has been developed. Starting from the known and easily available glucose diacetone, pachastrissamine has been synthesized in nine linear steps with an overall yield of 17.3%. As we have added the side chain at the penultimate step, our strategy is endowed with sufficient flexibility for the synthesis of pachastrissamine analogues with variation of side chain or alteration of its length.

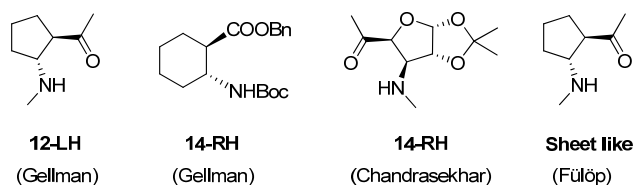
Chapter II

Synthesis of novel furano β -amino acids from D-xylose and their homo-oligomers

Introduction

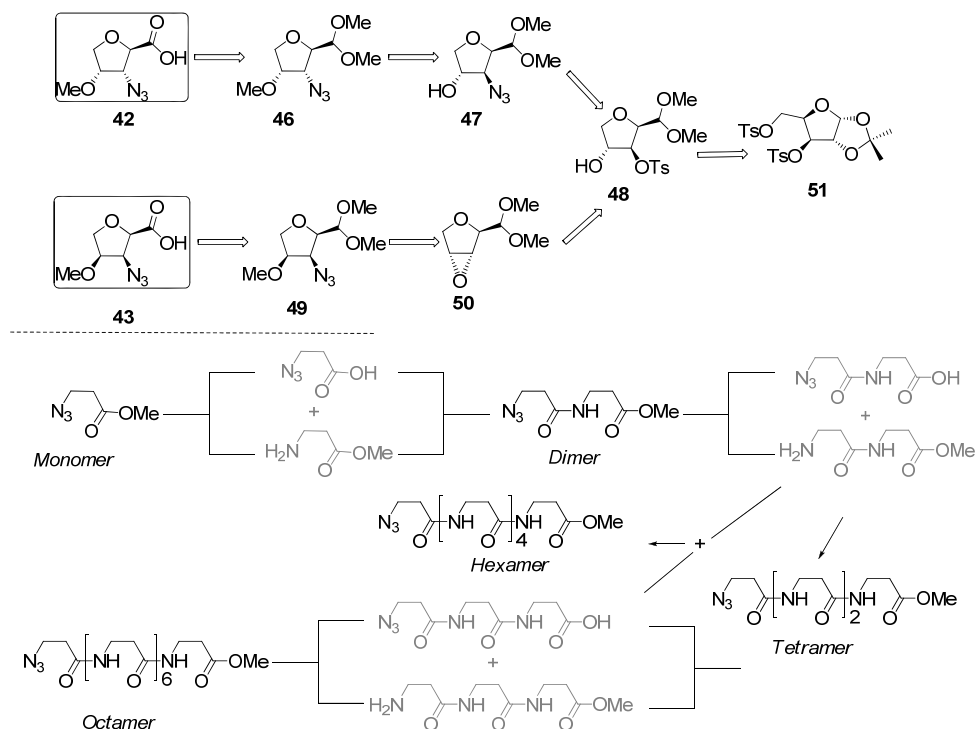
Recently Seebach and Gellman groups have introduced the β -amino acids and their oligomers as a stable mimics natural peptides. β -Peptides have been identified for three different helical secondary structures (14-helix, 12-helix and 10/12 helix). Gellman found that β -peptides with *trans*-substituted cyclohexane rings strongly favor a 14-helix, β -peptides with *trans*-substituted cyclopentane rings favor 12-helix, where as the *cis*-configured cyclopentane β -amino acid was found to form a sheet structure. Very recently, the synthesis of homo-oligomers of a sugar derived β -furano amino acid has been reported. Interestingly, the sugar derived *cis*- β -furano amino acid was found to form a stable 14-helix in solution where the corresponding *cis*- β -CPA oligomers formed sheet like structure (Figure 3). The rigid conformation of furanose ring has been attributed for the observed strong 14-helix. In this context, following sugar derived *cis*- and *trans*-furano β -amino acids **42** and **43** respectively, having a *cis*-methoxy α - to the amine unit have been designed to address the role of furanose conformation and also the steric/electronic influence of adjacent substituents on the secondary structure of the corresponding oligomers.

Figure 3: Structures of β -amino acids synthesized by Gellman, Chandrasekhar and Fülöp



The indented synthesis of these two diastereomeric furano amino acids is an extension of our ring-transposition approach that we have adopted for the above mentioned jaspine synthesis (Figure 4).

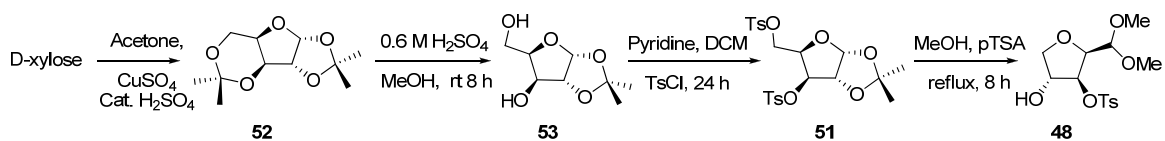
Figure 4: β -Amino acid, and retrosynthetic scheme and flow diagram for synthesis of homo-oligomers



Synthesis of dimethylacetal **48**

The synthetic endeavor began with the conversion of D-xylose into D-xylose diacetonide **52** (prepared from D-glucose by treating it with conc. H_2SO_4 , anhydrous CuSO_4 , in acetone). Selective deprotection of 3,5-isopropylidene group by using 0.8% H_2SO_4 in methanol gave diol **53** (Scheme 8). Diol **53** on was protected with tosyl by treated with tosyl chloride in pyridine to procure the compound **51**. Having the tosyl protected compound **51** in hand, the next task was acid mediated acetonide deprotection with concomitant 2,5-ring closure to give dimethylacetal **48**.

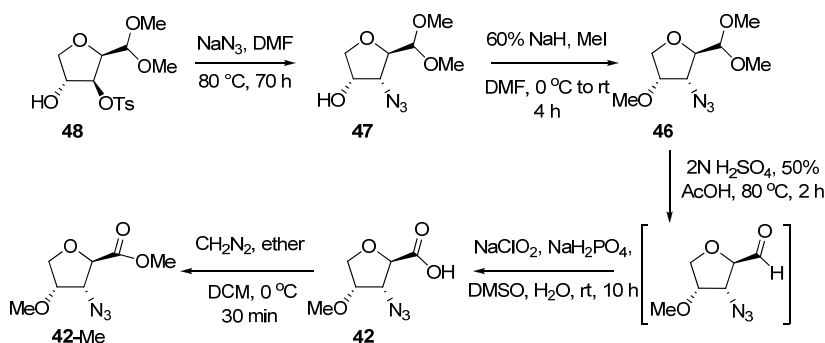
Scheme 8: Synthesis of dimethylacetal **48**



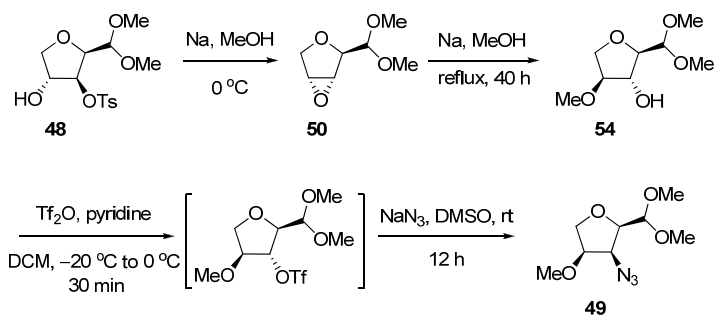
Synthesis of *trans*-furano- β -amino acid **42**

The compound **48** was treated with sodium azide in DMF solvent to give **47**. The hydroxyl group of **47** was methylated to give **46**, then acetal **46** was converted to aldehyde followed by acid formation using sodium chlorite and sodium dihydrogen phosphate in DMSO and water. Monomer **42** was converted to ester **42-Me** using diazomethane (Scheme 9).

Scheme 9: Synthesis of *trans*- β -azido acid **42** its methyl ester **42-Me**



Scheme 10: Synthesis of azide **49**

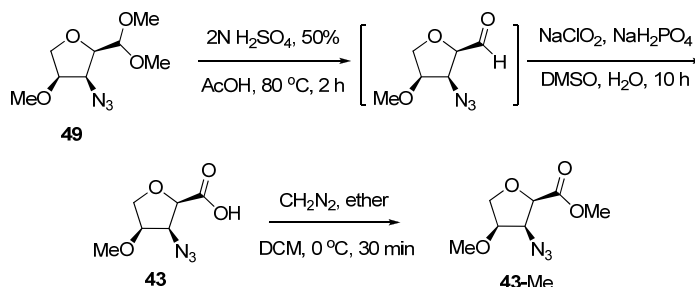


Synthesis of *cis*-furano- β -amino acid **43**

The compound **48** can be converted into **50** by base treatment, then epoxide was opened regioselectively with sodium methoxide. The hydroxyl group of **54** was transformed to the corresponding azide by treatment with Tf_2O in pyridine followed by reacting the intermediate triflates with NaN_3 in DMF (Scheme 10). Dimethyl acetal **49** was converted to aldehyde followed by acid formation using sodium chlorite and sodium

dihydrogen phosphate in DMSO and water. Monomer **43** was converted to ester **43-Me** using diazomethane (Scheme 11).

Scheme 11: Synthesis of acid **43 & ester **43-Me****



Synthesis of homo-oligomers from β -amino acid **42**

The monomers acid and amine were used to prepare dimer **55**, Tetramer **56**, hexamer **57**, and octamer **58** by using standard coupling protocol where EDCI and HOBT combination was used for peptide coupling (Figure 5)

Once we have the Oligomers **55–58** in our hand now the objective was set to examine the existence of a secondary structure resulting from the intra-strand hydrogen bonding. Circular Dichroism is one of the simple tool to find the existence of any secondary structure. Indeed the CD spectra of oligomers **55–58** in trifluoroethanol as shown in (Figure 6), suggest the existence of a 12-helix in solution.

Figure 5:

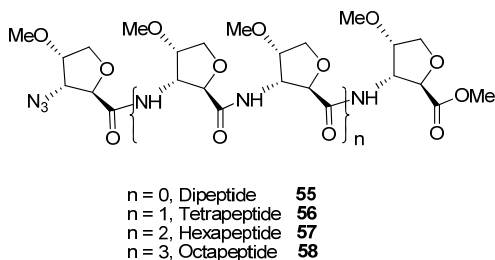
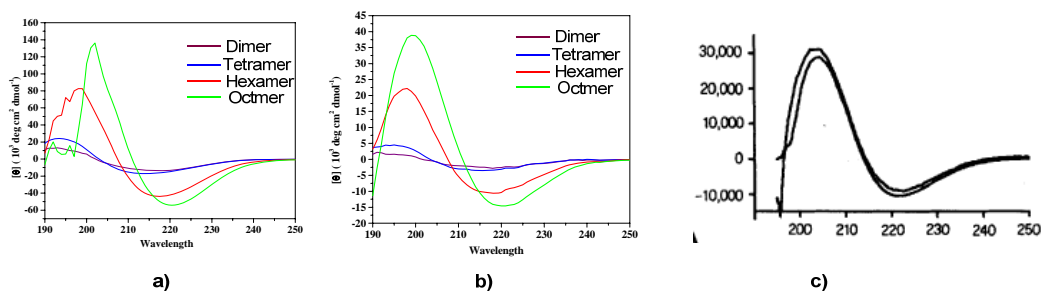
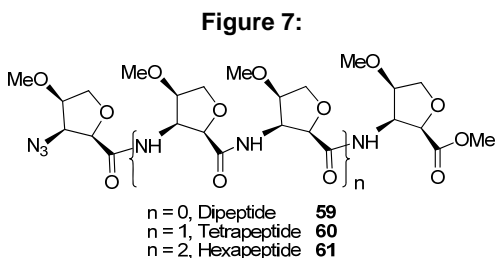


Figure 6: The CD Spectral of di, tetra, hexa and octamers (a) at 0.1 mmol and (b) at 0.02 mmol and c) the CD spectra of hexamer of *trans*-ACPC at 0.1 mmol and 0.02 mmol



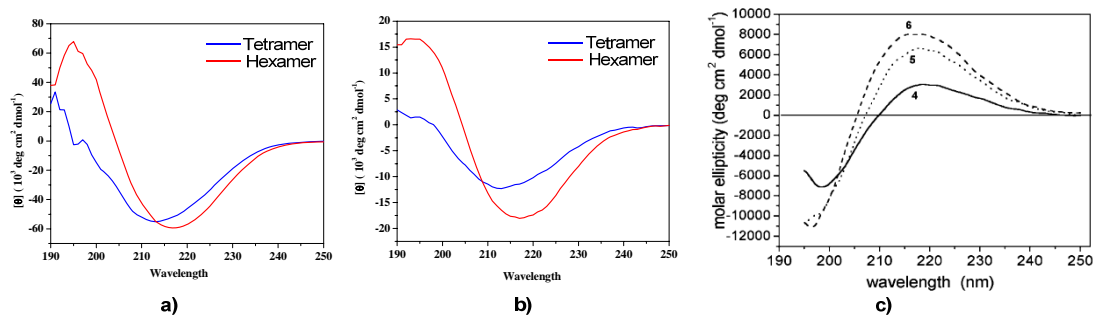
Synthesis of homo-oligomers from β -amino acid 43

The monomers acid and amine were used to prepare dimer **59**, Tetramer **60**, and hexamer **61** by using standard coupling protocol where EDCI and HOBt combination was used for peptide coupling (Figure 7).



The CD spectra of oligomers **59-61** in trifluoroethanol as shown in (Figure 8), suggest the existence of a 14-helix in solution.

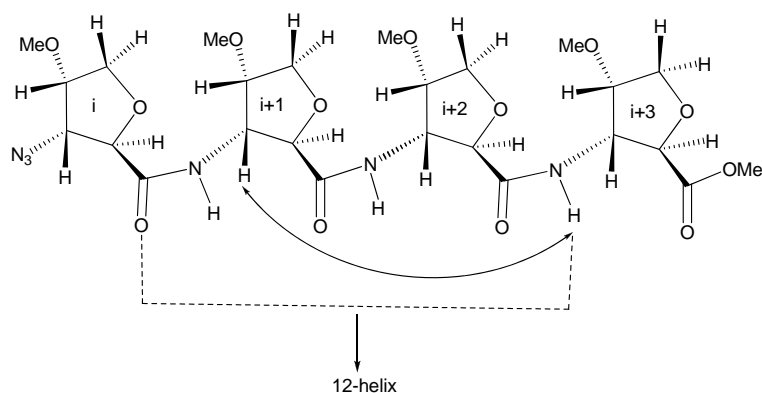
Figure 8: The CD Spectral of *cis* tetra and hexamers (a) at 0.1 mmol and (b) at 0.02 mmol and c) the CD spectra of related *cis*-AFA having 14-membered helix



Discussion and Conclusion

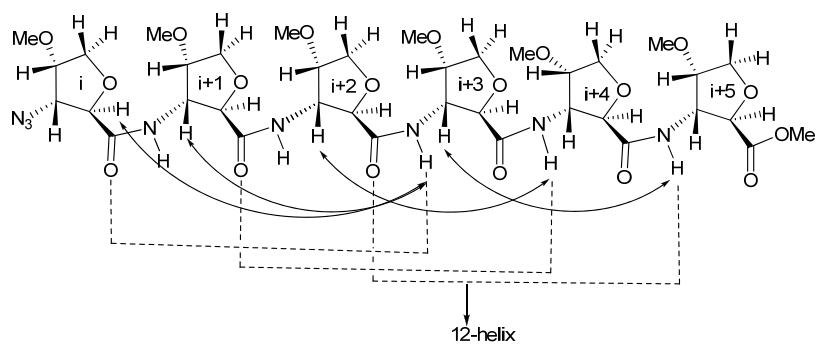
The secondary structure of *trans*- β -FAA tetramer **56** was assigned with the help of the inter-residue *nOes* noticed. Amongst the various *nOes* observed in the NOESY of the **56**, $C_{\beta}H_{(i+1)}/NH_{(i+3)}$ (Figure 9) indicates the presence of a single 12-helix pitch. However, the CD-ellipticity of this tetramer is substantially weak.

Figure 9: Characteristic *nOes* supporting a 12-helix



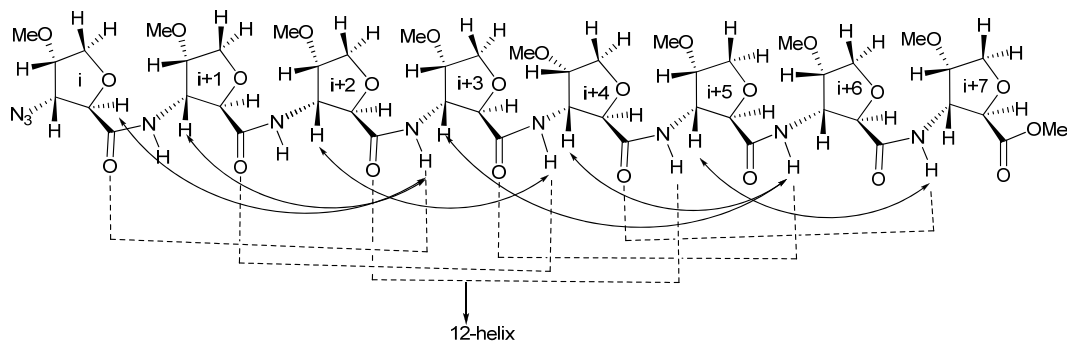
Next, we analyzed the various inter-residue *nOes* observed in the NOESY of the *trans*-hexamer **57**. The interpretation of some of the observed long-range *nOes* is complicated by the overlapping of two of the five NH protons. Four characteristic *nOes* $C_{\beta}H_{(i+1)}/NH_{(i+3)}$, $C_{\alpha}H_{(i)}/NH_{(i+3)}$, $C_{\beta}H_{(i+2)}/NH_{(i+4)}$ and $C_{\beta}H_{(i+3)}/NH_{(i+5)}$ found indicated the presence of a left-handed 12-helix, which was further supported by the concentration independent CD maxima and minima recorded for this hexamer (Figure 10).

Figure 10: Characteristic *nOes* supporting a 12-helix



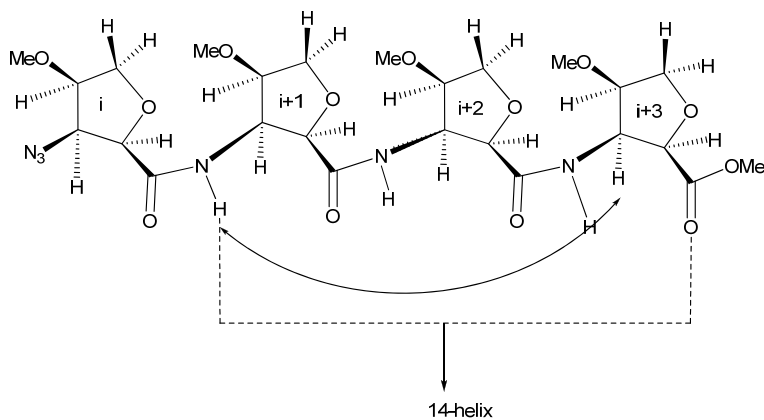
Due to the well separation of all the NH signal, many of the inter-residue *nOes* could be assigned which indeed strongly indicated hydrogen bonding pattern leading to a left-handed 12-helix. Some of the important inter-residue *nOes* - $C_{\alpha}H_{(i)}/NH_{(i+3)}$, $C_{\beta}H_{(i+1)}/NH_{(i+3)}$, $C_{\beta}H_{(i+2)}/NH_{(i+4)}$, $C_{\beta}H_{(i+4)}/NH_{(i+6)}$, $C_{\beta}H_{(i+5)}/NH_{(i+7)}$ and $C_{\beta}H_{(i+3)}/NH_{(i+6)}$ are illustrated in the Figure 11.

Figure 11: Characteristic *nOes* supporting a 12-helix



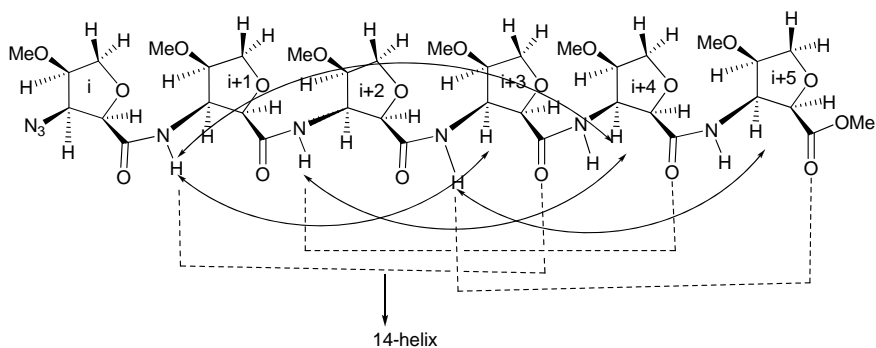
The secondary structure of *cis*- β -FAA tetramer **60** was assigned with the help of inter-residue *nOes* noticed. All protons at NH and C _{β} of each residue were well separated in CDCl₃ solvent. Amongst the various *nOes* observed in the NOESY of the **60**, one characteristic *nOes* *i.e.* $NH_{(i+1)}/C_{\beta}H_{(i+3)}$ found indicated the presence of a left-handed 14-helix (Figure 12).

Figure 12: Characteristic *nOes* supporting a 14-helix



Due to the well separation of all the NH signals and the C_β of each residue, four characteristic nOes $NH_{(i+1)}/C_\beta H_{(i+3)}$, $NH_{(i+1)}/C_\beta H_{(i+4)}$, $NH_{(i+2)}/C_\beta H_{(i+4)}$ and $NH_{(i+3)}/C_\beta H_{(i+5)}$ found indicated the presence of a left-handed 14-helix (Figure 13).

Figure 13: Characteristic nOes supporting a 14-helix



In summary, from CD and 2D NMR study we have concluded that the designed homo-oligomers of *trans*-furano- β -amino acid are capable of forming left-handed 12-helical conformation in the solution, while the *cis*-furano- β -amino acid homo-oligomers were found to be adopting a left-handed 14-helix structure.

CHAPTER-I

Section-I: The total synthesis of stagonolide B and 4-*epi*-stagonolide B

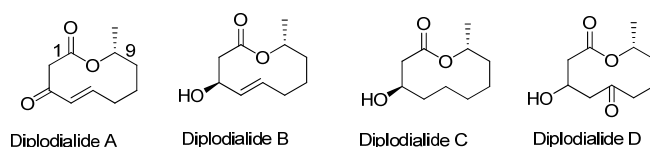
Introduction

Amongst the medium size rings in general and among the ten membered rings in particular, the nonenolides (10-membered lactones) are prevalent and most abundant in nature.¹ The jasmine lactone, isolated in 1942 from the essential oil of *Jasminum grandiflorum*, was the first representative member of this family and its structure was confirmed twenty years later.² Up to 1975, it was the only known naturally occurring decalactone. Over the last four decades a series of natural compounds having the 10-membered macrolactone ring have been isolated. These medium-sized macrolides are secondary metabolites biosynthesized mainly by fungi, bacteria and marine organisms, with only a few being produced by plants or insects. The common types of ten-member lactones frequently observed in nature are monocyclic polyketalides, oxylipins, bicyclic aliphatic and aromatic. Representative examples and their source, bio-activities are presented here.

Polyketalides

Polyketalides are the most common congeners of the ten member family of lactones. Diplodialides are the first described group of monocyclic ten-membered ring lactones (Figure 1). Diplodialides A, B and C were isolated in 1975 by Ishida and Wada, from the plant pathogenic fungus *Diplodia pinea*.³ Diplodialide A showed inhibitory activity against steroid hydroxylase. The isolation of diplodialide D, as well as the full structural elucidation of all the four metabolites were reported by the same authors.⁴

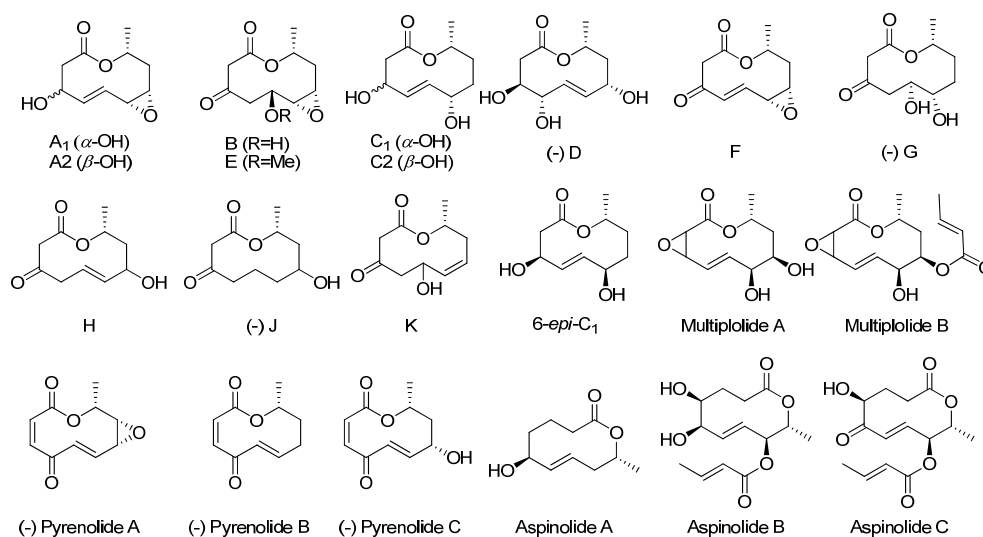
Figure 1: Structures of Diplodialides A–D



Another series of ten member lactones named decarestrictines, were isolated from different strains of *Penicillium* species (Figure 2) in early 1990s and shown to be inhibitors of cholesterol biosynthesis, demonstrated by both *in vivo* and *in vitro*

studies.⁵ Most of them consists of a ten member macrolactone skeleton with different oxo-functionalities at C(3) and C(7). Five of them (A₁, A₂, B, E, and F) bear an epoxide unit between C(6)–C(7), eight of them (A₁, A₂, C₁, C₂, D, F, H and K) possess a double bond and seven of the decarestrictines (B, E, F, G, H, J and K) are β-keto lactones. The most biologically active amongst these natural products, decarestrictine D, was simultaneously and independently isolated from the canadian tuckahoe (the sclerotium of the fungus *Polyporus tuberaster*) and was named tuckolide by the authors.⁶ A C(6)-epimer of decarestrictine C₁ was isolated in 2004 from the fungus *Cordyceps militaris* and exhibited antimalarial activity against *Plasmodium falciparum* K1.⁷ The epoxy lactones multiplolides A and B (isolated from *Xylaria multiplex*), are also closely related to the decarestrictine family.⁸

Figure 2: Structurally Related Nonenolides Decarestrictines (A₁–K), Pyrenolides & Multiplolides

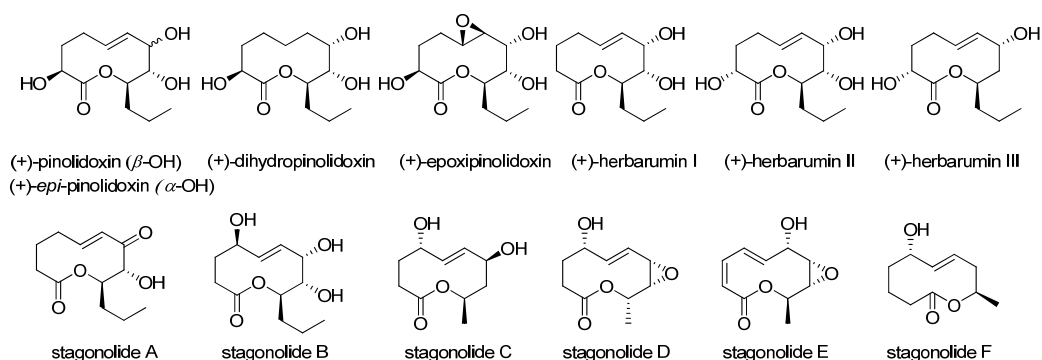


Pyrenolides A, B and C were isolated from *Pyrenophora teres*.⁹ Pyrenolide A was also detected in the culture filtrates of *Ascochyta hyalospora*.¹⁰ These highly functionalized unsaturated keto-lactones, which differ only by the pattern of oxidation at the C(7) and C(8) positions, exhibit growth inhibiting and morphogenic activities toward fungi. Aspinolides A–C are reported to be found in the cultures of *Aspergillus ochraceus* in 1997.¹¹

In 1993, Evidente *et al.* isolated pinolidoxin, a nonenolide containing an *n*-propyl group at C(9) from *Ascochyta pinoda*, as well as three related compounds, namely *epi*-pinolidoxin, dihydropinolidoxin and epoxy-pinolidoxin (Figure 3).¹²

Assayed on pea and bean leaves, the first three compounds were shown to be highly toxic, whereas epoxy-pinolidoxin was inactive. Herbarumins, structurally similar to the pinolidoxin were isolated by Rivero-Cruz *et al.* from the different source *Phoma (P. herbarum)* and were found to interact with the bovine brain calmodulin, inhibiting the activation of the enzyme cAMP phosphodiesterase.¹³

Figure 3: Structurally Related Nonenolides Pinolidoxins, Herbarumins and Staganolides



In 2007, Berestetskiy and co-workers described the isolation, chemical and biological characterization of a new nonenolide produced by *Stagonospora cirsi* (a pathogen of *Cirsium arvense*) in liquid cultures, named staganolide (Figure 3).¹⁴ The relative and the absolute configuration of staganolide A was established by converting it to the known herbarumin I employing a NaBH_4 reduction of the keto group. Later, in 2008, Evidente *et al.* reported the isolation of five new nonenolides from the same fungus, grown in solid culture.¹⁵ Considering their origin and structural similarity, these five new nonenolides were named as staganolides B–F. Considering the similar spectral data of staganolides with that of the previously reported natural products herbarumins, the connectivity of the free hydroxyl groups in staganolides were assigned and their relative orientations have been proposed as given in Figure 3.

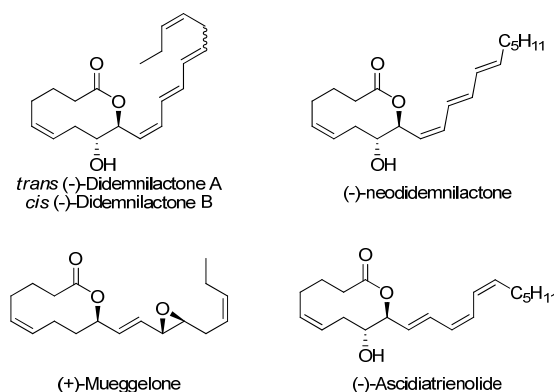
Oxylipins

In general, oxylipins are oxygenated fatty acid metabolites. One of the most biologically important groups of oxylipins in mammalian system is the eicosanoid. These eicosanoids are potent modulators of immune responses in addition to playing a role in numerous basic host physiological processes.¹⁶ Didemnilactones A and B, and neodidemnilactone, consisting of ten member lactone associated with hydrophilic side

chain at the C(9) carbon (Figure 4) were isolated in the early 1990s by Niwa *et al.*¹⁷ These eicosanoid lactones were found in the colonial marine tunicate *Didemnum moseleyi* and showed moderate inhibitory activity against lipoxygenase.

In 1997, an 18-carbon epoxy lactone was isolated from the cyanobacterium *Aphanizomenon flos-aquae*.¹⁸ This compound was shown to be an inhibitor of fish development and later (Figure 4) isolated from the blue-green alga *Gloeotrichia* sp. collected in Montana's lakes¹⁹ and was named as mueggelone. Ascidiatrienolides A–C, isolated in 1989 from the colonial marine ascidian *Didemnum candidum*, was first assigned as being nine-membered-ring lactones.²⁰ Later the structure of ascidiatrienolide A was revised to a ten-membered ring lactone, isomeric in the side chain with neodidemnilactone.²¹

Figure 4: Eicosanoid Decanolactones



In recent years, a number of bicyclic ten member lactones such as Sch642305, xestodecalactones A–C, sporostatin, apicularens, nargenicin and coloradocin with moderate to high complexity were isolated²². They are structurally and biologically important additions to the family of nonenolides. Many of the natural products described here were synthesized and their structures have been established.²³ It needs to be emphasized here that the number of strategies used for macrocycle construction is rather small. The methodologies included are mainly the Corey–Nicolaou²⁴ and Yamaguchi lactonizations²⁵ as well as the ring closing metathesis (RCM) approaches. In this context, the RCM reaction is well fitted and presently it is a fascinating tool in the field of organic synthesis.²⁶

Construction of the nonenolides employing ring closing metathesis and remarkable effect of allylic substituents on the outcome

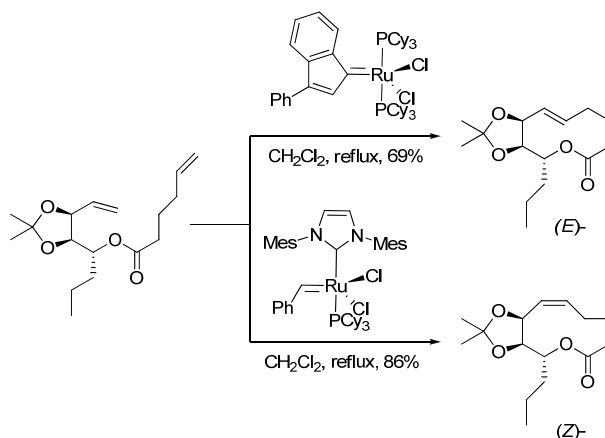
Macrocyclic secondary metabolites containing 8–10 membered rings are a subject of continuous interest to the synthetic chemists, as they are core structures of many natural products with a wide range of bioactivity.²⁷ Due to the difficulties caused by entropy as well as enthalpy, the construction of a medium size ring is not a straightforward proposition.^{28,29} The entropic factor is disfavored by the carbon chain becoming too long and thus the probability of a reaction taking place between the two chain termini decreases. The enthalpy factor is mainly created by steric interactions which lead to the torsional or Pitzer strain, bond angle deformation or Baeyer strain, stereoelectronic effect and *trans* annular interaction.^{30,31} The last two are particularly more important for medium size lactone rings. Simple methods used for the synthesis of smaller size rings have been also extended for the synthesis of medium size rings,³² but they are less effective and in most of the cases difficulties arose due the complexity in preparation of required intermediates designed for the macrocyclisation and experimentally demanding conditions which were not suitable when multifunctional, complex and natural products were the synthetic targets. Therefore, much more effort has been put forward toward the development of alternative strategies for the synthesis of medium size ring systems.³³

The olefin metathesis reaction has become a powerful tool in organic synthesis since the development of well defined single component ruthenium and molybdenum alkylidene catalysts that addressed the construction of the rings ranging from cyclobutane to macrocycles. Since the first construction of a 10-membered lactone using ring closing metathesis (RCM) by Fürstner in 1997,³⁴ synthesis of numerous naturally occurring ten-membered ring lactones, were documented by employing the RCM construct.³⁵ Though RCM has become a multipurpose reaction in nonenolides synthesis, the outcome of the reaction is sensitive to multiple factors, such as the nature of catalyst, steric crowding around the newly forming ring-olefin and sometimes even the success of RCM is substrate specific.

Fürstner's group has documented the early reports on the nature of the catalyst and the outcome of the RCM in their total synthesis of herbarumin I. They observed different results when different metathesis catalysts were employed (Scheme 1).³⁶ The

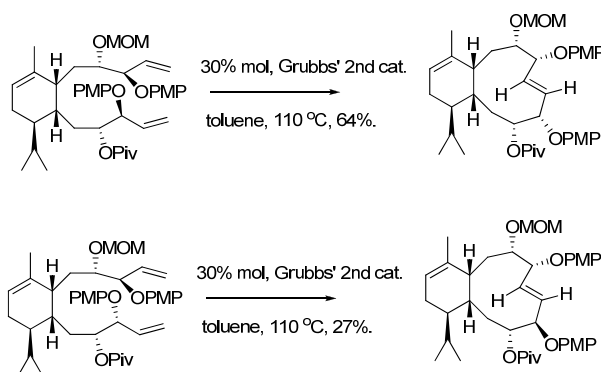
E/Z-selectivity depends on the catalyst employed and this has been attributed to ring strain of the cyclic intermediate from the di-olefinic precursors.

Scheme 1: *Fürstner Synthesis of Herbarumins*



During the course of their total synthesis of Eleutherobin, Gennerai and co-workers studied the role of protecting groups and the stereochemistry of the allylic hydroxyl groups on the 10-membered carbocycle construction.³⁷ The RCM was protective groups specific. With a PMP protection on both the allylic hydroxyl groups, 10-membered carbocycles with *2E*-ene-1,4-*cis*- or *trans*-diol were obtained under forced RCM conditions, the former being obtained in good yields and the latter in poor yields. For similar substrates having either with MOM or methyl ether protecting groups, the RCM led mainly to oligomerization (Scheme 2).

Scheme 2: *Dependence of RCM based 10-membered carbocycle construction on protecting groups as well as the stereochemistry of the allylic hydroxyl groups*

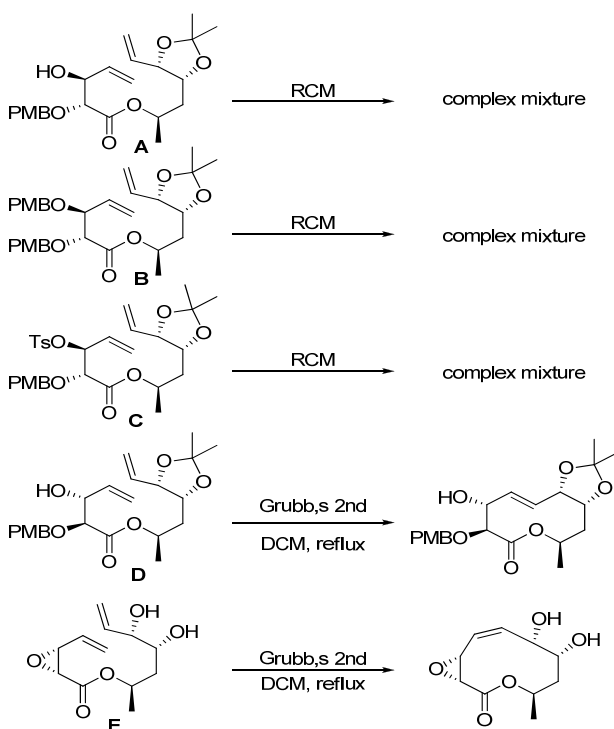


These results have been analyzed by Gennari with the help of DFT calculations and proposed that the *trans*-ruthena-cyclobutane derivatives are

thermodynamically more stable which indeed addressed the formation of *E*-olefins (which are thermodynamically unstable compared to their *Z*-isomers) exclusively under kinetically controlled conditions.^{37b,52,53}

Dealing with the total synthesis of multiplolide A, we have noticed a substrate specific RCM reaction.³⁸ Amongst the four similar substrates (**A–D**) employed, only one of the substrates (**D** 1,4-*cis*-diol) provided the desired 10-membered macrolactone. Whereas, the other three substrates **A–C** having a 1,4-*trans*-diol configuration, led to oligomerization and an epoxy substrate **E** resulting with the undesired stereochemistry of double bond (Scheme 3, Figure 5).

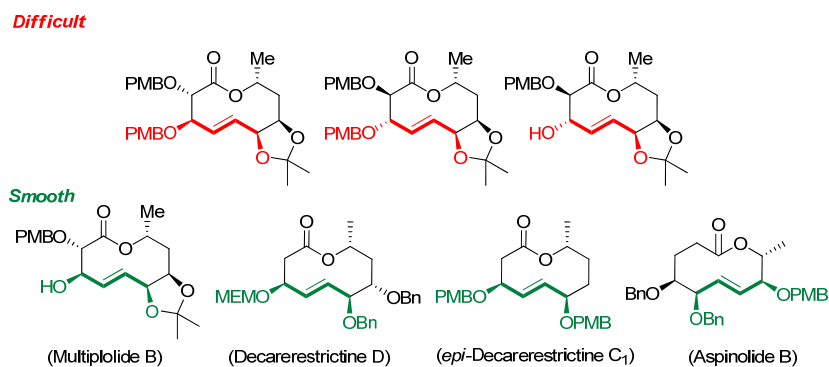
Scheme 3: Substrate specific outcome of RCM



This has prompted us to examine the available RCM based nonenolides construction having the 2-ene-1,4-diol unit. We were intrigued by the fact that they all dealt with the RCM of the substrates leading to a *syn*-1,4-diol configured nonenolides. It was quite striking to notice that, though several natural nonenolides having 1,4-*anti*-diol configuration are reported, no report concerning their synthesis employing the RCM are present in the literature. Reported synthesis of these nonenolides (Decarestrictine C₂ and Decarestrictine D) employed a macrolactonization³⁹ and

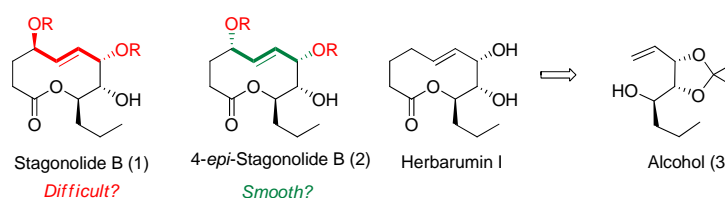
intramolecular Nozaki–Hiyama–Kishi coupling⁴⁰ (Aspinolide B and Decarestrictine D) as the central ring constructs.

Figure 5: The relative stereochemistry of the allylic hydroxy groups and the anticipated output of RCM



Intrigued by this, we have selected the staganolide B as a synthetic target which presents such *2E-ene-anti-1,4-diol* unit. We anticipated that the RCM will be a difficult proposition for a successful macrolide construction. We have also identified the *4-epi-Staganolide B* since it disposes a *2E-ene-syn-1,4-diol* unit, it should be a facile target to be constructed *via* RCM. The fact that staganolide B shares the complete structural features of herbarumin I except the presence of a C(4) hydroxy group with (*R*)-configuration and as our retrosynthetic disconnection will also provide the same alcohol intermediate **3** as one of the coupling partner, a brief account of the available methods for the preparation of **3** follows.

Figure 6: Staganolide B and its C(4)-epimer and the projected alcohol fragment **3**

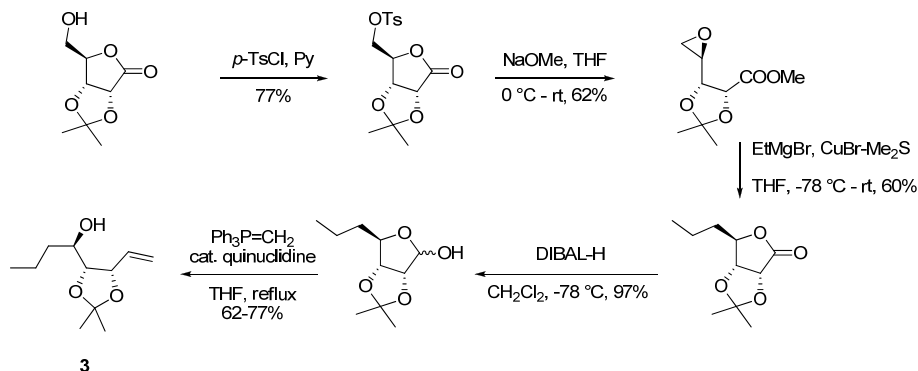


Reported syntheses of the triol fragment **3** and its enantiomer *ent-3*

The synthesis of alcohol **3** was first reported by Fürstner in 2002 during their total synthesis of herbarumins. They have used the three stereogenic centers of the D-ribonolactone which matched exactly with that of **3**. The synthesis of compound **3** was started with commercially available 2,3-*O*-isopropylidene-D-ribonolactone which

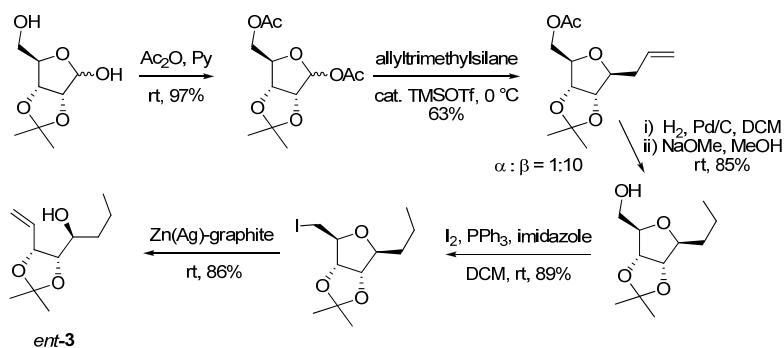
was converted to its tosyl derivative under standard conditions. The lactone was then converted to an epoxide derivative under basic condition using NaOMe. The synthesis was completed with subsequent epoxide opening with ethyl Grignard followed by DIBAL-H reduction and one carbon Wittig homologation.

Scheme 4: The first synthesis of acid **3** by Fürstner's group



The same group had also described a synthetic protocol for the enantiomer of **3** (*ent-3*). Considering the pseudosymmetry present in D-ribose, a C-glycosidation using allyl trimethylsilane of the 1,5-diacetate was utilized which produced β -isomer as the major product.

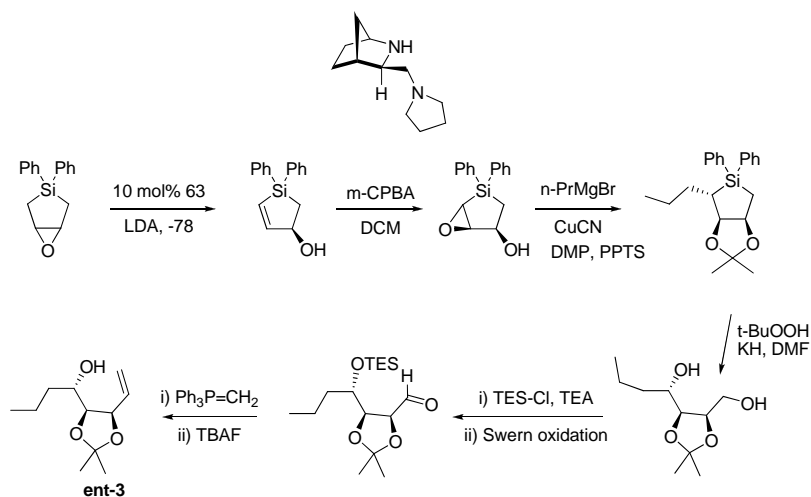
Scheme 5: Synthesis of enantiomer of alcohol **3**



After hydrogenation followed by decetylation, the primary hydroxyl group of the resulting C-propylribose was converted to the corresponding iodide. Finally, the furan ring was fragmented according to Bernet-Vasella protocol to complete the synthesis of the fragment *ent-3* (Scheme 5).³⁶

Although lengthy, an innovative synthesis of the fragment *ent-3* was published by Kozmin *et al.* in 2002.⁴¹ Their strategy began with the enantioselective isomerization of a silacyclopentane epoxide using LDA in the presence of a chiral ligand. The second –OH group was installed by applying a sequence of diastereoselective epoxidation and opening with propyl grignard to afford a functionalized silacyclopentane 2,3-diol. After protection of diol, silacyclic scaffold was removed under oxidative conditions. Finally, by a sequence of simple and straightforward way, they have completed the synthesis of *ent-3* (Scheme 6), and utilized the same for the total synthesis of herbarumin I and pinolidoxin.

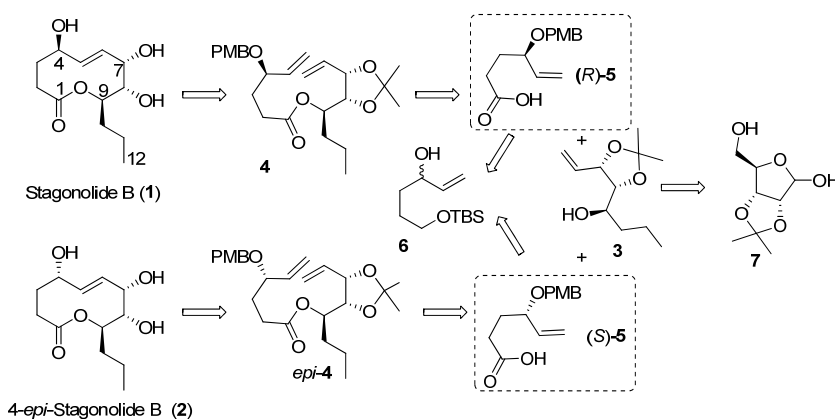
Scheme 6: An innovative synthesis of *ent-3* by Kozmin *et al.*



Present Work

Stagonolide B was isolated in 2008 by Evidente *et al.* from the solid cultures of *Stagonospora cirsii* (a pathogen of *Cirsium arvense*) along with the four other new nonenolides.¹⁵ The connectivity of the free hydroxyl groups and their relative orientations in stagonolides was proposed by correlating their spectral data with the previously reported natural products herbarumins data. Stagonolide B presents a *2E*-ene-1,4-*trans*-diol unit which we have identified as one of the tough task to construct by employing ring closing metathesis based upon ours as well as the others earlier observations.³⁸ The 4-*epi*-stagonolide has also been selected as a target for the total synthesis considering the fact that RCM of the substrates leading to a 1,4-*cis*-diol configured nonenolides seems to be facile.

Figure 7: Retrosynthetic analysis for stagonolide B and 4-*epi*-stagonolide B



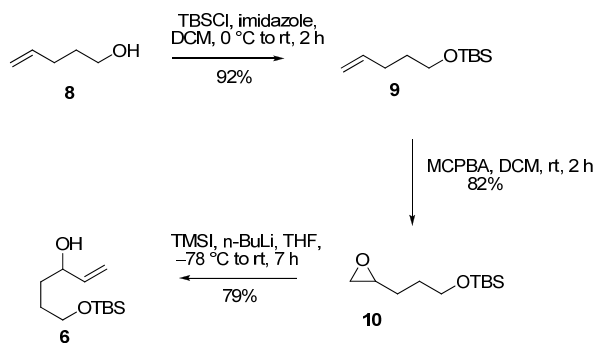
A detailed retrosynthetic planning for stagonolide B and its C(4)-epimer is given in the Figure 7. After the application of the RCM transform, the enantiomeric acids (*R*)-5 and (*S*)-5, and the alcohol 3 were identified as the key coupling partners for the synthesis of stagonolide B (1) and its C(4)-epimer (2). Easily available D-ribose has been selected as a starting point for the chiral pool synthesis of the known alcohol fragment 3. The synthesis of the enantiomeric acids (*R*)-5 and (*S*)-5 was planned through the enzymatic resolution of the allyl alcohol 6. A PMB protection on the allylic-OH of the acid coupling partners was selected as a safe handle to change

the steric nature of the adjacent functional groups that have been shown to influence the outcome of the RCM.

Synthesis of the acid fragment (*R*)-5

The advanced coupling fragments we identified for the synthesis of stagonolide B and its 4-*epimer* are enantiomeric acids (*R/S*)-5. As shown in Scheme 7, the synthesis started with the TBS protection of 4-pentene-1-ol (**8**) using TBSCl, imidazole in DCM to obtain **9**. Epoxidation of **9** using MCPBA in DCM followed by a one carbon extension of the resulting epoxide using trimethyl sulphonium iodide and *n*-BuLi in THF gave the key allyl alcohol **6** in good yields.⁴² In the ¹H NMR spectrum of **6**, the terminal olefinic protons were resonated at δ 5.07 as a ddd and the internal proton as a ddd at δ 5.85. A triplet in the ¹³C NMR spectrum at δ 114.2 ppm confirmed the presence of a *SP*² methylene carbon in the compound **6**. Other analytical data was in accordance with the assigned structure of compound **6**.

Scheme 7: Synthesis of epoxide **10**

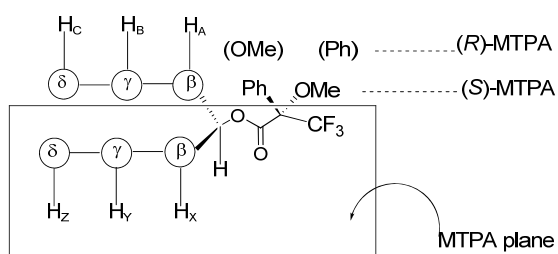


The enzymatic resolution of alcohol **6** was carried out using *Amano PS* in the presence of vinyl acetate in benzene:petether (1:3) at 40 °C.⁴³ The progress of the reaction was monitored carefully by thin layer chromatography and the reaction was stopped after 50% of *rac*-**6** was consumed. The resulting acetate **11** and the alcohol **6** were separated by simple column chromatography.

Modified Mosher's ester method for determining absolute stereochemistry⁴⁴

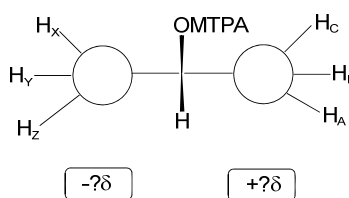
Determination of the absolute stereochemistry of organic compounds has become an important aspect in natural product synthesis. The limitations involved in physical methods such as exciton chirality method and X-ray crystallography forced synthetic chemists for a more reliable alternative. Although there are several chemical methods used to predict the absolute configuration of organic substances, Mosher's method using 2-methoxy-2-phenyl-2-(trifluoromethyl)acetic acid (MTPA) esters has been most frequently used. The modified Mosher's ester method (1H) is one of the simple and efficient ways to determine the absolute stereochemistry of the secondary alcohols and amine stereo centers in organic molecules. Mosher proposed that, in solution, the carbonyl proton, ester carbonyl and trifluoromethyl group of the MTPA moiety lie in the same plane (Figure 8).

Figure 8: MTPA plane of a MTPA ester



The plane and the conformation of MTPA group was called as the MTPA plane and ideal conformation respectively. In the MTPA plane, H_A, H_B, H_C...and H_X, H_Y, H_Z...are on the right and left sides of the plane respectively. Due to the diamagnetic effect of the benzene ring, the H_A, H_B, H_C... NMR signals of (R)-MTPA ester should appear upfield to those of the (S)-MTPA ester. The reverse should hold true for H_X, H_Y, H_Z.... Hence, the difference $\Delta\delta = (\delta_S - \delta_R) \times 1000$ should be positive for protons on the right side of the MTPA plane and the difference should be negative for those protons which were left side of the MTPA plane.

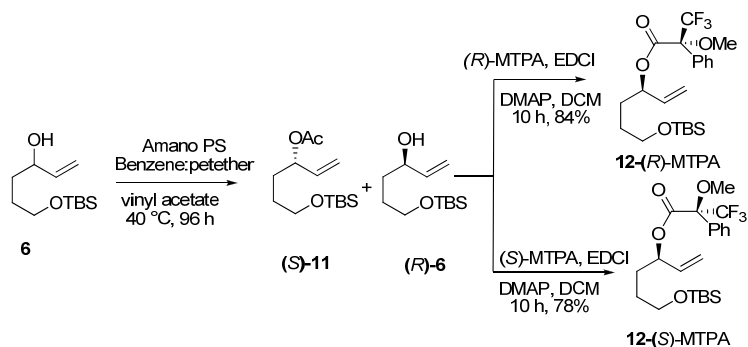
Figure 9: Model for determination of absolute stereochemistry



The Mosher's method can be summarized as follows:

- Assign as many proton signals as possible with respect to each of the (R) and (S) – MTPA esters.
- Obtain $\Delta\delta = (\delta_S - \delta_R) \times 1000$ values for all protons.
- Arrange the protons with positive $\Delta\delta$ values right side and those with negative $\Delta\delta$ values on the left side of the model.
- Once the molecule satisfies all the conditions, the stereochemistry of the model is the absolute stereochemistry of the compound in question.

Scheme 8: Synthesis of Moscher esters of alcohol (*R*)-6



Next, we proceeded to determine the absolute stereochemistry of alcohol **6** by employing the Mosher ester method and turned out to be (*R*). Thus, the free –OH of (*R*)-**6** was transformed to the corresponding (*R*)- and (*S*)-Moscher esters **12-(*R*)-MTPA** and **12-(*S*)-MTPA** in 84% and 78% yields (Scheme 8) by employing the standard protocols.⁴⁴ The ¹H NMR spectra of esters **12-(*R*)-MTPA** and **12-(*S*)-MTPA** were recorded and all possible protons were assigned (Table 1). The difference $\Delta\delta = (\delta_S - \delta_R) \times 1000$ was calculated and it was found that the molecule exactly fits the Mosher model of alcohol with an (*R*)-configuration, satisfying all the conditions (Figure 10).

Table 1: The assigned chemical shifts of H-C(1) – H-C(5)

	1	2	3	4	5
(<i>S</i>)-MTPA	5.23	5.72	1.76	1.49	3.57
(<i>R</i>)-MTPA	5.31	5.82	1.71	1.41	3.54
$\Delta\delta = (\delta_S - \delta_R) \times 1000$	-80	-100	+50	+80	+30

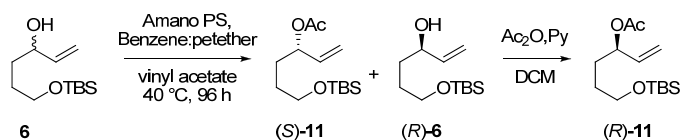
Figure 10: The absolute structure of alcohol **6**



The enantiomeric excess of the acetate **11** and alcohol (*R*)-**6** was obtained by GC analysis. The hydroxyl group of (*R*)-**6** was converted to acetate (*R*)-**11** using

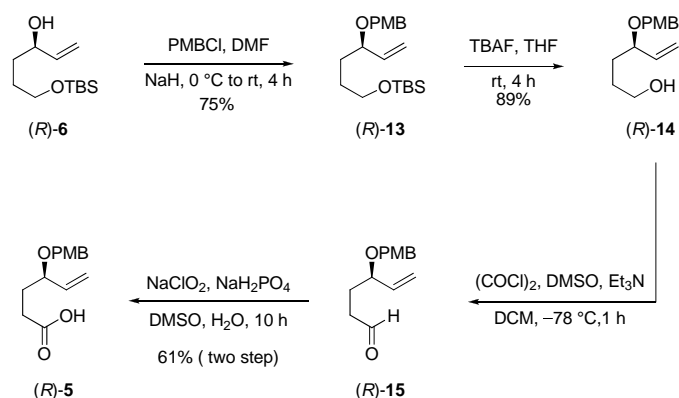
acetic anhydride and pyridine in DCM (Scheme 9). The GC analysis of (*R*)-**11** shows 82% *e.e* with retention time 25.47 min, whereas GC analysis of (*S*)-**11** showed 97% *e.e* with retention time (Rt) 25.39 min.

Scheme 9: Synthesis of acetate (*R*)-**11** and (*S*)-**11**



After ascertaining the absolute stereochemistry, protection of the hydroxyl group of (*R*)-**6** as its PMB ether was carried out by treating it with sodium hydride followed by PMB-Cl. Subsequently, the TBS-ether of (*R*)-**13** was removed using TBAF in THF at rt.⁴⁵ Oxidation of alcohol (*R*)-**14** under Swern conditions⁴⁶ (oxalyl chloride, DMSO and Et₃N in DCM at -78 °C) gave the aldehyde (*R*)-**15** which was further oxidized to the corresponding acid (*R*)-**5** by treating with NaClO₂ and NaH₂PO₄·H₂O in the presence of DMSO and H₂O.⁴⁷ The structure of acid (*R*)-**5** was confirmed by the spectral and analytical data. For example, in the IR spectrum of (*R*)-**5**, a band at 1710 cm⁻¹ corresponding to the -C=O stretching confirmed the presence of an acid group. Other analytical data such as the ¹H NMR and ESI-MS were in accordance with the proposed structure (Scheme 10).

Scheme 10: Synthesis of acid (*R*)-**5**

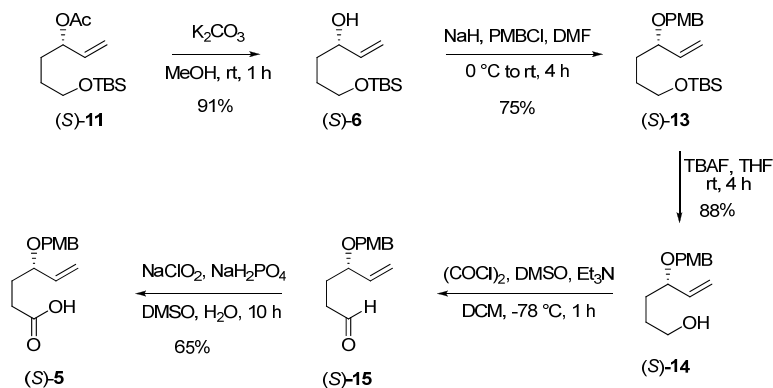


Synthesis of the acid fragment (*S*)-**5**

The synthesis started with the deacetylation of acetate (*S*)-**11** under standard Zemplén's conditions. The resulting alcohol (*S*)-**6** was then subjected for the same

sequence of reactions as used for the enantiomer (*R*)-**5** synthesis (Scheme 11) to procure acid (*S*)-**5**.

Scheme 11: Synthesis of acid (*S*)-5****



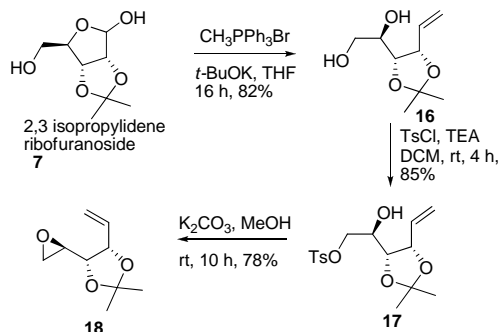
Synthesis of the alcohol fragment **3**

Considering the similar relative stereochemistry of the alcohol fragment **3** with that of D-ribose at C(2), C(3) and C(4), we have chosen ribose acetonide **7** as suitable starting material. The known ribose 2,3-acetonide **7** was prepared according to the reported procedure and subjected to one carbon Wittig homologation to afford the 1,2-diol **16**.⁴⁸ As the separation of the **16** from the side products of the Wittig reaction was found to be tedious, we have proceeded further for the tosylation of the primary hydroxyl of **16** by using tosyl chloride and triethyl amine in DCM at room temperature to afford the tosyl derivative **17** in 58% yield over two steps.

The formation of mono-tosyl compound was confirmed by spectral and analytical data. For instance, in the ¹H NMR spectrum of **17**, three sharp singlets at δ 1.28, 1.37 and 2.43 corresponding to the isopropylidene methyls and the methyl group attached with the sulfonyl aromatic ring appeared. Two separate doublets at δ 7.33 and 7.79 with a coupling constant 8 Hz are due to the *para*-disubstituted symmetric aromatic ring protons. Next, the epoxide **18** was prepared by treating tosylate **17** with potassium carbonate in methanol.⁴⁹ The volatile epoxide **18** was isolated in 78% yield as colourless oil. In the ¹H NMR spectrum of **18**, the epoxide methylene protons appeared at δ 2.66 (dd, $J = 2.5, 5.0$ Hz) and at 2.81 (dd, $J = 3.9, 5.0$ Hz). The internal methyne proton resonated at δ 2.94 (ddd, $J = 2.6, 3.9, 7.2$ Hz). Two singlets of the isopropylidene group observed at δ 1.36 and 1.50. The signals of the oxirane ring

carbons were found at relatively up field δ 45.7 (CH₂) and 49.7 (CH). Other peaks in both the spectra were in agreement with the assigned structure (Scheme 12).

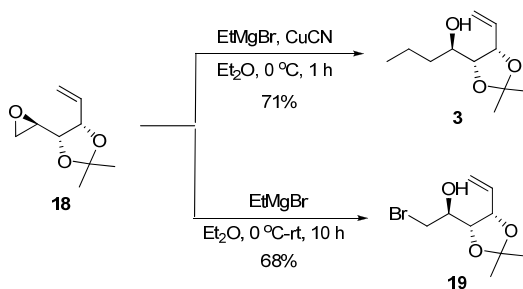
Scheme 12: Synthesis of epoxide **18**



Our next task was to open the epoxide with a two carbon Grignard reagent. Generally, the opening of an unsymmetric oxirane ring results from the less hindered side. Organolithium and copper reagents were used much more frequently. However, since Grignard reagents exist as an equilibrium mixture of RMgX, R₂Mg and MgX₂, all of which can react with epoxides, their reactions with substituted epoxides are complicated by various side reactions that often lead to a mixture of products. Considering above discussed difficulties, we have decided to use copper (I) cyanide. In addition to the overall efficiency of the epoxide opening reaction, use of copper cyanide forces the reaction in a desired fashion. Thus, the addition of the epoxide **18** to a suspension of alkyl cuprate prepared separately with EtMgBr and CuCN in ether afforded the crucial alcohol fragment **3** (Scheme 13).

The presence of a strong peak of highest m/z at 223.1 [M+Na]⁺, 239.1 [M+K]⁺ in the ESI mass spectrum of **3** and the presence of a triplet at δ 0.92 ($J = 6.9$ Hz) due to the terminal aliphatic methyl group in its ¹H NMR spectrum were a clear indication of ethyl incorporation. The terminal olefin protons of **3** appeared at δ 5.30 (br. d, $J = 10.3$ Hz) and 5.41 (br. d, $J = 17.2$ Hz). A fine ddd at δ 6.03 (ddd, $J = 7.7, 10.2, 17.2$ Hz) was due to the internal double bond proton. Corresponding signals of olefinic carbon were observed at δ 118.5 (CH₂) and 134.7 (CH) in the ¹³C NMR spectrum of compound **3**. All the observed data were superimposed with the reported data of the same intermediate used for total synthesis of herbarumin I, published by Fürstner.³⁶

Scheme 13: Synthesis of alcohol 3

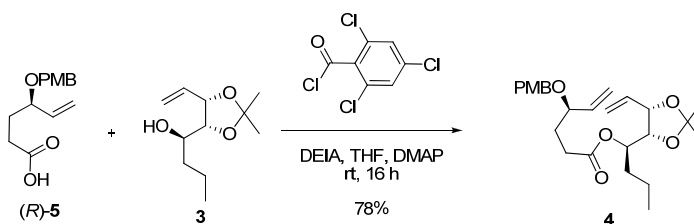


In absence of CuCN, the halohydrin **19** resulting from the involvement of bromide ion as a competing nucleophile, was isolated as the major product. The bromohydrin **19** was fully characterized with the help of spectral as well as analytical data.

Coupling of alcohol **3** and acid (*R*)-**5**

After completing the synthesis of crucial intermediates (*R*)-**5**, (*S*)-**5** and **3**, the next task was the execution of the key macrolide construction. Considering the simplicity of the acid fragment (*R*)-**5**, initially we tried the coupling with common activating reagent such as DCC and EDCI. With DCC and in the presence of DMAP, very low conversion (20%) was observed even after 3 days. Whereas, with EDCI, under standard conditions, the acid and alcohol were intact even after prolonged stirring. Next, we shifted to the Yamaguchi esterification method considering its wide spread application in the synthesis of highly functionalized esters and macrolactones under mild conditions.⁵⁰

Scheme 14: Synthesis of ester 4

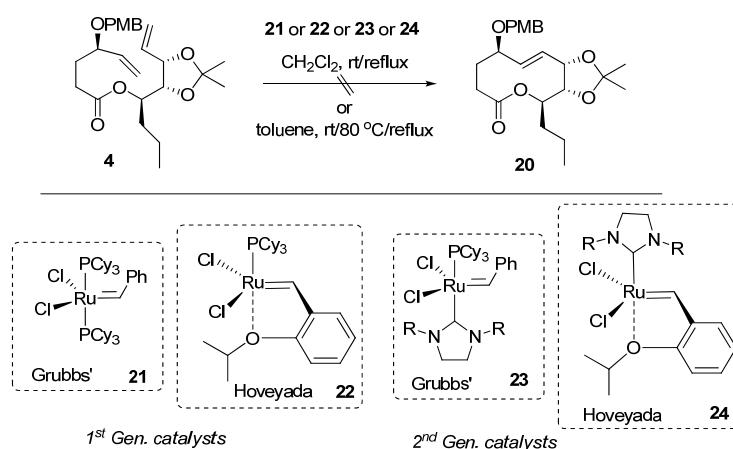


As prescribed, first the Yamaguchi reagent (2,4,6-trichlorobenzoyl chloride) was coupled with the carboxylic acid (*R*)-**5** in the presence of Hünig's base. After the formation of the intermediate mixed anhydride, the alcohol **3** and a stoichiometric

amount of DMAP were introduced and the contents were stirred at room temperature until the complete disappearance of the mixed anhydride. This afforded the desired diene-ester **4** in very good yields (Scheme 14). In the ^1H NMR spectrum of diene **4**, the characteristic four terminal olefinic protons appeared as multiplets ranging from δ 5.17–5.36 while the internal protons resonated at δ 5.75–5.84 as a multiplet. The acyloxy CH appeared at δ 4.91 (dt, $J = 4.0, 7.4$ Hz). The carbons of the terminal olefin methylenes, ester carbonyl carbons appeared in ^{13}C NMR at δ 117.6, 118.5 and 172.5 ppm respectively. All other protons and carbons in NMR spectra appeared with their respective chemical shifts, thereby confirming the structure of ester **4**. The structure of **4** was further supported by ESI-MS and elemental analysis.

The next critical step was the ring closing metathesis reaction of **4**. The compound **4** was subjected for ring closing metathesis in DCM and in toluene with Grubbs' 1st & 2nd generation catalysts and also with Hoveyda 1st & 2nd generation catalysts (**21–24**, Scheme 15) at different temperatures. However, these reactions resulted in the formation of complex product mixtures. To circumvent this problem, we have opted for the PMB deprotection which indeed was selected *a priori* as a safe handle. The PMB deprotection was carried out with DDQ to afford the diene ester **25**.

Scheme 15: The attempted RCM of **4** & the structures of the catalysts employed

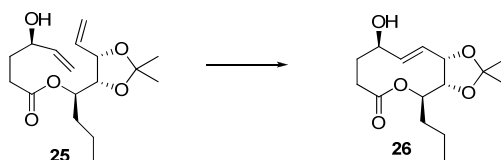


As the isopropylidene should be intact during the removal of PMB-ether, the use of acidic reagents such as AcOH, TFA, AlCl_3 , 1M HCl was not opted. The presence of diene functionality in the molecule has blocked the hydrogenation reaction conditions employing catalyst such as Pd, Pt, Raney nickel. Considering

these, the choice of reagents was restricted to either CAN or DDQ.³⁸ Gratifyingly, treatment of the compound **4** with DDQ in DCM:H₂O mixture gave **25** (Scheme 16). The structure of **25** was well supported by ¹H, ¹³C NMR and mass spectral analysis. For example, in the ¹H NMR spectrum, peaks corresponding to aromatic protons were absent. In the mass spectrum, the peaks corresponding to *m/z* 335.4 (100%)[M+Na]⁺, 351.4 (13.2%)[M+K]⁺ were observed.

After the selective PMB deprotection, the RCM of diene **25** was attempted under several conditions employing the available 1st and 2nd generation catalysts of Grubbs' and Hoyeda-Grubbs' in solvents such as dichloromethane, benzene and toluene either at rt or at reflux temperatures. In all the cases, the reactions resulted with the formation of untracable products mixture. In this disguise, when we switched to dichloroethane as a solvent,^{51,35e} and employed 2nd gen. Grubbs'/Hoyeda-Grubbs' catalysts in stoichiometric amounts. We could notice the molecular ion peaks corresponding to the product in the LCMS.

Table 2: Various conditions/catalysts employed for the RCM of diene **25**

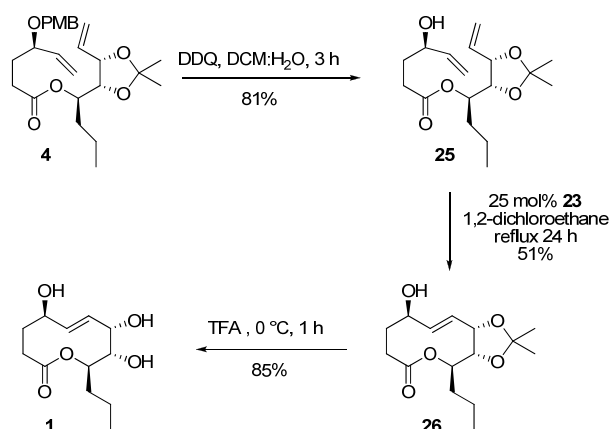


Entry	Catalyst	solvent	conditions	Yield (%)
1	23 (5 mol %)	toluene	80 °C, 8h	complex
2	24 (5 mol %)	DCM	Reflux, 8h	complex
3	23 (5 mol %)	benzene	Reflux, 8h	complex
4	23 and 24 (5 mol %)	DCE	Reflux, 8h	5-10%
5	23 (25 mol %)	DCE	Reflux, 24h	51%
6	23 (1 equiv)	DCE	Reflux, 72h	52%

After examining the various reaction parameters, the RCM of **25** could be conducted successfully using 25 mol% of 2nd gen. Grubbs' catalyst in dichloroethane at reflux temperatures (Scheme 16). The compound isolated was

found to be contaminated with the higher-oligomers, albeit showing the characteristic signals of the cyclization product. For example, the presence of *trans* double bond was evident from ^1H NMR, showing signals at δ 6.12 (ddd, $J = 1.4, 3.5, 16.1$ Hz) and 5.82 (ddd, $J = 2.1, 3.4, 16.1$ Hz). The large coupling constant 16.1 Hz is typical value for *trans* protons of C–C double bond. Presence of strong peak of highest m/z 307.1 (100%) $[\text{M}+\text{Na}]^+$ supported the structure of **26**.

Scheme 16: Total synthesis of stagonolide B



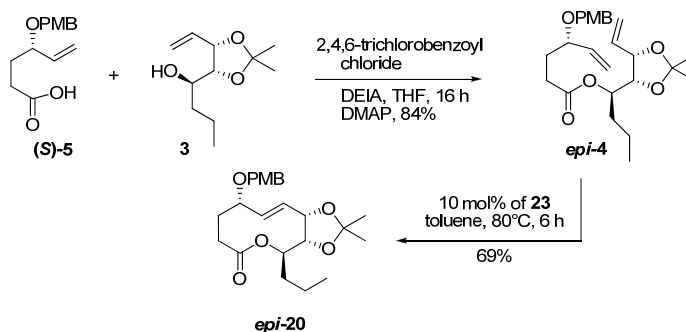
As the isolation of pure macrolide from the RCM reaction was found to be a tedious job, we have proceeded further for its deprotection to complete the synthesis of stagonolide B. The compound **26** was treated with TFA at 0 °C for 1h to afford the stagonolide B after chromatographic purification. The spectral and analytical data of **1** were in agreement with the data reported for natural stagonolide B. For instance, in the ^1H NMR spectrum, the C(12)-Me resonated as a triplet at δ 0.90 ($J = 7.4$ Hz). The C(5) olefin appeared at δ 5.63 (dt, $J = 2.7, 16.1$ Hz) whereas the C(6)-H resonated at δ 5.99 (dt, $J = 1.7, 16.1$ Hz). The br. singlet at δ 4.61 was assigned to the C(4)-H and the OMe br. singlet at δ 4.50 was assigned to the C(7)-H. The decoupling at δ 2.29 C(7)-H shows doublet of triplet ($J = 2.6, 4.6$ Hz). In the ^1H NMR spectrum, the clear doublet of a triplet at δ 4.94 ($J = 2.5, 9.6$ Hz) was due to the C(9) proton and after decoupling at δ 1.90 C(9) proton it become a triplet ($J = 9.5$ Hz). The D₂O experiment shows disappearance of br. singlet at δ 2.46 and br. doublet at δ 2.24 of C(7)-OH. Other resonances were fully in agreement with the assigned structure **1**. Specific rotation of the synthesized stagonolide B (**1**) was $[\alpha]_{\text{D}}^{25} = \text{Lit. } +27.1$ (c 0.9, CHCl₃)^{15a}

$[\alpha]_D^{25} = +20$ (0.1, CHCl_3) was similar in sign and magnitude to that of natural stagonolide B thus confirming the assigned absolute configuration.

Synthesis of 4-*epi*-stagonolide B

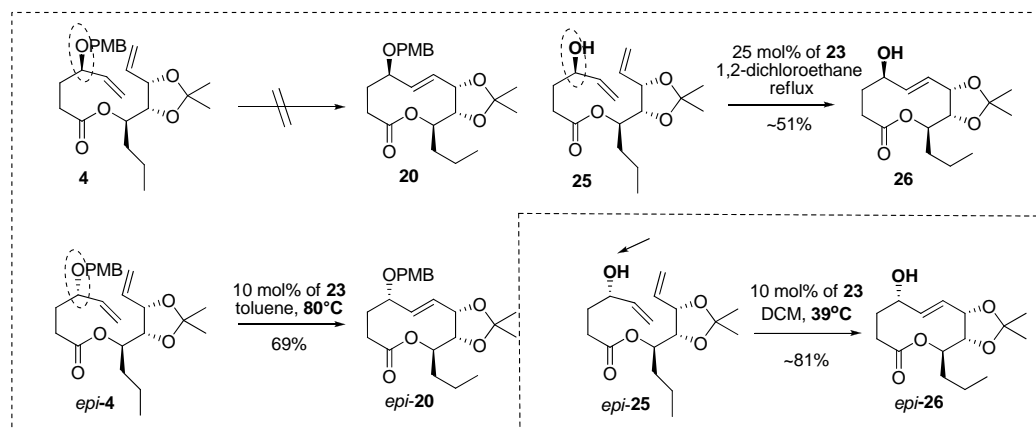
At the outset, to check the validity of our assumption, 4-*epi*-stagonolide B (**2**) has been synthesized by one of my colleague. In the initial strategy developed, the acid fragment (*S*)-**5** has been prepared by a different route employing a chiral pool approach. The diene *epi*-**4** was prepared by the coupling of (*S*)-**5** and the alcohol **3** (Scheme 17). The RCM of *epi*-**4** was found to be facile with Grubbs' 2nd generation catalyst in toluene at 80 °C and gave the desired *E*-isomer *epi*-**20** exclusively.

Scheme 17: Synthesis of ester compound **8**



The difference in the outcome of the RCM reaction with the dienes **4** and *epi*-**4** is as anticipated and supported our argument about the influence of the relative stereochemistry of the allylic hydroxyl groups on the outcome of the RCM. However, it was quite interesting to note that the ring closing metathesis of diene *epi*-**4** was not facile in CH_2Cl_2 or in toluene at room temperature. This, taken together with the fact that the RCM of diene **4** gave mainly oligomers under various conditions employed and that the RCM of the corresponding diene *epi*-**4** without the PMB protection resulted with the required RCM product in moderate yields, indicate that the steric bulk present on these hydroxy groups also influences the efficiency of the RCM. In this context we hypothesized that the RCM of the diene *epi*-**25** having a free hydroxyl and also the requisite *syn*-configuration should be even more facile when compared with the corresponding PMB-protected diene (Figure 11).

Figure 11: The compilation of the results of the RCM of various dienes prepared

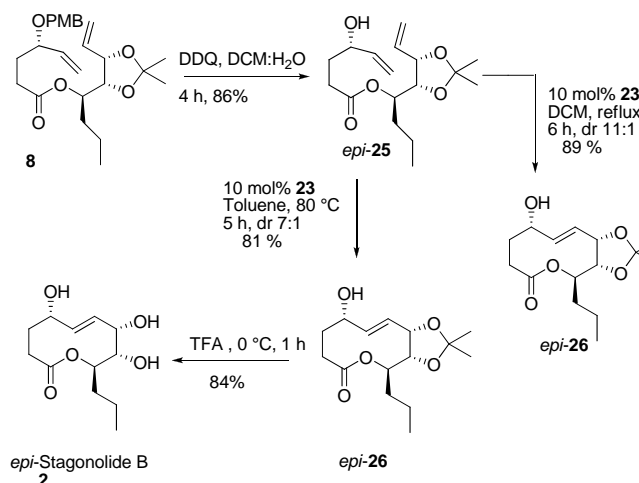


In order to probe in this direction, the diene *epi-4* has been prepared using the acid (*S*)-**5** (prepared by the present resolution protocol) and coupled with the alcohol **3** as described earlier. The spectral data of compound *epi-4* was in agreement with the data reported by my colleague. The compound *epi-4* was subjected for selective PMB deprotection to afford the requisite diene *epi-25*. The structure of *epi-25* was well supported by ^1H , ^{13}C NMR, and mass spectrum. In the ^1H NMR spectrum of compound *epi-25*, the characteristic two internal protons resonated at δ 5.18–5.26 as multiplet. The acyloxy CH proton appeared at δ 4.91 (dt, $J = 3.5, 7.6$ Hz). The carbon of the terminal olefin methylenes and ester carbonyl carbon appeared in the ^{13}C NMR spectrum at δ 115.1, 118.6 and 173.0 ppm respectively. The presence of a strong peak of highest m/z 335.2 (100%) [$\text{M}+\text{Na}$] $^+$ supported the structure of *epi-25*.

The RCM of *epi-25* could be carried out smoothly in dichloromethane at reflux temperature and *E/Z* noneolides *epi-26* were obtained in a 11:1 ratio. Carrying the reaction under conditions similar those for *epi-25* (toluene, 80 °C) resulted in an increase of *Z*-isomer 7:1 (Scheme 18). Presence of *trans* double bond in *epi-26* was evident from ^1H NMR, showing signals at δ 5.64 (ddd, $J = 1.7, 8.6, 15.9$ Hz) and 5.81 (dd, $J = 3.3, 15.9$ Hz). The large coupling constant 15.9 Hz is typical value for *trans* protons of C–C double bond. The acetonide methyl groups appeared at δ 1.36 and 1.54 as sharp singlet. The quaternary carbon of lactone resonated at δ 175.0 ppm in the ^{13}C NMR spectrum. Other observations were according to the assigned structure.

To achieve the synthesis of 4-*epi*-stagonolide B (**2**), the compound *epi*-**26** was treated with neat TFA for 1 h at 0 °C and compound **2** was obtained as crystalline solid in 85% isolated yield. The spectral data of compound **2** was in good agreement with the data reported earlier by my colleague.

Scheme 18: Synthesis of 4-*epi*-Stagonolide B **2**

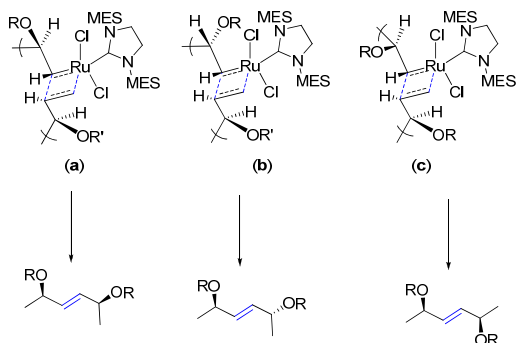


These results are indicative of the RCM rate acceleration by the co-operative OH-ruthenium interactions.

Discussion

First, the difference in the outcome of the RCM reaction with the dienes **4** and *epi*-**4** is quite striking. This could be due to the conformational constraints during the formation of the ruthenacyclobutane.^{36,37} We believe that the difficulties noticed in the construction of the stagonolide B and also in carbocycles especially the low yields obtained with the allyl alcohols leading to a 10-membered macrocycle with a 1,4-*trans*-diol configuration might be because of the steric hindrance which persists on both the faces during the formation of the ruthenacyclobutane (Figure 12b). For the formation of a macrocycle with a 1,4-*cis*-diol configuration (with *epi*-**4**), such steric crowding is absent as both these allylic groups lie on the same face (Figure 12a). Such a strain free transition state could also be obtained by a simple rotation around the C–C bond while the dimerization (Figure 12c) and this will be the serious competing reaction when the ring closure was sterically demanding.

Figure 12: The possible transition state structures of *trans*-ruthena-cyclobutane derivatives resulting macrolides with (a) 1,4-*cis*-diol, (b) 1,4-*trans*-diol macrolides and (c) self dimerization.



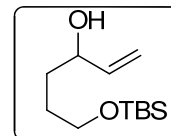
The feasibility of RCM with *epi*-**25** (where one of the allylic hydroxy groups is free) to some extent, could be explained by anticipating a co-operative O–H...Cl–Ru hydrogen bonding.^{52c} Acceleration of RCM reactions rates with free allylic hydroxyl groups is well documented.⁵³ It has been shown recently that such acceleration by an allylic–OH group was also regio-^{52a,b} and stereoselective^{52c}. This argument was further supported by the facile and more productive RCM of diene *epi*-**25** which occurred at 39 °C in DCM (the corresponding PMB ether required heating at 80 °C)

Conclusions

The first total synthesis of stagonolide B (**1**) confirming its absolute stereochemistry has been documented. A combination of the chiral pool approach and enzymatic resolution has been adopted to synthesize the key coupling partners. The 4-*epi*-stagonolide B (**2**) has also been synthesized to check the influence of the relative stereochemistry of allylic hydroxy groups and their protecting groups on the efficiency of the RCM and on the rate acceleration by the catalyst. Though these limited examples provide clues as to where the RCM could be a difficult proposition, a more comprehensive examination is needed with a broad range of substrates varying the stereochemistry of other centers and also without any conformational rigidity such as an acetonide protecting group. Work in this direction is progressing in our lab.

Experimental

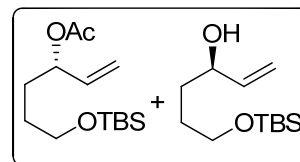
4-*O*-(*tert*-Butyldimethylsilyl)-hex-5-ene-1,4-diol (**6**)



A solution of trimethyl sulphonium iodide (7.5 g, 36.7 mmol) in THF (100 mL) was cooled to -78 °C and treated with *n*-BuLi (13.8 ml, 32.4 mmol) and stirred for 20 min. To this, a solution of **10** (2.0 g, 9.2 mmol) in THF (10 mL) was added slowly and stirred at -78 °C for 1 h and at rt for 6 h. The reaction mixture was partitioned between water and EtOAc. The aqueous phase was extracted with EtOAc. The combined organic phase was dried (Na_2SO_4), filtered and concentrated under reduced pressure. The purification of residue by silica gel column chromatography (5% ethyl acetate in petroleum ether) gave **6** (1.67 g, 79%) as colorless oil.

IR (CHCl_3) ν : 3370, 2930, 2858, 1472, 1256, 835 cm^{-1} . **^1H NMR** (200 MHz, CDCl_3): δ 0.04 (s, 6H), 0.88 (s, 9H), 1.57–1.67 (m, 4H), 2.77 (br. s, 1H), 3.63 (br. t, $J = 5.8$ Hz, 2H), 4.11 (dd, $J = 5.8, 11.0$ Hz, 1H), 5.06 (ddd, $J = 1.2, 1.7, 10.4$ Hz, 1H), 5.21 (dt, $J = 1.6, 17.2$ Hz, 1H), 5.85 (ddd, $J = 5.9, 10.4, 17.2$ Hz, 1H). **^{13}C NMR** (50 MHz, CDCl_3): δ -5.4 (q), 18.3 (s), 25.9 (q), 28.7 (t), 34.3 (t), 63.3 (t), 72.6 (d), 114.2 (t), 141.2 (d) ppm. **ESI-MS** m/z : 231.4 (42.8%, $[\text{M}+\text{H}]^+$), 253.4 (100%, $[\text{M}+\text{Na}]^+$), 269.4 (28.6%, $[\text{M}+\text{K}]^+$). **Anal. Calcd for $\text{C}_{12}\text{H}_{26}\text{O}_2\text{Si}$** : C, 62.55; H, 11.37; Found: C, 62.41; H, 11.66%.

Amino PS mediated resolution of *rac*-**6**



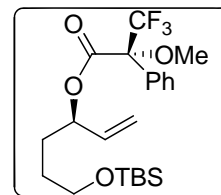
A suspension of *rac*-**6** (2.2 g, 9.5 mmol), *Amino PS* (600 mg) and vinyl acetate (4.4 mL, 47.8 mmol) in benzene-petroleum ether (50 mL, 1:2) was heated at 40 °C for 96 h. The contents were filtered and the filtrate was concentrated under reduced pressure. The residue was purified by silica gel column chromatography (2→5% ethyl acetate in petroleum ether) to afford alcohol (*R*)-**6** (0.9 g, 41 %) and acetate (*S*)-**11** (1.1 g, 42%) as colorless oils.

(4R)-4-O-(tert-Butyldimethylsilyl)-hex-5-ene-1,4-diol [(R)-6]: $[\alpha]_D^{25} = -1.9$ (c 1.0, CHCl₃). **IR (CHCl₃)** v: 3370, 2930, 2858, 1472, 1256, 835 cm⁻¹. **¹H NMR (200 MHz, CDCl₃):** δ 0.04 (s, 6H), 0.88 (s, 9H), 1.57–1.67 (m, 4H), 2.77 (br. s, 1H), 3.63 (t, *J* = 5.8 Hz, 2H), 4.11 (br. q, *J* = 5.7 Hz, 1H), 5.06 (ddd, *J* = 1.3, 1.6, 10.3 Hz, 1H), 5.21 (dt, *J* = 1.5, 3.1, 17.2 Hz, 1H), 5.85 (ddd, *J* = 5.8, 10.3, 17.3 Hz, 1H). **¹³C NMR (50 MHz, CDCl₃):** δ -5.4 (q), 18.3 (s), 25.9 (q), 28.7 (t), 34.3 (t), 63.3 (t), 72.6 (d), 114.2 (t), 141.2 (d) ppm. **ESI-MS *m/z*:** 231.4 (42.8%, [M+H]⁺), 253.4 (100%, [M+Na]⁺), 269.4 (28.6%, [M+K]⁺). **Anal. Calcd for C₁₂H₂₆O₂Si:** C, 62.55; H, 11.37; Found: C, 62.67; H, 11.53%.

(4S)-1-O-Acetyl-4-O-(tert-butyldimethylsilyl)-hex-5-ene-1,4-diol [(S)-11]: Rt = 25.47 (Flow rate: 1.1073 ml/min, 60 °C/10 min, 5 °C/min → 80 °C the 10 °C/min → 140 °C and 10 °C/min → 220 °C/5 min). $[\alpha]_D^{25} = -6.0$ (c 1.0, CHCl₃). **IR (CHCl₃)** v: 2955, 2858, 1742, 1560, 1473, 1248, 1100, 835 cm⁻¹. **¹H NMR (200 MHz, CDCl₃):** δ 0.03 (s, 6H), 0.87 (s, 9H), 1.44–1.72 (m, 4H), 2.05 (s, 3H), 3.60 (t, *J* = 6.2 Hz, 2H), 5.12–5.28 (m, 1H), 5.79 (ddd, *J* = 6.2, 10.4, 17.4 Hz, 1H). **¹³C NMR (50 MHz, CDCl₃):** δ -5.5 (q), 18.3 (s), 21.2 (q), 25.9 (q), 28.3 (t), 30.5 (t), 62.2 (t), 74.5 (d), 116.6 (t), 136.5 (d), 170.3 (s) ppm. **ESI-MS *m/z*:** 295.3 (100%, [M+Na]⁺). **Anal. Calcd for C₁₄H₂₈O₃Si:** C, 61.72; H, 10.36; Found: C, 61.64; H, 10.19%.

(R)-11: Rt = 25.40 (Flow rate: 1.1073 ml/min, 60 °C/10 min, 5 °C/min → 80 °C the 10 °C/min → 140 °C and 10 °C/min → 220 °C/5 min). $[\alpha]_D^{25} = +5.2$ (c 1.0, CHCl₃). **Anal. Calcd for C₁₄H₂₈O₃Si:** C, 61.72; H, 10.36; Found: C, 61.84; H, 10.19%.

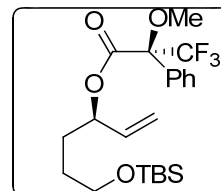
Preparation of 12-(R)-MTPA



To a solution of alcohol **(R)-6** (25 mg, 0.1 mmol) in dry CH₂Cl₂ (5 mL) was added **R-(+)-MTPA** (26 mg, 0.1 mmol) and the reaction mixture was cooled to 0 °C. To this, EDCI (31 mg, 0.16 mmol) was added in one portion followed by catalytic amount of DMAP (5 mg) and stirred at rt. for 10 h. The reaction mixture was quenched with ice and the organic phase was separated, washed with water (2 X 5 mL), brine (5 mL), dried over Na₂SO₄, filtered and concentrated. The residue obtained was purified by column chromatography (2→5% ethyl acetate in petroleum ether) to afford ester **12-(R)-MTPA** (40 mg, 82%) as colorless oil.

¹H NMR (200 MHz, CDCl₃): δ 0.01 (s, 6H), 0.86 (s, 9H), 1.33–1.50 (m, 2H), 1.66–1.77 (m, 2H), 3.51–3.60 (m, 5H), 5.26 (ddd, *J* = 0.8, 1.3, 10.2 Hz, 1H), 5.35 (br. tt, *J* = 1.1, 17.2 Hz, 1H), 5.48 (q, *J* = 6.8 Hz, 1H), 5.82 (ddd, *J* = 7.1, 10.4, 17.3 Hz, 1H), 7.36–7.41 (m, 3H), 7.49–7.54 (m, 2H).

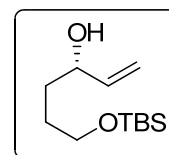
Synthesis of 12-(*S*)-MTPA



To a solution of alcohol (*R*)-**6** (25 mg, 0.1 mmol) in dry CH₂Cl₂ (5 mL) was added (*S*)-(-)-MTPA (26 mg, 0.1 mmol) and the reaction mixture was cooled to 0 °C. To this, EDCI (31 mg, 0.16 mmol) was added in one portion followed by catalytic amount of DMAP (5 mg) and stirred at rt. for 10 h. The reaction mixture was quenched with ice and the organic phase was separated, washed with water (2 X 5 mL), brine (5 mL), dried over Na₂SO₄, filtered and concentrated. The residue obtained was purified by column chromatography (2→5% ethyl acetate in petroleum ether) to afford ester **12-(*S*)-MTPA** (38 mg, 78%) as colorless oil.

¹H NMR (200 MHz, CDCl₃): δ 0.02 (s, 6H), 0.87 (s, 9H), 1.40–1.58 (m, 2H), 1.69–1.83 (m, 2H), 3.53–3.63 (m, 5H), 5.16–5.40 (m, 2H), 5.42–5.43 (m, 1H), 5.82 (ddd, *J* = 3.5, 7.4, 10.4 Hz, 1H), 7.32–7.41 (m, 3H), 7.48–7.53 (m, 2H).

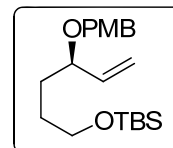
(4*S*)-4-*O*-(*tert*-Butyldimethylsilyl)-hex-5-ene-1,4-diol [(*S*)-**6**]



To a solution of (*S*)-**11** (2 g, 7.3 mmol) in methanol (20 mL) was added K₂CO₃ (2 g, 14.7 mmol) and reaction mixture stirred at rt for 1 h and filtered and the filtrate was concentrated under reduced pressure. The residue was purified by silica gel column chromatography (2→5% ethyl acetate in petroleum ether) to afford alcohol (*S*)-**6** (1.5 g, 91%) as colorless oil.

[α]_D²⁵ = +1.8 (*c* 1, CHCl₃); **Anal. Calcd for C₁₂H₂₆O₂Si:** C, 62.55; H, 11.37; Found: C, 62.70; H, 11.41%.

(4*R*)-1-*O*-(4-Methoxybenzyl)-4-*O*-(*tert*-butyldimethylsilyl)-hex-5-ene-1,4-diol [(*R*)-13]

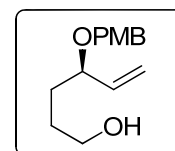


To a cooled solution of (*R*)-6 (3.4 g, 14.7 mmol) in anhydrous DMF (35 mL), NaH (60% dispersion in mineral oil, 620 mg, 15.5 mmol) was added slowly and stirred for 5 min. Then PMB-Cl (2.2 mL, 16.2 mmol) was added and continued at room temperature for 4 h. The reaction mixture was partitioned between water and EtOAc and the aqueous layer was extracted with EtOAc. The combined organic layer was dried (Na₂SO₄) and concentrated under reduced pressure. The purification of residue by silica gel column chromatography (1→ 3% ethyl acetate in petroleum ether) to afford (*R*)-13 (3.82 g, 75%) as colorless oil.

$[\alpha]_D^{25} = +13.4$ (*c* 0.7, CHCl₃). **IR (CHCl₃)** ν : 2954, 2857, 1613, 1514, 1250, 1097, 835 cm⁻¹. **¹H NMR (200 MHz, CDCl₃)**: δ 0.03 (s, 6H), 0.89 (s, 9H), 1.50–1.68 (m, 4H), 3.59 (br. t, *J* = 5.8 Hz, 2H), 3.67–3.77 (m, 1H), 3.79 (s, 3H), 4.28 (d, *J* = 11.5 Hz, 1H), 4.53 (d, *J* = 11.5 Hz, 1H), 5.19 (br. ddd, *J* = 0.8, 1.9, 16.2 Hz, 1H), 5.22 (br. ddd, *J* = 0.7, 1.9, 11.2 Hz, 1H), 5.65 (br. ddd, *J* = 7.6, 11.2, 16.2 Hz, 1H), 6.86 (br. d, *J* = 8.6 Hz, 2H), 7.25 (br. d, *J* = 8.6 Hz, 2H). **¹³C NMR (50 MHz, CDCl₃)**: δ -5.35 (q), 18.3 (s), 25.9 (q), 28.6 (t), 31.8 (t), 55.1 (q), 63.0 (t), 69.6 (t), 80.0 (d), 113.7 (d), 116.9 (t), 129.2 (d), 130.8 (s), 139.2 (d), 159.0 (s) ppm. **ESI-MS *m/z***: 351.0 (100%, [M+H]⁺). **Anal. Calcd for C₂₀H₃₄O₃Si**: C, 68.52; H, 9.78; Found: C, 68.61; H, 9.88%.

(*S*)-13: $[\alpha]_D^{25} = -17.5$ (*c* 1, CHCl₃); **Anal. Calcd for C₂₀H₃₄O₃Si**: C, 68.52; H, 9.78; Found: C, 68.19; H, 9.92%.

(4*R*)-1-*O*-(4-Methoxybenzyl)-hex-5-ene-1,4-diol [(*R*)-14]



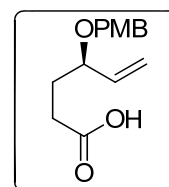
To a cooled solution of (*R*)-13 (3.0 g, 8.5 mmol) in dry THF (40 mL) was added TBAF (2.68 g, 10.2 mmol) and stirred at rt for 4 h. The reaction mixture was partitioned in sat. ammonium chloride and ethyl acetate and the aqueous layer was extracted with ethyl acetate. The combined extracts were dried (Na₂SO₄) and concentrated under reduced pressure. The purification of residue by silica gel column

chromatography (25% ethyl acetate in petroleum ether) gave (*R*)-**14** (1.80 g, 89% yield) as a colorless oil.

$[\alpha]_D^{25} = +19.4$ (*c* 0.9, CHCl₃). IR (CHCl₃) ν : 3020, 2928, 2855, 1612, 1514, 1215, 1035, 758 cm⁻¹. ¹H NMR (200 MHz, CDCl₃): δ 1.59–1.67 (m, 4H), 1.96 (br. s, 1H), 3.57–3.63 (m, 2H), 3.71–3.79 (m, 4H), 4.27 (d, *J* = 11.4 Hz, 1H), 4.53 (d, *J* = 11.4 Hz, 1H), 5.21 (br. ddd, *J* = 0.9, 1.8, 16.2 Hz, 1H), 5.23 (br. ddd, *J* = 0.7, 1.8, 11.3 Hz, 1H), 5.76–5.83 (m, 1H), 6.86 (br. d, *J* = 8.6 Hz, 2H), 7.25 (br. d, *J* = 8.6 Hz, 2H). ¹³C NMR (50 MHz, CDCl₃): δ 28.8 (t), 32.3 (t), 55.2 (q), 62.8 (t), 69.8 (t), 80.1 (d), 113.8 (d), 117.2 (t), 129.4 (d), 130.4 (s), 138.7 (d), 159.1 (s) ppm. ESI-MS *m/z*: 237.4 (8.3%, [M+H]⁺), 259.4 (100%, [M+Na]⁺), 275.4 (20.8%, [M+K]⁺). Anal. Calcd for C₁₄H₂₀O₃: C, 71.16; H, 8.53; Found: C, 70.9; H, 8.69%.

(*S*)-**14**: $[\alpha]_D^{25} = -23.6$ (*c* 1, CHCl₃); Anal. Calcd for C₁₄H₂₀O₃: C, 71.16; H, 8.53; Found: C, 71.02; H, 8.73%.

(4*R*)-4-(4-Methoxybenzyloxy)hex-5-enoic acid [(*R*)-5**]**



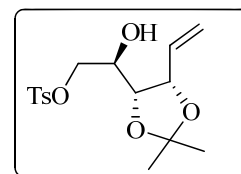
At -78 °C, a solution of DMSO (1.8 mL, 25.4 mmol) in CH₂Cl₂ (30 mL) was treated with oxalyl chloride (1.9 mL, 21.1 mmol) and stirred for 20 min. To this, alcohol (*R*)-**14** (2.0 g, 8.4 mmol) was added slowly and stirring was continued at -78 °C for another 1 h. To this, triethyl amine (6 mL, 43 mmol) was added and the contents were allowed to warm to rt. The reaction mixture was poured into aqueous NH₄Cl (10 mL) and extracted with EtOAc. The combined organic layer was washed with water (20 mL), dried (Na₂SO₄) and concentrated under reduced pressure and the resulting crude aldehyde was used directly for next step.

To a cooled solution of above aldehyde (1.8 g) in DMSO (10 mL) and aq. NaH₂PO₄·2H₂O (0.8 g in 5 mL water) a solution of sodium chlorite (1.8 g, 19.8 mmol) in water (10 mL) was introduced slowly and the resulting mixture was stirred at rt for 10 h. The reaction mixture was diluted with water and extracted with ethyl acetate. The organic extract was dried (Na₂SO₄) and concentrated. The crude product was purified by silica gel column chromatography (25→30% ethyl acetate in petroleum ether) to obtain acid (*R*)-**5** (1.28 g, 61%) as colorless oil.

(R)-5: $[\alpha]_D^{25} = +23.2$ (*c* 1.0, CHCl₃). IR (CHCl₃) ν : 3076, 1710, 1612, 1514, 1422, 1249, 1035, 910, 734 cm⁻¹. ¹H NMR (200 MHz, CDCl₃): δ 1.81–1.94 (m, 2H), 2.43 (br. dd, *J* = 7.1 Hz, 2H), 3.73–3.83 (m, 4H), 4.27 (d, *J* = 11.4 Hz, 1H), 4.53 (d, *J* = 11.4 Hz, 1H), 5.26 (br. ddd, *J* = 0.7, 1.8, 10.9 Hz, 1H), 5.25 (br. ddd, *J* = 0.9, 1.8, 16.6 Hz, 1H), 5.65–5.82 (m, 1H), 6.6 (br. d, *J* = 8.7 Hz, 2H), 7.25 (br. d, *J* = 8.7 Hz, 2H). ¹³C NMR (50 MHz, CDCl₃): δ 30.1 (t), 30.1 (t), 55.2 (q), 69.8 (t), 78.8 (d), 113.7 (d), 117.8 (t), 129.4 (d), 130.3 (s), 138.1 (d), 159.1 (s), 179.2 (s) ppm. ESI-MS *m/z*: 273.2 (100%, [M+Na]⁺), 289.2 (12.4%, [M+K]⁺). Anal. Calcd for C₁₄H₁₈O₄: C, 67.18; H, 7.25; Found: C, 67.55; H, 7.32.

(S)-5: $[\alpha]_D^{25} = -27.4$ (*c* 1.0, CHCl₃). Anal. Calcd for C₁₄H₁₈O₄: C, 67.18; H, 7.25; Found: C, 67.83; H, 7.12%.

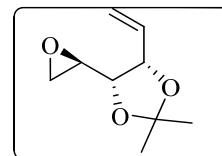
1,2-Dideoxy-2,3-*O*-isopropylidene-5-*O*-(*p*-tolunesulfonyl)-*D*-ribo-hex-1-enitol (17)



A solution of diol **16** (10.0 g, 53.2 mmol) in dry CH₂Cl₂ (150 mL) was cooled to 0 °C and treated with TsCl (10.25 g, 53.7 mmol) followed by TEA (22.3 mL, 161 mmol) and stirred at rt for 4 h. Then reaction mixture was partitioned between water and CH₂Cl₂ and the aqueous layer was extracted with CH₂Cl₂. The combined organic layer was washed with water, dried (Na₂SO₄) and concentrated under reduced pressure. The crude product was purified by column chromatography (25% ethyl acetate in petroleum ether) to afford **17** (15.46 g, 85%) as pale yellow oil.

$[\alpha]_D^{25} = 25.5$ (*c* 1.1, CHCl₃). ¹H NMR (200 MHz, CDCl₃): δ 1.28 (s, 3H), 1.37 (s, 3H), 2.38 (br. s, 1H), 2.43 (s, 3H), 3.76–3.87 (m, 1H), 3.97 (dd, *J* = 6.1, 8.8 Hz, 1H), 4.05 (dd, *J* = 6.6, 10.3 Hz, 1H), 4.28 (dd, *J* = 2.2, 10.3 Hz, 1H), 4.66 (br. tt, *J* = 1.2, 6.3 Hz, 1H), 5.25 (dt, *J* = 1.2, 10.4 Hz, 1H), 5.40 (dt, *J* = 1.4, 17.2 Hz, 1H), 5.91 (ddd, *J* = 6.6, 10.4, 17.2 Hz, 1H), 7.33 (br. d, *J* = 8.3 Hz, 2H), 7.79 (br. d, *J* = 8.3 Hz, 2H). ¹³C NMR (100 MHz, CDCl₃): δ 21.5 (q), 25.1 (q), 27.4 (q), 68.0 (d), 72.2 (t), 76.9 (d), 78.1 (d), 109.0 (s), 118.1 (t), 127.9 (d), 129.8 (d), 132.5 (s), 133.0 (d), 144.9 (s) ppm. Anal. Calcd for C₁₆H₂₂O₆S: C, 56.12; H, 6.48; Found: C, 55.89 ; H, 6.51%.

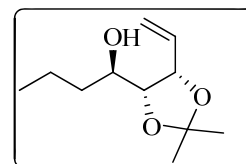
1,2-Dideoxy-2,3-*O*-isopropylidene-4,5-anhydro-D-ribo-hex-1-enitol (18**)**



To a solution of **17** (8.52 g, 24.9 mmol) in methanol (75 mL), solid K_2CO_3 (10.32 g, 74.7 mmol) was added at rt and stirred for 10 h. The solids were removed by filtration. The filtrate was diluted with water and extracted with diethyl ether (3x75 mL). The combined organic extract was washed with water, dried (Na_2SO_4) and concentrated at reduced pressure. The residue thus obtained was purified by column chromatography to afford **18** (3.30 g) as light oil in 78% yield.

$[\alpha]_D^{25}$: +18.8 (*c* 1, $CHCl_3$). IR ($CHCl_3$) ν : 2991, 2930, 1601, 1383, 1253, 1217, 1042, 872 cm^{-1} . 1H NMR (200 MHz, $CDCl_3$): δ 1.36 (s, 3H), 1.50 (s, 3H), 2.66 (dd, $J = 2.5, 5.0$ Hz, 1H), 2.81 (dd, $J = 3.9, 5.0$ Hz, 1H), 2.94 (ddd, $J = 2.6, 3.9, 7.2$ Hz, 1H), 3.74 (dd, $J = 6.5, 7.2$ Hz, 1H), 4.72 (tt, $J = 1.0, 6.7$ Hz, 1H), 5.34 (ddd, $J = 1.0, 1.6, 10.4$ Hz, 1H), 5.46 (br. dt, $J = 1.4, 1.6, 17.1$ Hz, 1H), 5.98 (ddd, $J = 6.8, 10.4, 17.1$ Hz, 1H). ^{13}C NMR (50 MHz, $CDCl_3$): δ 25.1 (q), 27.6 (q), 45.7 (d), 49.7 (d), 78.6 (d), 78.9 (d), 109. (s), 118.8 (t), 132.4 (d) ppm. Anal. Calcd for $C_9H_{14}O_3$: C, 63.51; H, 8.29; Found: C, 63.35; H, 8.18%.

(3*S*,4*R*,5*S*)-3,4-*O*-Isopropylidene-oct-1-ene-3,4,5-triol (3**)**

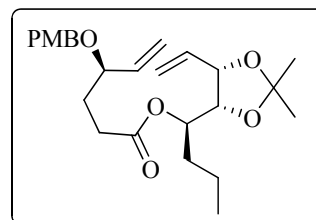


At 0 °C, a suspension of CuCN (1.64 g, 18.2 mmol) in dry ether (10 mL) was treated with a solution of EtMgBr [prepared from Mg (1.85 g, 76 mmol) and ethyl bromide (3.42 mL, 45.6 mmol)] in ether (30 mL) was added slowly and the contents were stirred at 0 °C for 20 min. To this, a solution of the epoxide **18** (2.59 g, 15.2 mmol) in ether (10 mL) was introduced and the mixture was stirred for another 1 h at 0 °C. The reaction mixture was quenched with cold water and extracted with ethyl acetate. The combined organic extract was dried (Na_2SO_4), concentrated and the resulting crude material was purified by column chromatography to afford alcohol **3** (2.1 g, 71%) as colorless oil.

$[\alpha]_D^{25}$ = +9.9 (*c* 1.3, $CHCl_3$). IR ($CHCl_3$) ν : 3437, 2987, 2959, 2936, 2874, 1458, 1428, 1381, 1253, 1217, 1168, 1099, 1067, 1033, 874 cm^{-1} . 1H NMR (200 MHz, $CDCl_3$): δ 0.92 (t, $J = 6.9$ Hz, 3H), 1.31–1.72 (m, 4H), 1.35 (s, 3H), 1.46 (s, 3H), 3.66 (br. t, $J = 8.5$ Hz, 1H), 3.96

(dd, $J = 6.5, 8.2$ Hz, 1H), 4.63 (br. t, $J = 6.9$ Hz, 1H), 5.30 (br. d, $J = 10.3$ Hz, 1H), 5.41 (br. d, $J = 17.2$ Hz, 1H), 6.03 (ddd, $J = 7.7, 10.2, 17.2$ Hz, 1H). ^{13}C NMR (50 MHz, CDCl_3): δ 14.0 (q), 18.3 (t), 25.3 (q), 27.8 (q), 35.8 (t), 69.7 (d), 78.9 (d), 80.7 (d), 108.6 (s), 118.5 (t), 134.7 (d) ppm. **Anal. Calcd for $\text{C}_{11}\text{H}_{20}\text{O}_3$** : C, 65.97; H, 10.07; Found: C, 65.83; H, 9.84%.

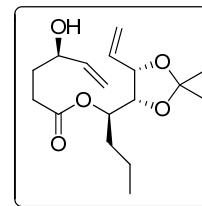
Preparation of Diene 4



To a solution of acid (*R*)-**5** (500 mg, 2.0 mmol) in dry THF (10 mL) were added 2,4,6-trichlorobenzoyl chloride (0.37 mL, 2.4 mmol) and *N,N*-diisopropyl ethyl amine (2.0 mL, 11.5 mmol) and the contents were stirred for 2 h at ambient temperature. After completion of mixed anhydride formation as indicated by TLC, DMAP (500 mg, 4 mmol) and a solution of alcohol **3** (400 mg, 2.0 mmol) in THF (2 mL) were added and the reaction mixture was stirred for 16 h at rt. The reaction was quenched with water and extracted with ethyl acetate. The combined organic phase was washed with saturated NaHCO_3 solution, water, dried (Na_2SO_4) and evaporated under reduced pressure. The crude product was purified by silica gel column chromatography (8→10% EtOAc in petroleum ether) to afford the diene **4** (673 mg, 78%) as light yellow oil.

$[\alpha]_{\text{D}}^{25} = +9.6$ (c 1.0, CHCl_3). **IR** (CHCl_3) ν : 2961, 2935, 2873, 1735, 1613, 1514, 1465, 1249, 910 cm^{-1} . ^1H NMR (200 MHz, CDCl_3): δ 0.88 (t, $J = 7.3$ Hz, 3H), 1.20–1.34 (m, 2H), 1.36 (s, 3H), 1.48 (s, 3H), 1.55–1.67 (m, 2H), 1.79–1.91 (m, 2H), 2.32 (d, $J = 8.4$ Hz, 1H), 2.36 (dd, $J = 0.9, 8.8$ Hz, 1H), 3.70–3.80 (m, 4H), 4.16 (dd, $J = 6.5, 7.4$ Hz, 1H), 4.25 (d, $J = 11.3$ Hz, 1H), 4.52 (d, $J = 11.3$ Hz, 1H), 4.60 (ddt, $J = 0.9, 6.4, 7.8$ Hz, 1H), 4.91 (dt, $J = 4.0, 7.4$ Hz, 1H), 5.17–5.36 (m, 4H), 5.64–5.74 (m, 1H), 5.75–5.84 (m, 1H), 6.88 (br. d, $J = 8.6$ Hz, 2H), 7.24 (br. d, $J = 8.6$ Hz, 2H). ^{13}C NMR (50 MHz, CDCl_3): δ 14.0 (q), 17.9 (t), 25.2 (q), 27.5 (q), 30.3 (t), 33.3 (t), 55.2 (q), 69.8 (t), 71.6 (d), 78.4 (d), 78.8 (d), 79.0 (d), 108.7 (s), 113.7 (2C, d), 117.6 (t), 118.5 (t), 129.3 (d), 130.5 (s), 133.2 (d), 138.3 (d), 159.1 (s), 172.5 (s) ppm. ESI-MS m/z : 455.6 (100%, $[\text{M}+\text{Na}]^+$), 471.5 (18.5%, $[\text{M}+\text{K}]^+$). **Anal. Calcd for $\text{C}_{25}\text{H}_{36}\text{O}_6$** : C, 69.42; H, 8.39; Found: C, 69.31; H, 8.42%.

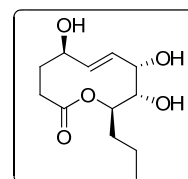
Synthesis of Compound 25



A suspension of **4** (400 mg, 0.9 mmol) and DDQ (600 mg, 2.6 mmol) in CH₂Cl₂:H₂O (50 mL, 18:1) was stirred for 3 h at rt. The reaction mixture was quenched with aqueous Na₂CO₃ solution and partitioned between water and CH₂Cl₂. The aqueous layer was extracted with CH₂Cl₂ and the combined organic layer was dried (Na₂SO₄) and concentrated. The residue was purified by silica gel chromatography (25% EtOAc in petroleum ether) to afford **25** (233 mg, 81%) as colourless oil.

$[\alpha]_D^{25} = +29.4$ (*c* 1.0, CHCl₃). **IR** (CHCl₃) *v*: 3453, 2962, 2875, 1732, 1645, 1382, 1217, 1066, 929 cm⁻¹. **¹H NMR** (200 MHz, CDCl₃): δ 0.88 (t, *J* = 7.3 Hz, 3H), 1.18–1.31 (m, 2H), 1.35 (br. s, 3H), 1.46 (br. s, 3H), 1.56–1.71 (m, 2H), 1.74–1.94 (m, 2H), 2.39 (br. dd, *J* = 2.7, 7.3 Hz, 1H), 2.35 (br. dd, *J* = 1.5, 7.3 Hz, 1H), 4.15 (d, *J* = 6.6 Hz, 1H), 4.19 (d, *J* = 6.6 Hz, 1H), 4.59 (ddt, *J* = 1.0, 6.6, 7.4 Hz, 1H), 4.91 (dt, *J* = 4.0, 7.3 Hz, 1H), 5.13 (dt, *J* = 1.3, 10.4 Hz, 1H), 5.21 (ddd, *J* = 0.9, 1.7, 10.4 Hz, 1H), 5.25 (br. dt, *J* = 1.4, 7.2 Hz, 1H), 5.33 (br. ddd, *J* = 1.1, 1.7, 15.8 Hz, 1H), 5.70–5.92 (m, 2H). **¹³C NMR** (50 MHz, CDCl₃): δ 14.0 (q), 17.9 (t), 25.2 (q), 27.5 (q), 30.3 (t), 31.4 (t), 33.3 (t), 71.9 (d), 72.0 (d), 78.3 (d), 78.8 (d), 108.8 (s), 115.1 (t), 118.5 (t), 133.1 (d), 140.3 (d), 172.9 (s) ppm. **ESI-MS** *m/z*: 335.4 (100%, [M+Na]⁺), 351.4 (13.2%, [M+K]⁺). **Anal. Calcd for C₁₇H₂₈O₅**: C, 65.36; H, 9.03; Found: C, 65.19; H, 9.29%.

Stagonolide B (1)



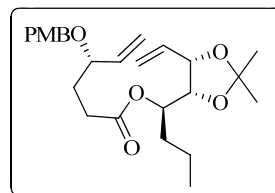
To a solution of diene **25** (50 mg, 0.16 mmol) in dry dichloroethane (20 mL), 2nd gen. Grubbs' catalyst (35 mg, 0.04 mmol) was added and the mixture was degassed under argon atmosphere thoroughly. The reaction mixture was refluxed for 24 h and solvent was removed under reduced pressure. The residue was purified by flash column chromatography (30% EtOAc in petroleum ether) gave impure macrolide (25 mg) as colorless liquid. The above compound (25 mg) was suspended

at 0 °C in TFA (2 mL) and stirred for 1 h. The reaction mixture was concentrated under reduced pressure and the residue was purified by column chromatography (70→100% EtOAc in petroleum ether) to obtain stagonolide B (**1**) as viscous liquid (15 mg, 39%).

$[\alpha]_D^{25} = +27.1$ (*c* 0.9, CHCl₃); Lit.^{9a} $[\alpha]_D^{25} = +20$ (0.1, CHCl₃). **IR** (CHCl₃) ν : 3409, 2927, 1729, 1560 cm⁻¹. **¹H NMR** (400 MHz, CDCl₃): δ 0.90 (t, *J* = 7.4 Hz, 3H), 1.23–1.30 (m, 1H), 1.32–1.42 (m, 1H), 1.57 (ddq, *J* = 4.9, 9.8, 14.3 Hz, 1H), 1.64 (br. s, 1H, -OH), 1.82–1.92 (m, 2H), 2.07 (br. ddd, *J* = 2.6, 5.5, 14.3 Hz, 1H), 2.12 (br. dt, *J* = 2.6, 14.4 Hz, 1H), 2.24 (br. d, *J* = 8.4 Hz, 1H, C7-OH), 2.44 (br. s, 1H, -OH), 2.45 (br. dt, *J* = 1.8, 14.4 Hz, decouple at 1.90→t, *J* = 13.4, 1H), 3.57 (br. t, *J* = 8.5 Hz, decouple at 2.48→dd, *J* = 2.6, 9.9 Hz, 1H), 4.47–4.53 (br. s, decouple at 2.29→dt, *J* = 2.6, 4.6 Hz, 1H), 4.59–4.64 (br. s, 1H), 4.94 (dt, *J* = 2.5, 9.6 Hz, decouple at 1.90→t, *J* = 9.5 Hz, 1H), 5.63 (dt, *J* = 2.7, 16.1 Hz, 1H), 5.99 (dt, *J* = 1.7, 16.1 Hz, 1H). **¹³C NMR** (100 MHz, CDCl₃): δ 13.9 (q), 18.0 (t), 27.8 (t), 31.6 (t), 33.6 (t), 68.6 (d), 70.2 (d), 73.6 (d), 73.6 (d), 127.1 (d), 127.2 (d), 176.5 (s) ppm. **ESI-MS *m/z***: 267.2 (100%, [M+Na]⁺). **Anal. Calcd for C₁₂H₂₀O₅**: C, 59.00; H, 8.25; Found: C, 59.22; H, 8.10%.

D₂O Exchange ¹H NMR (400 MHz, CDCl₃ + D₂O) : δ 0.90 (t, *J* = 7.4 Hz, 3H), 1.23–1.30 (m, 1H), 1.32–1.42 (m, 1H), 1.56 (ddq, *J* = 4.9, 9.8, 14.3 Hz, 1H), 1.82–1.92 (m, 2H), 2.07 (br. ddd, *J* = 2.6, 5.5, 14.3 Hz, 1H), 2.12 (br. dt, *J* = 2.6, 14.4 Hz, 1H), 2.46 (br. dt, *J* = 2.8, 14.4 Hz, 1H), 3.56 (dd, *J* = 2.5, 9.8 Hz, 1H), 4.45 (br. dt, *J* = 2.6, 4.6 Hz, 1H), 4.60 (br. s, 1H), 4.75 (br. s, 1H, -OH), 4.93 (dt, *J* = 2.5, 9.6 Hz, 1H), 5.63 (dt, *J* = 2.7, 16.1 Hz, 1H), 5.99 (dt, *J* = 1.7, 16.1 Hz, 1H).

Preparation of Diene *epi*-4

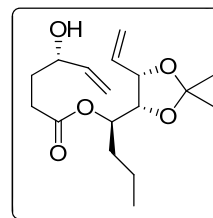


To a solution of acid (*S*)-**5** (240 mg, 0.96 mmol) in dry THF (5 mL), the 2,4,6-trichlorobenzyl chloride (0.22 mL, 1.44 mmol) followed by *N,N*-diisopropylethyl amine (0.83 mL, 4.79 mmol) were added and the mixture was stirred for 2 h at ambient temperature. After completion of mixed anhydride formation as indicated by TLC, a solution of alcohol **3** (192 mg, 0.96 mmol) in THF (2 mL) was introduced and the contents were stirred for 16 h at rt. The reaction mixture was quenched with cold water and extracted with ethyl acetate. The combined organic phase was washed with

aq. NaHCO₃ solution and water, dried (Na₂SO₄) and evaporated under reduced pressure. The crude product was purified by silica gel column chromatography (8→10% EtOAc in petroleum ether) to procure *epi-4* (348 mg, 84%) as light yellow oil.

$[\alpha]_D^{25}$: -2.8 (*c* 1.4, CHCl₃). IR (CHCl₃) ν : 2932, 2872, 1737, 1644, 1613, 1514, 1464, 1442, 1372, 1301, 1172, 1067, 1037, 928, 872, 821 cm⁻¹. ¹H NMR (200 MHz, CDCl₃): δ 0.89 (t, *J* = 7.2 Hz, 3H), 1.23–1.36 (m, 2H), 1.36 (s, 3H), 1.48 (s, 3H), 1.56–1.71 (m, 2H), 1.77–1.96 (m, 2H), 2.19–2.48 (m, 2H), 3.70–3.79 (m, 1H), 3.79 (s, 3H), 4.16 (dd, *J* = 6.6, 7.4 Hz, 1H), 4.26 (d, *J* = 11.4 Hz, 1H), 4.52 (d, *J* = 11.4 Hz, 1H), 4.59 (ddt, *J* = 1.0, 6.7, 7.4 Hz, 1H), 4.91 (dt, *J* = 4.0, 7.4 Hz, 1H), 5.16–5.23 (m, 2H), 5.26–5.36 (m, 2H), 5.63–5.88 (m, 2H), 6.87 (br. d, *J* = 8.6 Hz, 2H), 7.24 (br. d, *J* = 8.6, 2H). ¹³C NMR (50 MHz, CDCl₃): δ 14.0 (q), 17.8 (t), 25.1 (q), 27.4 (q), 30.3 (t, 2C), 33.3 (t), 55.2 (q), 69.7 (t), 71.6 (d), 78.3 (d), 78.7 (d), 79.0 (d), 108.7 (s), 113.7 (d), 117.6 (t), 118.3 (t), 129.2 (d), 130.5 (s), 133.2 (d), 138.3 (d), 159.1 (s), 172.4 (s) ppm. Anal. Calcd for C₂₅H₃₆O₆: C, 69.42; H, 8.39; Found: C, 69.31; H, 8.41%.

Diene *epi-25*

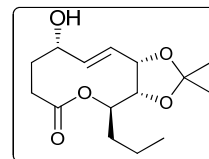


To a solution of *epi-4* (100 mg, 0.23 mmol) in CH₂Cl₂:H₂O (15 mL, 18:1), DDQ (157 mg, 0.69 mmol) was added and stirred for 3 h at rt. The reaction mixture was quenched with aqueous NaHCO₃ solution and partitioned between water and CH₂Cl₂. The aqueous layer was extracted with CH₂Cl₂ and the combined organic layer was dried (Na₂SO₄) and concentrated. The residue was purified by silica gel chromatography (25% EtOAc in petroleum ether) to procure *epi-25* (60 mg, 86%) as colorless oil.

$[\alpha]_D^{25}$ = +30.5 (*c* 1.0, CHCl₃). IR (CHCl₃) ν : 3453, 2961, 2864, 1732, 1643, 1388, 1215, 1061, 924 cm⁻¹. ¹H NMR (400 MHz, CDCl₃): δ 0.89 (t, *J* = 7.4 Hz, 3H), 1.23–1.34 (m, 2H), 1.35 (br. s, 3H), 1.47 (br. s, 3H), 1.58–1.71 (m, 2H), 1.74–1.89 (m, 2H), 2.35 (br. dd, *J* = 2.7, 7.4 Hz, 1H), 2.30–2.43 (m, 2H), 4.13 (br. dd, *J* = 6.0 Hz, 1H), 4.17 (dd, *J* = 6.7, 7.4 Hz, 1H), 4.59 (br. t, *J* = 7.2 Hz, 1H), 4.91 (dt, *J* = 3.5, 7.6 Hz, 1H), 5.13 (br. dt, *J* = 1.2, 10.5 Hz, 1H), 5.18–5.26 (m, 2H), 5.32 (br. dt, *J* = 1.2, 17.0 Hz, 1H), 5.74–5.88 (m, 2H). ¹³C NMR (100 MHz, CDCl₃): δ 14.0 (q), 17.9 (t), 25.2 (q), 27.5 (q), 30.3 (t), 31.4 (t), 33.3 (t), 71.9 (d), 72.1

(d), 78.3 (d), 78.8 (d), 108.8 (s), 115.1 (t), 118.6 (t), 133.1 (d), 140.3 (d), 173.0 (s) ppm. **ESI-MS m/z** : 335.2 (100%, $[M+Na]^+$). **Anal. Calcd for $C_{17}H_{28}O_5$** : C, 65.36; H, 9.03; Found: C, 65.24; H, 9.15%.

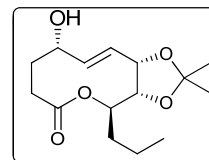
RCM of Compound *epi-26*



To a degassed solution of diene *epi-25* (40 mg, 0.12 mmol) and 2nd gen. Grubbs' catalyst (11 mg, 0.012 mmol) in dry DCM (40 mL) was heated to reflux under argon atmosphere for 6 h and concentrated. The residue was purified by flash chromatography to furnish *epi-26* (32 mg, 89%) as colourless semisolid.

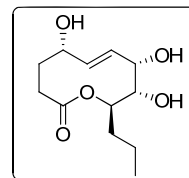
$[\alpha]_D^{25} = +55.1$ (c 0.5, $CHCl_3$). **IR ($CHCl_3$)** ν : 3467, 3020, 1732, 1542, 1452, 1349, 1216, 1046 cm^{-1} . **1H NMR (400 MHz, $CDCl_3$)**: δ 0.9 (t, $J = 7.3$, 3H), 1.26–1.35 (m, 2H), 1.36 (s, 3H), 1.41–1.50 (m, 2H), 1.54 (s, 3H), 1.70–1.78 (m, 1H), 1.98–2.05 (m, 2H), 2.29–2.35 (m, 1H), 3.95 (dd, $J = 4.7, 10.1$ Hz, 1H), 4.13–4.20 (m, 1H), 4.68 (br.ddd, 1.9, 3.1, 4.7 Hz, 1H), 4.92 (ddd, $J = 2.7, 8.9, 10.1$ Hz, 1H), 5.64 (ddd, $J = 1.7, 8.6, 15.9$ Hz, 1H), 5.81 (dd, $J = 3.3, 15.9$ Hz, 1H). **^{13}C NMR (100 MHz, $CDCl_3$)**: δ 13.9 (q), 17.8 (t), 26.2 (q), 28.4 (q), 31.2 (t), 33.6 (t), 34.1 (t), 70.8 (d), 75.6 (d), 75.7 (d), 78.6 (d), 109.3 (s), 126.7 (d), 128.1 (d), 175.0 (s) ppm. **ESI-MS m/z** : 307.1 (100% $[M+Na]^+$). **Anal. Calcd for $C_{15}H_{24}O_5$** : C, 63.36; H, 8.51; Found: C, 63.25; H, 8.39%.

RCM of Compound *epi-26* in toluene



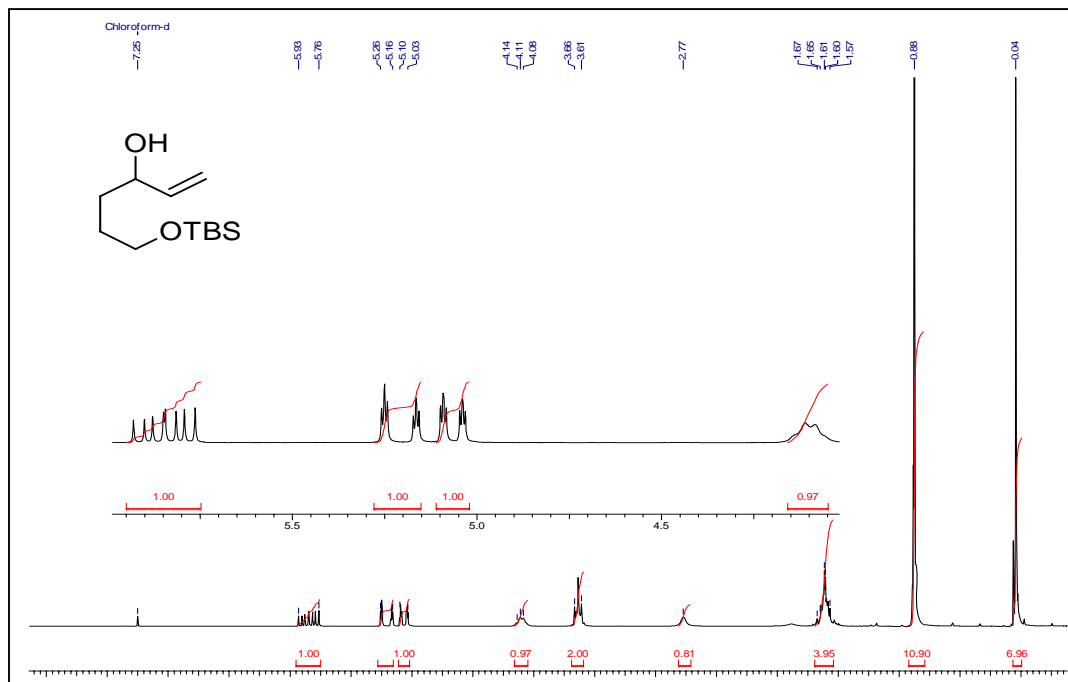
To a degassed solution of diene *epi-25* (40 mg, 0.12 mmol) and 2nd gen. Grubbs' catalyst (11 mg, 0.012 mmol) in dry toluene (40 mL) was heated to 80 °C under argon atmosphere for 6 h and concentrated. The residue was purified by flash chromatography to furnish *epi-26* (27 mg, 81%) as colourless semisolid.

4-*Epi*-Stagonolide B 2

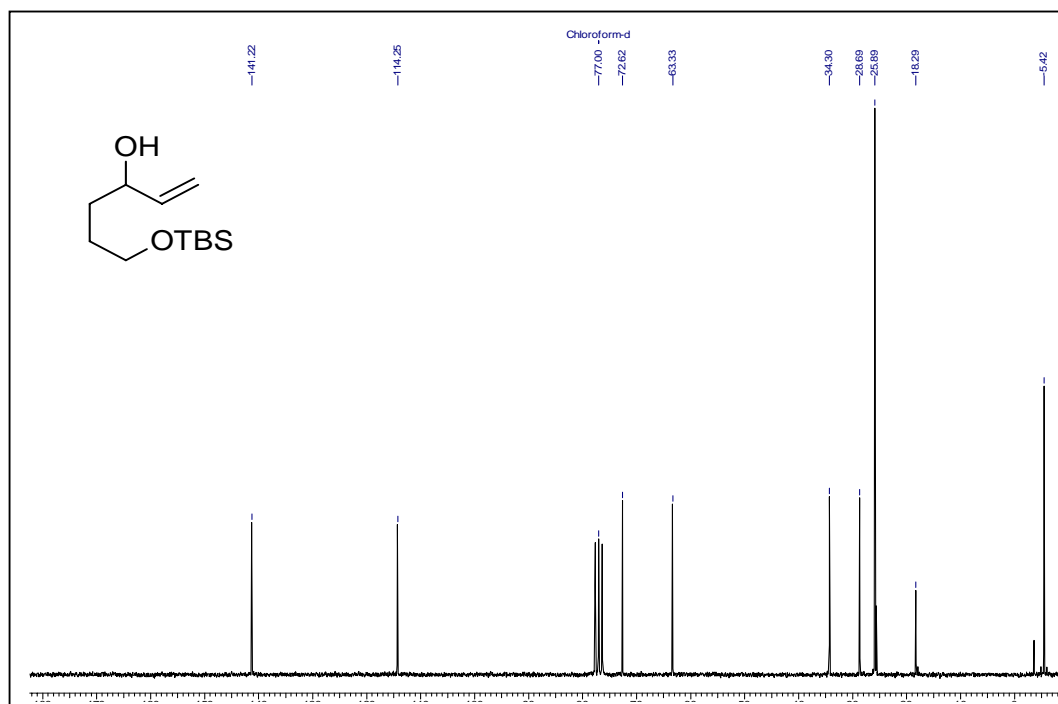


A solution of compound *epi*-**26** (10 mg, 0.00 mmol) and TFA (1 mL) was stirred at 0 °C for 1 h. The reaction mixture was concentrate under reduced pressure and the residue was purified by column chromatography (70→100% EtOAc in petroleum ether) to procure *epi*-stagonolide B (**2**) as colorless solid (7 mg, 84%).

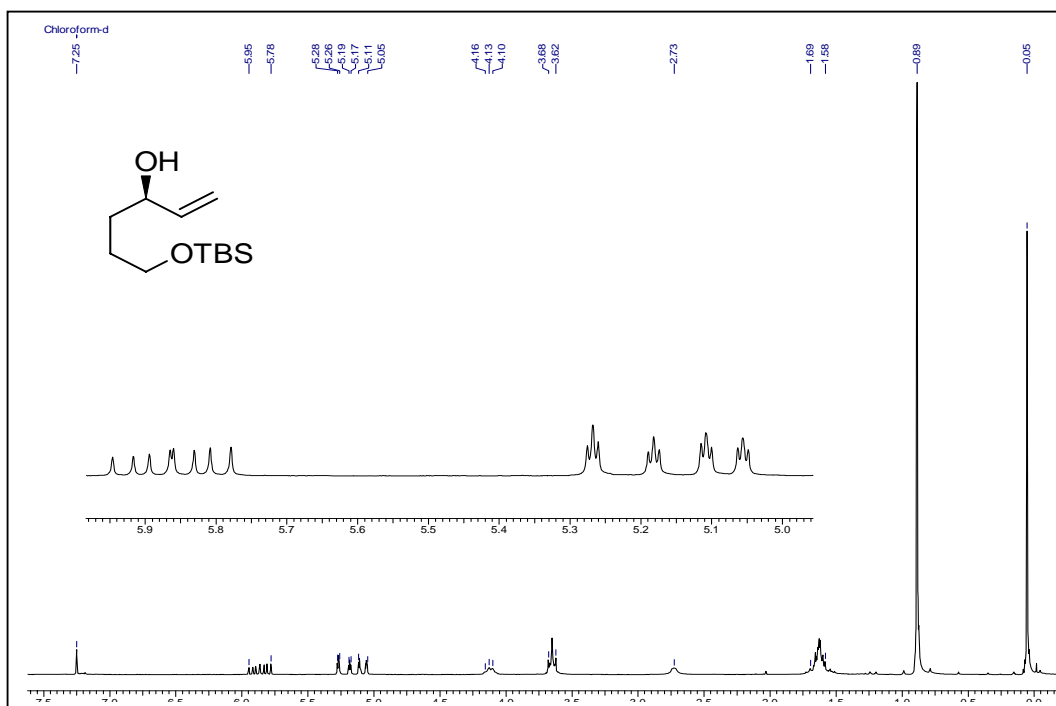
MP: 185–187 °C. $[\alpha]_D^{25}$: +10.7 (*c* 0.5, CH₃OH). IR (CHCl₃) ν : 3390, 2921, 1730, 1563 cm⁻¹. ¹H NMR (400 MHz, CD₃OD): δ 0.88 (t, *J* = 7.4 Hz, 3H), 1.19–1.34 (m, 2H), 1.39–1.48 (m, 1H), 1.73–1.82 (m, 2H), 1.85–1.91 (m, 1H), 2.00 (dt, *J* = 1.4, 13.3 Hz, 1H), 2.23 (ddd, *J* = 2.0, 6.2, 13.9 Hz, 1H), 3.46 (dd, *J* = 1.7, 9.6 Hz, 1H), 4.02 (dt, *J* = 4.6, 10.8 Hz, 1H), 4.35 (br. s, 1H), 5.10 (dt, *J* = 2.4, 9.6 Hz, 1H), 5.46 (ddd, *J* = 1.6, 9.1, 15.5 Hz, 1H), 5.74 (dd, *J* = 1.6, 15.5 Hz, 1H). ¹³C NMR (100 MHz, CD₃OD): δ 14.4 (q), 18.9 (t), 32.5 (t), 33.9 (t), 35.1 (t), 71.8 (d), 73.6 (d), 74.6 (d), 75.9 (d), 128.1 (d), 133.5 (d), 176.3 (s) ppm. ESI-MS *m/z*: 245.2 (100%, [M+H]⁺).



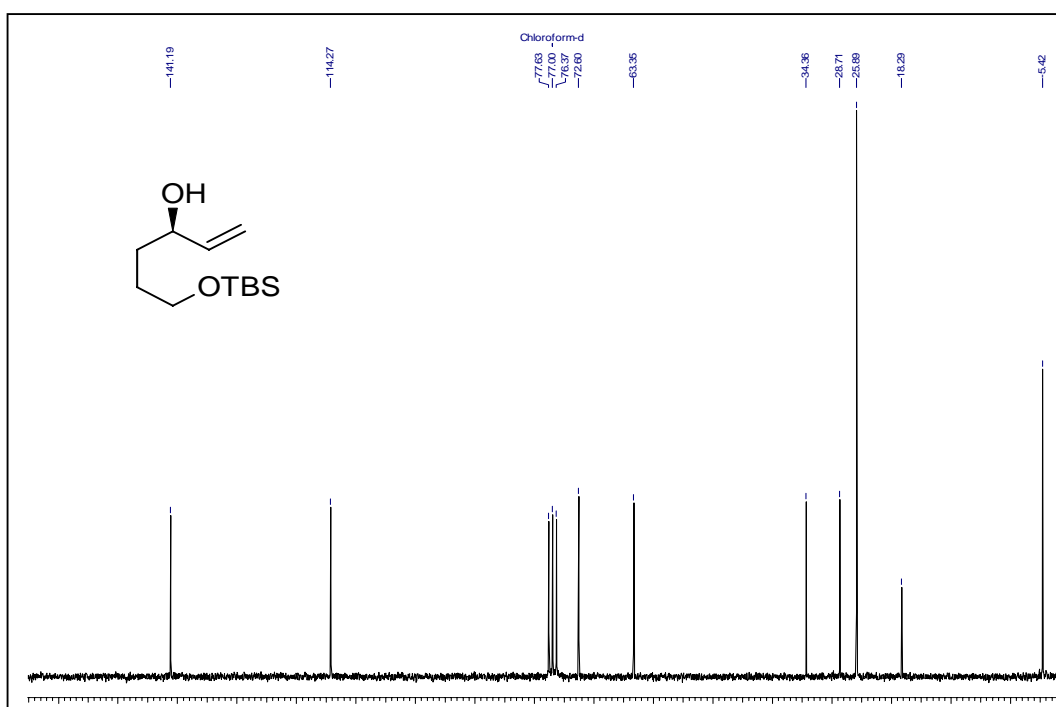
^1H NMR Spectrum of *rac*-6 in CDCl_3



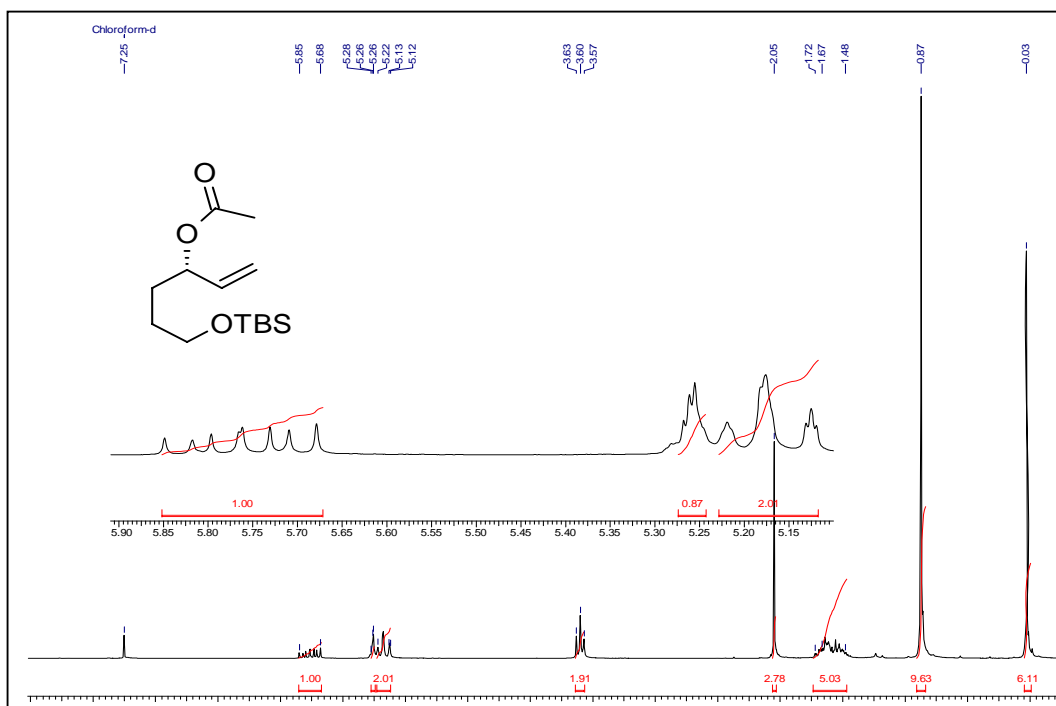
^{13}C NMR Spectrum of *rac*-6 in CDCl_3



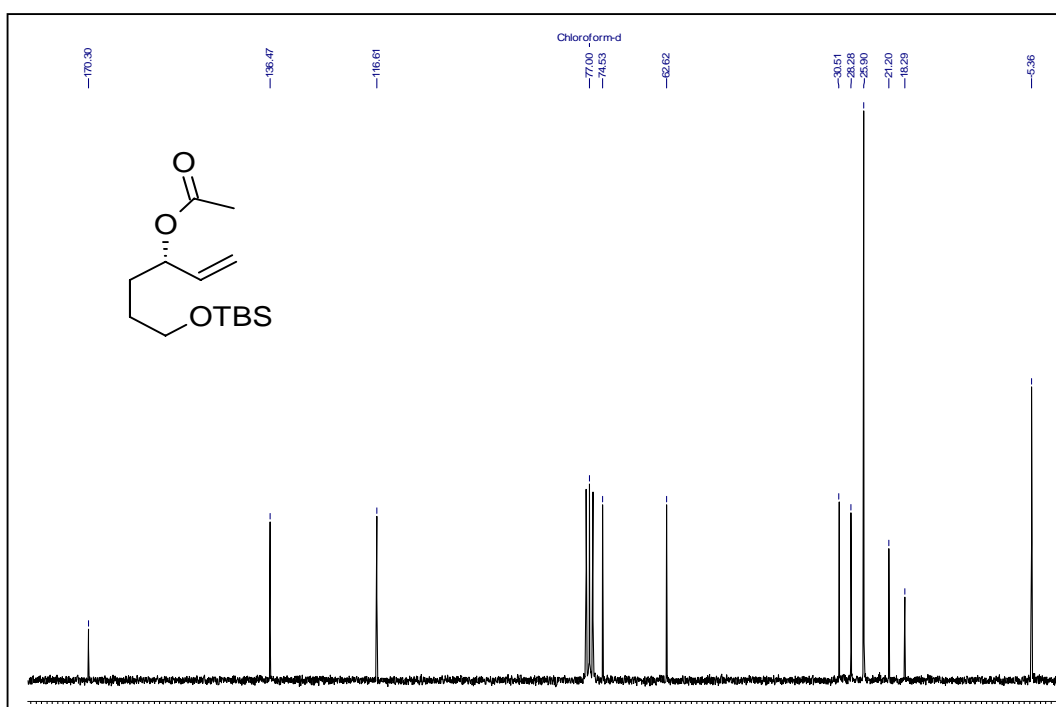
^1H NMR Spectrum of (R)-6 in CDCl_3



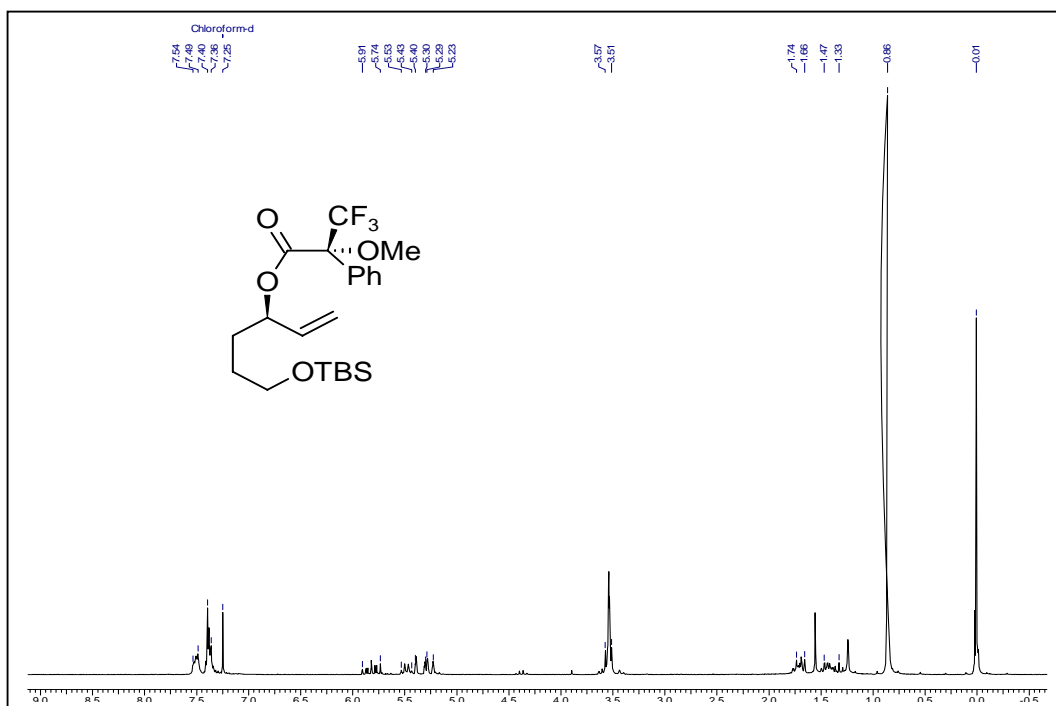
^{13}C NMR Spectrum of (R)-6 in CDCl_3



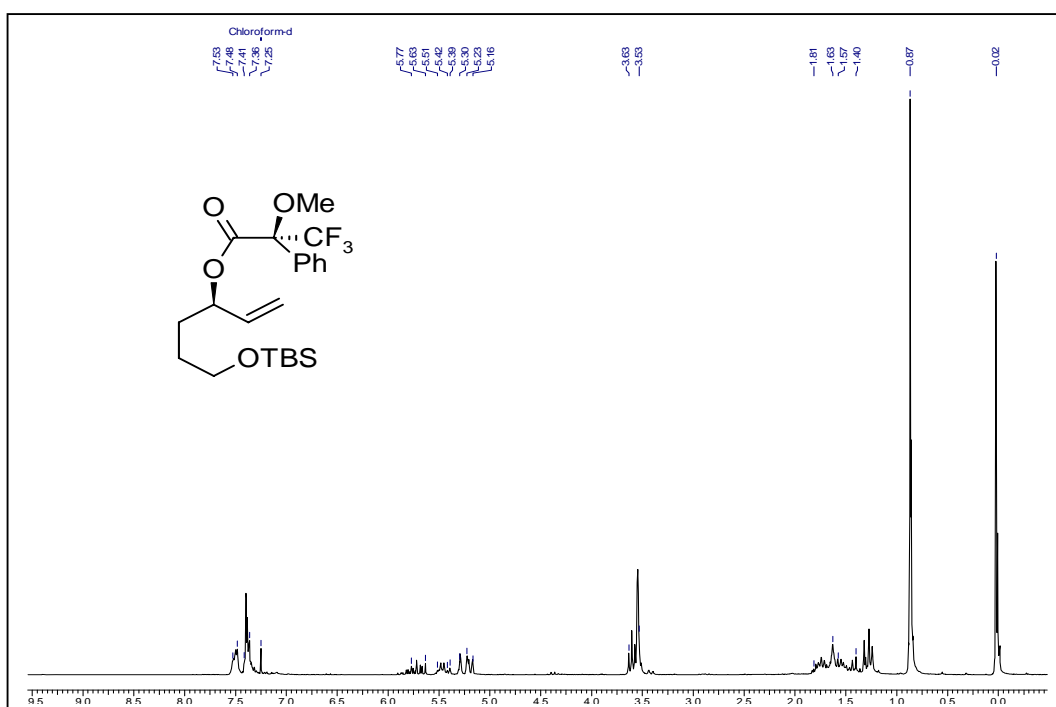
¹H NMR Spectrum of (S)-11 in CDCl₃



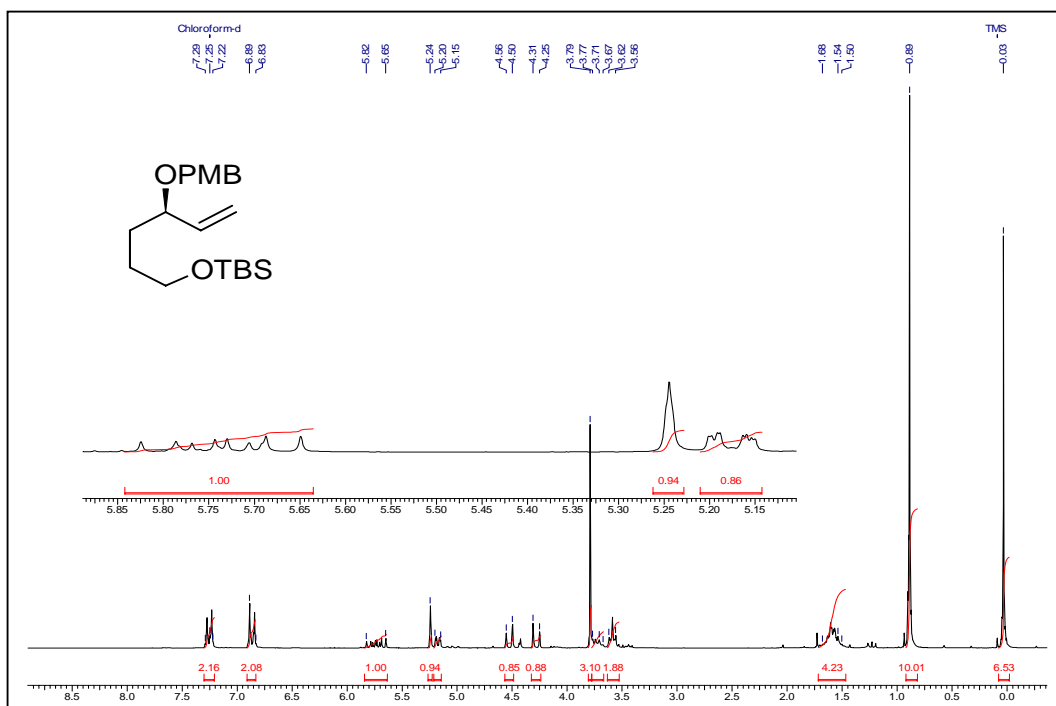
¹³C NMR Spectrum of (S)-11 in CDCl₃



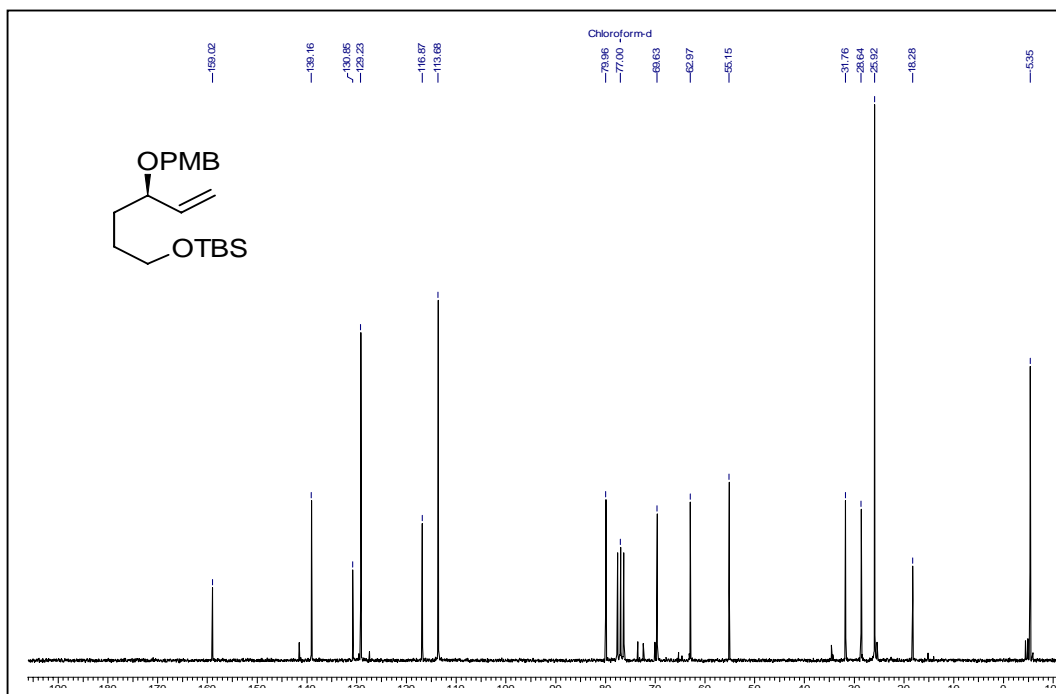
¹H NMR Spectrum of 12-(*R*)-MTPA in CDCl₃



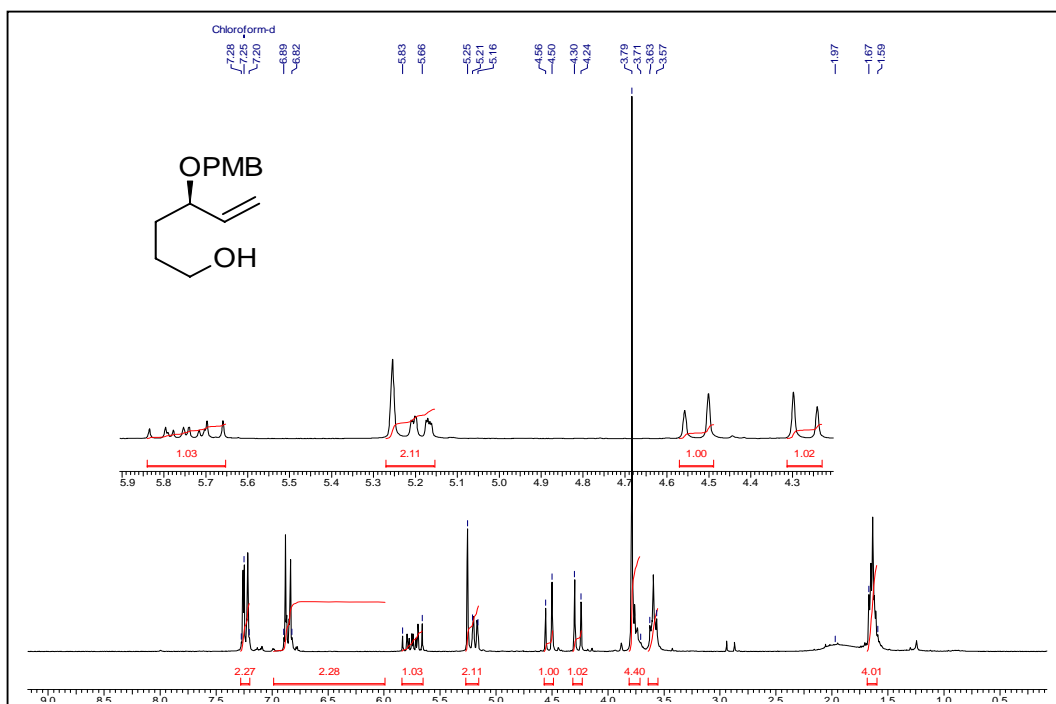
¹H NMR Spectrum of 12-(*S*)-MTPA in CDCl₃



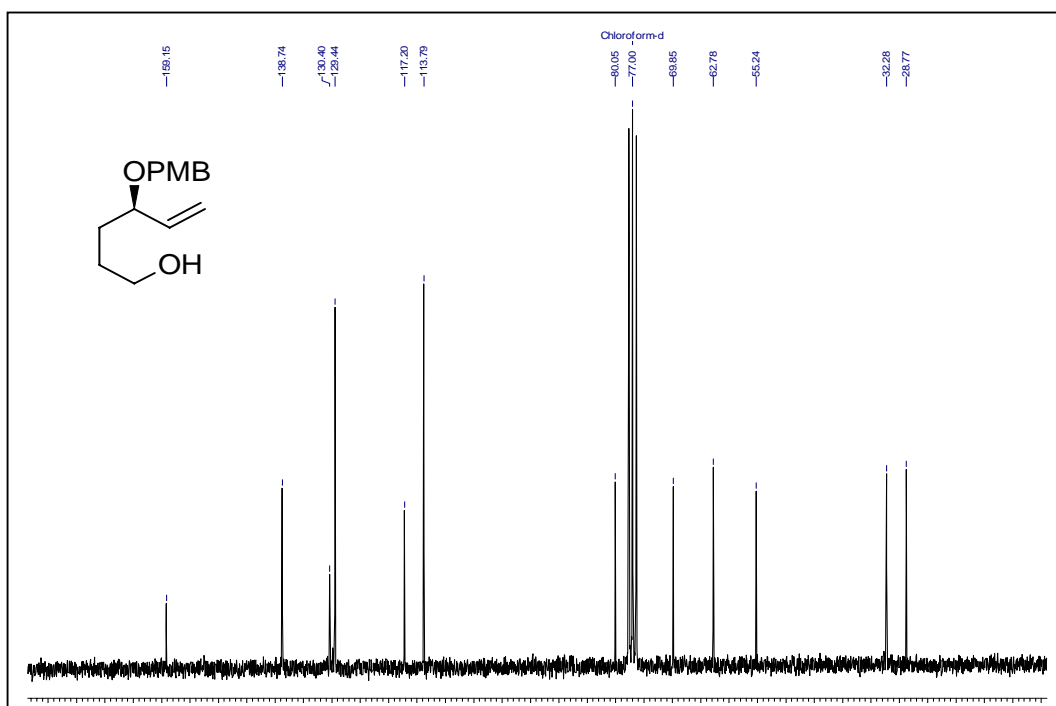
¹H NMR Spectrum of (R)-13 in CDCl₃



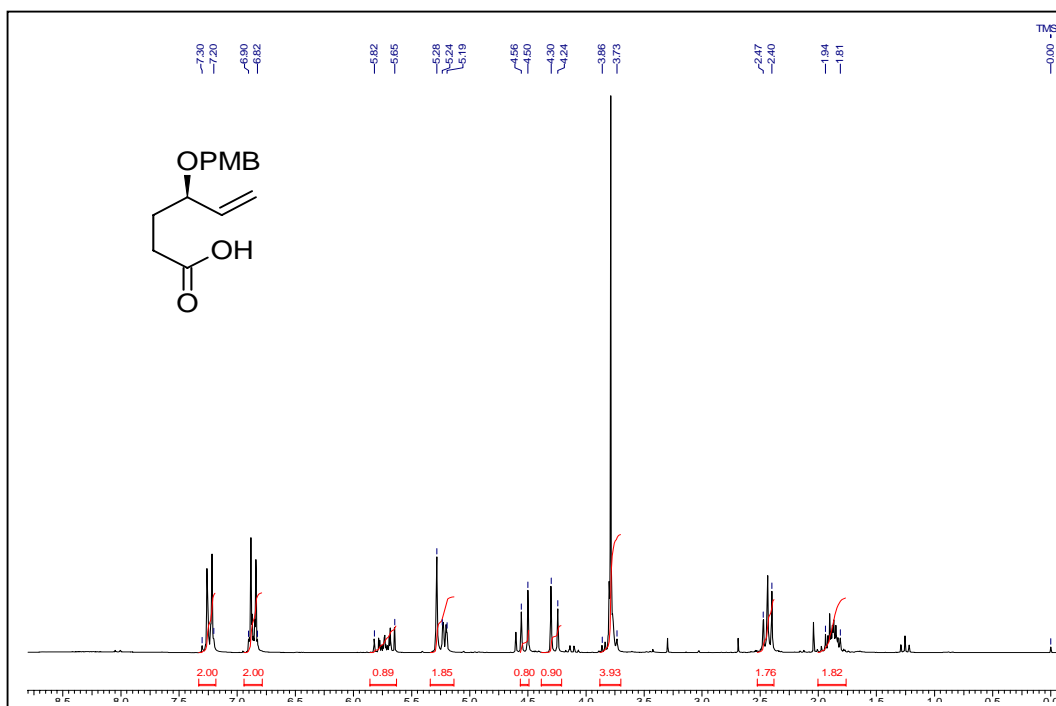
¹³C NMR Spectrum of (R)-13 in CDCl₃



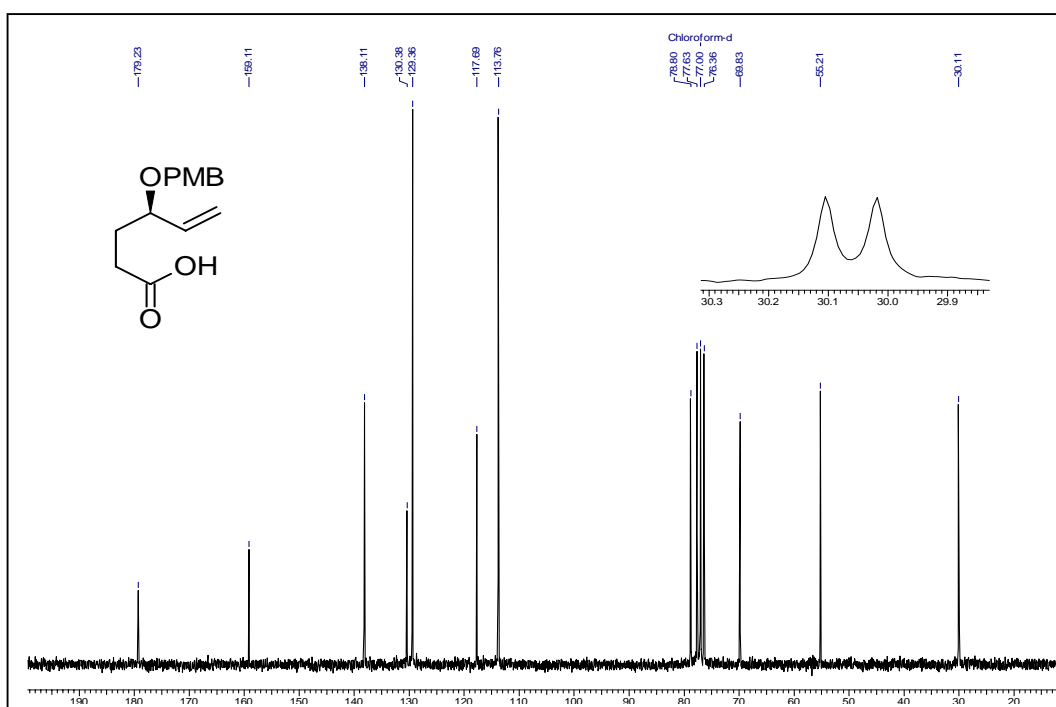
¹H NMR Spectrum of (*R*)-14 in CDCl₃



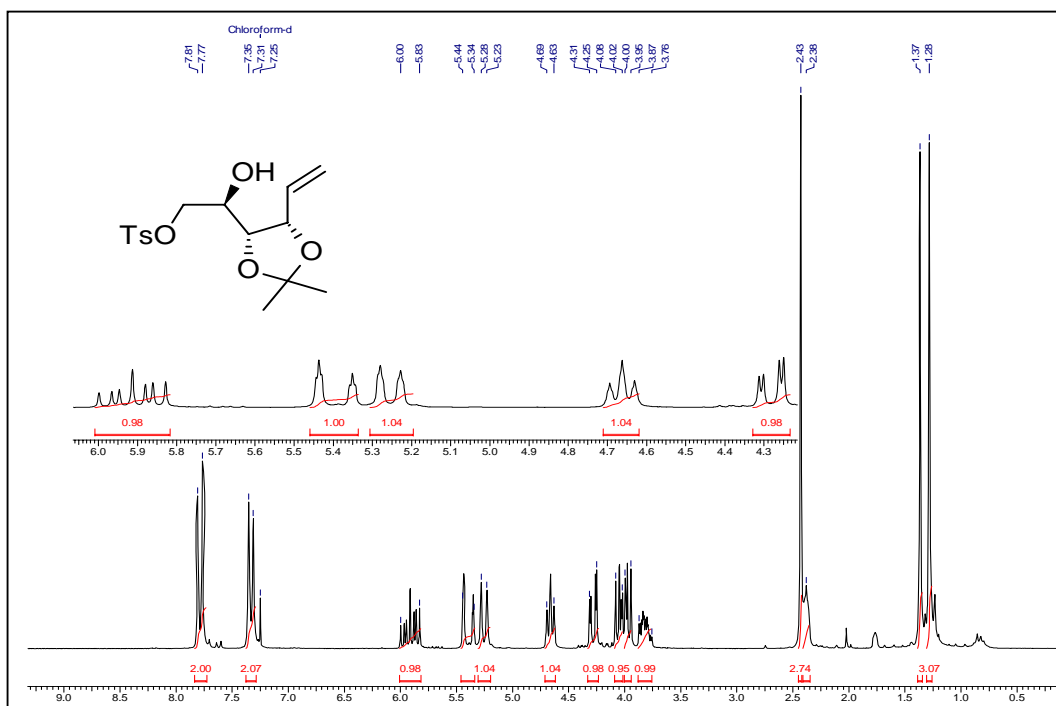
¹³C NMR Spectrum of (*R*)-14 in CDCl₃



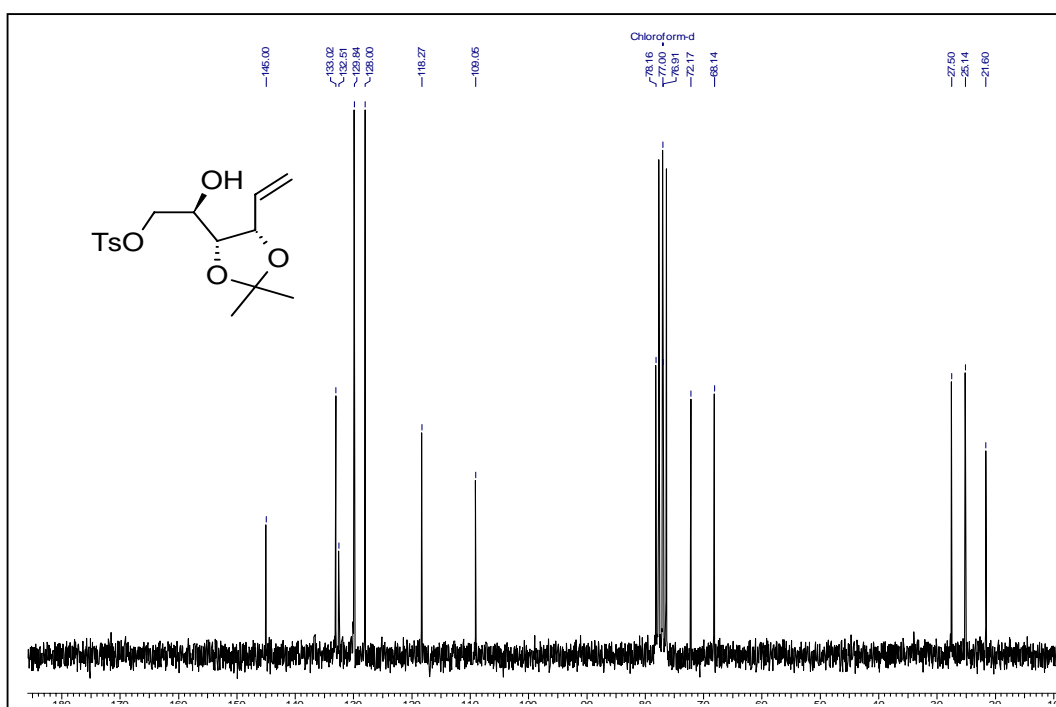
¹H NMR Spectrum of (R)-5 in CDCl₃



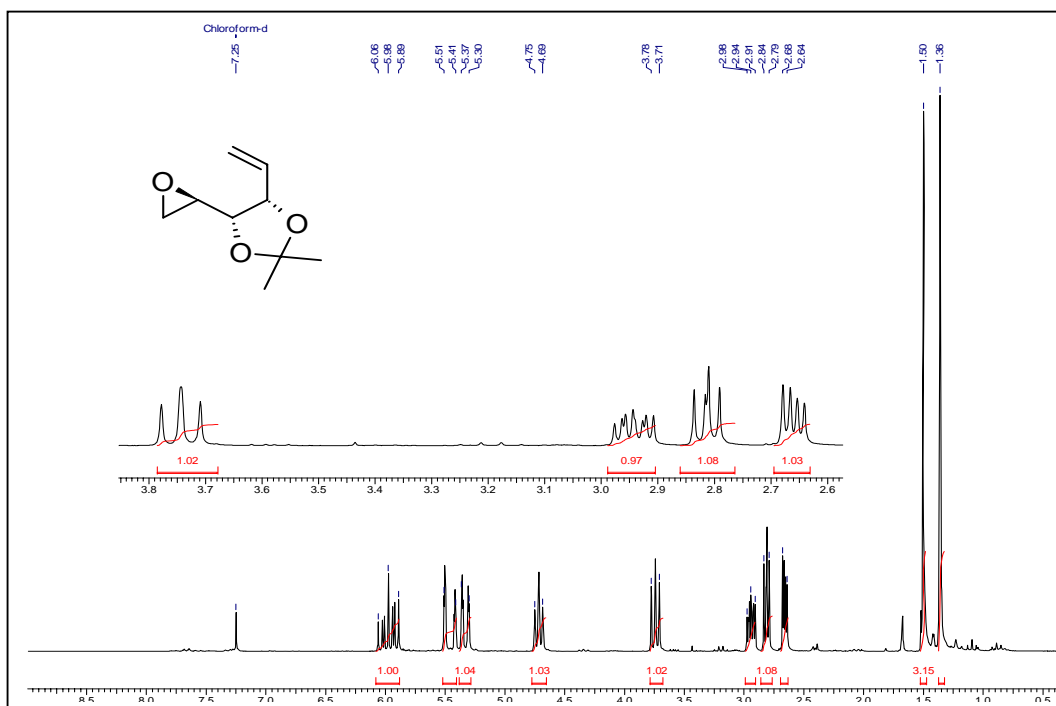
¹³C NMR Spectrum of (R)-5 in CDCl₃



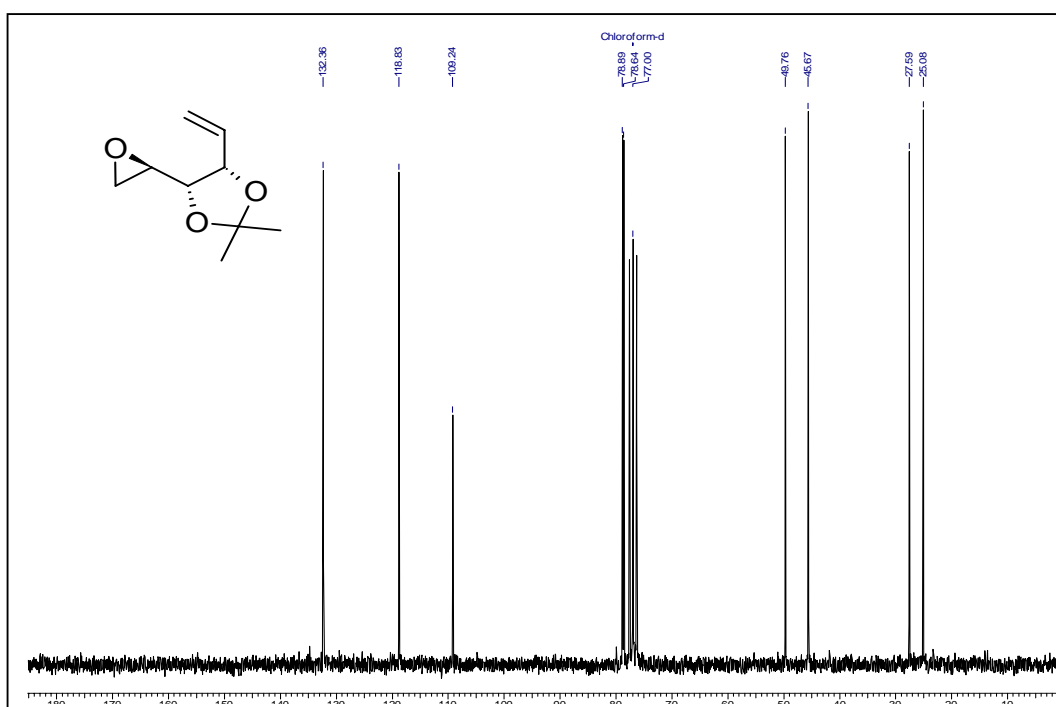
¹H NMR Spectrum of 17 in CDCl₃



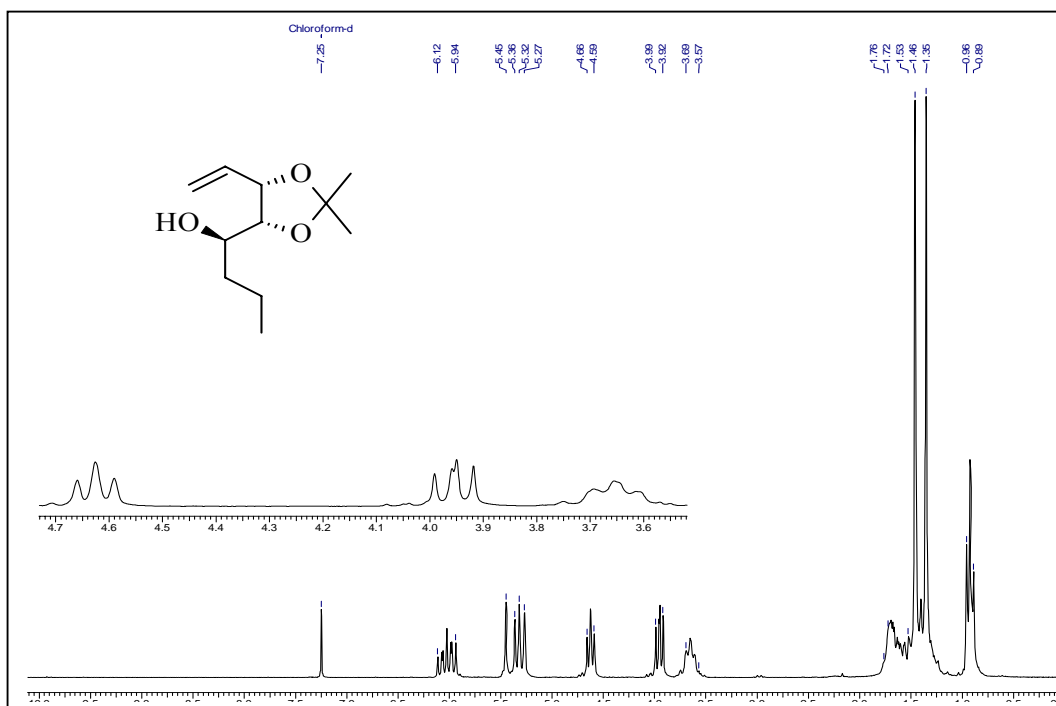
¹³C NMR Spectrum of 17 in CDCl₃



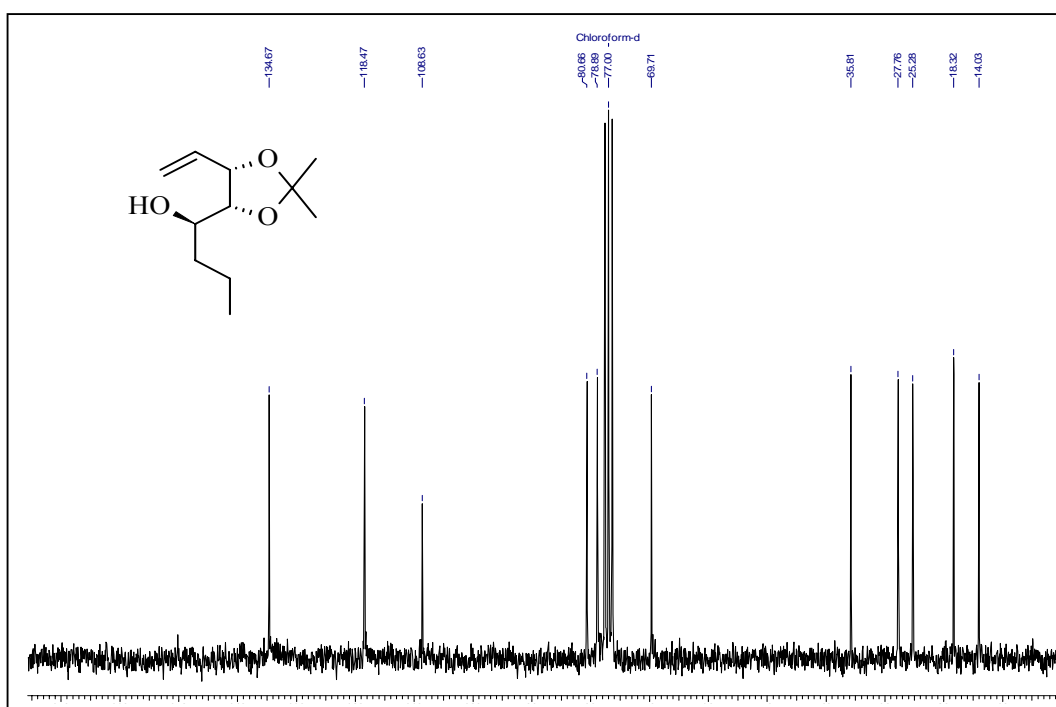
^1H NMR Spectrum of 18 in CDCl_3



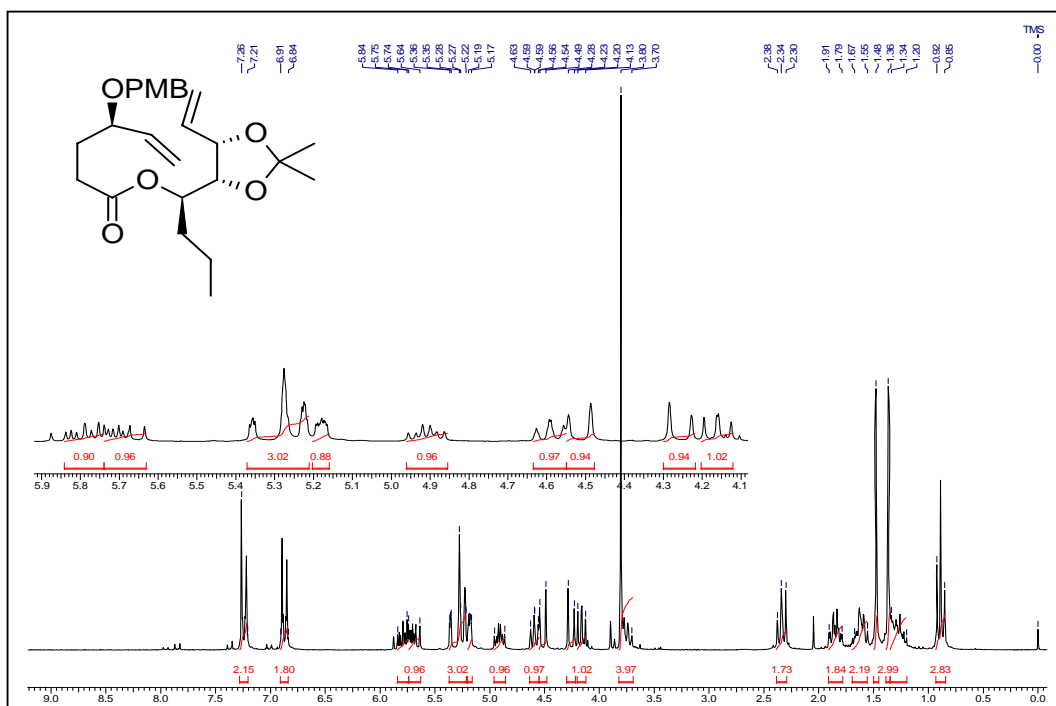
^{13}C NMR Spectrum of 18 in CDCl_3



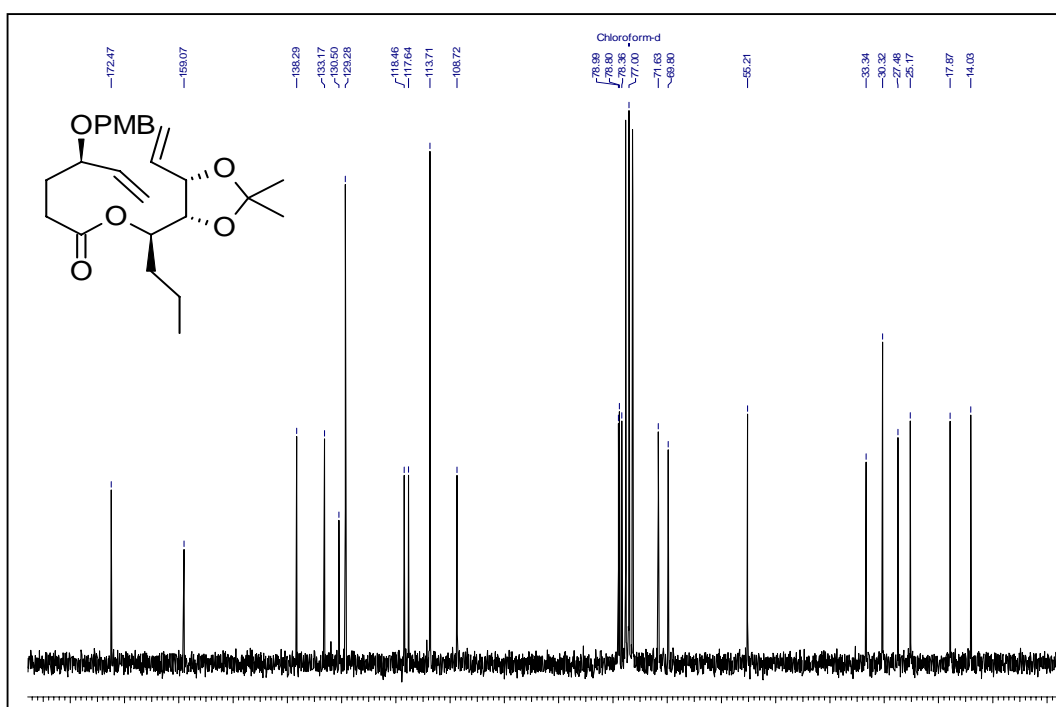
¹H NMR Spectrum of 3 in CDCl₃



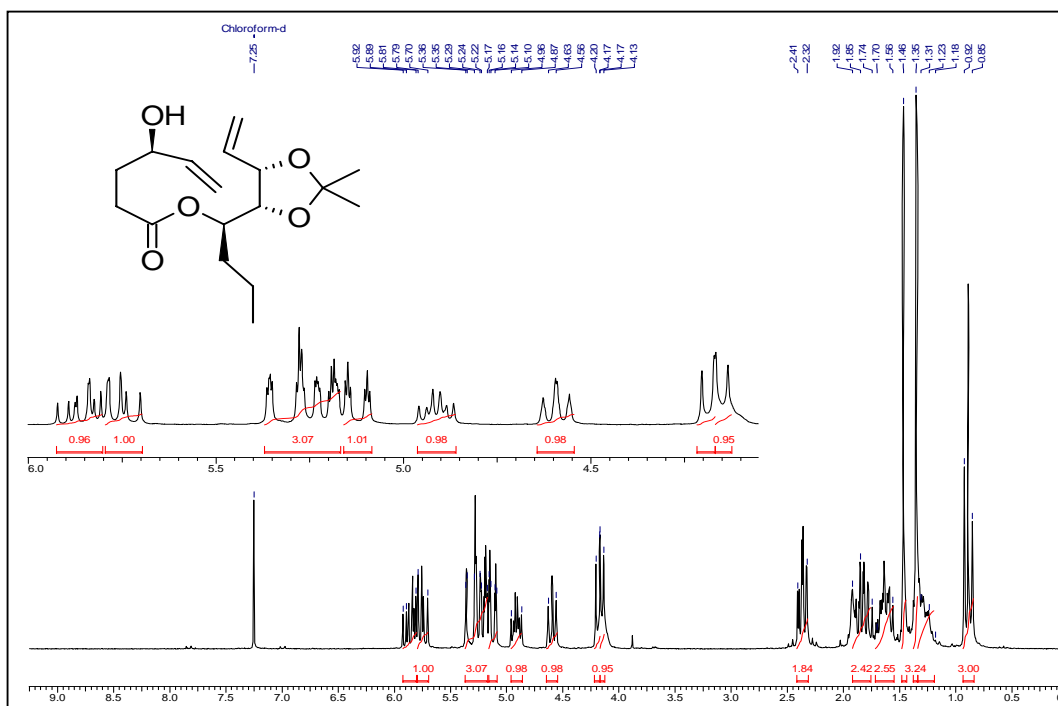
¹³C NMR Spectrum of 3 in CDCl₃



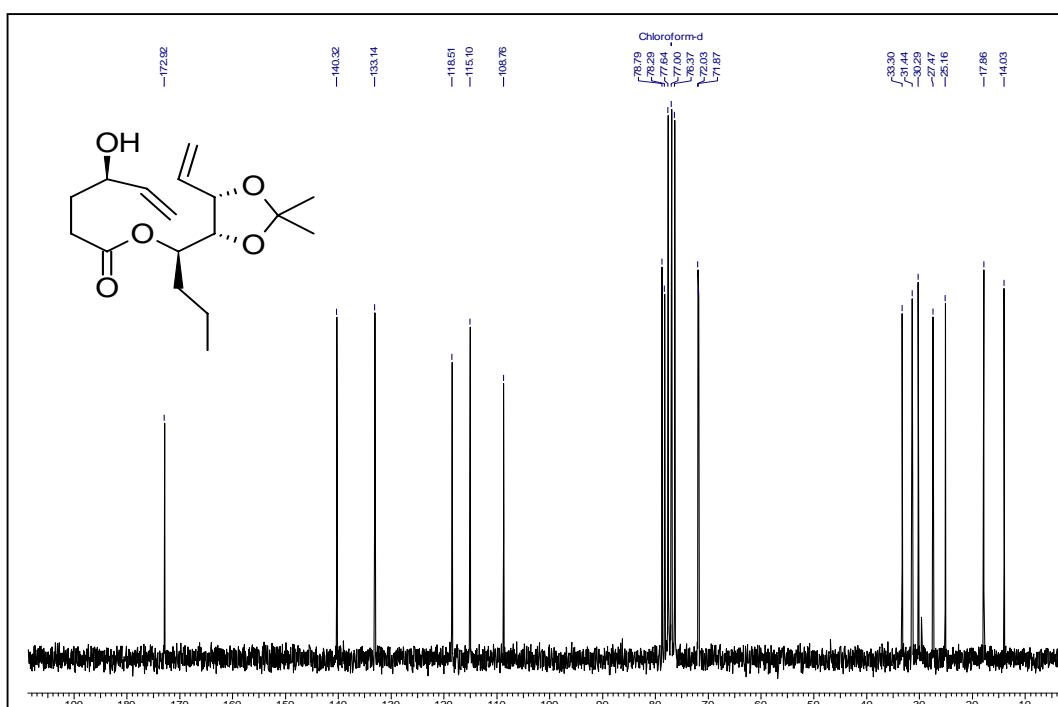
¹H NMR Spectrum of 4 in CDCl₃



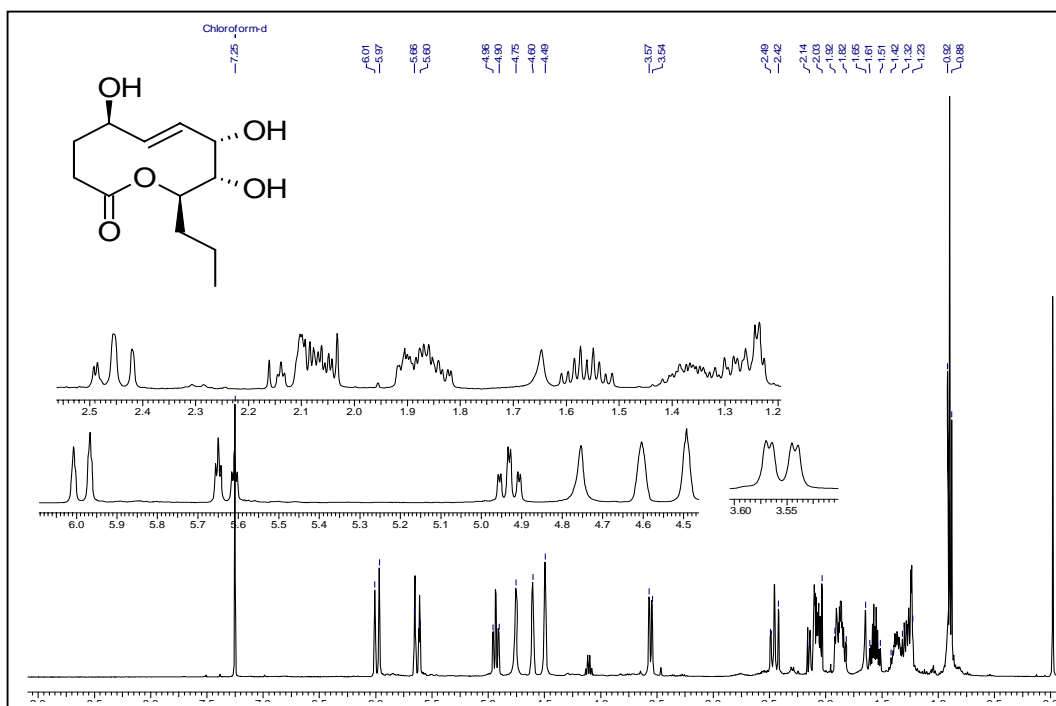
¹³C NMR Spectrum of 4 in CDCl₃



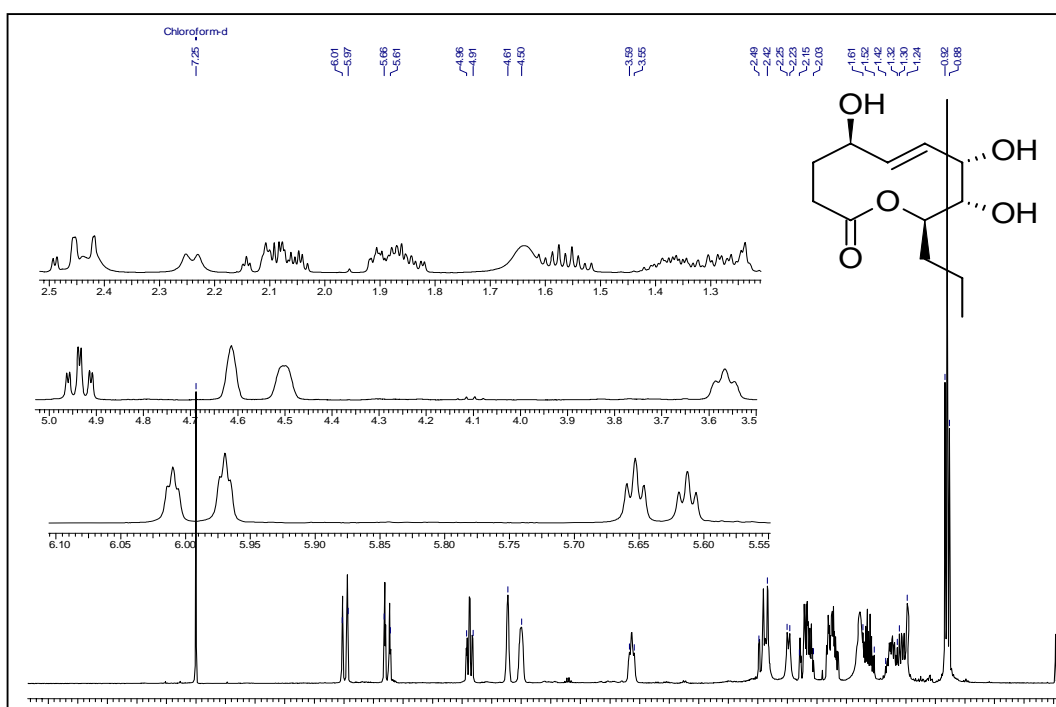
^1H NMR Spectrum of 25 in CDCl_3



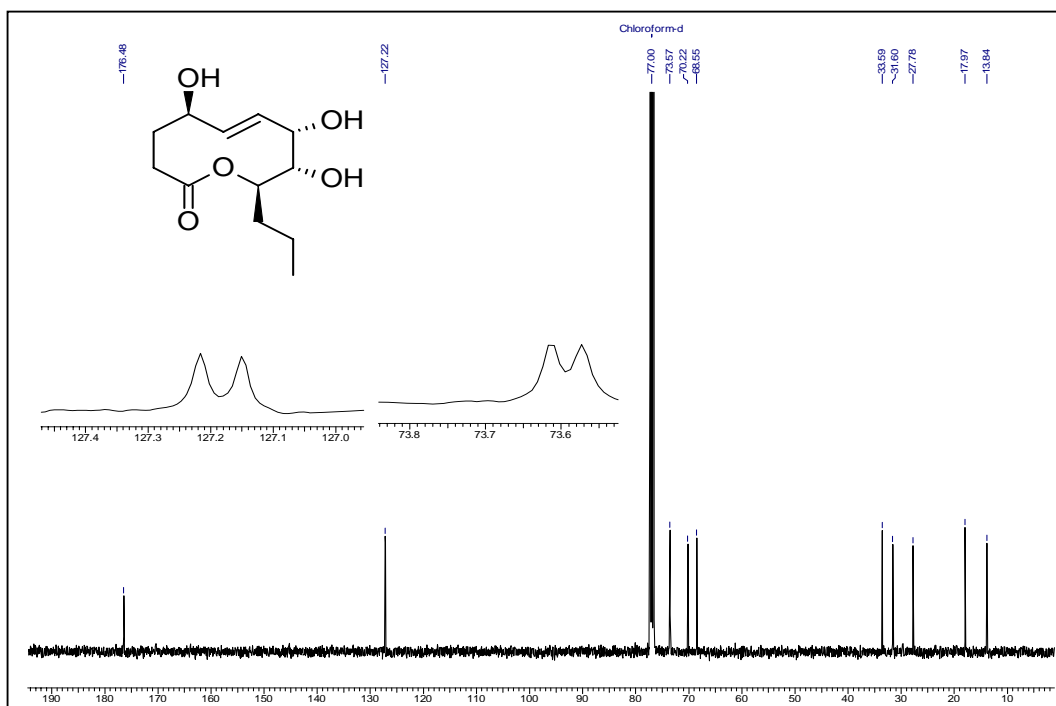
^{13}C NMR Spectrum of 25 in CDCl_3



^1H NMR Spectrum of stagonolide B in CDCl_3

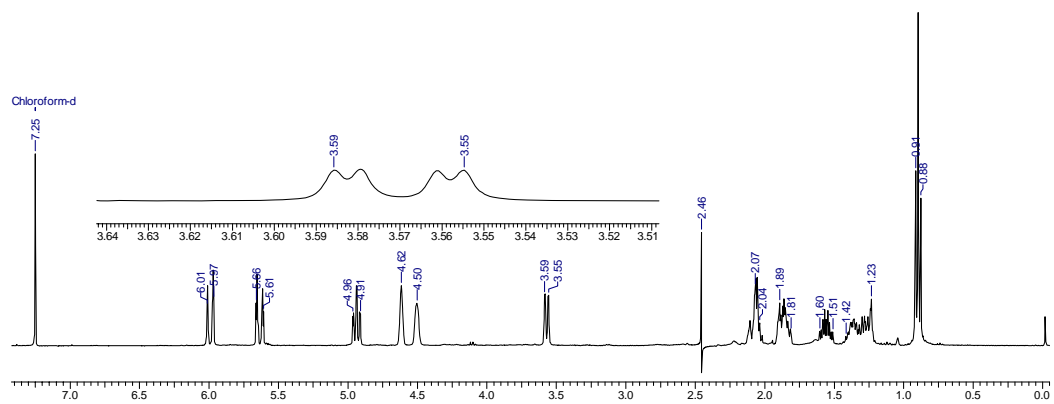


^1H NMR Spectrum of stagonolide B in $\text{CDCl}_3+\text{D}_2\text{O}$

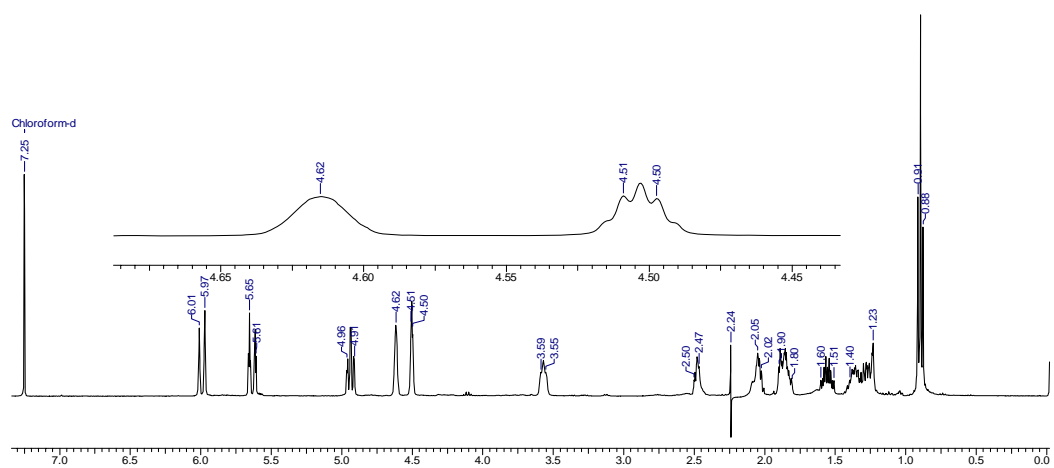


^{13}C NMR Spectrum of stagonolide B in CDCl_3

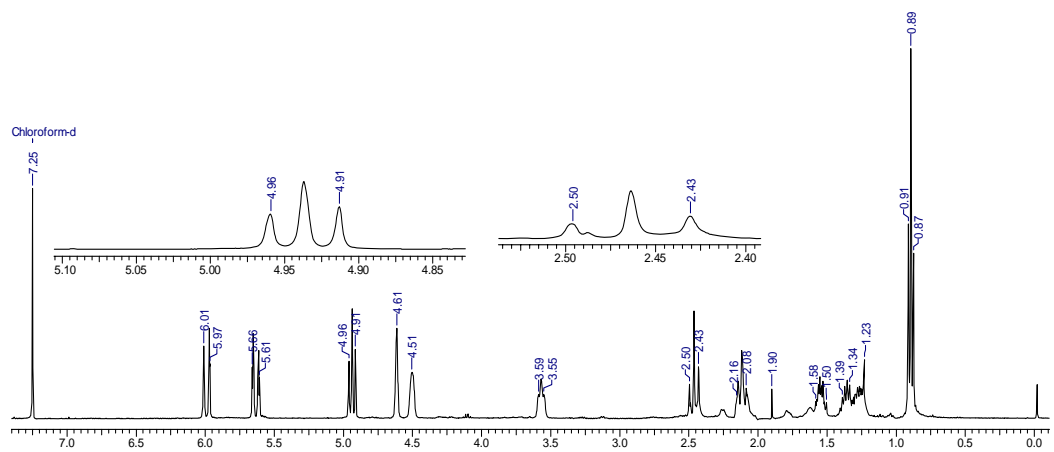
The decoupling ^1H NMR Spectrum of stagonolide B in CDCl_3 .



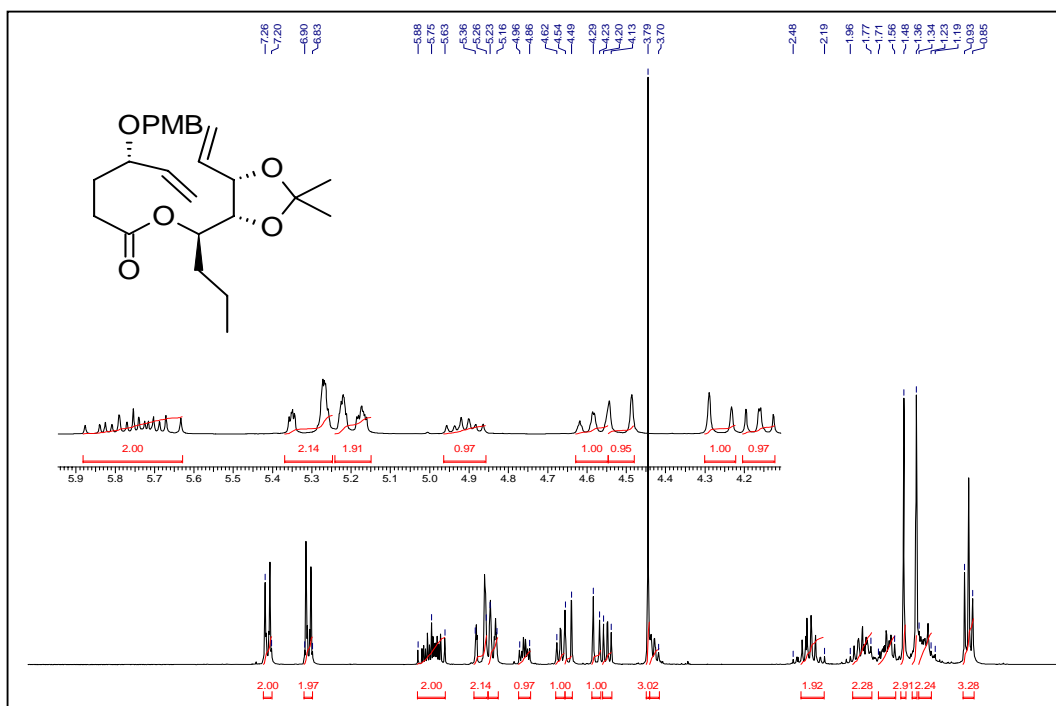
Decoupling at δ 2.48



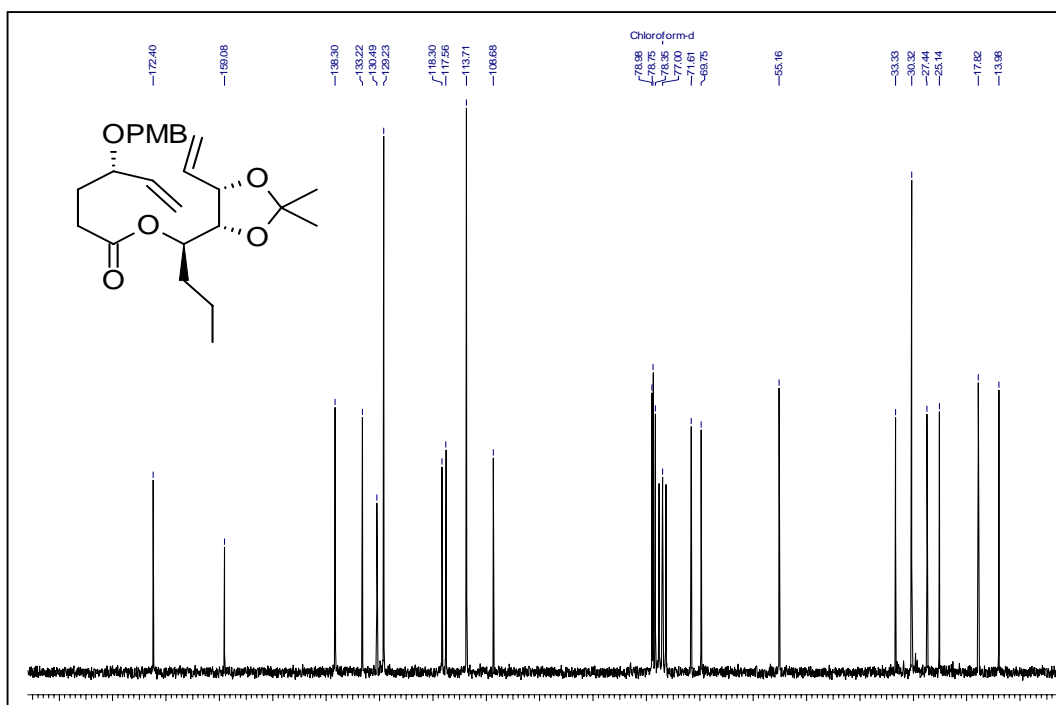
Decoupling at δ 2.29



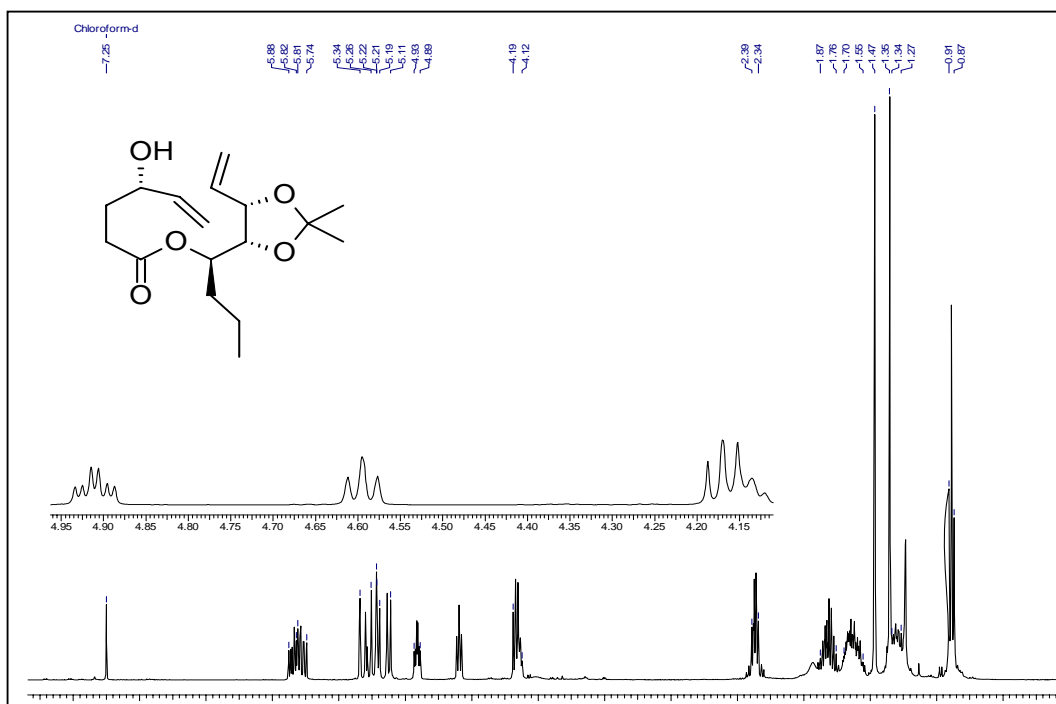
Decoupling at δ 1.90



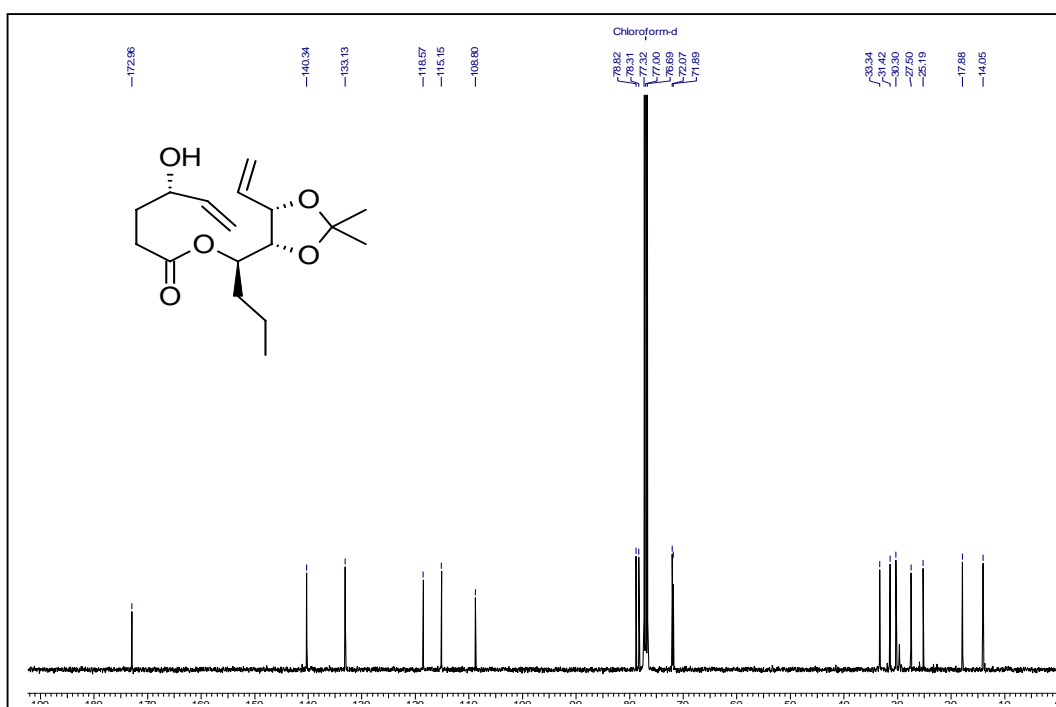
¹H NMR Spectrum of *epi*-20 in CDCl₃



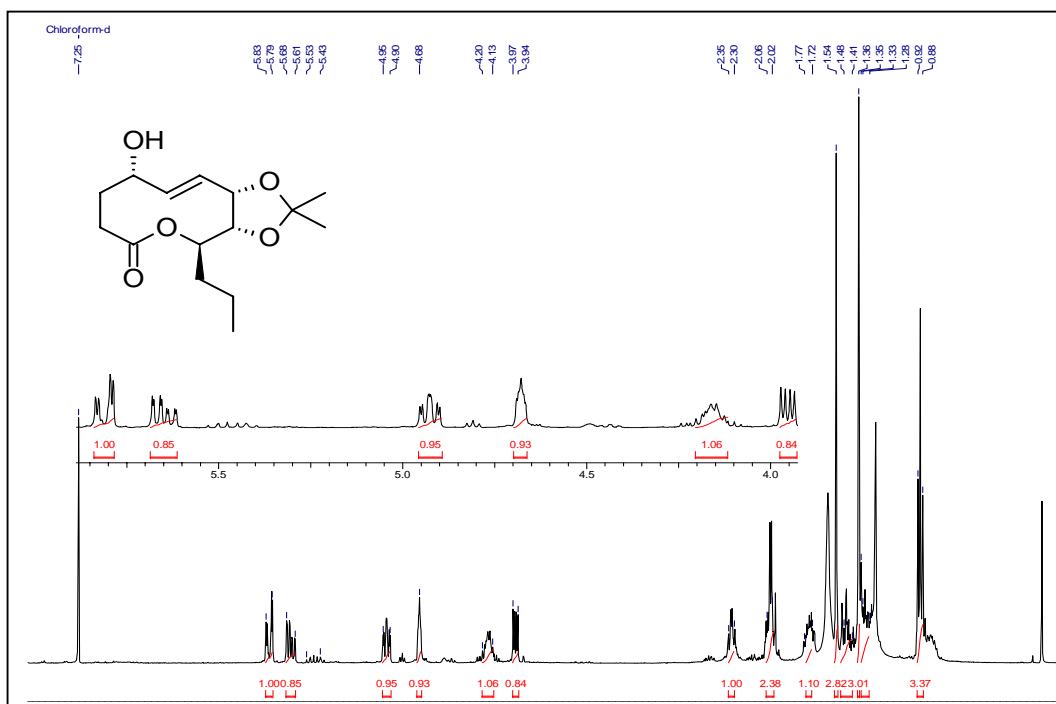
¹³C NMR Spectrum of *epi*-20 in CDCl₃



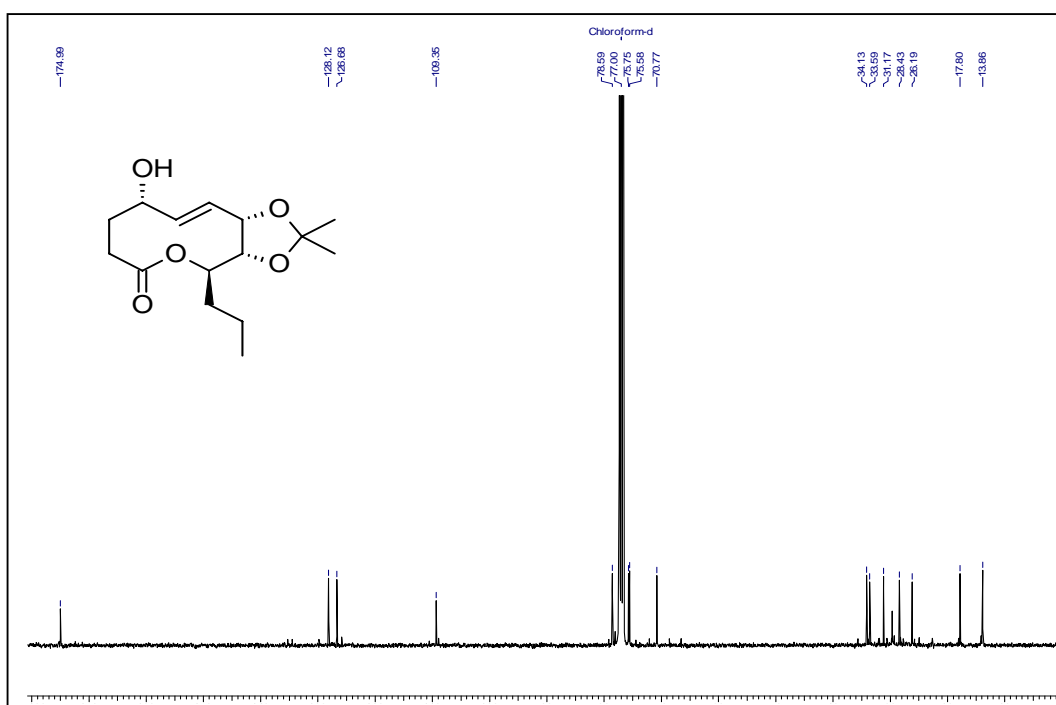
¹H NMR Spectrum of *epi*-25 in CDCl₃



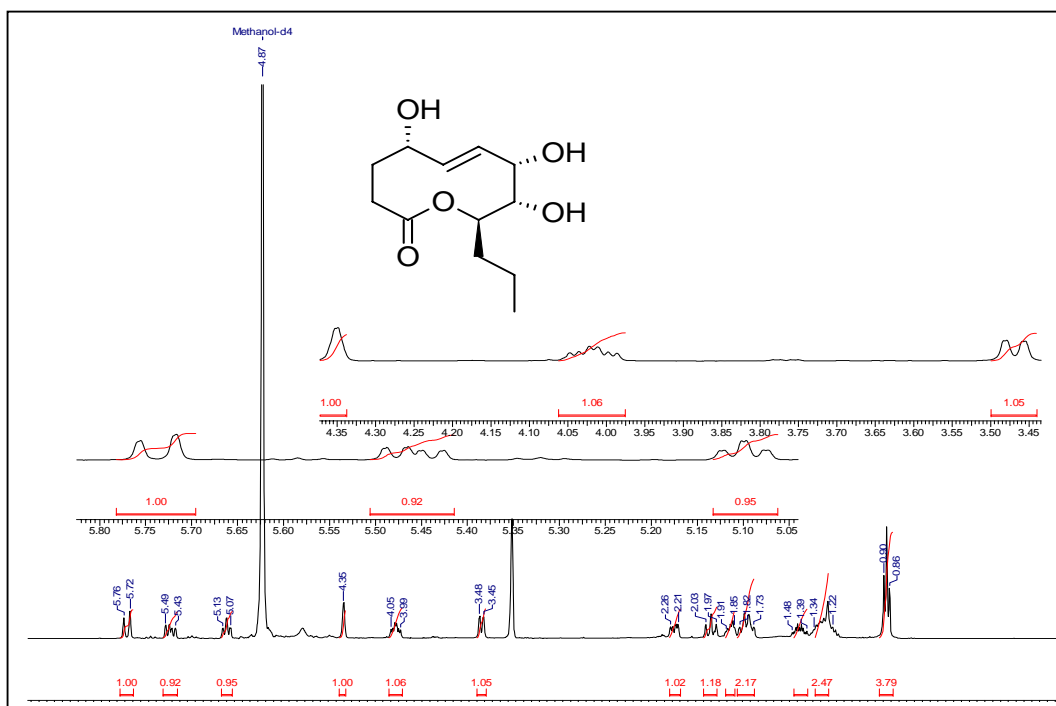
¹³C NMR Spectrum of *epi*-25 in CDCl₃



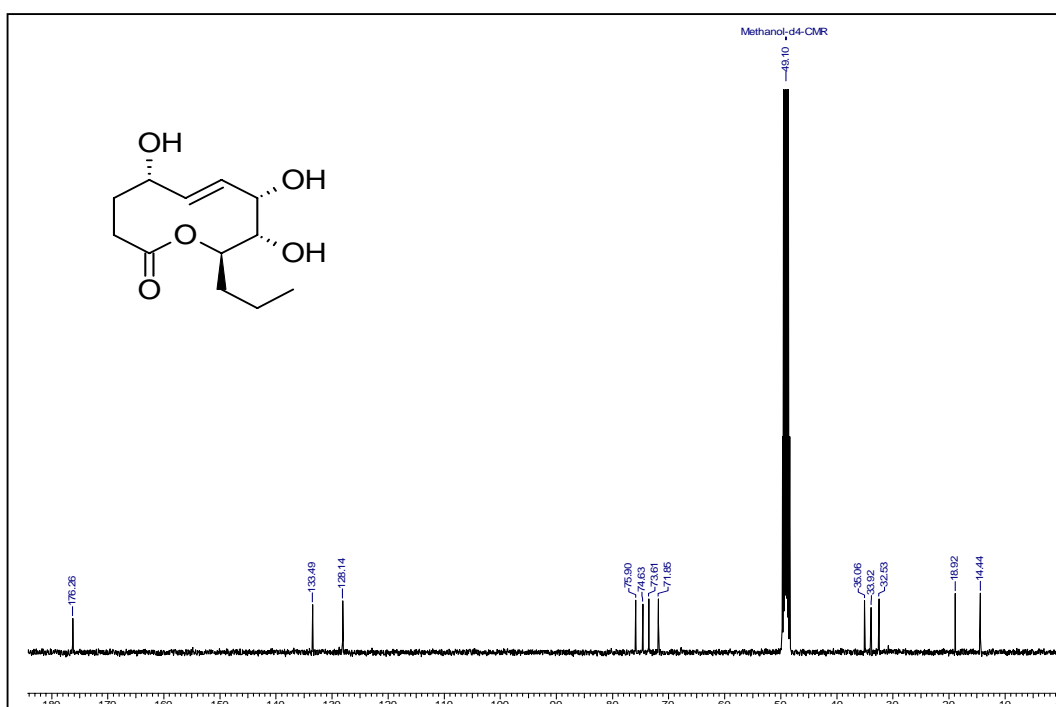
¹H NMR Spectrum of *epi*-26 in CDCl₃ (solvent used for reaction is DCM)



¹³C NMR Spectrum of *epi*-26 in CDCl₃ (solvent used for reaction is DCM)



¹H NMR Spectrum of 4-*epi*-stagonolide B in CDCl₃



¹³C NMR Spectrum of 4-*epi*-stagonolide B in CDCl₃

References

1. a) Rousseau, G. *Tetrahedron* **1995**, *51*, 2777. b) Dräger, G.; Kirschning, A.; Thiericke, R.; Zerlin, M. *Nat. Prod. Rep.* **1996**, *13*, 365.
2. a) Naves, Y. R.; Grampoloff, A. V. *Helv. Chim. Acta* **1942**, *25*, 1500. b) Demole, E.; Willhalm, B.; Stoll, M. *Helv. Chim. Acta* **1964**, *47*, 1152.
3. a) Ishida, T.; Wada, K. *J. Chem. Soc., Chem. Commun.* **1975**, 209.
4. a) Wada, K.; Ishida, T. *J. Chem. Soc., Chem. Commun.* **1976**, 340. b) Wada, K.; Ishida, T. *J. Chem. Soc., Perkin Trans.* **1979**, *1*, 1154.
5. a) Grabley, S.; Granzer, E.; Hutter, K.; Ludwig, D.; Mayer, M.; Thiericke, R.; Till, G.; Wink, J.; Phillips, S.; Zeeck, A. *J. Antibiot.* **1992**, *45*, 56. b) Gohrt, A.; Zeeck, A.; Hutter, K.; Kirsch, R.; Kluge, H.; Thiericke, R. *J. Antibiot.* **1992**, *45*, 66. c) Grabley, S.; Hammann, P.; Hutter, K.; Kirsch, R.; Kluge, H.; Thiericke, R.; Mayer, M.; Zeeck, A. *J. Antibiot.* **1992**, *45*, 1176.
6. Ayer, W. A.; Sun, M.; Browne, L. M.; Brinen, L. S.; Clardy, J. *J. Nat. Prod.* **1992**, *55*, 649.
7. Rukachaisirikul, V.; Pramjit, S.; Pakawatchai, C.; Isaka, M.; Supothina, S. *J. Nat. Prod.* **2004**, *67*, 1953.
8. Surat B.; Kittakoo P.; Masahiko I.; Daraporn P.; Morakot T.; Yodhathai T. *J. Nat. Prod.* **2001**, *64*, 965.
9. a) Nukina, M.; Sassa, T.; Ikeda, M. *Tetrahedron Lett.* **1980**, *21*, 301. b) Nukina, M.; Ikeda, M.; Sassa, T. *Agric. Biol. Chem.* **1980**, *44*, 2761.
10. Venkatasubbaiah, P.; Chilton, W. S. *J. Nat. Prod.* **1992**, *55*, 461.
11. Fuchser, J.; Zeeck, A. *Liebigs Ann. Recuell.* **1997**, 87.
12. Evidente, A.; Lanzetta, R.; Capasso, R.; Vurro, M.; Bottalico, A. *Phytochemistry* **1993**, *34*, 999.

13. a) Rivero-Cruz, J. F.; Garcia-Aguirre, G.; Cerda-Garcia-Rojas, C. M.; Mata, R. *Tetrahedron* **2000**, *56*, 5337. b) Rivero-Cruz, J. F.; Garcia-Aguirre, G.; Cerda-Garcia-Rojas, C. M.; Mata, R.; *J. Nat. Prod.* **2003**, *66*, 511.
14. Yuzikhin, O.; Mitina, G.; Berestetskiy, A. *J. Agri. Food Chem.* **2007**, *55*, 7707.
15. a) Evidente A.; Cimmino A.; Berestetskiy A.; Mitina G.; Andolfi A.; Motta A.; *J. Nat. Prod.* **2008**, *71*, 31. b) Evidente A.; Cimmino A.; Berestetskiy A.; Andolfi A.; Motta A. *J. Nat. Prod.* **2008**, *71*, 1897.
16. Funk, C. D. *Science* **2001**, *294*, 1871.
17. a) Niwa, H.; Inagaki, H.; Yamada, K. *Tetrahedron Lett.* **1991**, *32*, 5127. b) Niwa, H.; Watanabe, M.; Inagaki, H.; Yamada, K. *Tetrahedron* **1994**, *50*, 7385.
18. Papendorf, O.; Konig, G. M.; Wright, A. D.; Chorus, I.; Oberemm, A. *J. Nat. Prod.* **1997**, *60*, 1298.
19. Stierle, D. B.; Stierle, A. A.; Bugni, T.; Loewen, G. *J. Nat. Prod.* **1998**, *61*, 251.
20. Lindquist, N.; Fenical, W. *Tetrahedron Lett.* **1989**, *30*, 2735.
21. Congrève, M. S.; Holmes, A. B.; Hughes, A. B.; Looney, M. G. *J. Am. Chem. Soc.* **1993**, *115*, 5815.
22. a) Chu, M.; Mierzwa, R.; Xu, L.; He, L.; Terracciano, J.; Patel, M.; Gullo, V.; Black, T.; Zhao, W.; Chan, T.-M.; McPhail, A. T. *J. Nat. Prod.* **2003**, *66*, 1527. b) Edrada, R. A.; Heubes, M.; Brauers, G.; Wray, V.; Berg, A.; Grafe, U.; Wohlfarth, M.; Muhlbacher, J.; Schaumann, K.; Bringmann, G.; Sudarsono; Proksch, P. *J. Nat. Prod.* **2002**, *65*, 1598. c) Kinoshita, K.; Sasaki, T.; Awata, M.; Takada, M.; Yaginuma, S. *J. Antibiot.* **1997**, *50*, 961. d) Jansen, R.; Kunze, B.; Reichenbach, H.; Höfle, G. *Eur. J. Org. Chem.* **2000**, 913. e) Celmer, W. D.; Chmurny, G. N.; Moppett, C. E.; Ware, R. S.; Watts, P. C.; Whipple, E. B. *J. Am. Chem. Soc.* **1980**, *102*, 4203. f) Rasmussen, R. R.; Scherr, M. H.; Whittern, D. N.; Buko, A. M.; McAlpine, J. B. *J. Antibiot.* **1987**, *40*, 1383;

- McAlpine, J. B.; Mitscher, L. A.; Jackson, M.; Rasmussen, R. R.; Velde, D. V.; Veliz, E. *Tetrahedron* **1996**, *52*, 10327.
23. a) Shiina, I. *Chem. Rev.* **2007**, *107*, 239. b) Dräger, G.; Kirschning, A.; Thiericke, R.; Zerlin, M.; *Nat. Prod. Rep.* **1996**, *13*, 365. c) Rousseau, G.; *Tetrahedron* **1995**, *51*, 2777. d) Ferraz, H. M. C.; Bombonato, F. I.; Longo, J. L. S. *Synthesis* **2007**, 3261.
24. Corey, E. J.; Nicolaou, K. C. *J. Am. Chem. Soc.* **1974**, *96*, 5614.
25. Inanaga, J.; Hirata, K.; Saeki, H.; Katsuki, T.; Yamaguchi, M. *Bull. Chem. Soc. Jpn.* **1979**, *52*, 1989.
26. Trnka, T. M.; Grubbs, R. H. *Acc. Chem. Res.* **2001**, *34*, 18.
27. a) Back, T. G. *Tetrahedron* **1977**, *33*, 3041. b) Roxburgh, C. J. *Tetrahedron* **1993**, *49*, 10749.
28. a) Illuminati, G.; Mandolini, L.; *Acc. Chem. Res.* **1981**, *14*, 95. b) Wiberg, K. B.; Waldron, R. F. *J. Am. Chem. Soc.* **1991**, *113*, 7697.
29. a) Ruggli, P.; *Liebigs Ann. Chem.* **1916**, *412*, 1. b) Sicher, J. *Progr. Stereochem.* **1962**, *3*, 202.
30. Dunitz, J. D. *Pure Appl. Chem.* **1971**, *25*, 495.
31. a) Huisgen, R.; Ott, H. *Tetrahedron* **1959**, *6*, 253. b) Wiberg, K. B.; Waldron, R. F.; Schulte, G.; Saunders, M. *J. Am. Chem. Soc.* **1991**, *113*, 971.
32. a) Back, T. G. *Tetrahedron* **1977**, *33*, 3041. b) Parenty, A.; Moreau, X.; Campagne, J. M. *Chem. Rev.* **2006**, *106*, 911. c) Gradillas, A.; Perez-Castells, J. *Angew. Chem. Int. Ed.* **2006**, *45*, 6086.
33. a) Petasis, N. A.; Patane, M. A. *Tetrahedron* **1992**, *48*, 5757. b) Mehta, G.; Singh, V. *Chem. Rev.* **1999**, *99*, 881. c) Minnaard, A. J.; Wijnberg, J. B.; de Groot, P. A. *Tetrahedron* **1999**, *55*, 2115. d) Rousseau, G. *Tetrahedron* **1995**, *51*, 2777. e) Longo, L. S. Jr.; Bombonato, F. I.; Ferraz, H. M. C. *Quim. Nova*

- 2007, 30, 415. f) Crimmins, M. T.; Emmitte, K. A.; *J. Am. Chem. Soc.* **2001**, 123, 1533. g) Evans, P. A.; Holmes, A. B. *Tetrahedron* **1991**, 47, 9131.
34. Fürstner A.; Thomas M.; *Synlett* **1997**, 1010.
35. a) Ferraz H. M. C.; Bombonato F. I.; Longo Jr L. S. *Synthesis* **2007**, 3261 and references cited there in. b) Deiters A.; Martin S. F. *Chem. Rev.* **2004**, 104, 2199. c) Gaich T.; Mulzer J. *Curr. Top. Med. Chem.* **2005**, 5, 1473. d) Conrad J. C.; Fogg D. E. *Curr. Org. Chem.* **2006**, 10, 185. e) Gradillas A.; Pérez-Castells J. *Angew. Chem. Int. Ed.* **2006**, 45, 6086. f) Riatto V. B.; Pilli R. A.; Victor M. M. *Tetrahedron* **2008**, 64, 2279. g) Boeda F.; Clavier H.; Nolan S. P. *Chem. Commun.* **2008**, 2726. h) Herndon J. W. *Coord. Chem. Rev.* **2009**, 253, 86.
36. a) Fürstner A. Radkowski K. *Chem. Commun.* **2001**, 671. b) Fürstner A.; Radkowski K.; Wirtz C.; Goddard R.; Lehmann C. W.; Mynott R. *J. Am. Chem. Soc.* **2002**, 124, 7061.
37. For the construction of 10-membered carbocycles having the 2-ene-1,4-diol unit see: a) Caggiano L.; Castoldi D.; Beumer R.; Bayón P.; Telsler J.; Gennari C. *Tetrahedron Lett.* **2003**, 44, 7913. b) Castoldi D.; Caggiano L.; Panigada L.; Sharon O.; Costa A. M.; Gennari C. *Chem. Eur. J.* **2006**, 12, 51. c) Gennari C.; Castoldi D.; Sharon O. *Pure App. Chem.* **2007**, 79, 173.
38. Ramana C. V.; Khaladkar T. P.; Chatterjee S.; Gurjar M. K. *J. Org. Chem.* **2008**, 73, 3817.
39. a) Arai, M.; Morita, N.; Aoyagi, S.; Kibayashi, C. *Tetrahedron Lett.* **2000**, 41, 1199. b) (a) Kobayashi, Y.; Asano, M.; Yoshida, S.; Takeuchi, A. *Org. Lett.* **2005**, 7, 1533. (b) Kobayashi, Y.; Yoshida, S.; Asano, M.; Takeuchi, A.; Acharya, H. P. *J. Org. Chem.* **2007**, 72, 1707.
40. a) Pilli, R. A.; Victor, M. M. *Tetrahedron Lett.* **1998**, 39, 4421. b) Pilli, R. A.; Victor, M. M. *J. Braz. Chem. Soc.* **2001**, 12, 373. c) Pilli, R. A.; Victor, M. M.; de Meijere, A. *J. Org. Chem.* **2000**, 65, 5910.
41. Liu D.; Kozmin S. A. *Org. Lett.* **2002**, 4, 3005.

42. Alcaraz J.; Harneet J. J.; Mioskowski C.; Martel J. P.; Le Gall T.; Shin D.-S.; Falck J. R. *Tetrahedron Lett.* **1994**, *35*, 5449.
43. a) Gotor-Fernandez V.; Brieva R.; Gotor V. *J. Mol. Cat. B.* **2006**, *40*, 111. b) Ghanem A. *Tetrahedron* **2007**, *63*, 1721. c) Chojnacka A.; Obara R.; Wawrzenczyk C. *Tetrahedron: Asymm.* **2007**, *18*, 101.
44. a) Dale J. A.; Dull D. L.; Mosher H. S. *J. Org. Chem.* **1969**, *34*, 2543. b) Ohtani I.; Kusumi T.; Kashman Y.; Kakisawa H. *J. Am. Chem. Soc.* **1991**, *113*, 4092.
45. Corey E. J.; Venkateshwaralu A. *J. Chem. Soc. Chem. Soc.* **1972**, *94*, 6190
46. Anthony J. M.; Shui-Lung H.; Swern, D. *J. Org. Chem.* **1978**, *43*, 2480.
47. Enrico D. *J. Org. Chem.* **1986**, *51*, 567.
48. Choi W. J.; Moon H. R.; Kim H. O.; Yoo B. N.; Lee J. A.; Shin D. H. Jeong L. *S. J. Org. Chem.* **2004**, *69*, 2634.
49. Sharma, G. V. M.; Chander A. S.; Krishnudu, K.; Krishna P. R. *Tetrahedron Lett.* **1997**, *38*, 9051.
50. Inanaga J.; Hirata K.; Saeki H.; Katsuki T.; Yamaguchi M. *Bull. Chem. Soc. Jpn.* **1979**, *52*, 1989.
51. Kawaguchi ,T.; Funamori, N.; Matsuya, Y.; Nemoto, H. *J. Org. Chem.* **2004**, *69*, 505.
52. a) Schuster, M.; Blechert, S. *Angew. Chem., Int. Ed.* **1997**, *36*, 2036. b) Grubbs, R. H.; Chang, S. *Tetrahedron* **1998**, *54*, 4413. c) Fürstner, A.; *Angew. Chem. Int. Ed.* **2000**, *39*, 3812. d) Trnka, T. M.; Grubbs, R. H. *Acc. Chem. Res.* **2001**, *34*, 18.
53. Selected reports that deal with the proximal substituent effects on the construction of medium rings by RCM: a) Hoye T. R.; Zhao H. *Org. Lett.* **1999**, *1*, 1123. b) Ramírez-Fernández , J.; Collado, I. G.; Hernández-Galán, R., *Synlett* **2008**, 339. c) Ghosh, S.; Ghosh, S.; Sarkar, N. *J. Chem. Sci.* **2006**, *118*, 223. d) Mitchell, L.; Parkinson, J. A.; Percy, J. M. Singh K. *J. Org. Chem.*

2008, *73*, 2389. e) Imahori T.; Ojima H.; Yoshimura Y.; Takahata H. *Chem. Eur. J.* **2008**, *14*, 10762. f) Imahori T.; Ojima H.; Tateyama H.; Mihara Y.; Takahata H. *Tetrahedron Lett.* **2008**, *49*, 265.

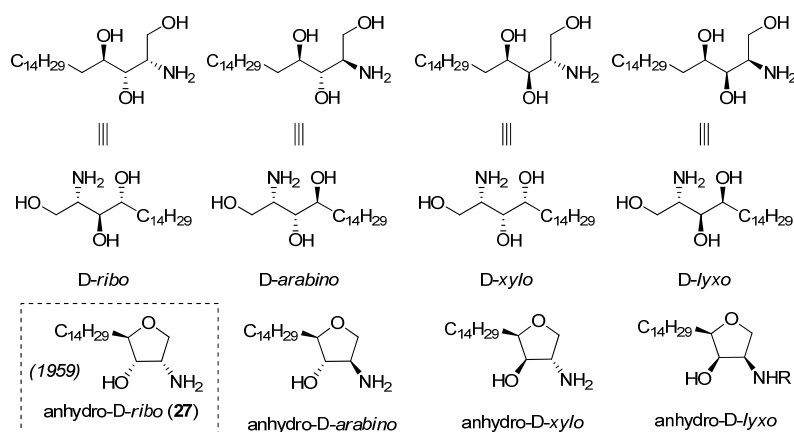
CHAPTER-I

**Section-II: Total synthesis of Jaspine B
(Pachastrissamine) from D-glucose**

Introduction

Sphingolipids are essential components of eukaryotic cells¹ and exhibit important physiological properties.² Phytosphingosines are a sub-class of the sphingolipid bases and consist of a 1,3,4-trihydroxy-2-amino unit at the head of a long hydrocarbon chain. Amongst these phytosphingosines, the most abundant phytosphingosine is *D-ribo*-phytosphingosine (**27**) comprising 18 carbon hydrocarbon chain (Figure 13).

Figure 13: Structures of C18 phytosphingosines

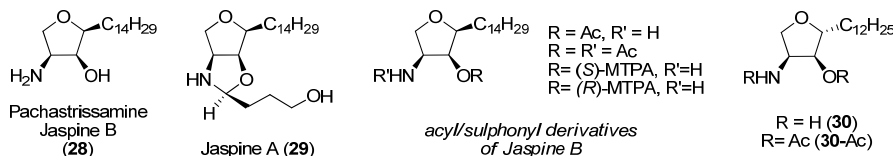


Anhydrophytosphingosines

O'Connell *et al.* isolated the first anhydrophytosphingosine (1,4-anhydro-D-*ribo*-phytosphingosine) in 1959 from corn phosphatide or cerebrin.³ The absolute stereochemistry of this compound as *D-ribo* was assigned with the help of the total synthesis of its truncated analogue **30**.⁴ Four decades after its isolation, another anhydrophytosphingosine named as Pachastrissamine (with *L-lyxo* configuration, also isolated and named as Jaspine B by another group) was isolated with important bioactivity.⁵ In 2002, Higa and co-workers reported the isolation and structure elucidation of second naturally occurring anhydrophytosphingosine derivative from a marine sponge, *pachastrissa* sp. and named as pachastrissamine (**28**) (Figure 14).⁶ Higa *et al.* elucidated the relative configuration of pachastrissamine by the NOE analysis of the *N,O*-diacetyl derivative, which indicated a *cis* relationship of all substituents around the tetrahydrofuran ring. The absolute configuration was determined by conversion of pachastrissamine to the corresponding (*R*)- and (*S*)-2-

methoxy-2-trifluoromethylphenyl acetyl (MTPA) derivatives and assigned the (*S*) configuration for C(2).

Figure 14: Structures of jaspine A (**29**)/B (**28**), and acetate/sulphonyl derivatives of Jaspine B



Later in 2003, Debitus and co-workers reported the isolation of two anhydrophytosphingosines from the marine sponge *Jaspis sp.*, which they named jaspines A (**29**) and B (**28**).⁵ Debitus group has also determined the relative and absolute configuration of jaspine A and jaspine B. First they prepared the *N,O*-diacetyl derivatives and compared the ¹H and ¹³C NMR data with that of the known truncated *N,O*-diacetyl-*D-ribo*-anhydrophytosphingosine derivative (**30-Ac**),⁵ which indicated an all-*cis* relationship of the substituents around the tetrahydrofuran ring. The absolute configuration was determined as (2*S*,3*S*,4*S*) *via* the NMR analyses of the (*S*)- and (*R*)-MTPA derivatives of *N*-acetyl jaspine B.

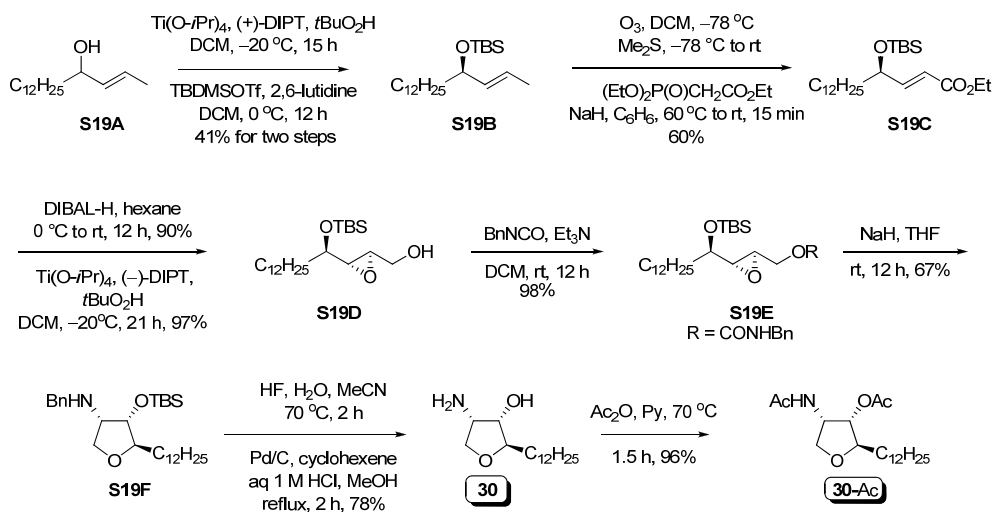
Synthesis of anhydrospingosines & Jaspine B

Since its isolation in 2002, there has been a great deal of interest from synthetic chemists concerning the total synthesis of pachastrissamine (Figure 14) because of its simple structure and promising anti-cancer activity. The screening of the jaspine B revealed its promising cytotoxic activity in the nanomolar range against P388, A549, HT29 and MEL28 (IC₅₀ = 0.001 μg/mL) cancer cell lines. This promising biological activity taken together with its simple structure, there have been several total synthesis reported prior to the initiation of our total synthesis of jaspine program. Even after our synthesis (2007), about 11 total syntheses have been reported. In the next few pages, the synthesis of anhydrospingosines in general and of jaspine B (reported prior to our synthesis) in particular will be described.

Synthesis of 2-carbon truncated 1,4-anhydro-D-ribo-phytosphingosine

The first anhydrophytosphingosine to be synthesized was a two carbon truncated 1,4-anhydro-D-ribo-phytosphingosine (**30**). Synthesis of **30** has been carried out to establish the absolute structure of the parent anhydrophytosphingosine **27**. The synthesis started with the kinetic resolution of allylic alcohol **S19A** under Sharpless asymmetric epoxidation conditions,⁷ which upon *O*-silylation afforded **S19B**. Subsequent ozonolysis of **S19B** followed by Horner-Wadsworth-Emmons olefination gave **S19C**.

Scheme 19: Total Synthesis of two carbon truncated 1,4-anhydro-D-ribo-sphingosine

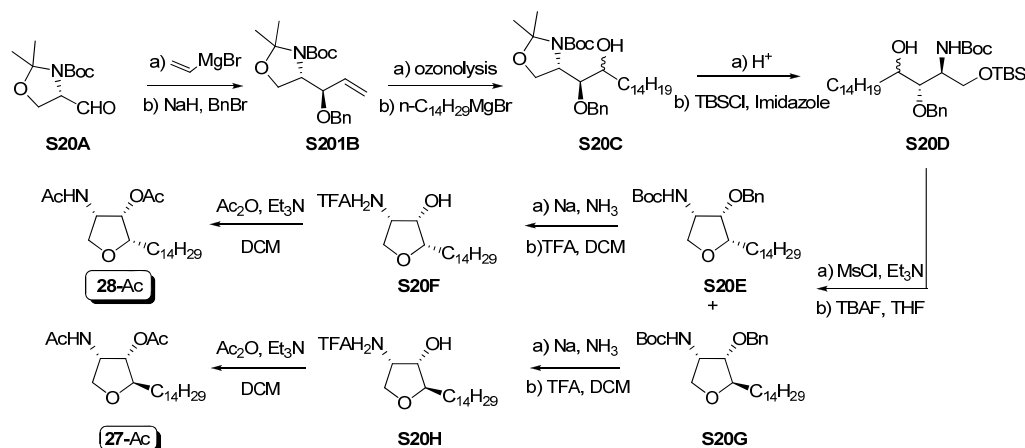


Reduction of the ester functionality of **S19C** with DIBAL-H, followed by second Sharpless asymmetric epoxidation gave the epoxide **S19D**. Treatment of **S19D** with benzylisocyanate gave the urethane **S19E** which upon treatment with NaH gave the N and O protected anhydrophytosphingosine **S19F**. Global deprotection of **S19F** gave **30** which was converted to its *N,O*-diacetyl derivative **30-Ac** for the characterization. The configuration of **30-Ac** (*2R,3S,4S*) was determined by ¹H NMR NOE studies (Scheme 19).⁴ Later, B. V. Rao and co-workers reported the first total synthesis of parent anhydrophytosphingosine en-route to the total synthesis of jaspine B.

1st Total synthesis of Jaspine B by B.V. Rao's group⁸

The first total synthesis of pachastrissamine (**28**) reported by Rao and co-workers used L-serine derived Garner's aldehyde **S20A**. Addition of vinylmagnesium bromide to **S20A** gave a separable 86:14 mixture of diastereoisomeric alcohols.⁹ The major diastereoisomer was converted to the corresponding benzyl ether **S20B** and subjected for the ozonolysis followed by addition of tetradecylmagnesium bromide to give an inseparable 70:30 mixture of the diastereoisomeric alcohols **S20C**. Protection and deprotection manipulations followed by mesylation and treatment of the mesylates with TBAF promoted desilylation and concomitant cyclization gave a separable 70:30 mixture of tetrahydrofurans, from which the all-*cis* diastereoisomer **S20E** and its C(2)-epimer **S20G** were isolated. Subsequent debenzylation and Boc-deprotection followed by diacetylation of **S20F** and **S20H** gave *N,O*-diacetyl jaspine B (**28-Ac**) and *N,O*-diacetyl 2-*epi*-jaspine B (**27-Ac**) respectively (Scheme 20).

Scheme 20: First total synthesis of Jaspine B by B. V. Rao's group

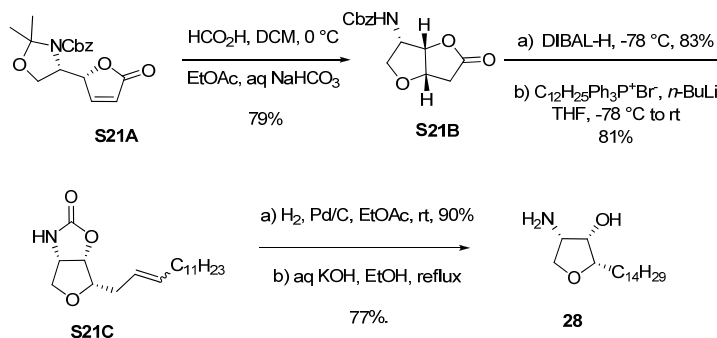


2nd Total Synthesis by Apurba Datta *et al.*¹⁰

In this synthesis, L-serine was converted into butenolide **S21A**. Treatment of **S21A** with formic acid enabled deprotection of the acetonide and subsequent Michael addition of the free hydroxyl group gave *cis*-fused bicyclic lactone **S21B**. Controlled reduction of **S21B** with DIBAL-H followed by Wittig olefination gave

S21C. Hydrogenation and cleavage of the resultant oxazolidinone of **S21C** afforded jaspine B (**28**) (Scheme 21).

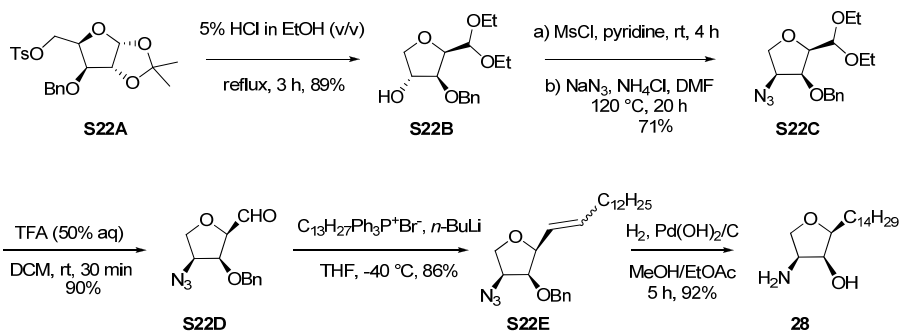
Scheme 21: The total synthesis of Jaspine B by Datta's group



3rd Total Synthesis by Linhardt's Group¹¹

During our synthesis in progress, Linhardt and co-workers reported the synthesis of jaspine B employing D-xylose. Tosylate **S22A** was prepared from D-xylose in three steps. Subsequent treatment with HCl in EtOH gave **S22B**, which upon mesylation and exposure to NaN₃ generated the azide derivative **S22C**. Hydrolysis of **S22C** with aqueous TFA afforded aldehyde **S22D** which after Wittig olefination gave an inseparable mixture of (*E*)- and (*Z*)-isomeric olefins **S22E**. Finally hydrogenation of **S22E** provided the pachastrissamine (**28**) (Scheme 22).

Scheme 22: Linhardt's total synthesis of jaspine B

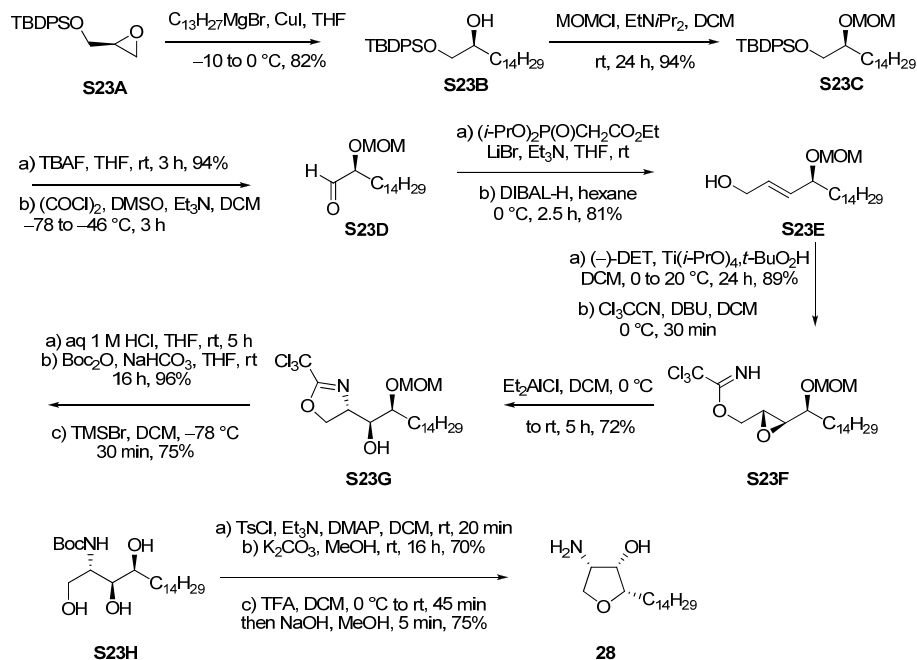


4th Total Synthesis by J. A. Marco *et al.*¹²

Marco and co-workers reported an enantiospecific synthesis of jaspine B from (*R*)-glycidol. The *O*-TBDPS protected (*R*)-glycidol **S23A** was initially treated

with tridecylmagnesium bromide in the presence of CuI to afford the corresponding alcohol **S23B**. Protection of free –OH in alcohol **S23B** as its MOM ether followed by desilylation, Swern oxidation, olefination and ester reduction gave the allylic alcohol **S23E**. Allylic alcohol **S23E** was subjected for Sharpless asymmetric epoxidation, with (–)-DET, and the resulting epoxide was treated with trichloroacetonitrile in the presence of DBU to give imino ester derivative **S23F**. Compound **S23F** was then reacted with Et₂AlCl to generate the oxazoline **S23G**, subsequent hydrolysis, *N*-Boc protection and MOM deprotection gave triol **S23H**. Triol **S23H** was then treated with TsCl, followed by K₂CO₃ in MeOH to induce cyclisation to give tetrahydrofuran derivative which on *N*-Boc deprotection gave pachastrissamine (**28**) (Scheme 23).

Scheme 23: Marco approach for synthesis of jaspine B

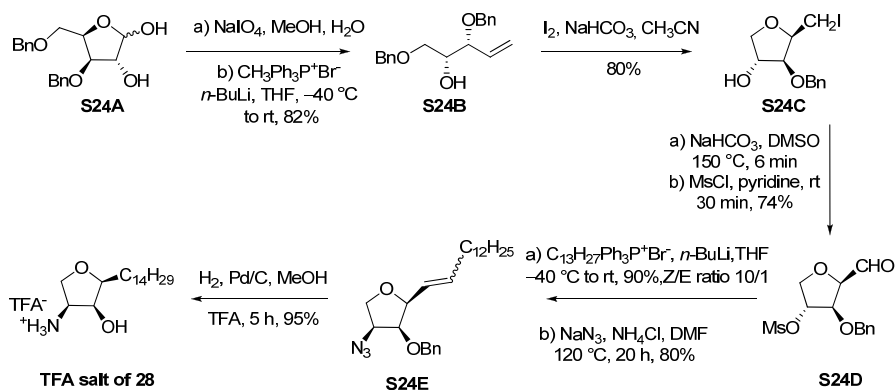


5th Total Synthesis by Du's group from D-Xylose

Subsequently, Du *et al.* reported an improved and scaleable synthesis of jaspine B from D-xylose.^{11b} In this approach, protected D-xylose derivative **S24A** was treated with NaIO₄ followed by Wittig reaction to afford **S24B**. The iodine-promoted debenzylative cycloetherification of **S24B** afforded the iodide **S24C**. Subsequent oxidation of the iodomethyl group followed by treatment with MsCl gave the mesylate **S24D**. Wittig olefination of **S24D** followed by displacement of

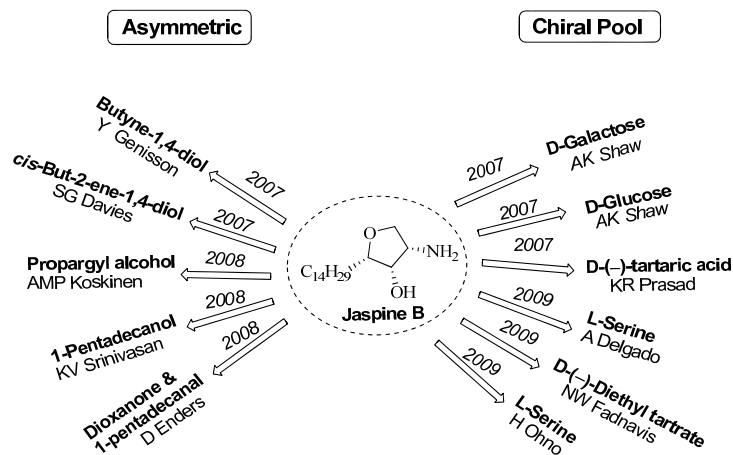
mesylate with NaN_3 gave **S24E**. Hydrogenation of **S24E** in MeOH containing 1% TFA furnished the target molecule pachastrissamine, in a salt form (Scheme 24).

Scheme 24: Du *et al*'s total synthesis of jaspine B



We have completed the 6th total synthesis of jaspine B and its enantiomer in 2007. Afterwards there were about 11 total syntheses reported. The starting material and author of the same has been presented in Figure 15.

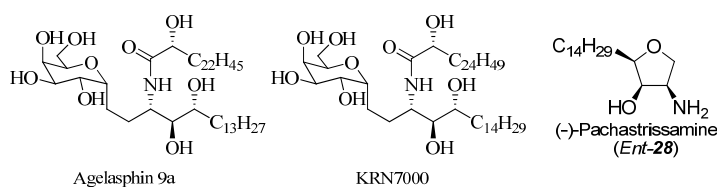
Figure 15



Present Work

Spingolipids are ubiquitous as components of cell membranes. Some unusual spingolipids have been described from marine organisms. An example is α -galactoceramide agelasphin, exhibiting potent *in vivo* antitumor activity but no *in vitro* cytotoxicity, from the sponge *Agelas mauritianus*.¹³ This discovery led Natori and co-workers to the development of a synthetic anticancer agent (coded KRN7000), which is now under clinical trials.¹⁴ Studies on the marine sponge *Pachastrissa sp.* by Higa and co-workers in 2002, led to the isolation of a cyclic anhydrophytosphingosine, which they named as pachastrissamine (**28**).⁶ Shortly after (in 2003), Debitus and co-workers reported the isolation of two anhydrophytosphingosines from the marine sponge *Jaspis sp.* and named as jaspine A (**29**) and jaspine B (**28**); pachastrissamine and jaspine B being identical.⁵ Jaspine B was reported to exhibit promising cytotoxic activity in the nanomolar range against P388, A549, HT29 and MEL28 (IC₅₀ = 1 ng/mL) cancer cell lines.

Figure 16:

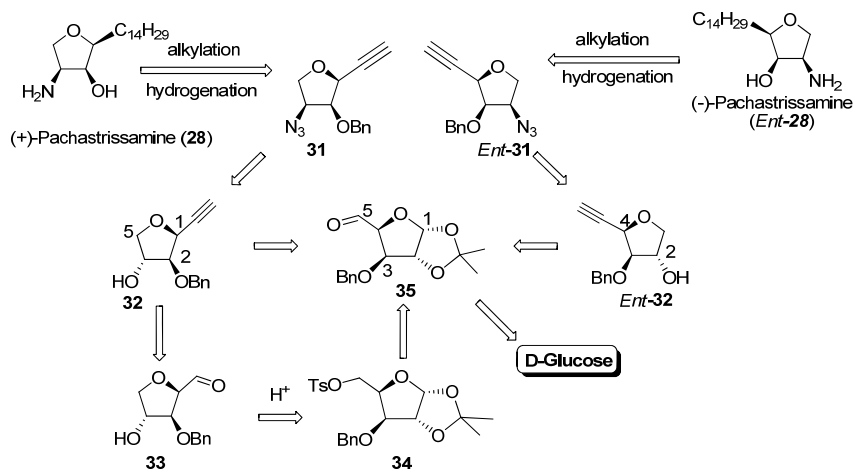


The promising biological activity and novel structural features of jaspine B (**28**) have inspired us for its synthesis. In order to gain rapid access to products of biological interests, we have initiated a program to synthesize the jaspine B and its enantiomer *Ent-28* with flexibility in modulating the side chain properties (Figure 16). In this section, we present our efforts on the synthesis of naturally occurring jaspine B beginning from cheaply available D-glucose.

Retrosynthetic analysis for both enantiomers of jaspine B from a common intermediate **35** is depicted in figure 30. Azidoalkynes **31** and *Ent-31*, which upon alkylation and hydrogenation should result in the synthesis of **28** and its enantiomer *Ent-28*, respectively. Alkyne functionality of azidoalkyne could be used for coupling reactions, and substitution of various alkyl halides to synthesize different analogues

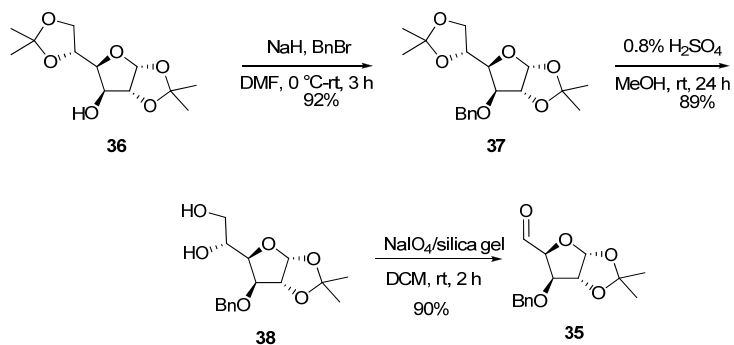
of jaspine B. We anticipated that the two enantiomeric furan systems **31** and *Ent*-**31** could be fashioned efficiently by employing selective Ohira-Bestmann alkylation at either end of **35**. The Bestmann alkylation at C(5) is a direct proposition. Whereas for the Ohira-Bestmann alkylation at C(1), we are interested to bring the acid mediated ring isomerisation of **34** (Figure 17).

Figure 17: Retrosynthetic analysis for jaspine B



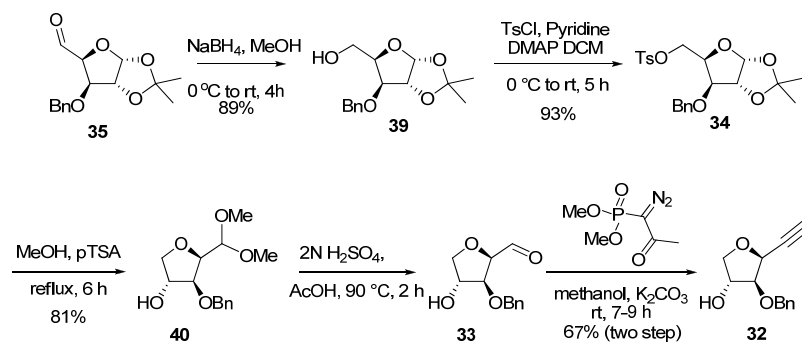
The synthetic endeavor began with the known diacetonide **36**. The free C(3)-OH in **36** was protected as its benzyl ether by treating it with benzyl bromide and sodium hydride in DMF to obtain compound **37**. Selective deprotection of 5,6-*O*-isopropylidene group by using 0.8% H₂SO₄ in methanol gave the diol **38** (Scheme 25). Diol **38** on oxidative cleavage by NaIO₄ adsorbed on silica gel in DCM afforded the aldehyde **35**.¹⁵

Scheme 25: Synthesis of aldehyde **35**



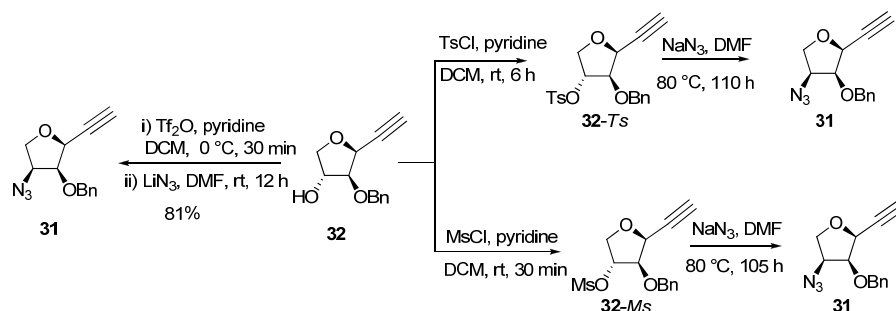
The crude aldehyde **35** was subjected to NaBH₄ reduction in methanol solvent.¹⁶ The hydroxyl group was then protected as its tosylate by treatment with tosyl chloride in pyridine to procure the compound **34**. Having the tosyl protected compound **34** in hand, the next task was acid mediated acetonide deprotection followed concomitant 2,5-ring closure to give dimethylacetal **40**.¹⁷

Scheme 26: Synthesis of alkynol **32**



The dimethylacetal **40** was converted to aldehyde using 2N H₂SO₄ and 50% acetic acid and resulting crude aldehyde **33** was treated with Ohira-Bestman reagent in MeOH/K₂CO₃ to afford the alkyne **32** (Scheme 26).¹⁸ The structure **32** of was established with the help of ¹H NMR, ¹³C NMR, mass and IR spectrum. In the ¹H NMR of alkyne **32**, the acetylenic proton resonated at δ 2.57 as a doublet with $J = 2.24$ Hz. The ¹³C spectrum revealed alkyne functionality at 76.4 ppm, (d) and 78.9 ppm, (s) and the IR spectrum showed acetylenic C–H stretching at 3305 cm⁻¹ and alkyne C≡C stretching at 2120 cm⁻¹.

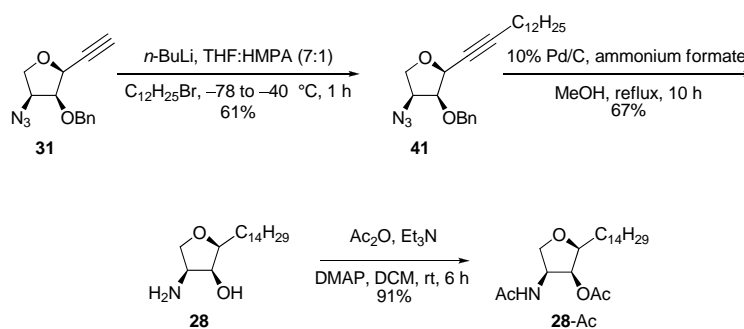
Scheme 27: Synthesis of azidoalkyne **31**



After having established an easy protocol for the preparation of the alkynol **32**, our next concern was the synthesis of the advanced azidoalkyne **31** and its further

elaboration into pachastrissamine. Various leaving groups at C(3)–O such as mesyl, tosyl, and triflate have been explored for the azide displacement reaction, amongst which, the reaction with triflate was found to be proceeding at rt. Thus the alkynol **32** was transformed to the corresponding azidoalkyne **31** by treatment with Tf₂O in pyridine followed by treating the intermediate triflate with LiN₃ in DMF at room temperature (Scheme 27). The spectral and analytical data of **31** were in well agreement with the proposed structure. In the ¹H NMR spectrum, alkyne-H showed doublet at 2.64 with *J* = 2.3 Hz and in the ¹³C NMR alkyne carbon resonated at 78.8 ppm as singlet and 76.4 ppm as doublet. In the IR spectrum, the absorption peaks at 2110 and 2125 cm⁻¹ indicated the presence of azide and alkyne functionality respectively.

Scheme 28: Synthesis of jaspine B



The next critical transformation to be carried out was alkylation of azidoalkyne **31**. After examining a set of bases and reaction conditions, we concluded that the alkylation of azidoalkyne **31** with 1-bromododecane was facile using *n*-BuLi in THF-HMPA and the alkylated product **41** was obtained in 61% yield (Scheme 28).¹⁹ The structural integrity of the alkylated product **41** was established with the help of NMR and mass spectral analyses. In the ¹H NMR spectrum, the nine long chain methylene protons showed broad singlet at δ 1.23, terminal methyl group showed triplet at δ 0.87 with coupling constant 6.9 Hz, mass spectrum showed peaks at 430.3 (100%, [M+NH₄]⁺), 435.2 (39.3%, [M+Na]⁺). Hydrogenolysis of **41** was affected by refluxing in methanol in the presence of ammonium formate and cat. 10% Pd/C to afford jaspine B as a white powder. The requisite jaspine B was characterized after chromatographic purification. The spectral and analytical data of synthetic **28** were identical with the data reported for the natural product **28** (Table

2). Specific rotation of the synthesized jaspine B (**28**) was $[\alpha]_D^{25} +10$ (c 0.7, MeOH) [lit. $[\alpha]_D +18^\circ$ (c 0.1, EtOH),⁶ and $[\alpha]_D^{20} +7$ (c 0.1, CHCl₃)⁵].

Further we have prepared the *N,O*-diacetate derivative by treatment of jaspine B with acetic anhydride and triethyl amine, cat. DMAP in DCM (Scheme 28). The ¹H NMR spectrum showed two singlets at δ 1.97 and 2.15, revealed the presence of two acetate groups, and other peaks in ¹H, ¹³C NMR were well comparable with reported data.⁵ The ¹³C NMR spectrum showed two singlets at 169.6 and 169.7 ppm for carbonyl carbons of two acetates. Other analytical data such as IR (1741 cm⁻¹), mass (m/z 385.2 (82.4%, [M+H]⁺), 407.3 (100%, [M+Na]⁺) and the structure of **28-Ac** was further established by single crystal X-ray analysis (Figure 18).

Figure 18: ORTEP Structure of Compound **28-Ac**

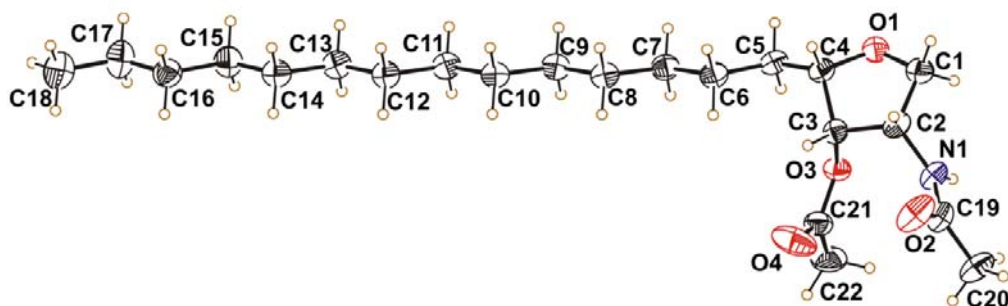


Table 2: ¹H NMR (CDCl₃, 500 MHz), ¹³C NMR (CDCl₃, 125 MHz) data of natural jaspine B and ¹H NMR (CDCl₃, 200 MHz), ¹³C NMR (CDCl₃) data of synthetic jaspine B.

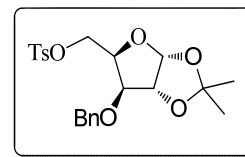
	Natural Jaspine B		Jaspine B	
	¹³ C	¹ H	¹³ C	¹ H
1a	72.2	3.51 (dd, $J = 7.0, 8.5$ Hz, 1H,)	72.3	3.35 (dd, $J = 4.05, 6.27$ Hz, 1H)
1b	72.2	3.95 (dd, $J = 7.0, 8.5$ Hz, 1H)	72.3	3.98 (dd, $J = 4.44, 6.40$ Hz, 1H)
2	54.2	3.68 (dt, $J = 5.0, 7.0$ Hz, 1H)	54.3	3.82 (dd, $J = 10.35, 15.33$ Hz, 1H)
3	71.6	3.88 (dd, $J = 3.5, 5.0$ Hz, 1H)	71.8	3.49 (dd, $J = 4.50, 10.43$ Hz, 1H)
4	83.1	3.75 (ddd, $J = 3.5, 7.0, 7.5$ Hz, 1H)	83.2	3.2 (dt, $J = 4.16, 6.72$ Hz, 1H)
5	29.3	1.71 (m, 2H,)		1.57–1.64 (m, 2H)
6–17	22.0–31.0	1.20–1.70 (m, 24H)		1.24–1.39 (m, 24H)
CH ₃	14.0	0.87 (t, $J = 6.5$ Hz, 3H)	31.9	0.87 (t, $J = 6.81$ Hz, 3H)
			22.6–29.7	
OH		2.10 (br. s)	14.1	2.22 (br. s)
NH ₂		2.10 (br. s)		

Conclusion

A simple chiral pool strategy for the total synthesis of jaspine B has been developed. Starting from the known and easily available glucose diacetone, pachastrissamine has been synthesized in nine linear steps with an overall yield of 17.3%. As we have added the side chain at the penultimate step, our strategy is endowed with sufficient flexibility for the synthesis of pachastrissamine analogues with variation of side chain or alteration of its length.

Experimental

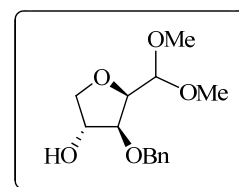
3-O-Benzyl-1,2-O-isopropylidene-5-O-p-toluenesulfonyl- α -D-xylofuranose (**34**)



At 0 °C, a solution of compound **39** (3 g, 10.7 mmol), pyridine (2 mL) and DMAP (100 mg) in dry CH₂Cl₂ (20 mL) was treated with *p*-toluenesulfonyl chloride (2.2 g, 11.7 mmol) and the reaction mixture was stirred for 5 h at rt. The reaction mixture was partitioned between water (40 ml) and CH₂Cl₂ (50 mL) and the organic layer was washed with saturated CuSO₄, water, brine, dried (Na₂SO₄) and concentrated. The crude product was purified over a silica gel column (8 to 10 % EtOAc in petroleum ether as an eluent) to obtain the tosylate **34** (4.32 g, 93%) as a colorless oil.

Mol. Formula: C₂₂H₂₆O₇S. [α]_D²⁵: -30.9 (*c* = 2.2, CHCl₃). **IR (CHCl₃)** ν : 3089, 2988, 1598, 1496, 1371, 1215, 1076, 832, 698, 665 cm⁻¹. **¹H NMR (CDCl₃, 200 MHz):** δ 1.28 (s, 3H), 1.43 (s, 3H), 2.41 (s, 3H), 3.94 (d, *J* = 3.0 Hz, 1H), 4.17 (dd, *J* = 5.8, 9.4 Hz, 1H), 4.2 (dd, *J* = 5.8, 14.9 Hz, 1H), 4.35 (dt, *J* = 3.0, 5.8 Hz, 1H), 4.44 (d, *J* = 11.8 Hz, 1H), 4.55 (d, *J* = 3.7 Hz, 1H), 4.61 (d, *J* = 11.8 Hz, 1H), 5.85 (d, *J* = 3.7 Hz, 1H), 7.21–7.27 (m, 4H), 7.30–7.34 (m, 3H) 7.75–7.79 (m, 2H). **¹³C NMR (CDCl₃, 50 MHz):** δ 21.5 (q), 26.2 (q), 26.7 (q), 66.9 (t), 71.9 (t), 77.4 (d), 81.1 (d), 81.9 (d), 105.1 (d), 112.0 (s), 127.6 (d), 127.9 (d), 128.0 (d), 128.4 (d), 129.8 (d), 132.5 (s), 136.9 (s), 144.9 (s) ppm. **ESI-MS *m/z*:** 435.16(2.5%, [M + 1]⁺), 452.17 (100%, [M + NH₄]⁺), 457.12 (72.5%, [M + Na]⁺). **Elemental Analysis Calcd.:** C, 60.81; H, 6.03%; Found: C, 60.72; H, 6.10%.

2,5-Anhydro-3-O-benzyl- α -D-xylose dimethyl acetal (**40**)

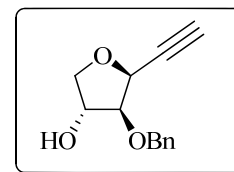


To a solution of compound **34** (6 g, 13.8 mmol) in methanol (150 mL), *p*-toluene sulphonic acid (300 mg) was added and the reaction mixture was stirred under reflux for 6 h. Then reaction mixture was neutralized with saturated sodium bicarbonate and concentrated. Residue was extracted with CH₂Cl₂ (2 x 75 mL) and the combined organic layer was dried (Na₂ SO₄) and concentrated. Purification of the

crude product by silica gel column chromatography (40 to 50% EtOAc in petroleum ether as an eluent) gave **40** (3 g, 81%) as a colorless oil.

Mol. Formula: C₁₄H₂₀O₅. [α]_D²⁵ = +37.6 (*c* = 3, CHCl₃). **IR (CHCl₃)** ν : 3427, 3012, 2940, 1497, 1454, 1216, 1087, 756, 698, 666 cm⁻¹. **¹H NMR(CDCl₃, 200 MHz):** δ 3.36 (s, 3H), 3.40 (s, 3H), 3.73 (d, *J* = 9.8 Hz, 1H), 3.91 (d, 3.5 Hz, 1H), 4.09 (dd, *J* = 3.9, 9.7 Hz, 1H), 4.14 (dd, *J* = 3.6, 9.7 Hz, 1H), 4.30 (br.d, *J* = 3.7 Hz, 1H), 4.52 (d, *J* = 11.8 Hz, 1H), 4.59 (d, *J* = 3.1 Hz, 1H), 4.62 (d, *J* = 7.9 Hz, 1H), 7.25–7.33 (m, 5H). **¹³C NMR (CDCl₃, 50 MHz):** δ 52.7 (q), 54.9 (q), 72.0 (t), 74.0 (d), 74.1 (t), 78.7 (d), 84.0 (d), 102.1 (d), 127.3 (d), 127.5 (d), 128.1 (d), 137.7 (s) ppm. **ESI-MS *m/z*:** 269.15 (21.8%, [M+1]⁺), 291.11 (100%, [M+Na]⁺). **Elemental Analysis Calcd.:** C, 62.67; H, 7.51%; Found: C, 62.7; H, 7.62%.

**(3R,4S,5S)-4-(Benzyloxy)-5-ethynyltetrahydrofuran-3-ol
(32)**



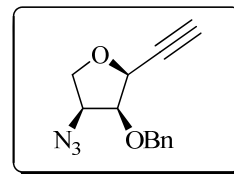
A suspension of acetal **40** (6 g, 22.3 mmol) in sulphuric acid (2N, 30 mL) and 50% acetic acid (30 mL) was heated at 90 °C for 2 h. The reaction mixture was cooled to room temperature and neutralized with sodium bicarbonate and extracted with CH₂Cl₂ (2 X 150 mL). The combined organic layer was washed with brine, dried (Na₂SO₄) and concentrated. The resulting crude aldehyde **33** was used directly for the next step without any further purification.

A suspension of above aldehyde **33**, dimethyl-1-diazo-2-oxopropylphosphonate (3.8 g, 19.7 mmol), potassium carbonate (2.8 g, 20.2 mmol) in methanol (20 ml) was stirred at 25 °C for 9 h. After the completion of reaction as indicated by TLC, methanol was removed and the crude product was partitioned between water and CH₂Cl₂. The aqueous layer was extracted with CH₂Cl₂ and the combined organic layer was dried (Na₂SO₄) and concentrated. Purification of the crude product by silica gel column chromatography (10 to 20% EtOAc in petroleum ether) gave **32** (3.27 g, 67%) as a colorless oil.

Mol. Formula: C₁₃H₁₄O₃. [α]_D²⁵ = -57.9 (*c* = 1, CHCl₃). **IR (CHCl₃)** ν : 3403, 3290, 3065, 2942, 2120, 1598, 1496, 1218, 1069, 754, 698, 666 cm⁻¹. **¹H NMR (CDCl₃, 200**

MHz): δ 2.15 (br.s, 1H), 2.57 (d, $J = 2.3$ Hz, 1H), 3.67 (dd, $J = 2.2, 9.8$ Hz, 1H), 3.91 (dd, $J = 2.3, 4.7$ Hz, 1H), 4.18 (dd, $J = 4.7, 9.8$ Hz, 1H), 4.34 (dt, $J = 2.3, 4.7$ Hz, 1H), 4.64 (d, $J = 11.9$ Hz, 1H), 4.77 (dd, $J = 2.2, 4.7$ Hz, 1H), 4.78 (d, $J = 11.9$ Hz, 1H), 7.27–7.38 (m, 5H). ¹³C NMR (CDCl₃, 50 MHz): δ 70.6 (d), 72.7 (t), 73.1 (t), 75.5 (d), 76.4 (d), 78.9 (s), 84.9 (d), 127.8 (d), 127.9 (d), 128.5 (d), 137.5 (s) ppm. **ESI-MS m/z :** 219.1(23.3%, [M+H]⁺), 236.2 (37.9%, [M+NH₄]⁺), 241.18 (100%, [M+Na]⁺), 257.1 (18.2%, [M+K]⁺). **Elemental Analysis Calcd.:** C, 71.54; H, 6.47%; Found: C, 66.44 ; H, 6.59%.

(2S,3S,4S)-4-Azido-3-(benzyloxy)-2-ethynyltetrahydrofuran (31)

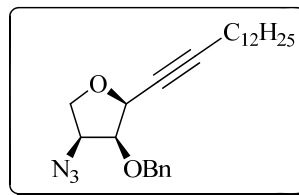


At -20 °C, a solution of **32** (1.6 g, 7.3 mmol) and pyridine (1.7 mL, 22 mmol) in CH₂Cl₂ (15 mL) was treated with triflic anhydride (1.5 mL, 8.8 mmol) and reaction was stirred for 30 min. The reaction mixture was diluted with CH₂Cl₂ (50 mL) and washed with cold 1N HCl and saturated NaHCO₃, brine and water. The organic extract was dried (Na₂SO₄) and concentrated under reduced pressure to obtain the intermediate triflate (quantitative) as a liquid and was used for the next step with out any further purification.

A solution of above triflate in DMF (10 mL) was cooled to 0 °C and treated with lithium azide (1.6 gm, 32.7 mmol) and the contents were stirred at room temperature for 12 h. The reaction mixture was diluted with EtOAc (100 ml), washed with water (3 X 20 mL), dried (Na₂SO₄) and concentrated under reduced pressure. Purification of the residue by column chromatography (5 to 10% EtOAc in petroleum ether) gave **31** (1.44 g, 81%) as a colorless oil.

Mol. Formula: C₁₃H₁₃N₃O₂. $[\alpha]_D^{25} = -69$ ($c = 1.3$, CHCl₃). **IR (CHCl₃) ν :** 3304, 3020, 2125, 2110, 1603, 1585, 1216, 759, 698, 638 cm⁻¹. **¹H NMR (CDCl₃, 200 MHz):** δ 2.64 (d, $J = 2.3$ Hz, 1H), 3.92–4.04 (m, 3H), 4.16 (br.dd, $J = 5.0, 6.1$ Hz, 1H), 4.71 (dd, $J = 2.3, 6.1$ Hz, 1H), 4.74 (d, $J = 6.2$ Hz, 1H), 4.83 (d, $J = 11.8$ Hz, 1H), 7.31–7.46 (m, 5H). **¹³C NMR (CDCl₃, 50 MHz):** δ 59.9 (d), 69.4 (t), 69.7 (d), 73.2 (t), 76.9 (d), 78.7 (s) 79.3 (d), 127.9 (d), 128.0 (d), 128.5 (d), 137.0 (s) ppm. **ESI-MS m/z :** 244.3 (100%, [M+H]⁺), 267.3 (27.17%, [M+Na]⁺), 283.39 (39.67%, [M+K]⁺). **Elemental Analysis Calcd.:** C, 64.19; H, 5.39; N, 17.27%; Found: C, 64.29; H, 5.21, N 17.18%.

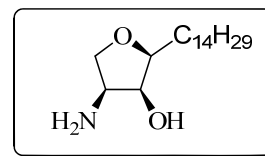
(2*S*,3*S*,4*S*)-4-Azido-3-(benzyloxy)-2-(tetradec-1-ynyl)tetrahydrofuran (41)



A solution of **31** (0.5 g, 2.06 mmol) in THF (15 mL) and HMPA (3 mL) was cooled to $-78\text{ }^{\circ}\text{C}$ and treated with *n*-BuLi (1.4 mL, 1.6 M in hexanes, 2.62 mmol) and stirred for 20 min. To this, dodecyl bromide (0.75 mL, 3.085 mmol) was added dropwise and the reaction mixture was warmed to $-30\text{ }^{\circ}\text{C}$ and allowed to stir for 1 h at this temperature. The reaction mixture was quenched by saturated aqueous solution of NH_4Cl and extracted with ethyl acetate. The combined organic extract was washed with brine, dried over (Na_2SO_4), filtered and concentrated under reduced pressure. The residue was purified by silica gel column chromatography (4% ethyl acetate in petroleum ether) to produce **41** (490 mg, 61% yield) as a colorless oil.

Mol. Formula: $\text{C}_{25}\text{H}_{37}\text{N}_3\text{O}_2$. $[\alpha]_{\text{D}}^{25} = -70.6$ ($c = 1$, CHCl_3). **IR** (CHCl_3) ν : 3018, 2927, 2855, 2108, 1497, 1455, 1215, 1059, 698, 668 cm^{-1} . **^1H NMR** (CDCl_3 , 200 MHz): δ 0.87 (t, $J = 6.7$ Hz, 3H), 1.23 (br.s, 18H), 1.43–1.57 (m, 2H), 2.25 (dt, $J = 2.0, 7.0$ Hz, 2H), 3.87 (dt, $J = 1.4, 5.5$ Hz, 1H), 3.94–4.05 (m, 2H), 4.11 (dd, $J = 5.4, 10.9$ Hz, 1H), 4.68–4.73 (m, 1H), 4.79 (d, $J = 12.6$ Hz, 1H), 4.82–4.99 (m, 1H), 7.29–7.45 (m, 5H). **^{13}C NMR** (CDCl_3 , 50 MHz): δ 14.1 (q), 19.0 (t), 22.7 (t), 28.4 (t), 28.9 (t), 29.1 (t), 29.3 (2t), 29.5 (t), 29.6 (t), 31.9 (t), 60.1 (d), 68.9 (t), 70.5 (d), 73.1 (t), 74.6 (d), 79.6 (s), 90.0 (s), 127.7 (d), 127.9 (d), 128.4 (d), 137.4 (s) ppm. **ESI-MS m/z :** 430.3 (100%, $[\text{M}+\text{NH}_4]^+$), 435.2 (39.3%, $[\text{M}+\text{Na}]^+$). **Elemental Analysis Calcd.:** C, 72.96; H, 9.06; N, 10.21%; Found: C, 72.78; H, 9.1; N, 10.05%.

Synthesis of Jaspine B (28)

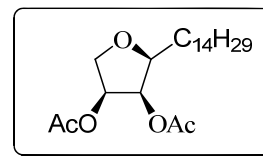


A suspension of **41** (150 mg, 0.36 mmol), 10% Pd/C (20 mg) and ammonium formate (230 mg, 3.64 mmol) in MeOH (4 mL) was refluxed for 10 h. The reaction mixture was filtered through celite and the celite pad washed with methanol. The

combined filtrate was concentrated under reduced pressure and purified by column chromatography (1:4:95, aq. NH₄OH/MeOH/CHCl₃) to obtain jaspine B (73 mg, 67%) as a white solid

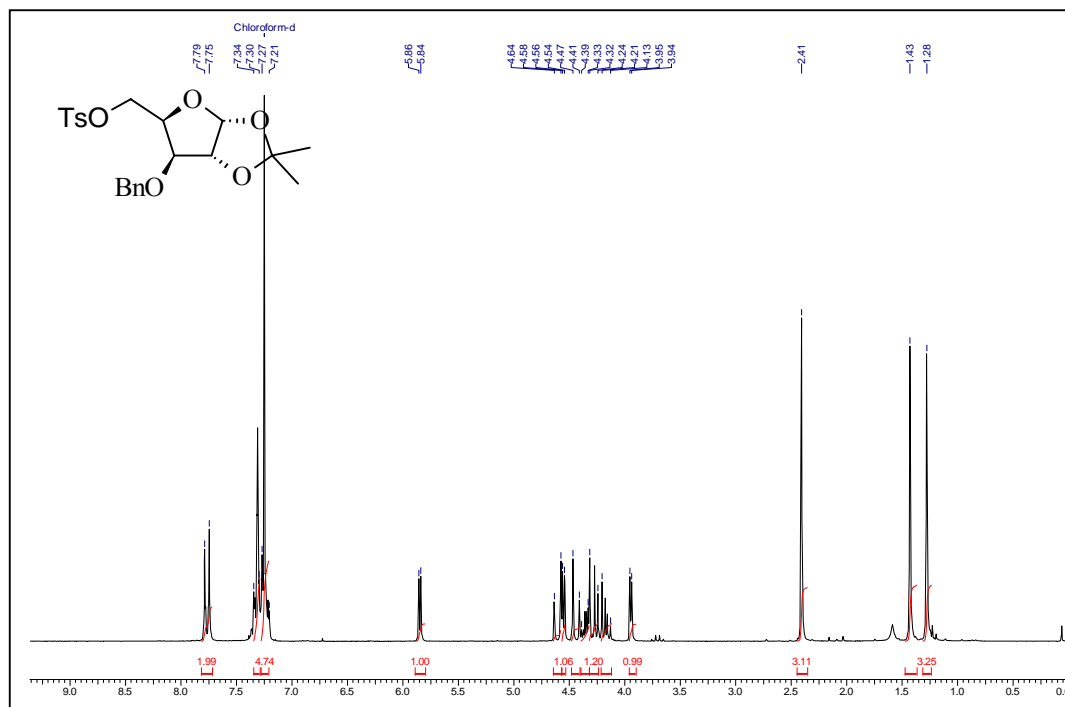
Mol. Formula: C₁₈H₃₇NO₂. [α]_D²⁵ = +10 (*c* = 0.7, MeOH). **IR (CHCl₃)** ν : 3341, 2926, 2855, 1466, 1215, 1046; 758 cm⁻¹. **¹H NMR (CDCl₃, 200 MHz):** δ 0.87 (t, *J* = 6.8 Hz, 3H), 1.24–1.39 (m, 24H), 1.57–1.64 (m, 2H), 2.22 (br. s, 2H), 3.2 (dt, *J* = 4.2, 10.6 Hz, 1H), 3.49 (dd, *J* = 4.5, 10.4 Hz, 1H), 3.82 (dd, *J* = 10.4, 15.3 Hz, 1H), 3.98 (dd, *J* = 4.4, 6.4 Hz, 1H), 4.35 (dd, *J* = 4.1, 6.3 Hz, 1H). **¹³C NMR (CDCl₃, DMSO-D₆, 100MHz):** δ 14.1 (q), 22.6 (t), 26.3 (t), 29.3 (t), 29.6 (t), 29.8, (t), 31.9 (t), 54.3 (d), 71.8 (d), 72.4 (t), 83.2 (d) ppm. **ESI-MS *m/z*:** 300.32 (100%, [M+1]).

N,O-Diacetyl pachastrissamine (28-Ac)

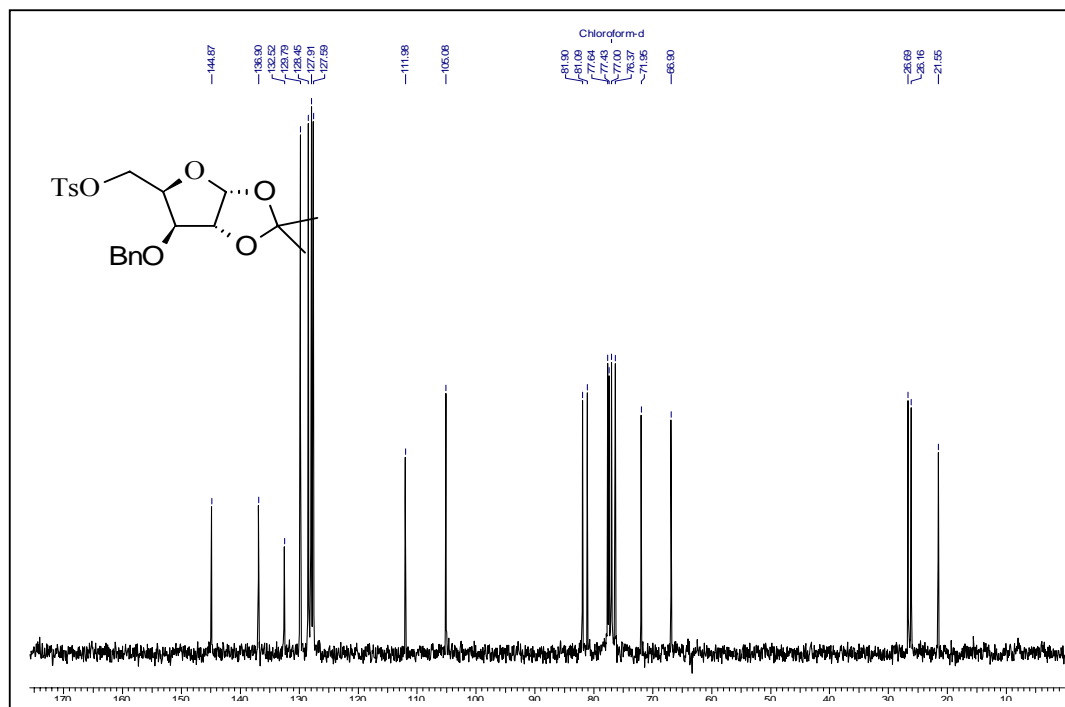


To a solution of **28** (300 mg, 0.1 mmol) in pyridine (1.5 mL), acetic anhydride (0.5 mL, 5.2 mmol) was added at 25 °C and stirred for 15 h. After completion of the reaction, pyridine and excess of acetic anhydride were removed under reduced pressure and the crude product was purified by silica gel column chromatography (50→70 % EtOAc in petroleum ether) to obtain **28-Ac** (35 mg, 91%) as a crystalline solid. Crystals of X-ray quality were obtained by a slow evaporation of dilute solution of **28-Ac** in ethyl acetate.

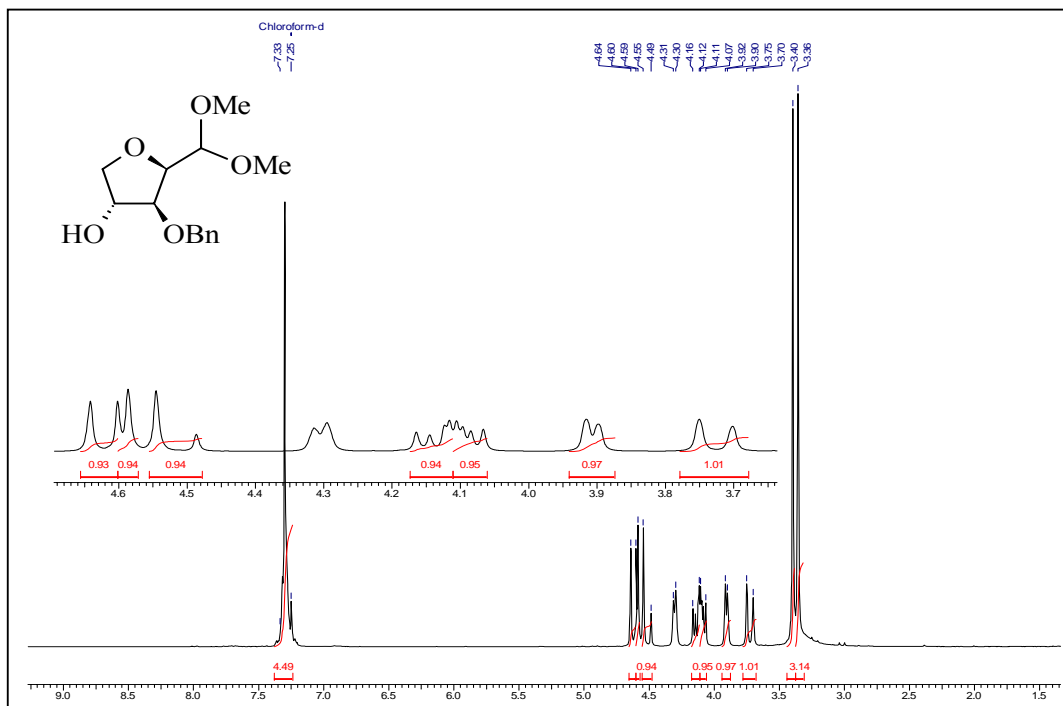
Mol. Formula: C₂₂H₄₀O₅. [α]_D²⁵ = -34.6 (*c* 1, CHCl₃). **IR (CHCl₃)** ν : 3019, 2927, 2855, 1743, 1676, 1550, 1467, 1374, 1215, 1049, 757 cm⁻¹. **¹H NMR (CDCl₃, 200 MHz):** δ 0.86 (t, *J* = 6.8 Hz, 3H), 1.23 (br.s, 24H), 1.40–1.48 (m, 2H), 1.97 (s, 3H), 2.15 (s, 3H), 3.58 (dd, *J* = 7.9, 8.6 Hz, 1H), 3.85–3.93 (m, 1H), 4.06 (dd, *J* = 8.1, 8.6 Hz, 1H), 4.80 (dq, *J* = 5.4, 8.0 Hz, 1H), 5.37 (dd, *J* = 3.4, 5.5 Hz, 1H), 5.61 (d, *J* = 8.2 Hz, 1H). **¹³C NMR (CDCl₃, 125 MHz):** δ 14.1 (q), 20.6 (q), 22.6 (t) 23.1 (q), 26.0 (t), 29.3 (2t), 29.4 (t), 29.5 (2t), 29.6 (2t), 31.9 (t), 51.3 (d), 69.9 (t), 73.5 (d), 81.20 (d), 169.8 (2xs) ppm. **ESI-MS *m/z*:** 385.2 (82.4%, [M+1]⁺), 407.3 (100%, [M+Na]⁺).



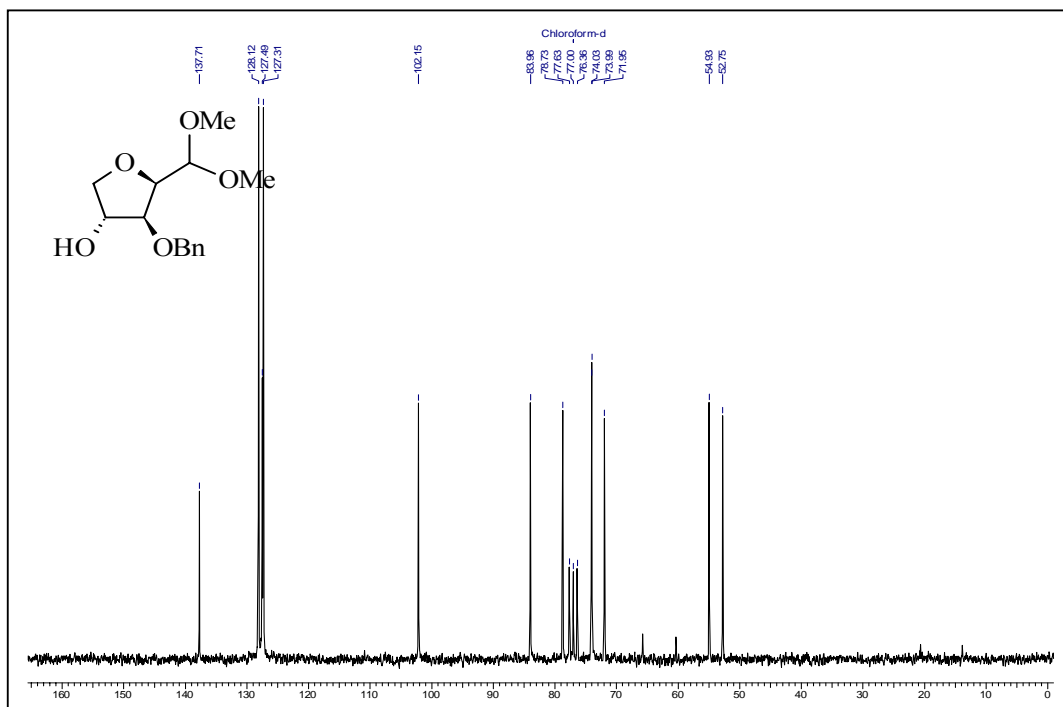
¹H NMR Spectrum of 34 in CDCl₃



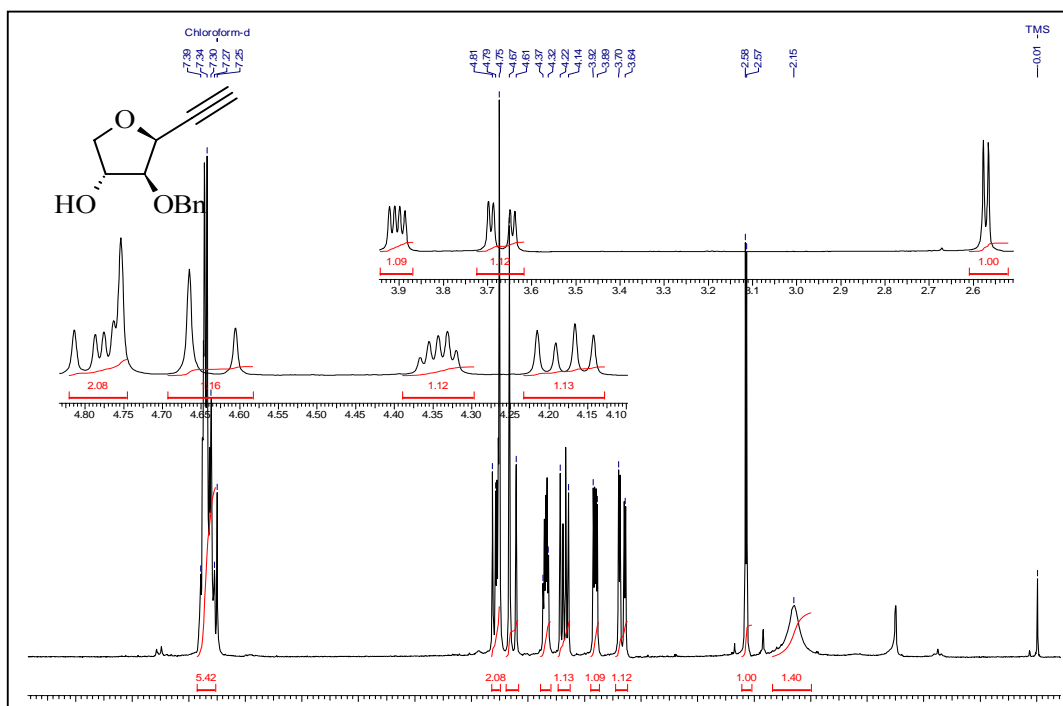
¹³C NMR Spectrum of 34 in CDCl₃



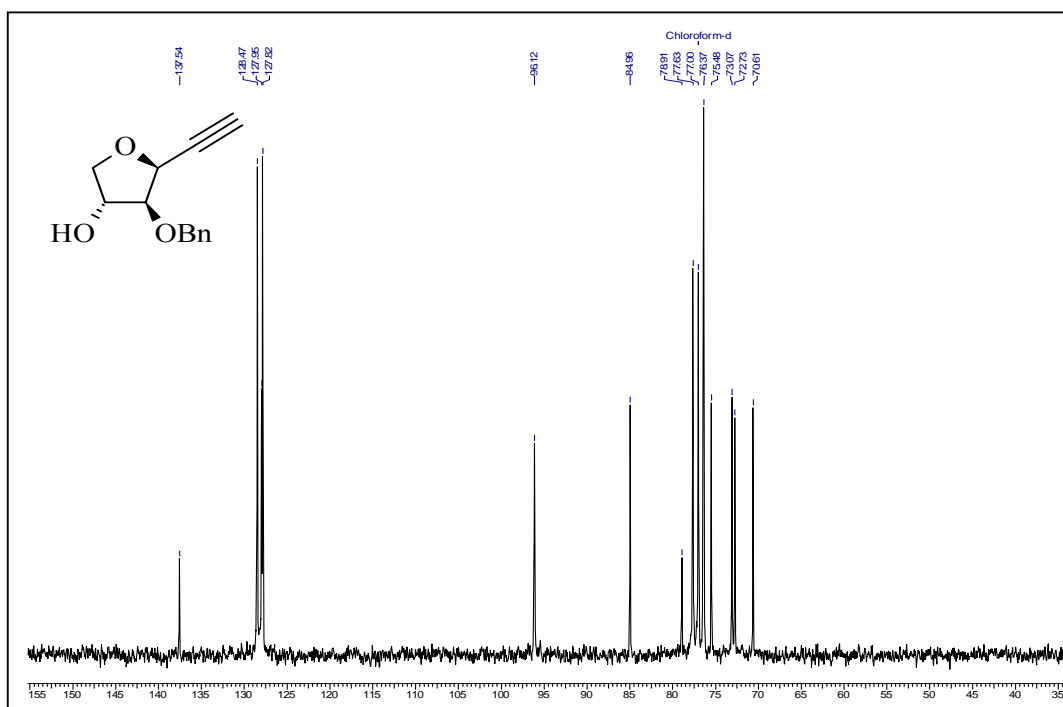
^1H NMR Spectrum of 40 in CDCl_3



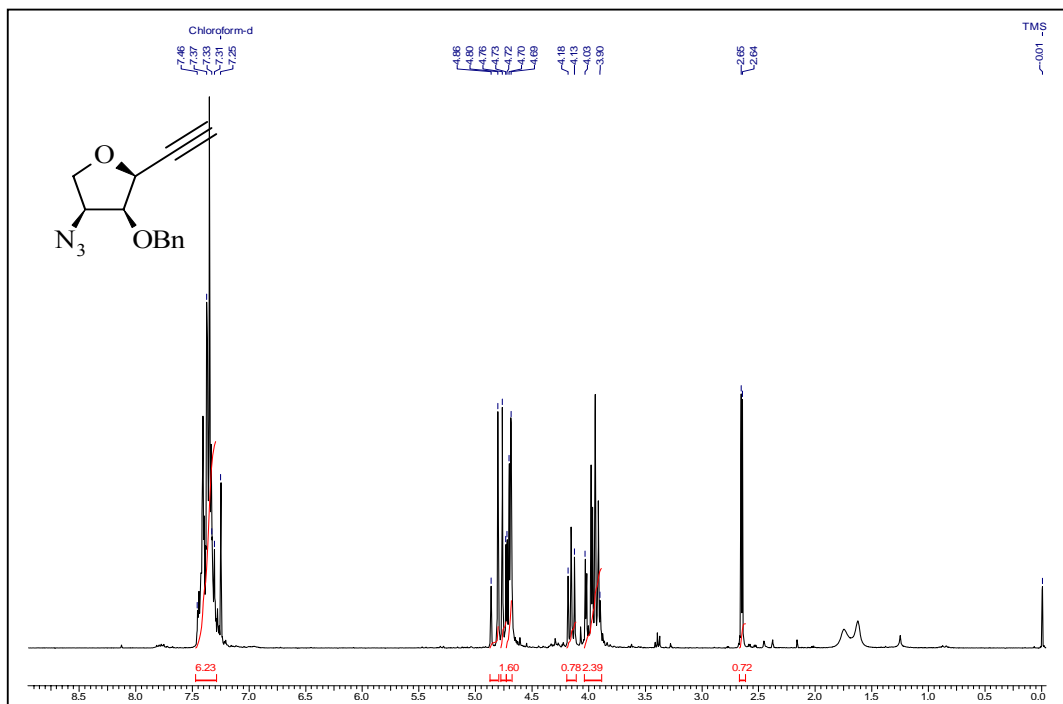
^{13}C NMR Spectrum of 40 in CDCl_3



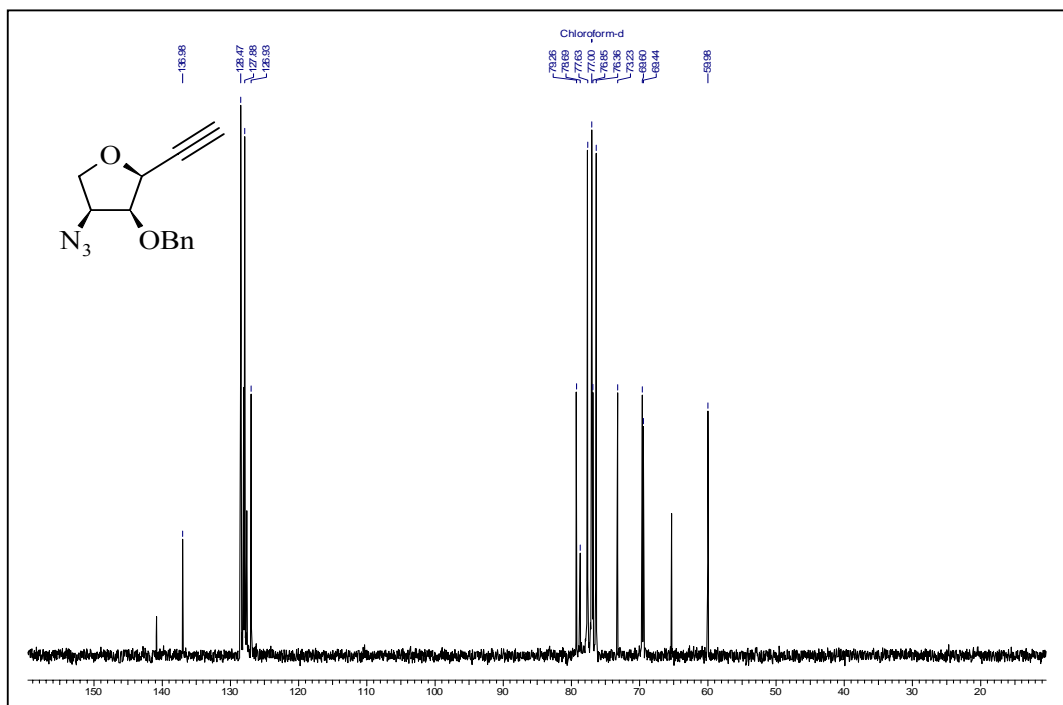
¹H NMR Spectrum of 32 in CDCl₃



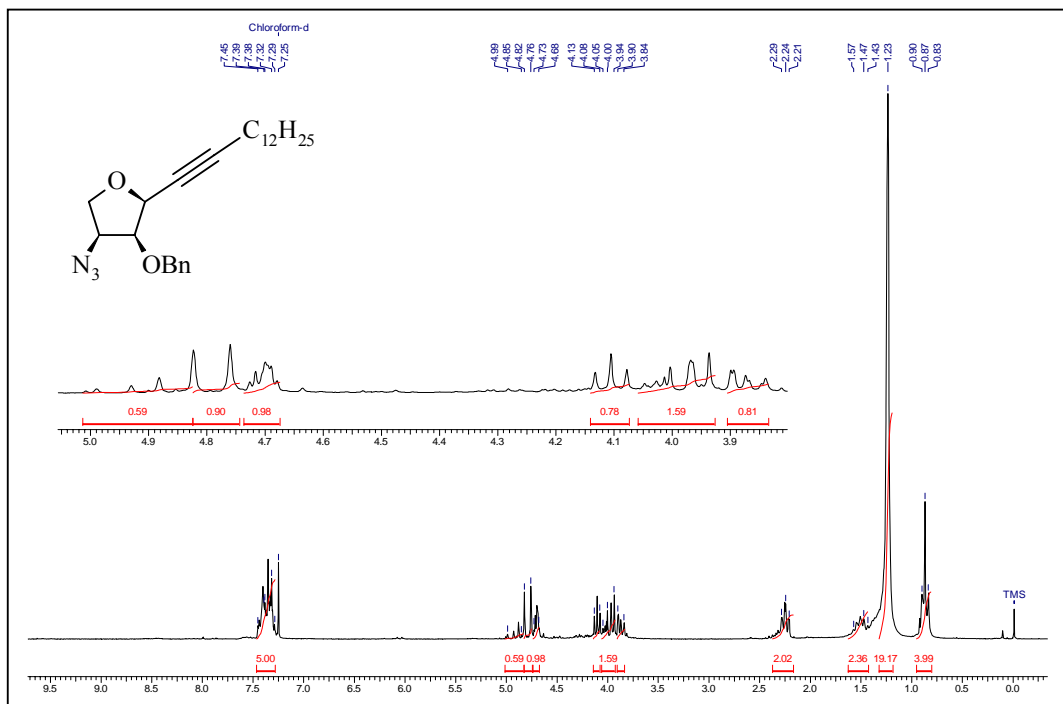
¹³C NMR Spectrum of 32 in CDCl₃



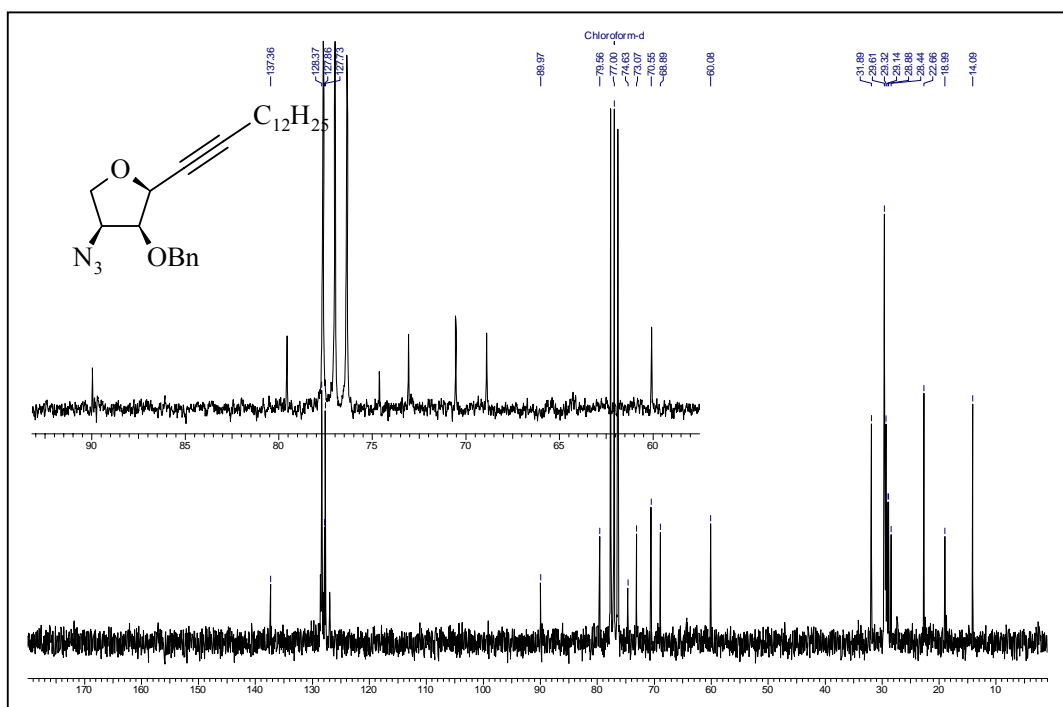
¹H NMR Spectrum of 31 in CDCl₃



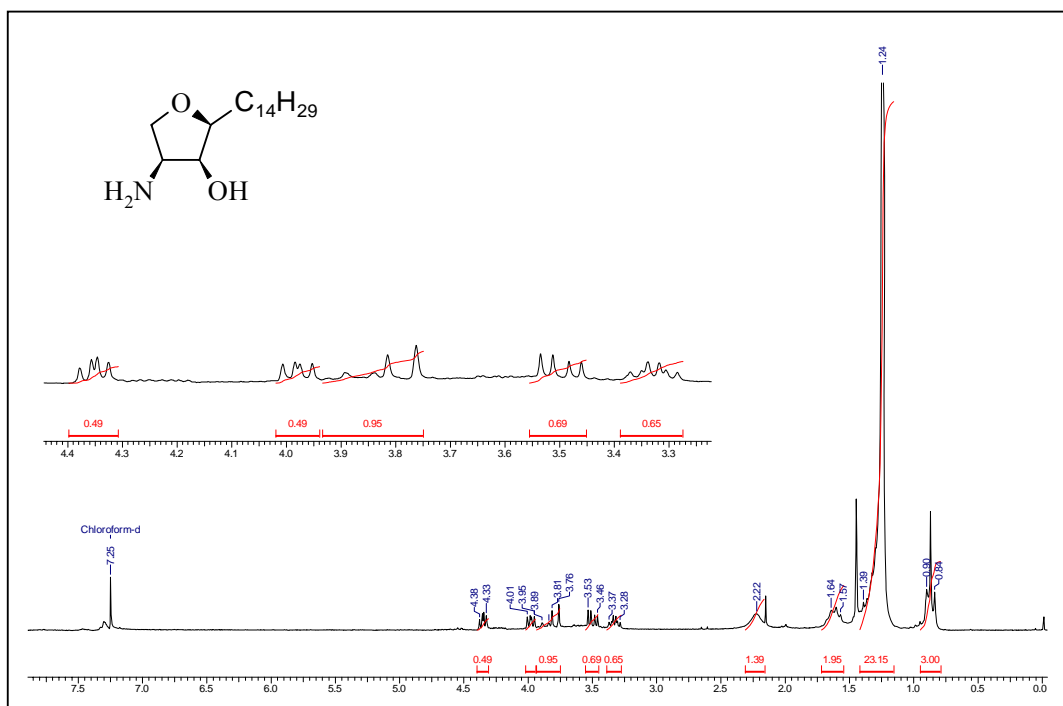
¹³C NMR Spectrum of 31 in CDCl₃



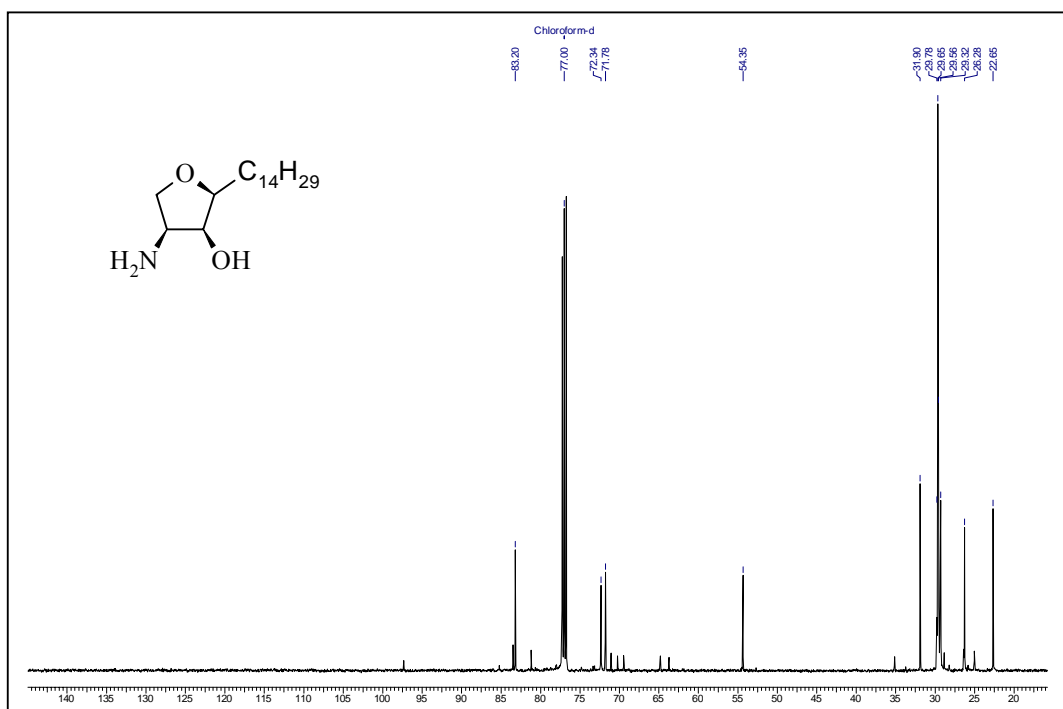
^1H NMR Spectrum of 41 in CDCl_3



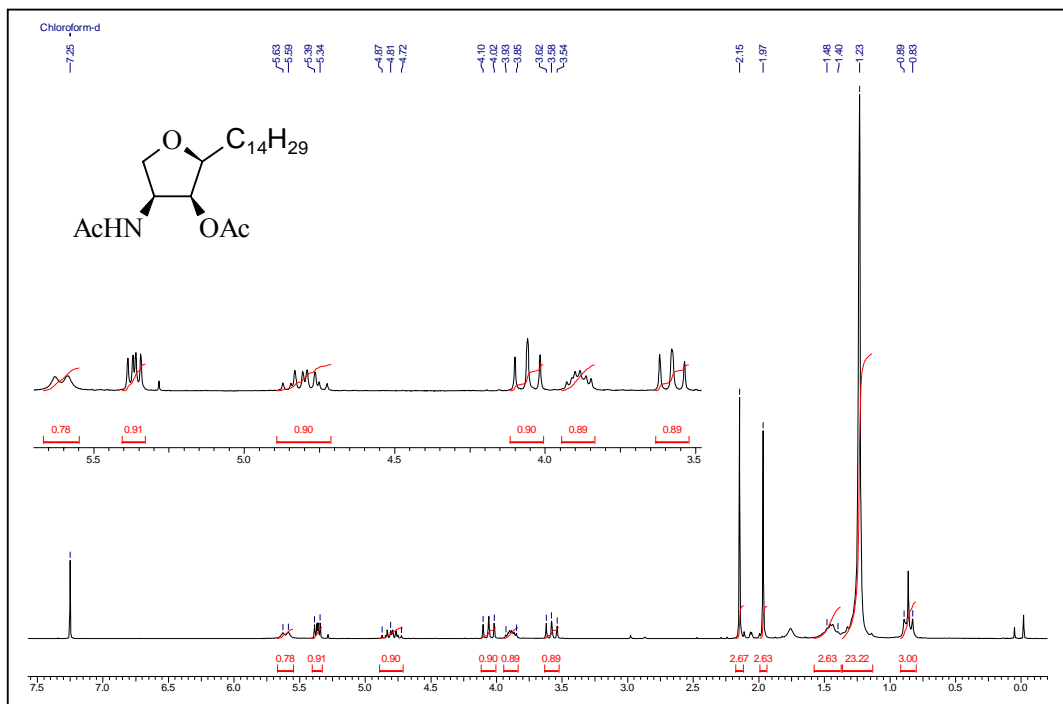
^{13}C NMR Spectrum of 41 in CDCl_3



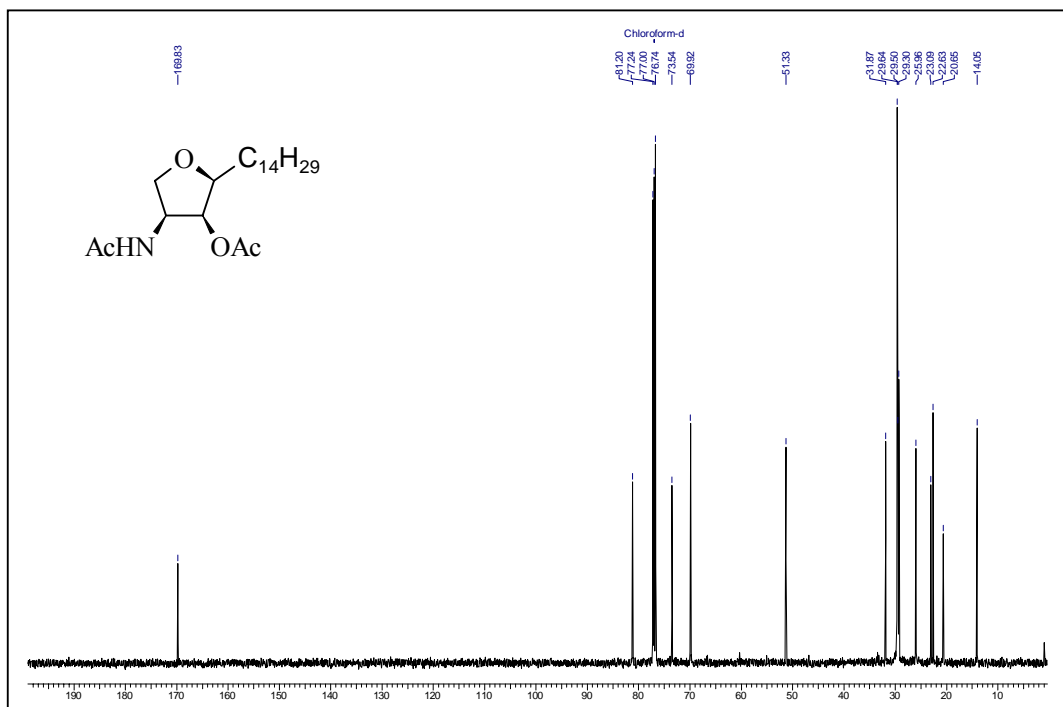
¹H NMR Spectrum of jaspine B (28) in CDCl₃



¹³C NMR Spectrum of jaspine B (28) in CDCl₃



¹H NMR Spectrum of 28-Ac in CDCl₃



¹³C NMR Spectrum of 28-Ac in CDCl₃

References

1. Cinque, B.; Di Marzio, L.; Centi, C.; Di Rocco, C.; Riccardi, C.; Cifone, M. G. *Pharmacol. Res.* **2003**, *47*, 421.
2. a) Ariga, T.; Jarvis, D. W.; Yu, R. K. J.; *Lipid Res.* **1998**, *1*, 1. b) Kobayashi, J.; Ishibashi, M. *Heterocycles* **1996**, *42*, 943.
3. O'Connell, P. W.; Tsien, S. H. *Arch. Biochem. Biophys.* **1959**, *80*, 289.
4. a) Sugiyama, S.; Honda, M.; Komori, T. *Liebigs Ann. Chem.* **1988**, 619. b) Sugiyama, S.; Honda, M.; Komori, T.; *Liebigs Ann. Chem.* **1990**, 1069. c) Birk, R.; Sandhoff, K.; Schmidt, R. R. *Liebigs Ann. Chem.* **1993**, 71.
5. Ledroit, V.; Debitus, C.; Lavaud, C.; Massiot, G. *Tetrahedron Lett.* **2003**, *44*, 225.
6. Kuroda, I.; Musman, M.; Ohtani, I. I.; Ichiba, T.; Tanaka, J.; Gravalos, D. G.; Higa, T. *J. Nat. Prod.* **2002**, *65*, 1505.
7. Pfenninger, A. *Synthesis* **1986**, 89.
8. Sudhakar, N.; Ravi Kumar, A.; Prabhakar, A.; Jagdeesh B.; Rao, B. V. *Tetrahedron Lett.* **2005**, *46*, 325.
9. Garner, P.; Park, J. M. *J. Org. Chem.* **1988**, *53*, 2979.
10. Morris, K, P.; Stauffer, C. S.; Datta, A. *Org. Lett.* **2005**, *7*, 875.
11. a) Du, Y.; Liu, J.; Linhardt, R. J. *J. Org. Chem.* **2006**, *71*, 1251. b) Liu, J.; Du, Y.; Dong, X.; Meng, S.; Xiao, J.; Cheng, L. *Carbohydr. Res.* **2006**, *341*, 2653.
12. Ribes, C.; Falomir, E.; Carda, M.; Marco, J. A. *Tetrahedron* **2006**, *62*, 5421.
13. Natori, T.; Morita, M.; Akimoto, K.; Koezuka, Y. *Tetrahedron* **1994**, *50*, 2771.
14. Sakai, T.; Koezuka, Y. *Exp. Opin. Ther. Patents* **1999**, *9*, 917.
15. Zhong, Y.L.; Shing, T. K. M. *J. Org. Chem.* **1997**, *62*, 2622.

16. a) Horton, D.; Swanson, F. O. *Carbohydr. Res.* **1970**, *14*, 159. b) Patil, N. T.; John, S.; Sabharwal, S. G.; Dhavale, D. D. *Bioorg. Med. Chem.* **2002**, *10*, 2155.
17. Defaye, D. H.; Muesser, M. *Carbohydr. Res.* **1971**, *20*, 305.
18. a) Ohira, S. *Synth. Commun.* **1989**, *19*, 561. b) Roth, G. J.; Liepold, B.; Muller, S. G.; Bestmann, H. J. *Synlett* **1996**, 521.
19. Weaving, R.; Roulland, E.; Monneret, C.; Florent, J. C. *Tetrahedron Lett.* **2003**, *44*, 2579.

CHAPTER-II

Synthesis of novel furano β -amino acids from D-xylose and their homo-oligomers preparation & secondary structural analysis

Introduction

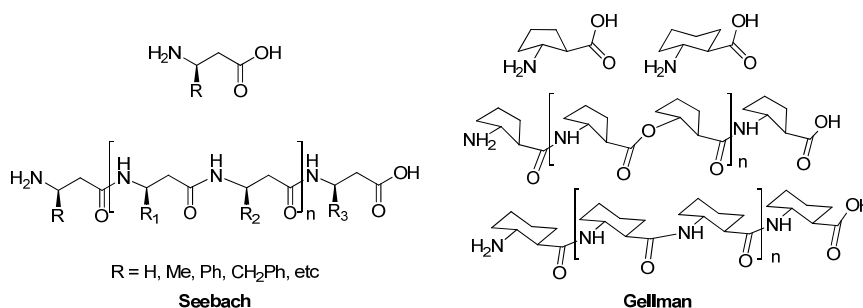
The biopolymers—carbohydrates as well as peptides and proteins are responsible for performing a variety of functions in a cell, such as catalysis, signal transduction, and strong and specific molecular recognition events. Recognition is the fundamental prerequisite at the outset of any biological event. Protein-protein and protein-carbohydrates interactions, though often weak govern a range of essential biological processes. A deeper understanding of such an event at the molecular level with the help of designed synthetic ligands is an essential aspect either to agonize or antagonize the concerned process. An important objective in modern bioorganic and medicinal chemistry concerns the design of synthetic models that mimic various aspects of biologically active molecules. The correct folding of these biopolymers is an important and crucial element, since any kind of interaction is observed only if the reactive groups are positioned in the correct spatial orientation to each other. In this context, mimicking the functions of biopolymers with the help of unnatural oligomers with backbones of discrete and predictable folding patterns (“foldamers”) has emerged as an important area during the last two decades. Amongst the three major biopolymers – *i.e.* nucleic acids, polypeptides and carbohydrates, mimicking the secondary structures of peptides is one of the well explored areas.

A number of very important physiological and biochemical functions of life are influenced by peptides. Peptides are the only biopolymers which have been well explored in medicinal chemistry and the number of drugs which consist of (modified) peptides or of peptide-related compounds are constantly increasing. However, the use of peptides as drugs is limited, because each living system employs several defense mechanisms preventing external peptide from getting into the metabolism. There are 20 proteinogenic amino acids which are linked by amide bonds during the ribosomal biosynthesis of peptides and proteins.

In recent years, several approaches have been put forward to address the mimicking of the secondary/tertiary structures on the one hand and the *in-vitro* stability of synthetic peptides for medicinal applications on the other. Seebach and Gellmann groups introduced the β -amino acids as elegant alternatives in this context

(Figure 19). With extensive structural analysis of their homo- and hetero oligomers, it has been shown that β -peptides form the more stable and diverse secondary structures. For example, β -Peptides have been identified for different helical secondary structures (14-helix, 12-helix and 10/12 helix, 10-helix and 8-helix). Most importantly, unlike the α -Peptides which only form distinct stable secondary structures in solution when they consist of at least 15-20 amino acids, even a simple β -hexapeptide can form a stable helical structure in solution.

Figure 19: The inaugural β -amino acids, β -peptides introduced by Seebach and Gellman



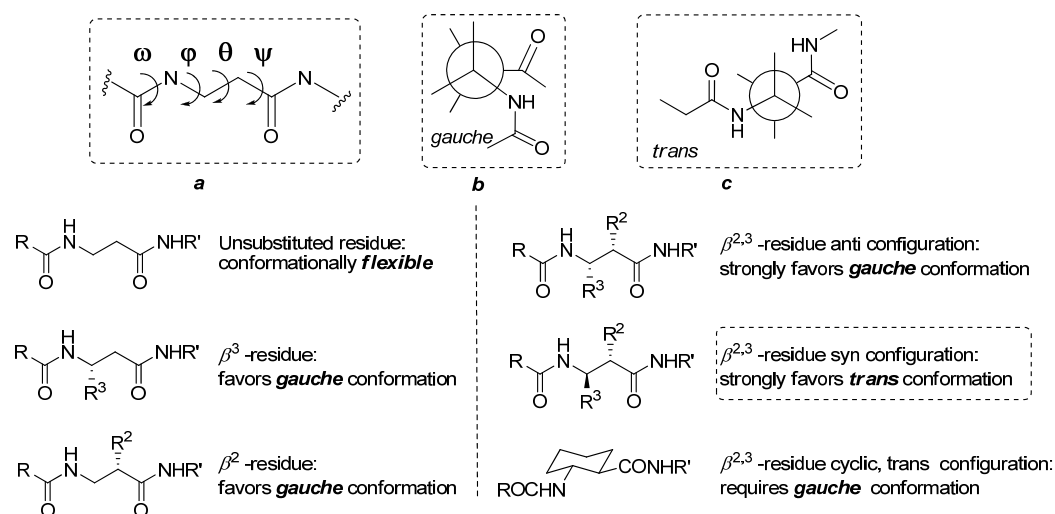
Various groups have established that the resulting β -peptides have superior stability against proteolytic degradation *in vitro* and *in vivo*. For example, β -Peptides have been used to mimic natural peptide-based antibiotics such as magainins. Magainin peptides are highly potent but difficult to use as drugs because they are degraded by proteolytic enzymes in the body. The use of β -Peptides and mixed α/β -peptides as stable mimics of natural peptides with applications ranging antibiotic,¹ anticancer,² anti-HIV functions,³ DNA⁴ and RNA⁵ binding and cell penetration⁶ has been well explored.

Conformational properties of β -amino acids

According to the convention of Balaram, the conformation of β -peptides can be analyzed in terms of the main chain torsional angles, which are designated the angles ω , φ , θ and ψ respectively (Figure 20a).⁷ After an extensive structural analysis, it has been proposed that these torsion angles depend mainly upon the substituents at the β^2 and β^3 -positions. The β -Alanine, analogous to the glycine in the α -amino acid, is highly flexible. Alkyl substituent at β^2 or β^3 -monosubstituted and β^2 , β^3 -disubstituted amino acids favors gauche conformation about the C²-C³ bond. In the cyclopentane and the cyclohexane rings, as in *trans*-2-aminocyclohexane carboxylic acid, *trans*-2,5-

diaminocyclohexanecarboxylic acid, *trans*-2-amino cyclopentanecarboxylic acid and *trans*-3-amino-pyrrolidine-4-carboxylic acid, they are strongly promoted to a *gauche* type conformation about C²–C³ torsional bond (Figure 20b)⁸. When substituents at C² and C³ are *syn*, a *trans* conformation about the C²–C³ bond is favored (Figure 20c), which encourages the formation of sheet like structure⁹. Wu and Wang found that β -dipeptides have a tendency to form folded helical and turn like conformation requiring a *gauche* conformation about the θ torsional angle defined by C²–C³ bond (Figure 20b).¹⁰

Figure 20: Torsion angles in β -peptide and effect of substitution on the torsional angle.



Helices

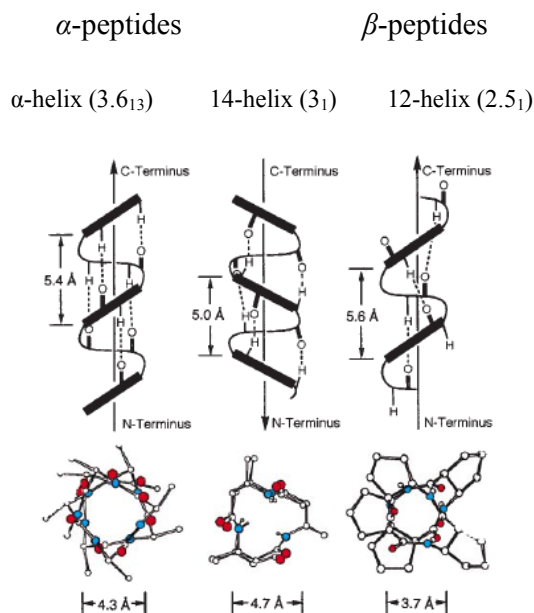
The nomenclature of helical conformations has varied widely in the literature. Gellmans nomenclature is more commonly used that depends on the number of atoms involved in the hydrogen bonded ring formed between donor and acceptor atoms. Gellman and Seebach have reported that β -peptides can form different helices by changing β -amino acid residue. Unlike the α -peptides, where the secondary structures are significantly affected by side chain properties, in β -peptides the secondary structure appears to be determined mainly by substitution patterns.

14-Helix

The 14-helix is formed by contiguous 14-membered hydrogen bonds between an amide proton at position i and a main chain carbonyl at position $i+2$. The β -peptide

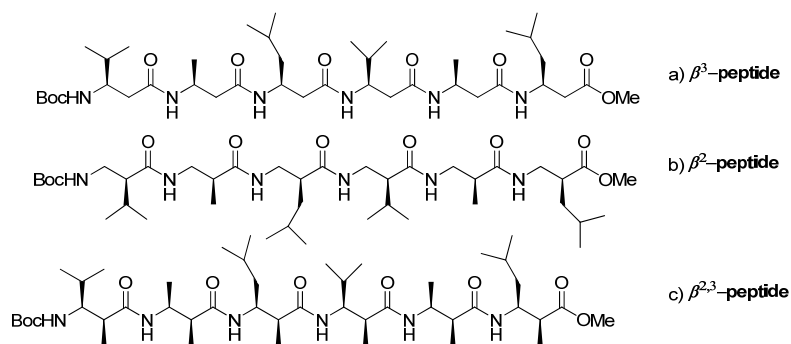
form 14-helical conformation was reported almost simultaneously by Gellman's and Seebach's groups.

Figure 21: Polarities, pitches, diameters and positioning of the side chain in α and β -peptide helices.



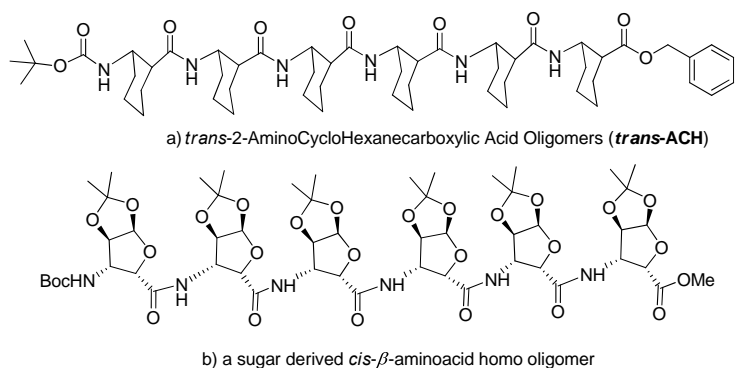
Seebach et al. have shown that β^2 - and β^3 -peptides adopt a 14-helix (also known as 3₁-helix by Seebach nomenclature) in organic solvent^{11,12} (Figure 22a,b). Later, Seebach found that (*S,S*)- $\beta^{2,3}$ -amino acid can also form 14-helix¹² (Figure 22c).

Figure 22: Observed 14-helix in β -peptides derived from acyclic β -amino acid oligomers



While Gellman's group reported that β -peptides with *trans*-2-aminocyclohexanecarboxylic acid (*trans*-ACHC) strongly favor a 14-helices in the solid and as well as in organic solvents¹³ (Figure 23a). Chandrasekhar¹⁴ has reported the formation of a stable 14-Helix in short oligomers of furanoid *cis*- β -Sugar-Amino acid (Figure 23b).

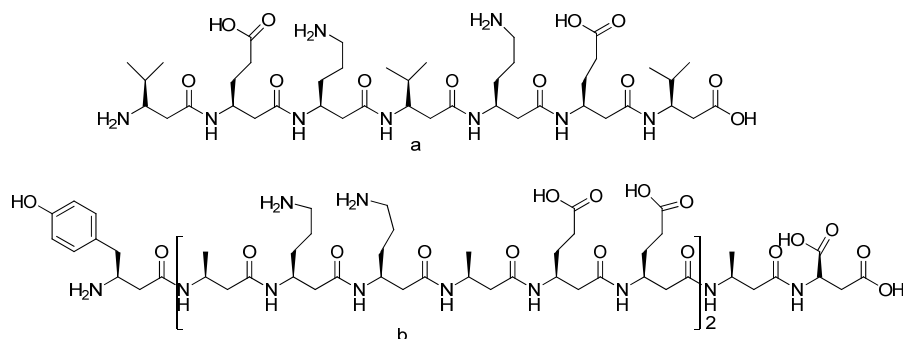
Figure 23: Observed 14-helix in β -peptides derived from cyclic β -amino acid oligomers



The comparative structural analysis of α -helix formed by the corresponding α -peptides and 14-helix reveals the following points:

1. only three β -amino acid residues are needed for a 14-helix, while 3.6 α -amino acids are required for a single winding of the α -helix
2. The pitch of an α -helix is 5.4 Å wide and its diameter is 4.3 Å, whereas the pitch of the 14-helix is only 5.0 Å wide. However the diameter is 4.7 Å (Figure 21)
3. The amide carbonyl and NH groups project toward the N- and C-terminus respectively in the 14-helix, resulting in a net dipole opposite to that of the α -helix
4. The helicity and dipole moment of the L- β -peptides are in the opposite direction compared to that of the α -helix formed by the corresponding α -peptides

Figure 24: 14-Helical β -peptide stabilized by salt bridges

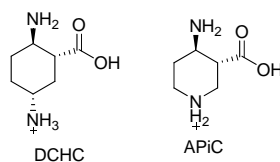


Seebach group designed the acyclic β -peptides to be capable of forming 14-helix in solution when stabilized by electrostatic interactions. β -Heptapeptide (Figure

24a)¹⁵ with salt bridge on two faces of the helix forms a 14-helix (in methanol and water) secondary structure confirmed by both CD and NMR. DeGrado group¹⁶ has shown that the 15-residue oligomer forms a 14-helix which is stabilized by a salt bridge (Figure 24b). These oligomers showed pH-dependent 14-helix formation with a folding maximal at neutral pH, which suggest that the salt bridges are required for folding.

There are couple of other reports which along similar lines demonstrate that even favorable secondary interactions between the helix dipole and salt bridges does stabilize a 14-helix in water.¹⁷ Interestingly, Gellman has shown that the salt bridge formation is not required for secondary structure stabilization by incorporation of constrained β -amino acid containing ACHC residues anticipating the need for salt bridges to promote folding in aqueous solution and folding displays no pH dependence (Figure 25).¹⁸

Figure 25: Cationic cyclically constrained β -amino acids that adopt 14-helical conformation

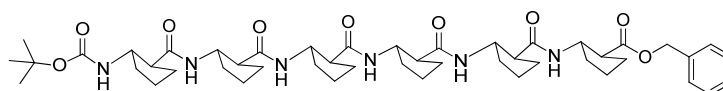


12-Helix

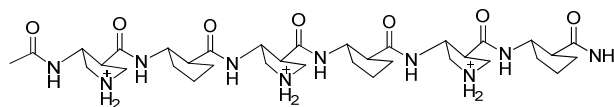
The 12-helix is also called as a 2.5₁-helix. The 12-helix repeats approximately every 2.5 residues. Gellman's group has reported β -peptides with *trans*-2-aminocyclopentanecarboxylic acid (ACPC)¹⁹ (Figure 26a) adopt a helical structure with 12-membered-ring hydrogen bonds (12-helix) both in organic solution and in the solid state.

Gellman's group has reported the CD spectra of 12-helix peptides which shows a maximum at 207 nm and a minimum at 222 nm.¹⁹ The β -peptides prepared from *trans*-3-amino-pyrrolidine-4-carboxylic acid (APC) and β -peptides containing alternating ACPC and APC residues have been shown to adopt a 12-helix in aqueous solution²⁰ (Figure 26b). The β -peptides containing ACPC, APC and (2*R*, 3*R*)-amino proline (AP) has been also adopt a 12-helix in aqueous solution²¹ (Figure 27). β -peptides of 3-substituted ACPC adopting 12-helix²² (Figure 28).

Figure 26: Observed 12-helix of β -peptides

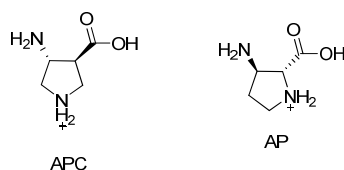


trans-2-Aminocyclopentanecarboxylic Acid Oligomers



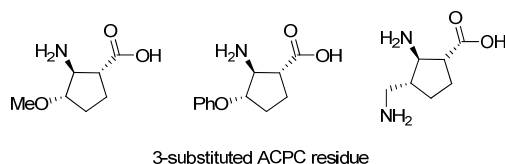
trans-3-amino-pyrrolidine-4-carboxylic acid oligomer

Figure 27: Cationic cyclically constrained β -amino acids



A 12-helix is formed by contiguous 12-membered hydrogen bonds between the amide carbonyl groups of the i^{th} residue and an amide proton of $i+3^{\text{th}}$ residue. The amide carbonyl and NH groups orient themselves toward the C- and N- termini respectively, giving rise to a net helix dipole with the same directionality as the α -helix.

Figure 28: Functionalized β -amino acids with five membered ring



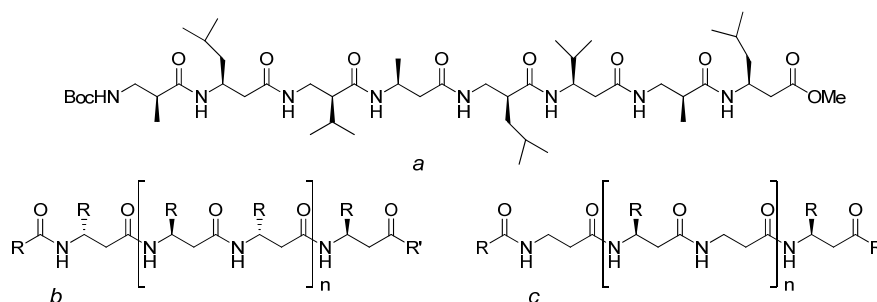
3-substituted ACPC residue

10/12-helix

Seebach's group studied β -peptides with alternating β^2 - and β^3 -monosubstituted residues and showed that they can adopt the 10/12-helix conformation^{11,23} (Figure 29a). Later on, unlike β^3/β^3 -peptides and β^3/β -hGly(homoglycine) peptides has been also found to form the 10/12-helix.²⁴ The C=O and N-H bonds point alternatively up and down along the axis of the helix, thus the net dipole is almost zero. As in the 14-helix, side chains of the β -amino acids i and $i+3$ reside above each other. The major difference between those two helices is the

polarity. The 10/12 helix has almost no resulting dipole moment of the molecule, while the 14-helix has one with the positive end at the C- and the negative at the N-terminus. The 14-helix consists of only one type of 14-membered turn whereas in the 10/12 helix has two different turns, the central 10-membered- and the two terminal 12-membered turns. Seebach group reported the CD spectra of 10/12-helix peptides shows intense signal peak at 205 nm.¹¹

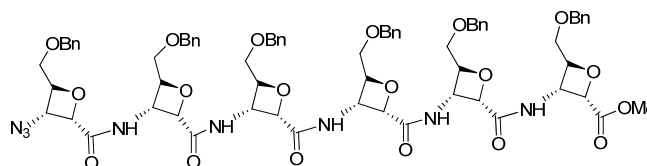
Figure 29: Observed 10/12-helix of β -peptides



10-Helix

Fleet's²⁵ group investigated secondary structure of β -hexapeptide stabilization by 10-membered hydrogen bonded rings for the first time in which the peptide backbone is constrained by *cis*-substituted oxetane rings (Figure 30). This secondary structure was confirmed by NMR analysis in nonpolar solvents. Molecular mechanics assisted conformational analysis of β -hexapeptide show left-handed helical structure.

Figure 30: β -Peptide that adopts a 10-helix conformation

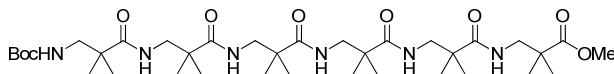


8-Helix

Crystal structure of the trimer and tetramer of achiral monomer 1-(aminomethyl)cyclopropanecarboxylic acid adopt a regular 8-helix,²⁶ which would have approximately two residues per turn (Figure 31). In an 8-helix, the amide carbonyl group is gauche to the two C $_{\alpha}$ -H bonds. Simple alkyl substituents do not favour the 8-helix. This conformational preference is mainly due to a

hyperconjugative interaction between the cyclopropane and the carbonyl group, instead of the steric effect.

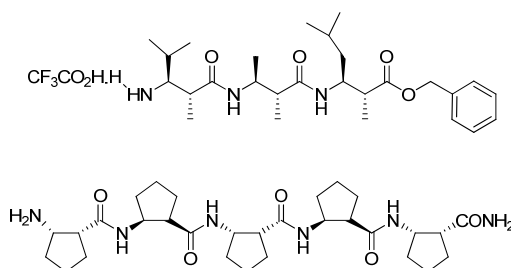
Figure 31: β -Peptide that adopt 8-helix conformation



Pleated sheet

Seebach and co-workers has reported first time sheet-type structure formation in β -peptides. There are two types of sheet secondary structure available in β -peptides, one in which each residue has an anti C^2-C^3 torsion angle and another in which each residue has a gauche C^2-C^3 torsion angle. Theoretical analysis of the dipeptide model indicates that the intrinsic hydrogen bond strength is large for both parallel and antiparallel sheets and affected little by substituents. $\beta^{2,3}$ -peptides have much stronger sheet forming abilities. The β -sheets formed by the α -peptides have little or no net dipole because the backbone carbonyls alternate in direction along each strand. In contrast, in β -peptide sheets, where C=O and N-H bonds point up and down alternatively the resulting pleated sheet is polar, since all carbonyls point in one direction, while all N-H bonds point in the opposite direction (Figure 32).^{9,27}

Figure 32: β -Peptide that adopts a sheet conformation

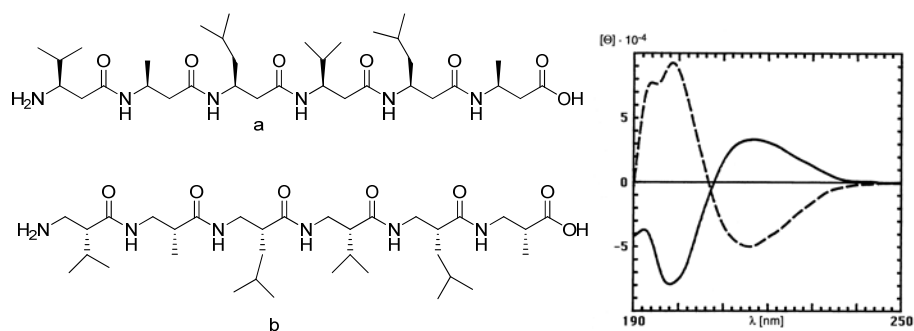


Circular Dichroism spectroscopy

Characteristic troughs and double troughs between 200 and 230 nm in the CD spectra of α -peptides and proteins are associated with β -sheet and α -helix secondary structures. Seebach et al. have reported that CD data for β -peptides constructed from β -substituted residues adopt 14-helices in organic solvent and show a minimum at 214 nm, a zero-point crossing at 206 nm, and a maximum at 198 nm. The CD spectra of several hexa- and heptapeptides, which adopt left-handed 14- helices as determined

by NMR or crystallography, show a maximum near 195 nm and a minimum near 215 nm (or vice versa for right-handed helices). The magnitude of the negative ellipticity at 215 nm varies somewhat from peptide to peptide.^{11,12,19} The CD pattern is characteristic for the presence of an left- or righthanded 14-helix (Figure 33).

Figure 33: CD-spectra of the β^3 -hexapeptide **a** (- -) forming a left-handed 14-helix and of the β^2 -hexapeptide **b** (-) forming a right-handed 14-helix in methanol

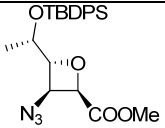
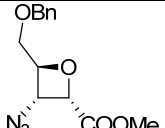
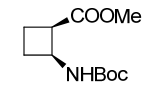

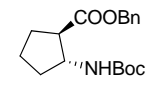

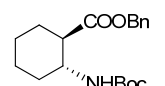
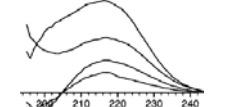
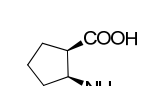
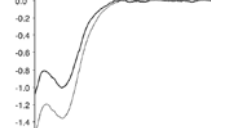
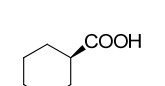
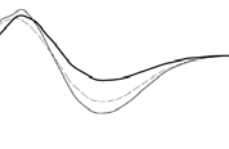
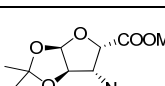
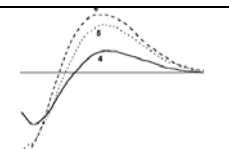


The intensity of the CD spectrum of the α -helix is known to depend on chain length, becoming more intense as the helix is lengthened. Similar behavior appears to be found for 14-helices. The CD spectra of many 10-15-residue peptides, which have been designed to adopt a 14-helical conformation, are more intense than their shorter counterparts.

Theoretical calculations²⁸ indicated that the π - π^* contribution to the CD spectrum of the 12-helix should be similar in shape to that of the 14-helix but that the sign should be reversed for a given helical handedness and the splitting between the parallel and perpendicular bands should be greater. The experimental spectra observed for a hexamer that forms a left-handed 12-helix is consistent with this analysis, showing a maximum near 205 nm and a minimum near 190 nm. Additionally, a negative band is observed near 220 nm, which is probably associated with the n - π^* transition. The presence of a maximum at 200-205 nm together with a minimum near 220 nm has not been observed in other secondary structures of β -peptides and may be diagnostic of the 12-helix. The circular dichroism spectrum of the right-handed 10/12-helical conformation shows an intense single peak near 205 nm with a mean residue ellipticity up to 60 000 deg cm² dmol⁻¹.

CD – Pattern of homo-oligomers of the cyclic β -amino acids

In the context of our investigation that deals with the cyclic furano- β -amino acids, available CD-data of various cyclic β -amino acids is compiled and given below.

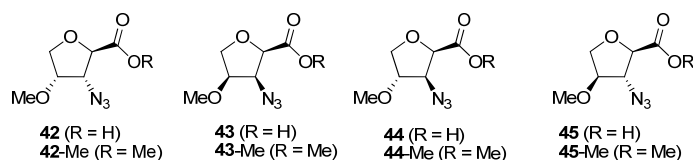
Monomer	Secondary Structure	Characteristic CD peaks in nm			
			Zero crossing		
	10-(LH)helix				CD not given
	10-(RH)helix				CD not given
	Strand	210		225	
	12-(LH)helix	204	214	221	
	14-(RH)helix			217	
	Sheet like	203			
	<i>tetramer</i> 10-(LH)helix <i>Pentamer and hexamer</i> 14-(RH)helix	197	207	217	
	14-(RH)helix	198	209	218	

A careful examination of the structures of synthesized sugar amino acids, especially dealing with the relative stereochemistry of the other functional groups, revealed the fact that they are more randomly synthesized and in a majority of the cases, only those diastereomers which are easy to synthesize are reported. This may be because of limitations imposed by the availability of all sugar monomers and no. of synthetic transformations involve. Additionally, some of the synthesized sugar amino acids are not devoid of either protecting groups or the high functionalization.

Nonetheless, studies addressing issues like correlation between the relative and absolute configuration of amino acid functionalities on the handedness of the helix, the effect of the adjacent substituents on the secondary structure have been not dealt in detail. Considering the above mentioned limitations, especially in the context to understand precisely the relation between the stereochemistry of substituents and the nature of the secondary structure, and also to minimize the no. of variables, we have designed the following sugar derived

The *trans* **42** and *cis* **43** furano β -amino acids respectively, having a methoxy *syn*-to the amine unit have been prepared in order to understand the effect of a *cis* alkoxy group on the secondary structure of the derived oligomers. The details of their synthesis and the structural analysis of the derived homo-oligomers will be described in the following section.

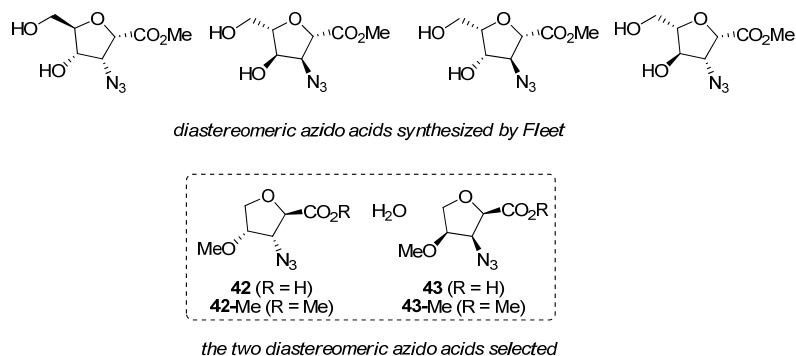
Figure 34: Designed diastereomeric furano- β -amino acids building blocks



Present Work

Sugar Amino Acids coined by H. Kessler are an important class of compounds which have been introduced in the area of peptido-mimetics recently.²⁹ The synthesis of the building blocks utilizes standard carbohydrate chemistry, whereas the assembly of different conjugates results from both state of the art peptide chemistry as well as carbohydrate chemistry. Very recently, a couple of groups have prepared sugar derived β -amino acids and showed that their oligomers mimic some secondary structure elements of peptides. However, as it has been mentioned earlier, the substituent and their stereochemistry on the furanoid template had not been considered and the selection was made purely on the easy availability of the sugar building block. Professor Fleet's group has made the synthesis of four possible diastereomers of a furanoid β -amino acid (Figure 35).³⁰ However, their further elaboration into the homo-/heterooligomers and their structural analysis has not been documented.

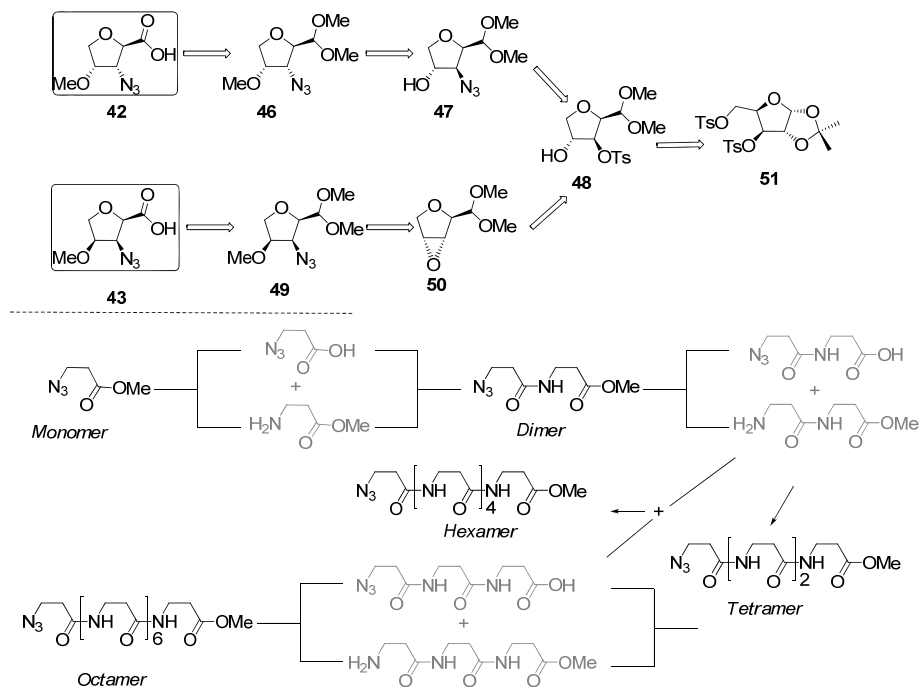
Figure 35: Structures of β -amino acids synthesized by Fleet and selected β -amino acids for synthesis



We have designed a set of four diastereomeric furanoid β -amino acids and intended to synthesize their homo-oligomers influence of the adjacent substituent on the secondary structures of furanoid beta-peptides. To start in this direction, first we have selected the *trans*- and *cis*-furanoid β -azido acids **42** and **43** having a β^d -methoxy group *syn*- to the azide group and the corresponding methyl esters **42-Me** and **43-Me** as suitable precursors for the iterative synthesis of the corresponding β -

peptides. A representative protocol for the synthesis of homo-oligomers is given in figure 36.

Figure 36: β -Amino acid, and retrosynthetic scheme and flow diagram for synthesis of homo-oligomers



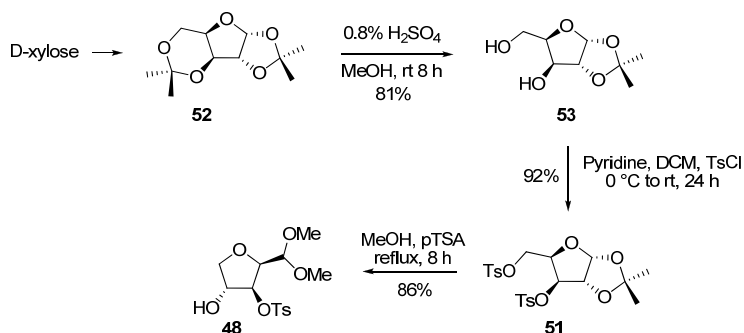
Synthesis of β -amino acids

We have intended to develop a practical strategy for the synthesis of monomeric units **42** and **43** on multi gram scales. The intended strategy for the synthesis of these two diastereomers is an extension of our ring-transposition approach that we used for the previously mentioned Jaspine B synthesis. Retrosynthetic analysis for the two azido acids is depicted in Figure 35. The acetal unit has been recognized as a surrogate for the acid group. The azido group was planned *via* a displacement of suitable *O*-tosyl or *O*-triflate derivatives. The methoxy group of **42** was planned by a simple protection of the azido alcohol **47**. Methoxy functionality of **43** could be fashioned via a regioselective opening of the epoxide **50** with methanol. The tosyl derivative **48** was identified as a suitable precursor for the preparation of the azido alcohol **47** and also of the key epoxide **50**. The tosylate **48** was planned by acid mediated ring isomerisation of the xylose derived ditosylate **51**.

Synthesis of intended dimethylacetal **48**

The synthesis began with the conversion of D-xylose into D-xylose diacetone **52**. Selective deprotection of 3,5-isopropylidene group was carried out by using 0.8% H₂SO₄ in methanol at ambient temperature to afford the diol **53** (Scheme 29). The diol **53** was converted to the corresponding ditosylate **51** by treating with tosyl chloride in pyridine.³¹ In the ¹H NMR spectrum of **51**, the presence of two tosyl groups was evident from the appearance of two arylmethyl singlets at δ 2.44 and 2.47 and eight aromatic protons multiplet at δ 7.31–7.80. The next task was acid mediated acetonide deprotection with concomitant 2,5-ring closure to give dimethylacetal **48**.³² This reaction can be effected in quantitative yields (on 100 g scale) by treating ditosylate **51** with *p*-toluenesulfonic acid in a solution of methanol at reflux temperature. The structure of **48** was established with the help of NMR, IR and mass spectroscopy techniques.

Scheme 29: Synthesis of dimethylacetal **48**



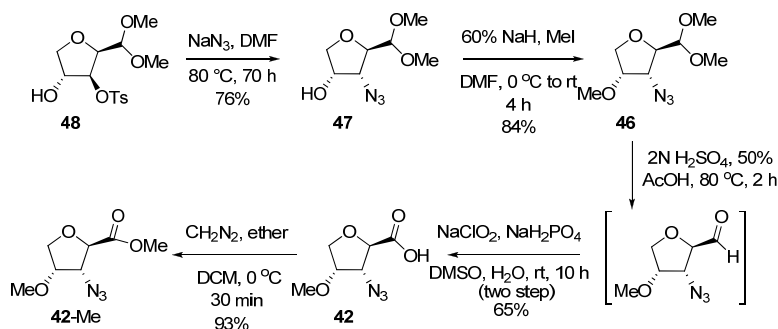
Synthesis of *trans*- β -azido acid **42** and its methyl ester **42-Me**

The tosyl displacement of **48** with azide nucleophile was carried out by treating it with sodium azide in DMF at 80 °C and the azidoalcohol **47** was obtained in 76% yield. In the ¹H NMR spectrum of **47**, the Ar–H signals were disappeared. The azide functionality was confirmed by a characteristic band at 2105 cm⁻¹ in the IR spectrum of **47**. The highest mass peak at m/z 226.6 (100%, [M+Na]⁺) and elemental analysis supported the assigned structure of **47**. The hydroxy group of **47** was converted to methyl ether **46** by treatment with 60% sodium hydride (dispersion in mineral oil) and methyl iodide in DMF. The addition of one methyl group was evident from the ¹H NMR spectrum where the signal due to methyl group resonated as a

singlet at δ 3.47. In the mass spectrum m/z 218.1 (18.2%, $[M+H]^+$), 235.2 (66.4%, $[M+NH_4]^+$), 240.1 (100%, $[M+Na]^+$), 256.2 (24.1%, $[M+K]^+$) confirmed the proposed constitution. The ^{13}C NMR spectrum and elemental analysis were also found to match with the proposed structure **46**.

The azido dimethylacetal **46** was hydrolysed using 2N H_2SO_4 and 50% acetic acid and the resulting crude aldehyde was used for the next step without further purification. The crude aldehyde was oxidized to the acid **42** employing $NaClO_2$ and $NaH_2PO_4 \cdot 2H_2O$ in $DMSO:H_2O$ at rt. The azido acid was purified by column chromatography and characterized by spectral data. In the IR spectrum of **42** the O-H stretching band was observed at 3357 cm^{-1} and C=O stretching at 1731 cm^{-1} . The carbonyl group was observed at 174.8 ppm in the ^{13}C NMR spectrum of compound **42**. Other analytical data such as mass and CHN were in accordance with the proposed structure of **42** (Scheme 30).³³

Scheme 30: Synthesis of *trans*- β -azido acid **42** its methyl ester **42-Me**

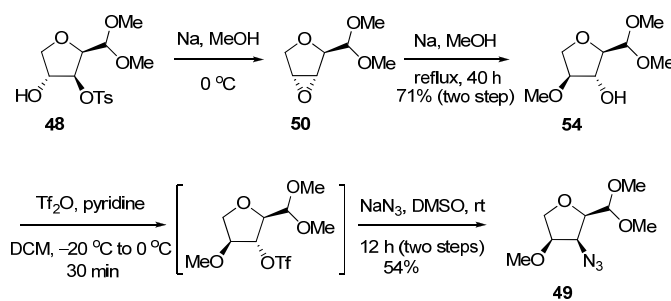


The next transformation to be carried out was esterification of acid **42**. This was successfully carried out by treating *trans*-acid **42** with diazomethane in CH_2Cl_2 :ether at $0\text{ }^\circ\text{C}$ and the methyl ester **42-Me** was obtained in 93% yield. The structure of **42-Me** was supported by 1H NMR and IR spectra. The presence of methyl ester was evident from the 1H NMR spectrum where an additional singlet at δ 3.79 integrating for three protons was seen to appear. In the IR spectrum, the O-H stretching disappeared and a C=O stretching band was observed at 1753 cm^{-1} . The carbonyl group was observed at 170.0 ppm in ^{13}C NMR spectrum. In the mass spectrum the characteristic mass peaks at m/z 224.6 (100% $[M+Na]^+$), 240.7 (16%, $[M+K]^+$) confirmed the proposed constitution of **42-Me**.

Synthesis of *cis*- β -azido acid **43** and its methyl ester **43-Me**

Synthesis of the *cis*-azido acid **43** began with the conversion of the monotosylate **48** into epoxide **50** by using Na in methanol. For the purpose of characterization, part of the above reaction was worked up and the resulting epoxide was purified and analyzed. A prolonged heating of the above reaction mixture gave **54** in excellent yields (Scheme 31). In the ^1H NMR spectrum, signal corresponding to methoxy group was appeared at δ 3.35 as singlet integrating for 3H. Other analytical data such as mass, ^{13}C NMR spectrum and CHN were in accordance with the proposed structure **54**.

Scheme 31: Synthesis of azide **49**

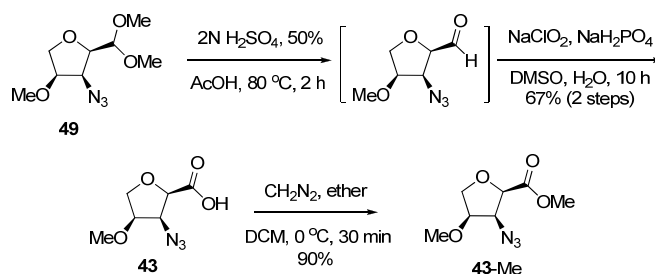


The next step was to convert alcohol **54** into the azide **49**. The displacement of the corresponding tosyl or mesyl derivatives of **54** was sluggish with sodium azide at 80 °C in DMF and showed only 30–40% conversion in eight days. Therefore we opted for a better leaving group such as a triflate. The hydroxy group of **54** was transformed to the corresponding triflate by treatment with Tf_2O in pyridine. The displacement of intermediate triflate employing NaN_3 in DMSO at room temperature was facile and gave the azido compound **49** in respectable yields. In the ^1H NMR spectrum of **49**, the methoxy signals were observed at δ 3.42, 3.44 and 3.45 as singlets, each integrating for three protons. The azide functionality was confirmed by characteristic band at 2108 cm^{-1} in the IR spectrum of **49**. The highest mass peak at m/z 240.2 (100%, $[\text{M}+\text{Na}]^+$) and elemental analysis supported the assigned constitution of **49**.

The dimethylacetal group of **49** was hydrolyzed to aldehyde by employing 2N H_2SO_4 and 50% acetic acid and the resulting crude aldehyde was oxidized to the acid **43** on treatment with NaClO_2 and $\text{NaH}_2\text{PO}_4 \cdot 2\text{H}_2\text{O}$ in $\text{DMSO}:\text{H}_2\text{O}$ at rt. In the IR

spectrum the O–H stretching was observed at 3371 cm^{-1} and the C=O stretching at 1735 cm^{-1} . The carbonyl group was observed at 171.3 ppm in ^{13}C NMR spectrum. In ^1H NMR spectrum, the dimethylacetal singlet was seen to disappear. In the mass spectrum m/z 210.2 (100%, $[\text{M}+\text{Na}]^+$) confirmed the proposed structure **43** (Scheme 32).

Scheme 32: Synthesis of acid **43 & ester **43-Me****



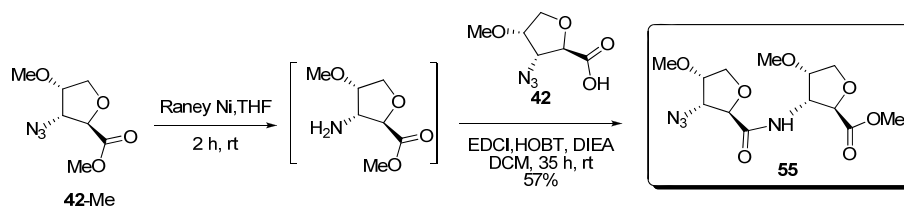
Next, the *cis*-acid **43** was treated with diazomethane in CH_2Cl_2 :ether at $0\text{ }^\circ\text{C}$ to afford ester **43-Me**. The structure of **43-Me** was supported by ^1H NMR and IR spectrum. Presence of methyl ester was visible in the ^1H NMR spectrum by the appearance of additional singlet at δ 3.78 integrating for three protons. In the IR spectrum, the O–H stretching disappeared and C=O stretching was observed at 1762 cm^{-1} . The carbonyl group was observed at 168.2 ppm in ^{13}C NMR spectrum. In the mass spectrum a peak at m/z 224.3 (100% $[\text{M}+\text{Na}]$) confirmed the proposed structure **43-Me**.

Liquid phase synthesis of homo-oligomers from *trans*- β -azido acid **42** and its methyl ester **42-Me**

With the necessary building blocks **42** and **42-Me**, our next concern was the synthesis of the corresponding oligomers. The synthesis of dimer was carried out in a two step sequence. First step is the reduction of azide functionality of ester **42-Me** by employing Raney nickel in THF under an atmosphere of hydrogen at rt to obtain the corresponding amine which was coupled with the acid **42** immediately by using EDCI and HOBt, DIPEA in CH_2Cl_2 at rt to afford the dimer **55** in 57% yield (Scheme 33).³⁴ Presence of an amide proton was evident from the ^1H NMR spectrum where a doublet at δ 7.13 with $J = 8.4\text{ Hz}$ integrating for one proton was appeared. In the ^{13}C NMR spectrum, ester carbonyl appeared at δ 171.18 and amide carbonyl appeared at 170.87. The ester functionality was confirmed by characteristic band at 1747 cm^{-1} and the

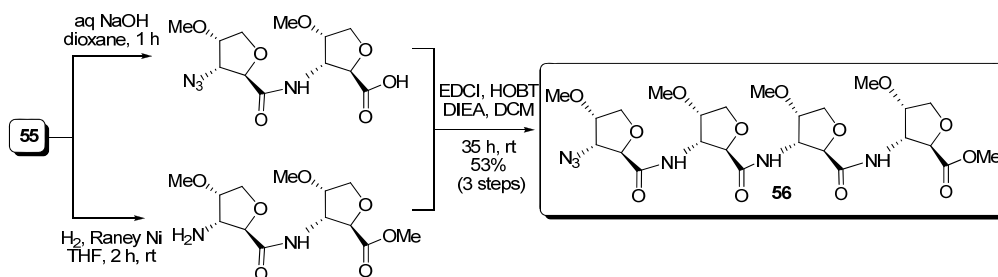
amide functionality was confirmed by the characteristic band at 1660 cm^{-1} in the IR spectrum of **55**. The highest mass peak at m/z 345.0 (100%, $[M+H]^+$) supported the assigned structure **55**.

Scheme 33: Synthesis of *trans*- β -FAA dimer



The tetramer synthesis started with the conversion of the dimer to the two requisite acid and amine units. Treatment of dimer **55** with aqueous sodium hydroxide in dioxane afforded the intermediate dimer-acid. The Raney nickel mediated hydrogenolysis of azide **55** in THF gave the intermediate dimer-amine. Finally, the coupling of these acid and amines was carried out by employing EDCI and HOBT, DIPEA in CH_2Cl_2 at rt. The tetramer **56** was purified by column chromatography and characterized by spectral and analytical data (Scheme 34).

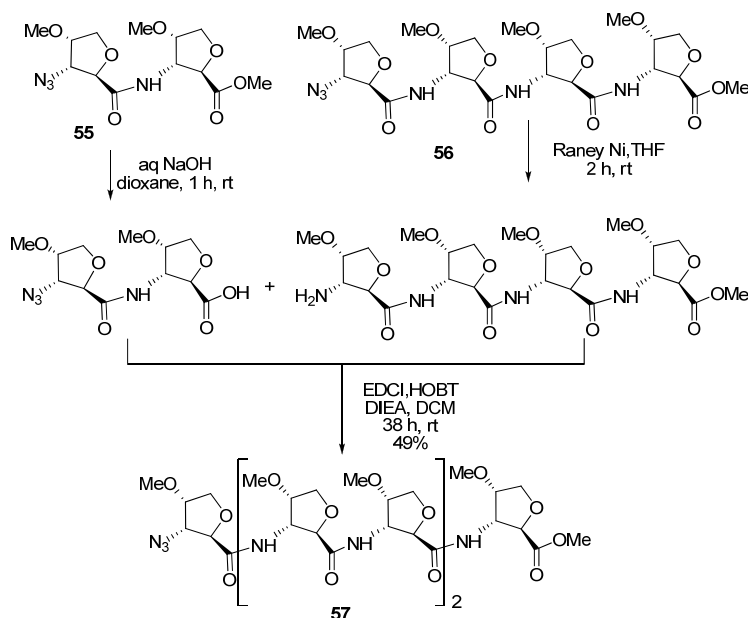
Scheme 34: Synthesis of *trans*- β -FAA tetramer



The presence of amide protons as a doublet at δ 7.21, 7.23 and 7.37 and singlets for five methoxy at δ 3.36, 3.36, 3.37 3.45 and 3.71 in ^1H NMR approved the tetramer structure **56**. Four quaternary carbon singlets in the ^{13}C NMR spectrum of tetramer **56**, one at δ 171.50 corresponding to carbonyl of ester and three at δ 170.39, 170.41 and 170.44 ppm corresponding to the amide carbonyls confirmed the requisite coupling. Absorptions due to the ester and amide carbonyl functionalities were seen separately in the IR spectrum, respectively at 1747 cm^{-1} and 1685 cm^{-1} . Mass spectra showed a peak at m/z 631.1 (100%, $[M+H]^+$) which corresponding to the tetramer structure **56**.

Encouraged by this result, we focused our efforts on preparing the higher oligomers. The synthesis of hexamer **57** was carried out by coupling crude tetramer-amine (prepared by the hydrogenolysis of tetramer **56**), with dimer-acid using EDCI and HOBt, DIPEA in CH₂Cl₂ at rt (Scheme 35).

Scheme 35: Synthesis of *trans*- β -FAA hexamer **57**

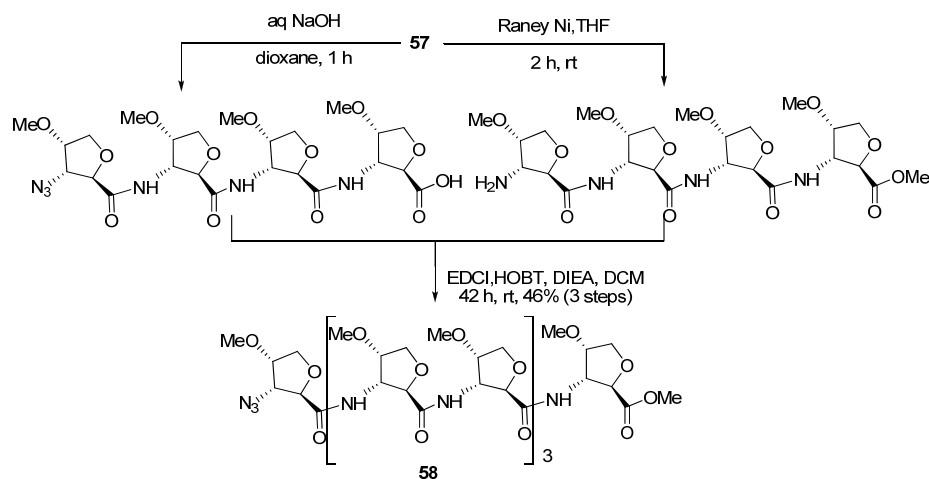


The formation of hexamer **57** was substantiated by the presence of five amide proton doublets at δ 7.26, 7.34, 7.36, 7.39 and 7.39 with $J = 8.3, 7.8, 8.2, 8.5$ and 8.5 Hz respectively in the ¹H NMR spectrum. The seven methoxy signals were observed at δ 3.35, 3.35, 3.36, 3.36, 3.37, 3.45 and 3.70, being the first six corresponding to the methyl ethers and last one for the methyl ester. In the ¹³C NMR spectrum, the characteristic ester carbonyl signal appeared at δ 171.65 and five amide carbonyls appeared at δ 170.38, 170.49, 170.58, 170.90 and 170.90 ppm. In the IR spectrum, absorption due to ester C=O stretching band appeared at 1746 cm^{-1} and the C=O stretching band of amide functionality was seen at 1682 cm^{-1} and the characteristic peak at 2112 cm^{-1} justified the presence of azide group. Further supplementations such as CHN and the mass peak noticed at m/z 939.5 (100%, $[M+\text{Na}]^+$) agreed to the assigned structure **57**.

Next, we focused our attention on the synthesis of octamer. For this purpose, the methyl ester of tetramer **57** was hydrolyzed with aqueous sodium hydroxide in

dioxane and the resulting tetramer-acid was coupled with the tetramer-amine employing EDCI and HOBT, DIPEA in CH₂Cl₂ at rt to afford octamer **58** (Scheme 36).

Scheme 36: Synthesis of *trans*- β -FAA octamer **58**



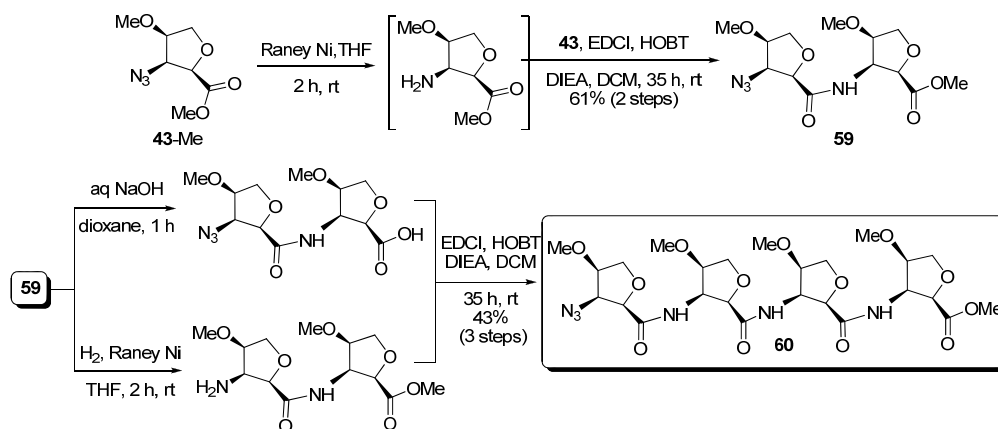
The constitution of the octamer **58** was investigated with the help of spectral and analytical data. In the ¹H NMR spectrum of octamer **58**, seven characteristic amide protons are present as doublet at δ 7.27, 7.28, 7.38, 7.48, 7.55, 7.65, 7.66 each integrating for one proton. The ¹³C NMR spectrum showed corresponding carbonyl singlets at δ 170.38, 170.48, 170.86, 171.05, 171.27, 171.29, 171.41, 171.73 ppm. The IR spectrum showed the C=O stretching of ester at 1744 cm⁻¹ and the C=O stretching of amide carbonyl at 1676 cm⁻¹. Azide functionality was confirmed by characteristic band at 2110 cm⁻¹. Also mass peak at m/z 1204 (100%, [M+H]⁺) agreed with the structure **58**.

Synthesis of *cis*- β -FAA homo-oligomers **59–61** from **43/43-Me**

A similar set of reactions used for the preparation of the *trans*- β -FAA homo-oligomers have been extended by employing the azido-acid **43** and the azido-ester **43-Me**. The dimer **59** was prepared by coupling the intermediate monomer-amine (prepared by the hydrogenolysis of the azide **43-Me** using Raney nickel) and acid **43** by employing EDCI and HOBT, DIPEA in CH₂Cl₂ at rt (Scheme 37). The structure of dimer **59** was investigated with the help of ¹H NMR, ¹³C NMR, IR and mass spectral data analysis. In the ¹H NMR of dimer **59**, the methoxy signals were observed at δ 3.28, 3.45 and 3.75 as a singlets each integrating for three protons. The distinguishing

amide proton appeared as a doublet at δ 7.39 with $J = 8.8$ Hz. The ^{13}C NMR spectrum, ester carbonyl carbon singlet appeared at δ 170.25 ppm and the amide carbonyl carbon appeared at 168.00 ppm. Absorption due to ester and amide carbonyl functionalities were seen in the IR spectrum at 1751 cm^{-1} and 1681 cm^{-1} respectively. The characteristic peak at 2107 cm^{-1} indicated the presence of the azide group.

Scheme 37: Synthesis of *cis*- β -FAA dimer **59 and *cis*- β -FAA tetramer **60****

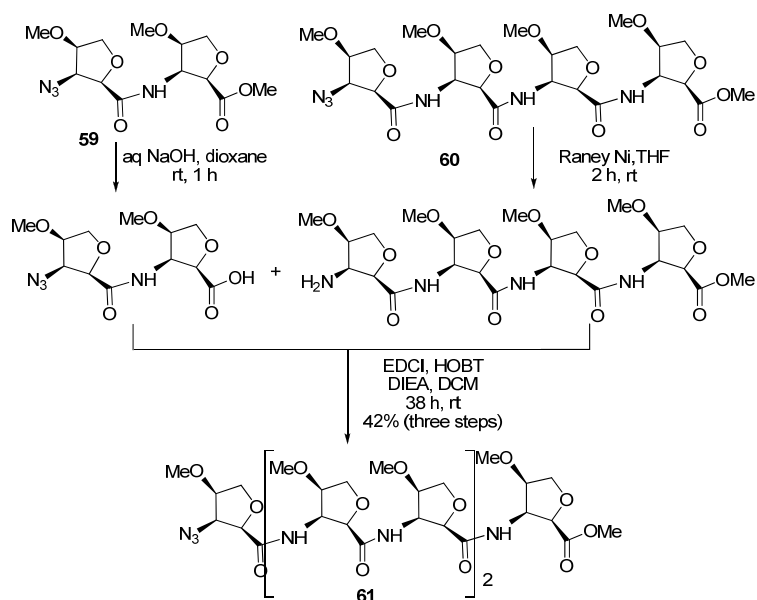


The synthesis of *cis*-tetramer **60** was started with the saponification of dimer to prepare dimer-acid and reduction of azide unit in the same dimer **59** gave the dimer-amine. Finally, coupling of these two fragments in the presence of EDCI and HOBt, DIPEA in CH_2Cl_2 furnished tetramer **60** in 43% overall yield (Scheme 37). The assigned structure of tetramer was well supported by spectral data. In the ^1H NMR spectrum of tetramer **60**, all amide protons were appeared as doublets at δ 7.76 ($J = 9.3$ Hz), 8.46 ($J = 8.5$ Hz) and 8.56 ($J = 8.6$ Hz). The carbonyl of ester appeared as a singlet at δ 168.30 ppm and the amide carbonyls appeared as singlets at δ 170.83, 171.83 and 171.83 ppm. In the IR spectrum of tetramer **60**, C=O stretching of ester and amide were observed at 1751 cm^{-1} and 1682 cm^{-1} respectively and the azide functionality of **60** appeared at 2118 cm^{-1} .

Hydrogenolysis of the azide group in the tetramer yielded the tetramer-amine which was coupled with the freshly prepared dimer-acid using EDCI and HOBt, DIPEA in CH_2Cl_2 at rt to procure hexamer **61** (Scheme 38). The hexamer product was confirmed by ^1H NMR, ^{13}C NMR, IR and mass spectrum. In the ^1H NMR spectrum of hexamer **61**, seven methoxy signal were observed at δ 3.25, 3.25, 3.26, 3.26, 3.28, 3.46 and 3.76 as singlets. The amide protons were resolved clearly in ^1H NMR

spectrum, and appeared as doublets at δ 7.76 ($J = 9.3$ Hz), 8.54 ($J = 7.6$ Hz), 8.59 ($J = 7.1$ Hz), 8.62 ($J = 7.4$ Hz) and 8.65 ($J = 7.5$ Hz). In the IR spectrum absorption due to ester C=O stretching band appeared at 1746 cm^{-1} and C=O stretching of amide functionality was seen at 1682 cm^{-1} , and the azide functionality was confirmed by characteristic band at 2112 cm^{-1} in the IR spectrum of **61**. The mass peak at m/z 939.5 (100%, $[M+Na]^+$) supported evidences for structure **61**.

Scheme 38: Synthesis of *cis*- β -FAA hexamer **61**



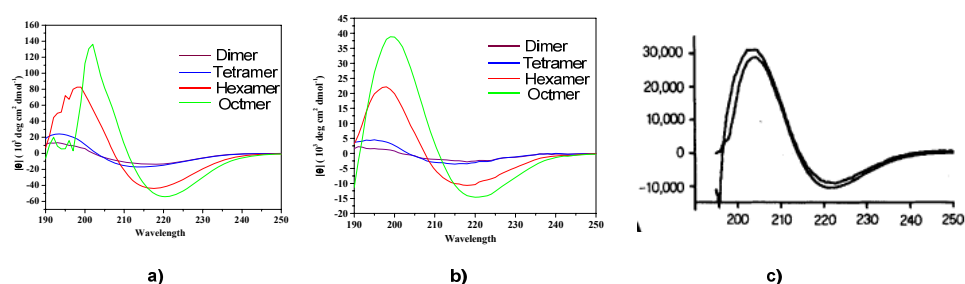
Next we attempted to synthesize the octamer by employing the amine and acids of the tetramer following the established protocols. However all the attempts were found to be futile. We also attempted to couple the amine of the hexamer with the dimer acid, which once again was a failure.

Secondary structural analysis of *trans*-FAA oligomers

The secondary structural analysis of the homo-oligomers of *trans*- β -FAA started with the recording of the CD spectra of dimer **55**, tetramer **56**, hexamer **57** and octamer **58**. The CD spectra of these four oligomers were measured in trifluoroethanol and at two different concentrations (0.1 mmol and 0.02 mmol). The CD spectra of dimer **55** and tetramer **56** did not show any significant ellipticity. The CD data for the hexamer and octamer suggests a distinct secondary structure and the sign and magnitude of the CD were found to be independent of concentration. The CD spectra

of hexamer **57** shows a maxima at 198 nm, zero crossing at 208 nm and minima at 218 nm. Similarly, CD spectra of octamer **58** showed a maxima at 200 nm, zero crossing at 211 nm and minima at 220 nm (Figure 37). This CD pattern suggest a left handed 12-helix in these two homo-oligomers which indeed has been observed with the *trans*-aminocyclopentane carboxylic acid (*trans*-ACPC) and also cyclic pyrrolidne based beta-amino acid homo-oligomers. For example, the hexamer of *trans*-ACPC show a maxima at 204 nm, zero crossing at 214 nm and minima at 221 nm.

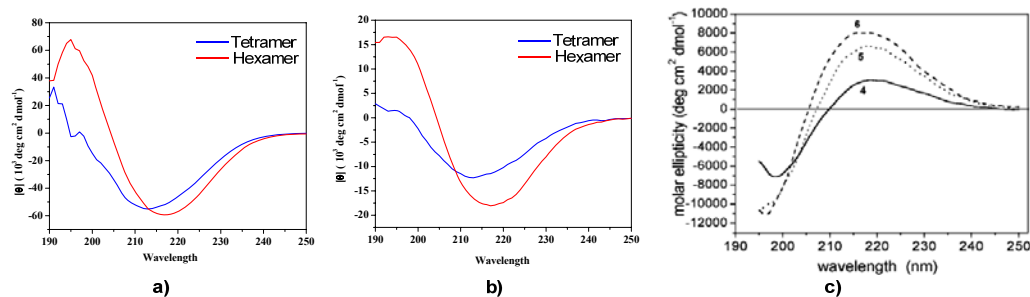
Figure 37: The CD Spectral of di, tetra, hexa and octamers (a) at 0.1 mmol and (b) at 0.02 mmol and c) the CD spectra of hexamer of *trans*-ACPC at 0.1 mmol and 0.02 mmol



Secondary structural analysis of *cis*-FAA oligomers

The CD spectra of tetramer **60** and hexamer **61** were measured in trifluoroethanol and at 0.1 mmol and 0.02 mmol concentrations. The CD data for the tetramer suggests a distinct secondary structure and also is independent of the concentration. Hexamer **61** showed a similar CD signature however with the increased ellipticity. The CD spectra of tetramer and hexamer showed a maxima at 196 nm. The zero crossing of the tetramer is at 198 nm and that of the hexamer is 204. The minimum of the tetramer is 214 nm and this has moved further 3 units to hexamer (Figure 38). This CD pattern suggests a left handed 14-helix in these two homo-oligomers which indeed has been observed with the *cis*- β -FAA carboxylic acid prepared by Chandrasekhar and co-workers. For example, Chandrasekhar's tetramer displays a minimum, zero crossing and a maximum at 198, 209, and 218 nm, respectively which has been ascribed to the presence of a right-handed 14-helix.

Figure 38: The CD Spectral of *cis* tetra and hexamers (a) at 0.1 mmol and (b) at 0.02 mmol and c) the CD spectra of related *cis*-AFA having 14-membered helix



Secondary Structural Analysis by 2D NMR

The secondary structural analysis of oligo peptides by 2D-NMR techniques has been well established. Though, the 1D NMR techniques like ^1H , ^{13}C and DEPT help to get the intra-residual connectivity to some extent, however, extensive 2D NMR (HSQC and HMBC) analysis is required to get the inter-residue connectivity. We have used COSY, HSQC and HMBC to characterize first the primary structure of these peptides and which has been cross checked to get the proximal through spatial connectivity with the help of NOESY such as the cross talk between the $\text{C}\alpha\text{H}_{(i)}/\text{NH}_{(i+2)}$, $\text{NH}_{(i)}/\text{NH}_{(i+1)}$, and $\text{C}\beta\text{H}_{(i)}/\text{NH}_{(i+2)}$. Inter-residue *nOes* are also present in most of the spectra. Additional *nOes* are observed in spectra of those peptides for which lowered tempered coefficients implicate amide protons involved in intramolecular H-bonding interaction and there exists a defined secondary structure. In case of α -peptides, characteristic *nOe* connectivities include $\text{NH}_{(i)}/\text{NH}_{(i+1)}$, $\text{C}\alpha\text{H}_{(i)}/\text{NH}_{(i+2)}$, and $\text{C}\beta\text{H}_{(i)}/\text{NH}_{(i+2)}$. Whereas, β -peptides with defined secondary structure show long range *nOes* like $\text{NH}_{(i)}/\text{NH}_{(i+1)}$, $\text{NH}_{(i)}/\text{C}\beta\text{H}_{(i+1)}$, $\text{NH}_{(i)}/\text{C}\beta\text{H}_{(i+2)}$, $\text{NH}_{(i)}/\text{C}\beta\text{H}_{(i+3)}$, $\text{C}\alpha\text{H}_{(i)}/\text{C}\beta\text{H}_{(i+3)}$, $\text{C}\alpha\text{H}_{(i)}/\text{C}\beta\text{H}_{(i+2)}$.

Secondary structural analysis of trans- β -FAA dimer 55

i) COSY (Correlation spectroscopy) of trans- β -FAA dimer 55: The detailed analysis of the COSY spectrum (Figure 39) of dimer **55** has been given and the inter-residue connectivities are shown (Figure 40) below.

Figure 39: Expansion of COSY spectrum of dimer 55

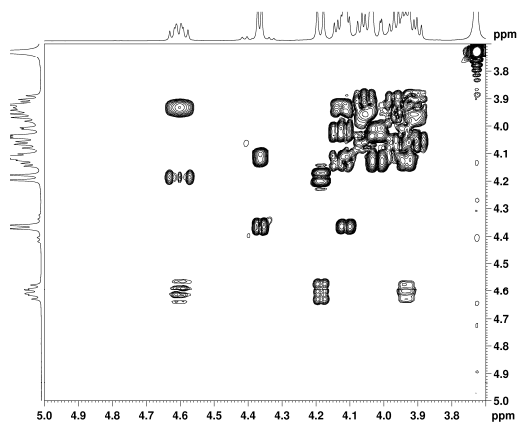
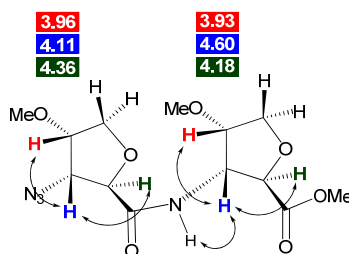
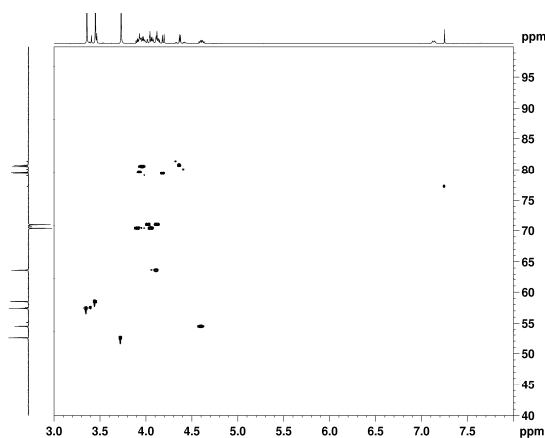


Figure 40: skeletal presentation of the dimer 55 obtained from COSY experiment



ii) HSQC (Heteronuclear Single Quantum Coherence) of *trans*- β -FAA dimer 55: This experiment identifies the carbon and ^1H which are connected to each other through single bond. Figure 41 shows the $^1J_{\text{C-H}}$ couplings of *trans*-dimer 55.

Figure 41: Expansion of HSQC spectrum of *trans* dimer 55



iii) *HMBC (Heteronuclear Multiple Bond Coherence) of trans-β-FAA dimer 55*: This experiment (Figure 42) identified the carbon and proton which are separated by two/three bonds depending on the coupling constant and dihedral angles. Figure 43 shows some of the characteristic $^2J_{C-H}/^3J_{C-H}$ couplings of dimer 55 observed.

Figure 42: Expansion of HMBC spectrum of trans-AHA dimer 55

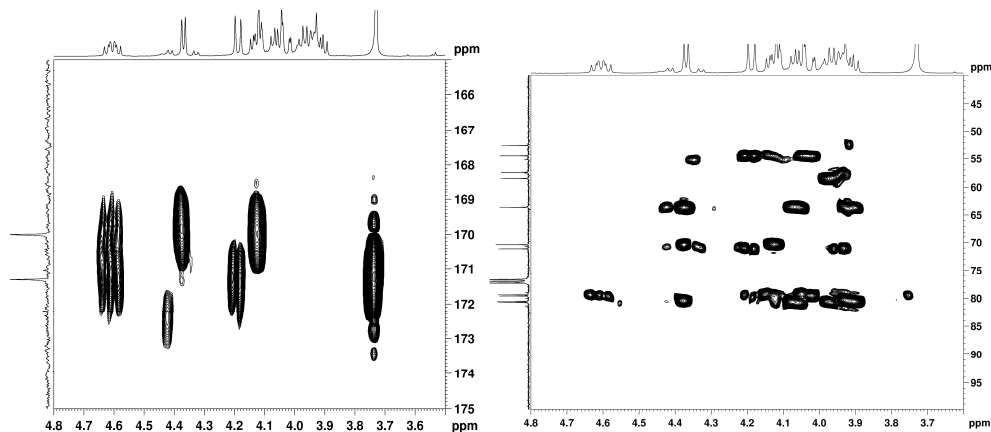
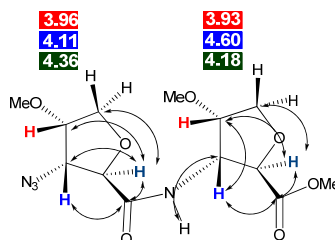


Figure 43: skeletal presentation of the dimer 55 obtained from HMBC experiment



iv) *NOESY (Nuclear Overhauser Effect) Spectrum of dimer 55*: The Figure 44 show some of the characteristic nOes of dimer 55 and Figure 45 shows the skeletal presentation.

Figure 44: Expansion of NOESY spectrum of dimer 55

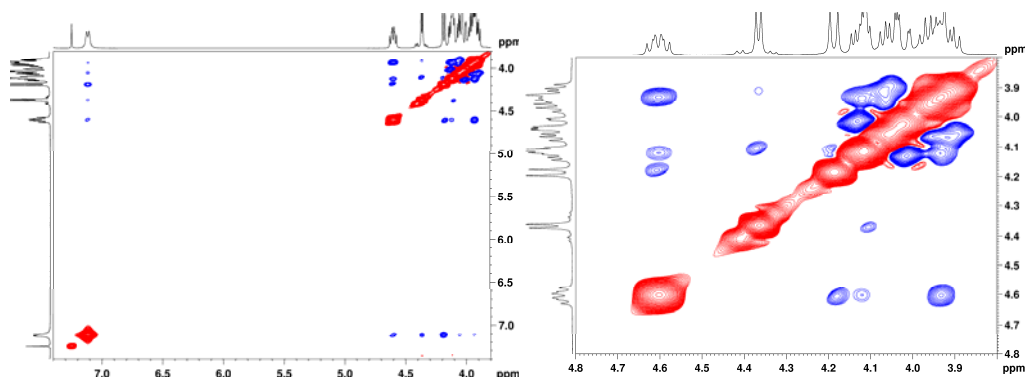
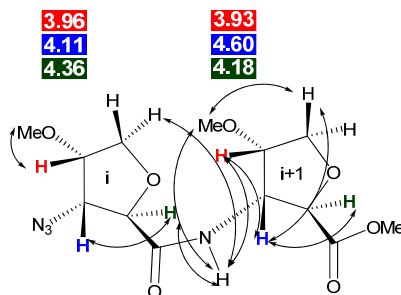


Figure 45: skeletal presentation of the dimer **55** obtained from nOes experiment



In the NOESY of the dimer **55**, $C_{\alpha}H_{(i+1)}/C_{\beta}H_{(i+1)}$, $C_{\beta}H_{(i+1)}/C_{\gamma}H_{(i+1)}$, $C_{\beta}H_{(i+1)}/C_{\delta}H_{(i+1)}$, $NH_{(i+1)}/C_{\gamma}H_{(i+1)}$, $C_{\delta}H_{(i+1)}/C_{\gamma}OMe_{(i+1)}$, $NH_{(i+1)}/C_{\alpha}H_{(i+1)}$ and $NH_{(i+1)}/C_{\gamma}OMe_{(i+1)}$ are the intraresidue nOes of the ester (i+1) ring that are observed. The inter-residue of (i) are $C_{\alpha}H_{(i)}/C_{\beta}H_{(i)}$ and $C_{\gamma}OMe_{(i)}/C_{\gamma}H_{(i)}$. Intra-residue $NH_{(i+1)}/C_{\delta}H_{(i)}$ and $NH_{(i+1)}/C_{\alpha}H_{(i)}$ nOes are also observed.

Table 3: 1H NMR chemical shift (δ in ppm) are in $CDCl_3$ for dimer **55**

Monomer Proton ↓	(i)	(i+1)
NH		7.11
α	4.36	4.18
β	4.11	4.60
γ	3.96	3.93
δ	4.05	4.12
δ'	3.91	4.02
-OMe	3.44	3.35

Secondary structural analysis of trans- β -AFA tetramer 56

i) *COSY of Tetramer 56:* Majority of inter residual connectivities are characterized with the help of the COSY spectrum of tetramer (Figure 46) and the representative connectivities and peak assignments are given in the Figure 47.

Figure 46: Expansion of COSY spectrum of tetramer 56

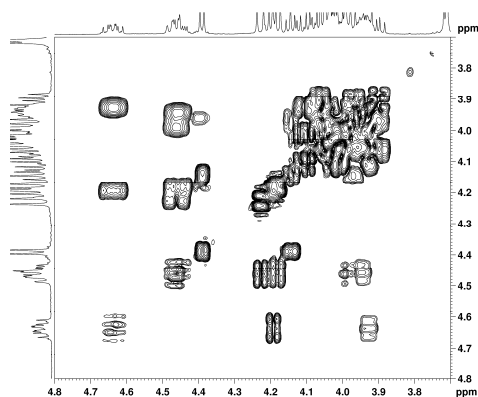
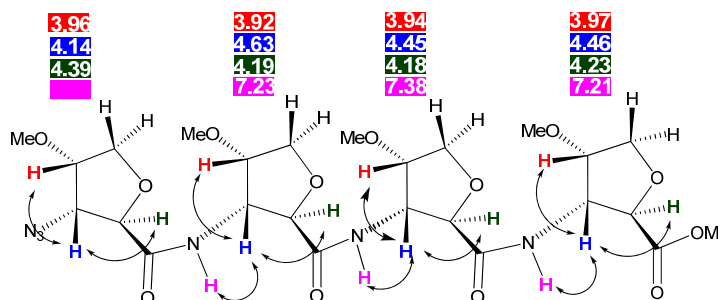
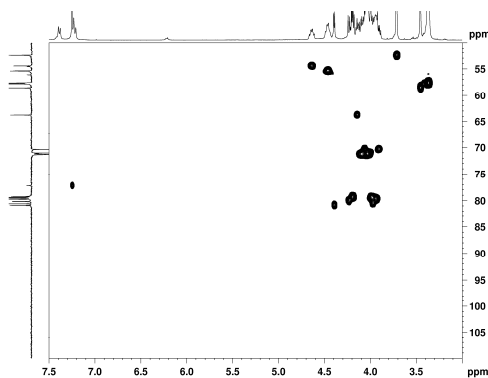


Figure 47: skeletal presentation of the tetramer 61 obtained from COSY experiment



ii) *HSQC of Tetramer 56*: This experiment identified the carbon and ^1H which are connected to each other through single bond. Figure 48 shows the $^1J_{\text{C-H}}$ couplings of tetramer 56.

Figure 48: HSQC spectrum of tetramer 56



iii) *HMBC of Tetramer 56*: The HMBC spectrum (Figure 49) and characteristic $^2J_{\text{C-H}}$ $^3J_{\text{C-H}}$ couplings of tetramer 56 (Figure 50) are given below.

Figure 49: Expansion of HMBC spectrum of tetramer 56

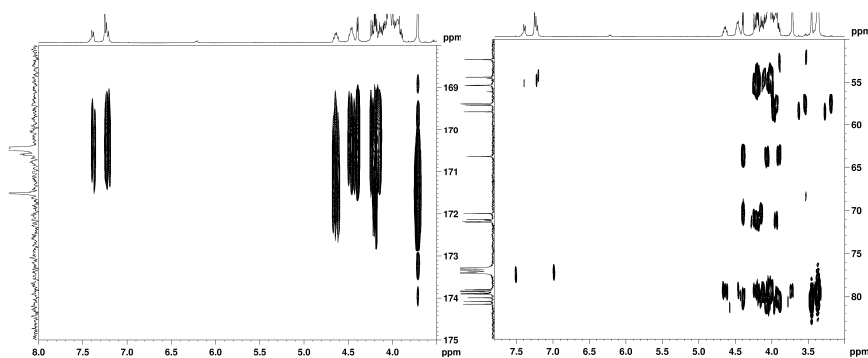
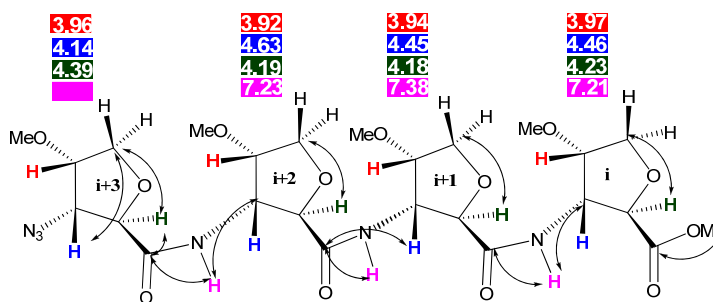
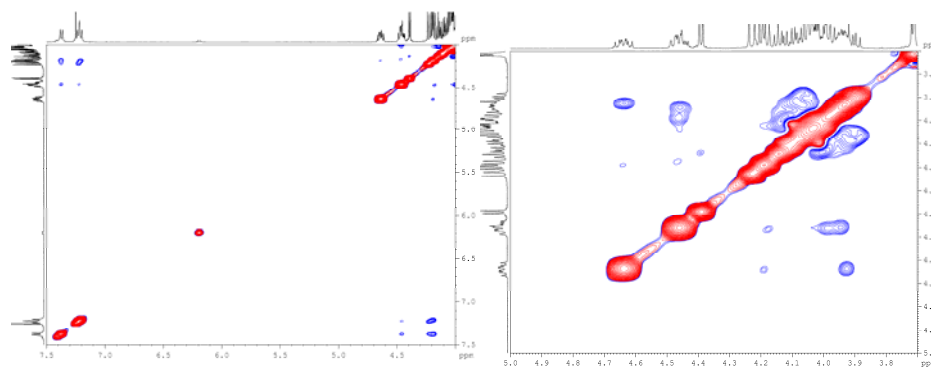


Figure 50: skeletal presentation of the tetramer 56 obtained from HMBC experiment



iv) NOESY analysis of Tetramer 56: The NOESY of tetramer 56 and the characteristic through spatial connectives are given in Figures 51 and 52 respectively.

Figure 51: Expansion of nOes spectrum of tetramer 56



The tetramer 56 shows nOes between $C_{\alpha}H_{(i+3)}/NH_{(i+3)}$, $C_{\beta}H_{(i+3)}/C_{\gamma}H_{(i+3)}$, $C_{\beta}H_{(i+3)}/C_{\delta}H_{(i+3)}$, $C_{\beta}H_{(i+2)}/NH_{(i+2)}$, $C_{\gamma}OMe_{(i+1)}/C_{\delta}H_{(i+1)}$, $C_{\alpha}H_{(i+1)}/C_{\beta}H_{(i+1)}$, $C_{\beta}H_{(i+1)}/C_{\gamma}H_{(i+1)}$, $NH_{(i+1)}/C_{\alpha}H_{(i+1)}$, $C_{\gamma}H_{(i+1)}/C_{\gamma}OMe_{(i+1)}$ and $C_{\gamma}H_{(i)}/C_{\gamma}OMe_{(i)}$ which are the intra-residue nOes. The observed inter-residue nOes of tetramer are between $C_{\beta}H_{(i+3)}/C_{\gamma}H_{(i+2)}$, $C_{\alpha}H_{(i+2)}/C_{\beta}H_{(i+3)}$, $C_{\alpha}H_{(i+1)}/NH_{(i+2)}$ and $C_{\delta}H_{(i+3)}/C_{\beta}H_{(i+1)}$.

Figure 52: skeletal presentation of the tetramer **56** obtained from *nOes* experiment

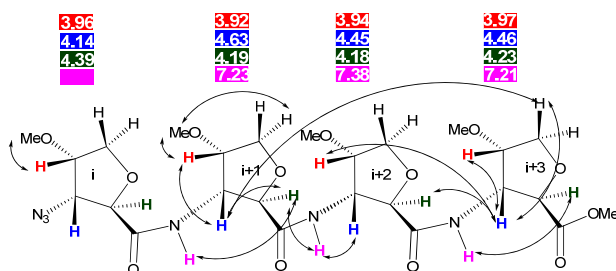


Table 4: ^1H NMR chemical shift (δ in ppm) are in CDCl_3 for tetramer **56**

Monomer →	(i)	(i+1)	(i+2)	(i+3)
Proton ↓				
NH		7.21	7.38	7.23
α	4.39	4.19	4.18	4.23
β	4.14	4.63	4.45	4.46
γ	3.96	3.92	3.94	3.97
δ	3.90	4.09	4.09	4.10
δ'	4.05	4.02	4.02	4.02
-OMe	3.45	3.36	3.37	3.35

Secondary structural analysis of *trans*- β -FAA hexamer **57**

i) *COSY* of hexamer **57**: Majority of inter residual connectivities of hexamer **57** are characterized with the help of the *COSY* spectrum (Figure 53) and the representative connectivities and peak assignments are given in the Figure 54.

Figure 53: Expansion of *COSY* spectrum of hexamer **57**

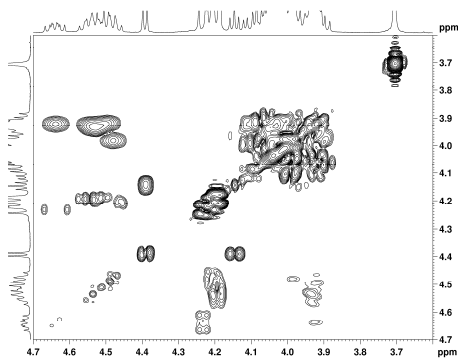
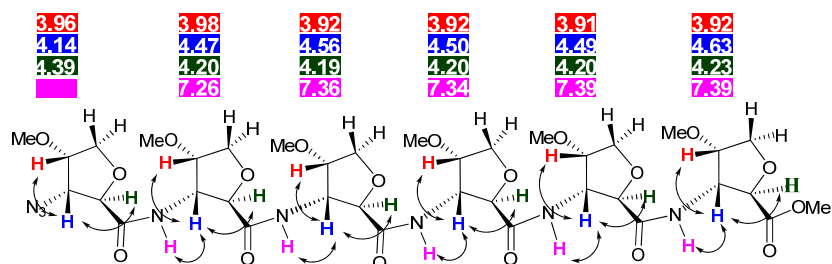
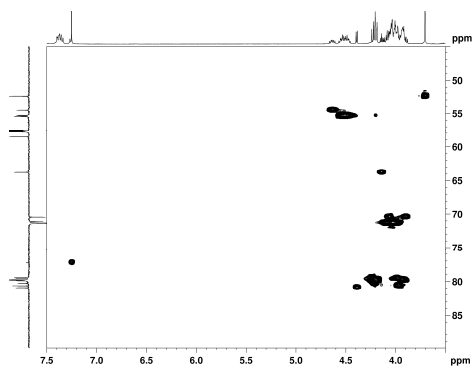


Figure 54: skeletal presentation of the hexamer **57** obtained from COSY experiment



ii) *HSQC analysis of hexamer 57*: This experiment identified the carbon and ^1H which are connected to each other through a single bond. Figure 55 shows the $^1J_{\text{C-H}}$ couplings of hexamer **57**.

Figure 55: HSQC spectrum of *trans* hexamer **57**



iii) *HMBC analysis of hexamer 57*: The HMBC spectrum (Figure 56) and characteristic $^2J_{\text{C-H}}/^3J_{\text{C-H}}$ couplings of hexamer **57** (Figure 57) are given below.

Figure 56: Expansion of HMBC spectrum of hexamer **63**

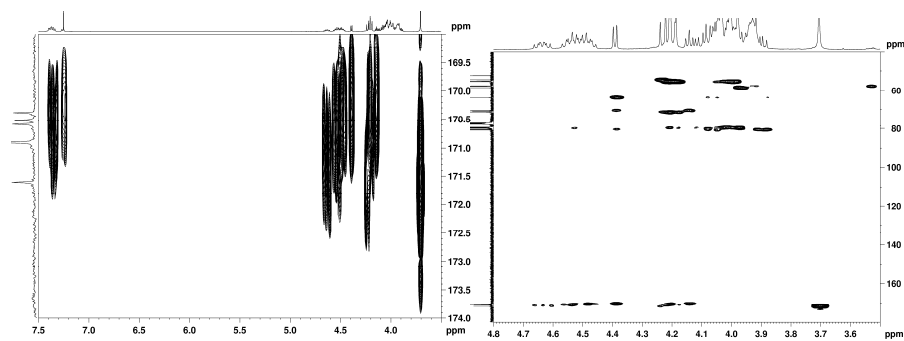
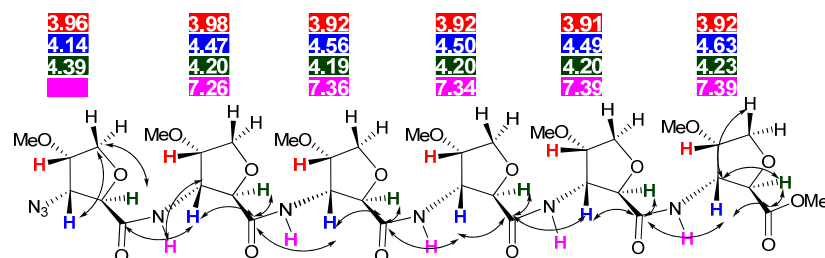
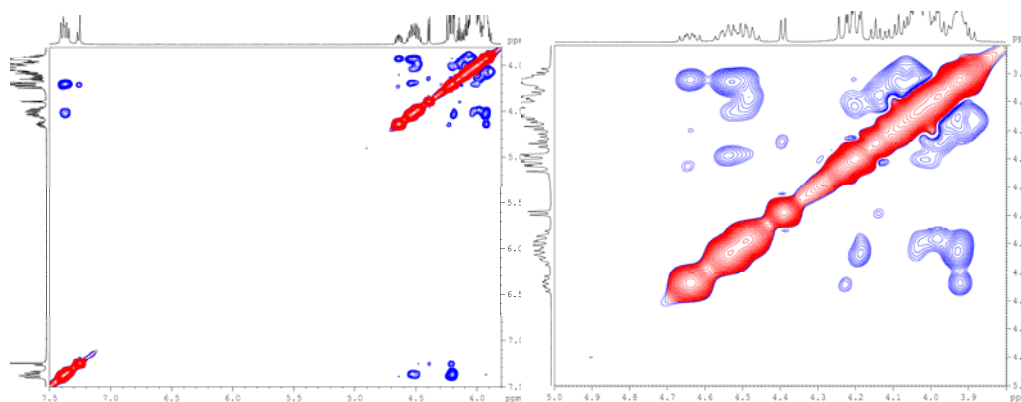


Figure 57: skeletal presentation of the hexamer **57** obtained from HMBC experiment



iv) *NOESY of hexamer 57*: The NOESY of hexamer **57** and the characteristic through spatial connectives are given in Figures 58 and 59 respectively.

Figure 58: Expansion of *nOe* spectrum of hexamer **57**



The hexamer **57** shows intraresidue *nOes* between $C_{\alpha}H_{(i+5)}/C_{\beta}H_{(i+5)}$, $C_{\beta}H_{(i+5)}/NH_{(i+5)}$, $C_{\beta}H_{(i+5)}/C_{\gamma}H_{(i+5)}$, $C_{\beta}H_{(i+5)}/C_{\delta}H_{(i+5)}$, $C_{\alpha}H_{(i+4)}/C_{\beta}H_{(i+4)}$, $C_{\beta}H_{(i+4)}/NH_{(i+4)}$, $NH_{(i+4)}/C_{\gamma}H_{(i+4)}$, $C_{\gamma}H_{(i+2)}/NH_{(i+2)}$, $NH_{(i+2)}/C_{\alpha}H_{(i+2)}$, $NH_{(i+2)}/C_{\beta}H_{(i+2)}$, $C_{\beta}H_{(i+1)}/NH_{(i+1)}$ and $NH_{(i+1)}/C_{\alpha}H_{(i+1)}$. The inter-residue *nOes* of hexamer are $NH_{(i+3)}/C_{\beta}H_{(i+2)}$, $NH_{(i+3)}/C_{\alpha}H_{(i+2)}$, $NH_{(i+1)}/C_{\alpha}H_{(i)}$.

Figure 59: skeletal presentation of the hexamer **57** obtained from *nOe* experiment

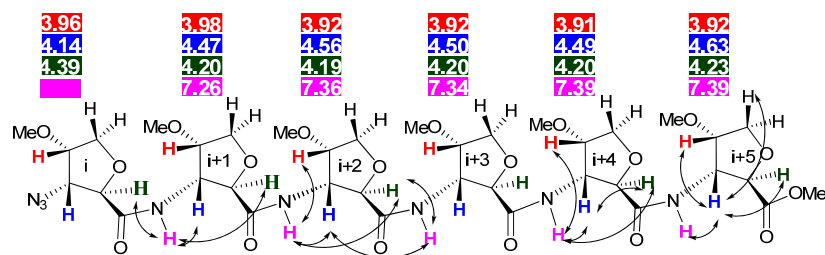


Table 5: ^1H NMR chemical shift (δ in ppm) are in CDCl_3 for *trans* hexamer

Monomer \ Proton	(i)	(i+1)	(i+2)	(i+3)	(i+4)	(i+5)
NH		7.26	7.36	7.34	7.39	7.39
α	4.39	4.20	4.19	4.20	4.20	4.23
β	4.14	4.47	4.56	4.50	4.49	4.63
γ	3.96	3.98	3.92	3.92	3.91	3.92
δ	3.89					3.98
δ'	4.02					4.10
-OMe					57.54	

Secondary structural analysis of *trans*- β -FAA octamer **58**

i) *COSY* of octamer **58**: Majority of inter residual connectivities of octamer **58** are established with the help of the *COSY* spectrum of (Figure 60) and the representative connectivities and peak assignments are given in the Figure 61.

Figure 60: Expansion of *COSY* spectrum of octamer **58**

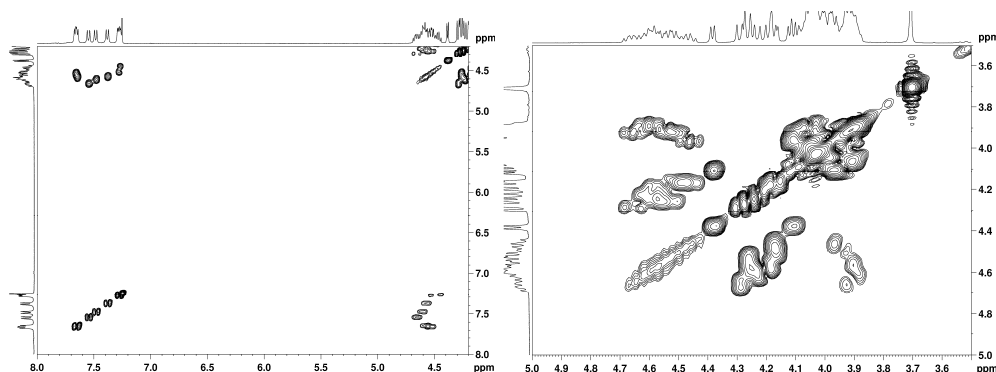
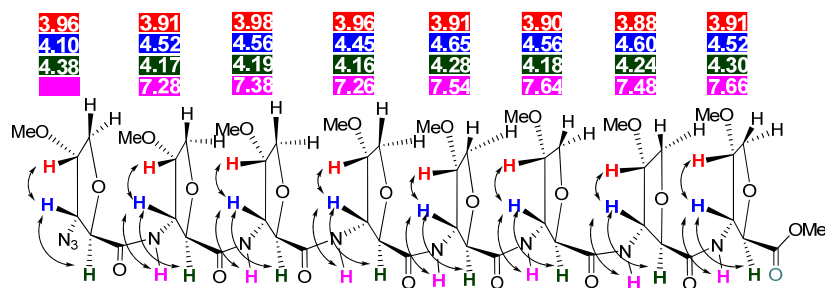
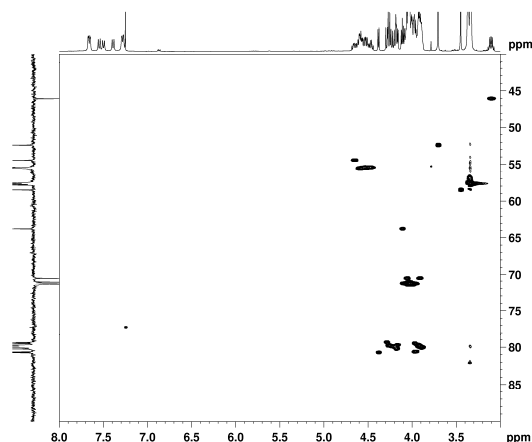


Figure 61: skeletal presentation of the octamer **58** obtained from *COSY* experiment



ii) *HSQC analysis of octamer 58*: This experiment identified the carbon and ^1H which are connected to each other through single bond. Figure 62 shows the $^1J_{\text{C-H}}$ couplings of octamer 58.

Figure 62: Expansion of HSQC spectrum of *trans* octamer 58



iii) *HMBC analysis of octamer 58*: The HMBC spectrum (Figure 63) and characteristic $^2J_{\text{C-H}}/^3J_{\text{C-H}}$ couplings of octamer 58 (Figure 64) are given below.

Figure 63: Expansion of HMBC spectrum of octamer 58

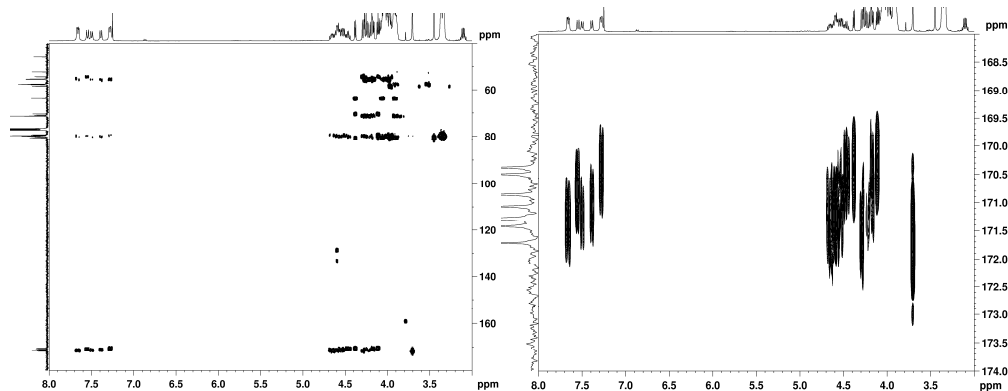
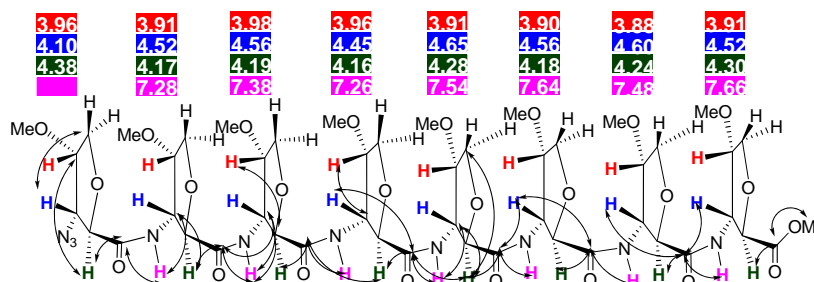


Figure 64: skeletal presentation of the octamer 58 obtained from HMBC experiment



iv) *NOESY analysis of octamer 58*: The NOESY of octamer **58** and the characteristic through spatial connectives are given in Figures 65 and 66 respectively.

Figure 65: Expansion of *nOe* spectrum of octamer **58**

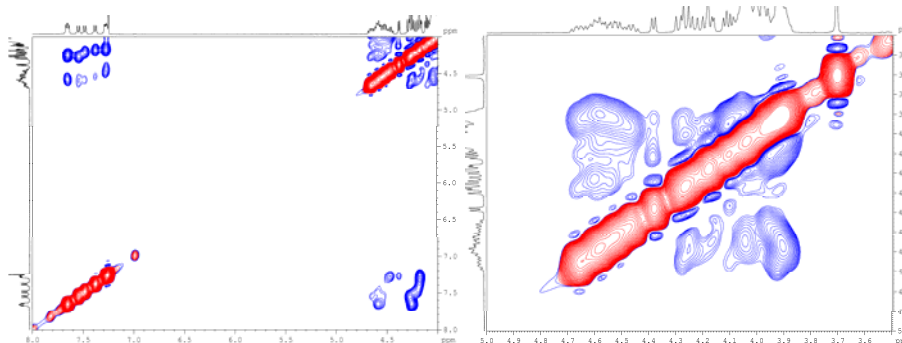
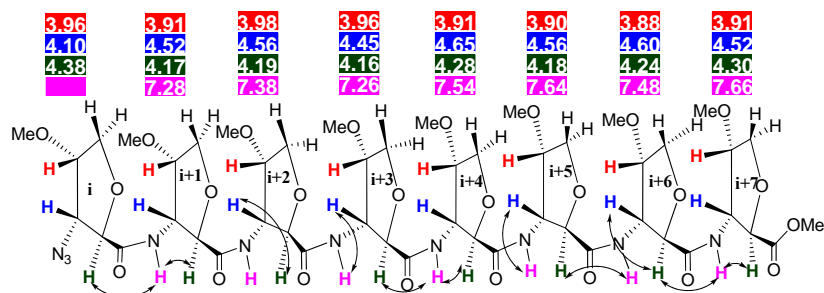


Figure 66: skeletal presentation of the octamer **58 obtained from *nOe* experiment**



The trans octamer shows $\text{NH}_{(i+7)}/\text{C}_\alpha\text{H}_{(i+6)}$, $\text{NH}_{(i+7)}/\text{C}_\alpha\text{H}_{(i+7)}$, $\text{C}_\alpha\text{H}_{(i+6)}/\text{C}_\beta\text{H}_{(i+6)}$, $\text{NH}_{(i+5)}/\text{C}_\beta\text{H}_{(i+5)}$, $\text{NH}_{(i+6)}/\text{C}_\alpha\text{H}_{(i+5)}$, $\text{NH}_{(i+5)}/\text{C}_\alpha\text{H}_{(i+4)}$, $\text{NH}_{(i+4)}/\text{C}_\alpha\text{H}_{(i+4)}$, $\text{NH}_{(i+3)}/\text{C}_\beta\text{H}_{(i+3)}$, $\text{NH}_{(i+1)}/\text{C}_\alpha\text{H}_{(i)}$, $\text{C}_\alpha\text{H}_{(i+2)}/\text{C}_\beta\text{H}_{(i+2)}$, $\text{C}_\alpha\text{H}_{(i+1)}/\text{NH}_{(i+1)}$ inter *nOes* of trans octamer.

Table 6: ^1H NMR chemical shift (δ in ppm) in CDCl_3 for octamer **58**

Monomer → Proton ↓	(i)	(i+1)	(i+2)	(i+3)	(i+4)	(i+5)	(i+6)	(i+7)
NH		7.28	7.38	7.26	7.54	7.64	7.48	7.66
α	4.38	4.17	4.19	4.16	4.28	4.18	4.24	4.30
β	4.10	4.52	4.56	4.45	4.65	4.56	4.60	4.52
γ	3.96	3.91	3.98	3.96	3.91	3.90	3.88	3.91
δ	4.05				4.02			
δ'	3.90				4.02			
-OMe								

Secondary structural analysis of *cis*- β -FAA dimer **59**

i) *COSY* of dimer **59**: The detailed analysis of the COSY spectrum (Figure 67) of dimer **59** has been given and the inter-residue connectivities are shown (Figure 68) below.

Figure 67: Expansion of COSY spectrum of dimer **65**

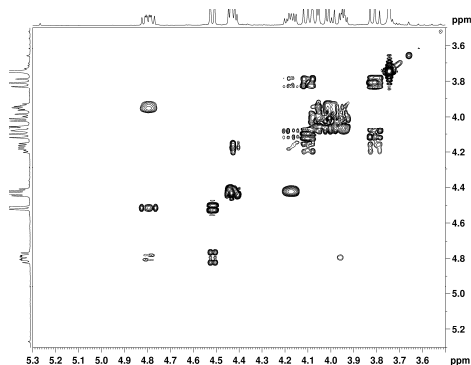
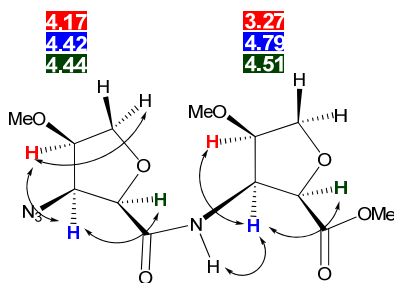
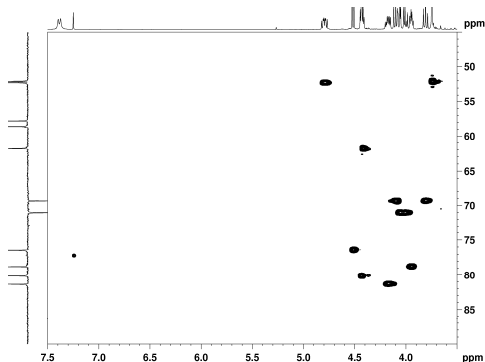


Figure 68: skeletal presentation of the dimer **59** obtained from COSY experiment



ii) *HSQC* analysis of dimer **59**: This experiment identifies the carbon and ^1H which are connected to each other through a single bond. Figure 69 shows the $^1J_{\text{C-H}}$ couplings of *cis*-dimer **59**.

Figure 69: Expansion of HSQC spectrum of dimer **59**



iii) *HMBC of cis-β-FAA dimer 59*: This experiment (Figure 70) identified the carbon and proton which are separated by two/three bonds depending on the coupling constant and dihedral angles. Figure 70 shows some of the characteristic $^2J_{C-H}/^3J_{C-H}$ couplings of dimer **59** observed.

Figure 70: Expansion of HMBC spectrum of dimer **59**

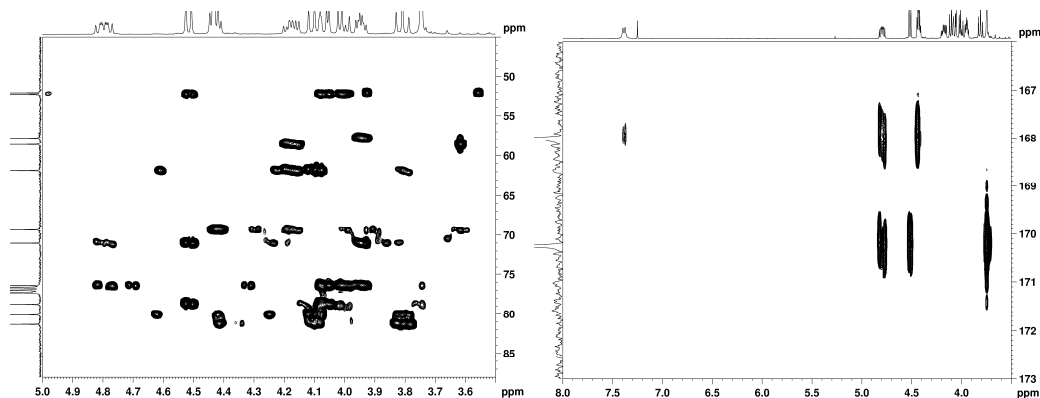
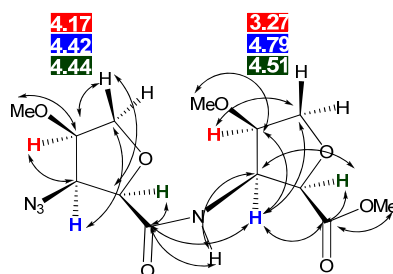


Figure 71: skeletal presentation of the dimer **59** obtained from HMBC experiment



iv) *NOESY analysis of dimer 59*: The Figure 72 show some of the characteristic *nOes* of dimer **59** and Figure 73 shows the skeletal presentation.

Figure 72: Expansion of *nOe* spectrum of dimer **59**

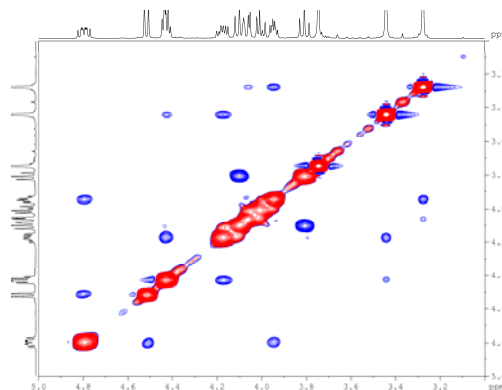
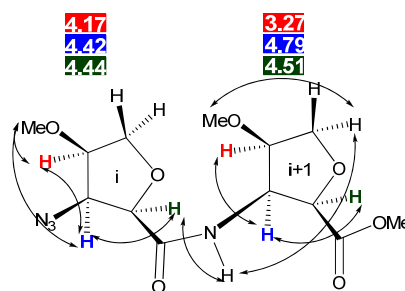


Figure 73: skeletal presentation of the dimer **59** obtained from nOe experiment



The cis dimer **59** shows intra-residue nOes between $C_{\alpha}H_{(i+1)}/C_{\beta}H_{(i+1)}$, $C_{\beta}H_{(i+1)}/C_{\gamma}H_{(i+1)}$, $C_{\gamma}OMe_{(i+1)}/C_{\delta}H_{(i+1)}$, $NH_{(i+1)}/C_{\delta}H_{(i+1)}$, $C_{\alpha}H_{(i)}/C_{\beta}H_{(i)}$, $C_{\beta}H_{(i)}/C_{\gamma}OMe_{(i+1)}$, $C_{\beta}H_{(i)}/C_{\gamma}H_{(i)}$ and $C_{\gamma}OMe_{(i)}/C_{\gamma}H_{(i)}$. The inter-residue nOes is $NH_{(i+1)}/C_{\alpha}H_{(i)}$

Table 7: 1H NMR chemical shift (δ in ppm) are in $CDCl_3$ for cis dimer **67**

Monomer →	(i)	(i+1)
Proton ↓		
NH		7.38
α	4.44	4.51
β	4.42	4.79
γ	4.17	3.94
δ	3.81	4.01
δ'	4.10	4.06
-OMe	3.44	3.27

Secondary structural analysis of cis- β -FAA tetramer **60**

i. COSY of tetramer 60: A majority of inter residual connectivities are characterized with the help of the COSY spectrum of tetramer (Figure 74) and the representative connectivities and peak assignments are given in the Figure 75.

Figure 74: Expansion of COSY spectrum of tetramer 60

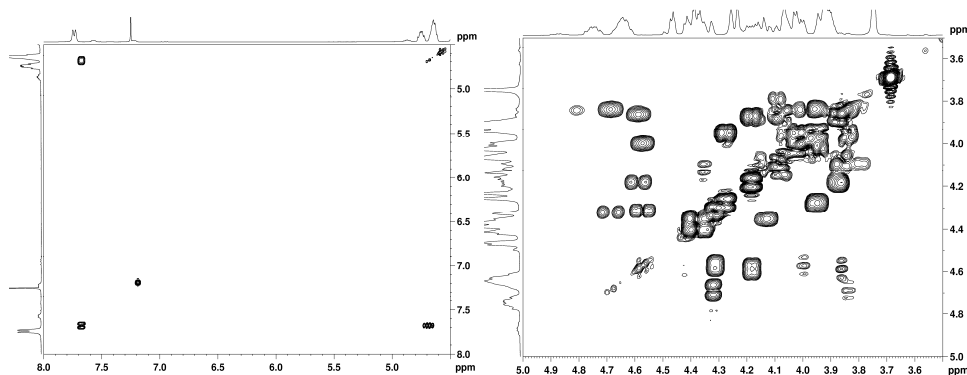
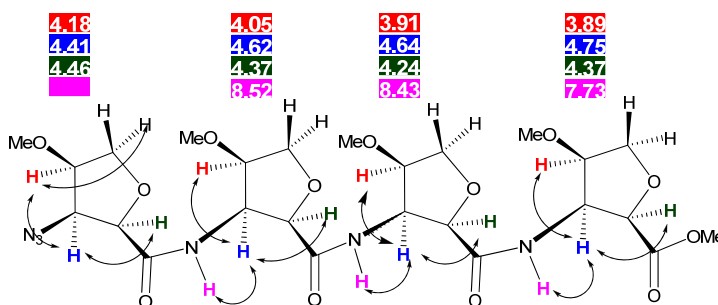
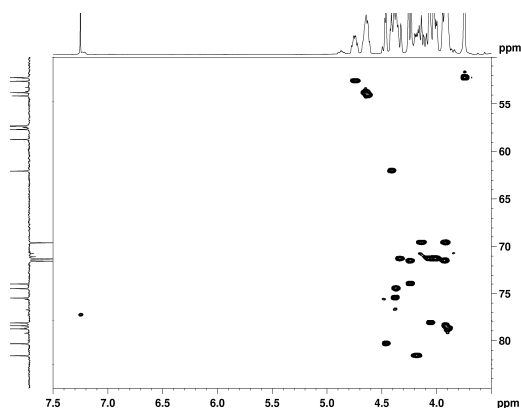


Figure 75: skeletal presentation of the cis tetramer 70 obtained from COSY experiment



ii) *HSQC analysis of tetramer 60*: This experiment identified the carbon and ^1H which are connected to each other through single bond. Figure 76 shows the $^1J_{\text{C-H}}$ couplings of tetramer 60.

Figure 76: Expansion of HSQC spectrum of tetramer 60



iii) *HMBC analysis of tetramer 60*: The HMBC spectrum (Figure 77) and characteristic $^2J_{\text{C-H}}/^3J_{\text{C-H}}$ couplings of tetramer 60 (Figure 78) are given below.

Figure 77: Expansion of HMBC spectrum of tetramer 60

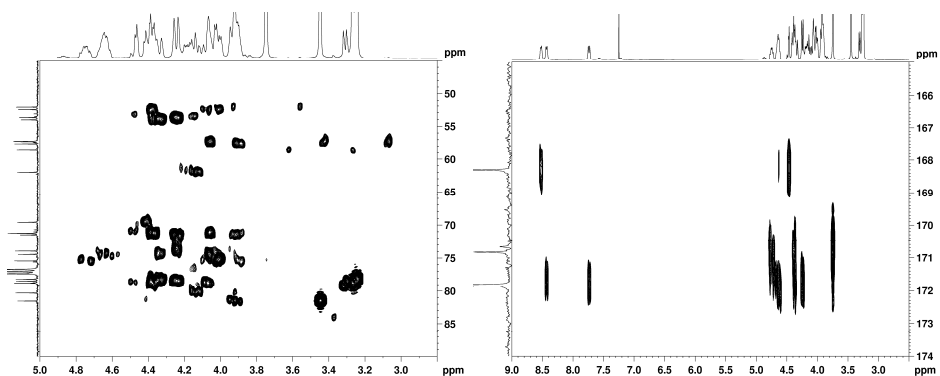
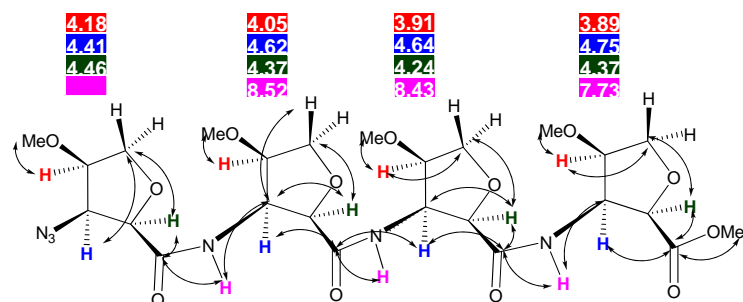
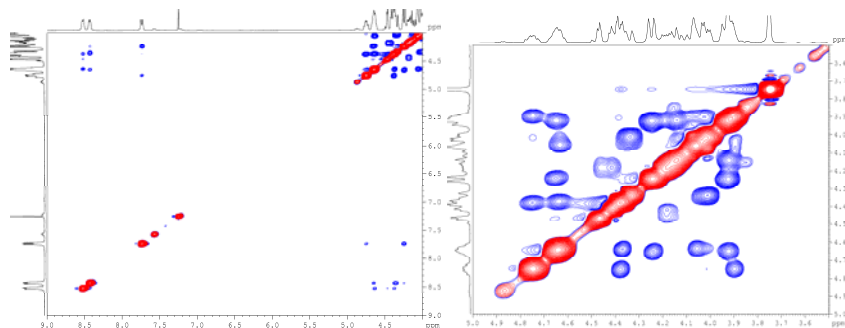


Figure 78: skeletal presentation of the tetramer 60 obtained from HMBC experiment



iv) NOESY analysis of tetramer 60: The NOESY of tetramer 60 and the characteristic through spatial connectives are given in Figures 79 and 80 respectively.

Figure 79: Expansion of nOe spectrum of tetramer 60



The tetramer 60 shows nOes of, $C_{\alpha}H_{(i+3)}/NH_{(i+3)}$, $C_{\beta}H_{(i+3)}/NH_{(i+3)}$, $C_{\gamma}H_{(i+3)}/NH_{(i+3)}$, $C_{\delta}H_{(i+3)}/NH_{(i+3)}$, $NH_{(i+3)}/C_{\gamma}OMe_{(i+2)}$, $EsterOMe/C_{\gamma}OMe_{(i+2)}$, $C_{\gamma}H_{(i+3)}/C_{\gamma}H_{(i+2)}$, $C_{\alpha}H_{(i+2)}/C_{\gamma}OMe_{(i+2)}$, $C_{\beta}H_{(i+2)}/NH_{(i+2)}$, $C_{\alpha}H_{(i+1)}/C_{\delta}H_{(i+1)}$, $C_{\alpha}H_{(i+1)}/C_{\beta}H_{(i+1)}$, $C_{\beta}H_{(i+1)}/C_{\gamma}H_{(i+1)}$, $NH_{(i+1)}/C_{\alpha}H_{(i+1)}$, $C_{\beta}H_{(i+1)}/NH_{(i+1)}$, $NH_{(i+1)}/C_{\alpha}H_{(i)}$, $C_{\gamma}H_{(i)}/C_{\gamma}OMe_{(i)}$ and $C_{\gamma}OMe_{(i)}/C_{\beta}H_{(i)}$ are the nOes of *cis*-tetramer observed.

Figure 80: skeletal presentation of the tetramer **60** obtained from nOe experiment

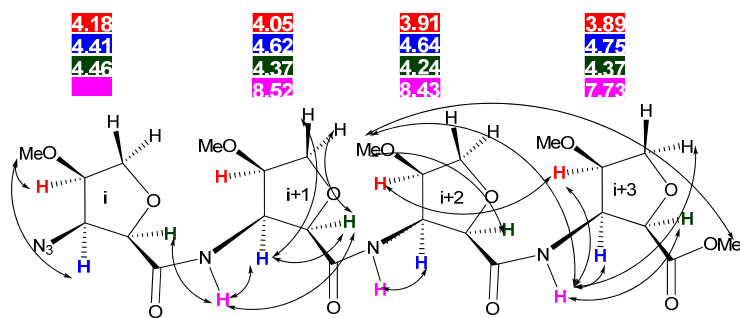


Table 8: ^1H NMR chemical shift (δ in ppm) in CDCl_3 for tetramer **60**

Monomer → Proton ↓	(i)	(i+1)	(i+2)	(i+3)
NH		8.52	8.43	7.73
α	4.46	4.37	4.24	4.37
β	4.41	4.62	4.64	4.75
γ	4.18	4.05	3.91	3.89
δ	4.13	4.33	4.24	4.06
δ'	3.91	4.01	3.92	
-OMe	3.45	3.24	3.25	3.27

Secondary structural analysis of *cis*- β -FAA hexamer **61**

i) COSY analysis of hexamer **61**: Majority of inter residual connectivities of hexamer **61** are characterized with the help of the COSY spectrum (Figure 81) and the representative connectivities and peak assignments are given in the Figure 82.

Figure 81: Expansion of COSY spectrum of hexamer **61**

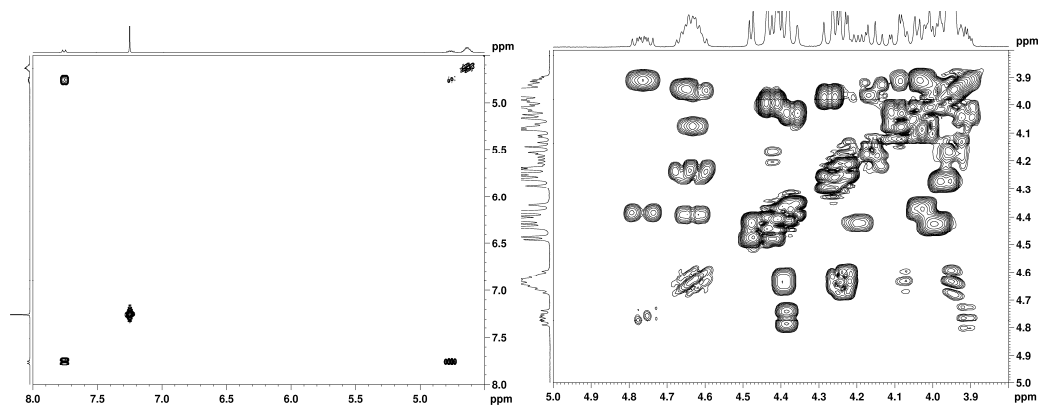
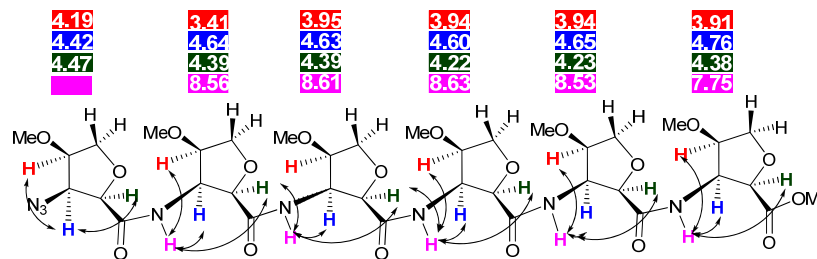
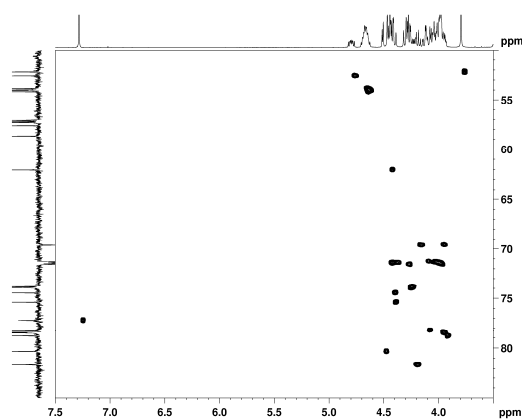


Figure 82: skeletal presentation of the hexamer **60** obtained from COSY experiment



ii) *HSQC analysis of hexamer 61*: This experiment identified the carbon and ^1H which are connected to each other through single bond. Figure 83 shows the $^1J_{\text{C-H}}$ couplings of hexamer **61**.

Figure 83: Expansion of HSQC spectrum of *cis* hexamer **72**



iii) *HMBC analysis of hexamer 61*: The HMBC spectrum (Figure 84) and characteristic $^2J_{\text{C-H}}$ / $^3J_{\text{C-H}}$ couplings of hexamer **61** (Figure 85) are given below.

Figure 84: Expansion of HMBC spectrum of hexamer **61**

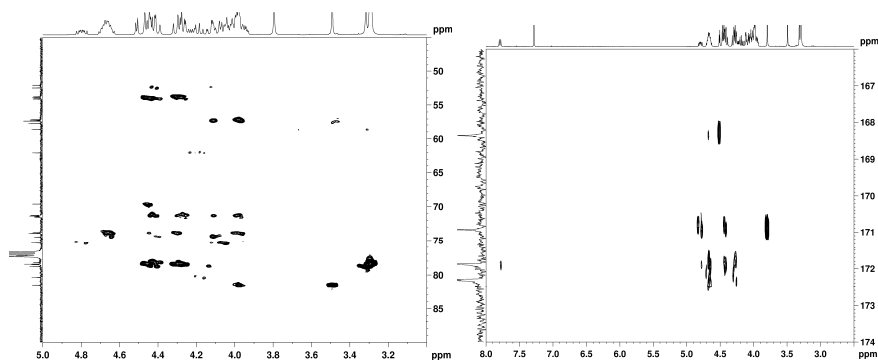
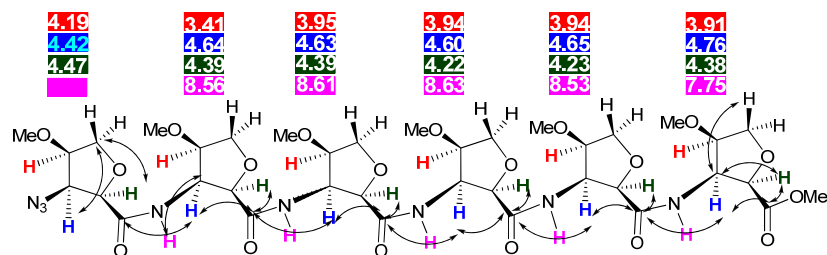


Figure 85: skeletal presentation of the hexamer **61** obtained from HMBC experiment



iv) NOESY analysis of hexamer **61**: The NOESY of hexamer **61** and the characteristic through spatial connectives are given in Figures 86 and 87 respectively.

Figure 86: Expansion of nOe spectrum of *cis* hexamer **72**

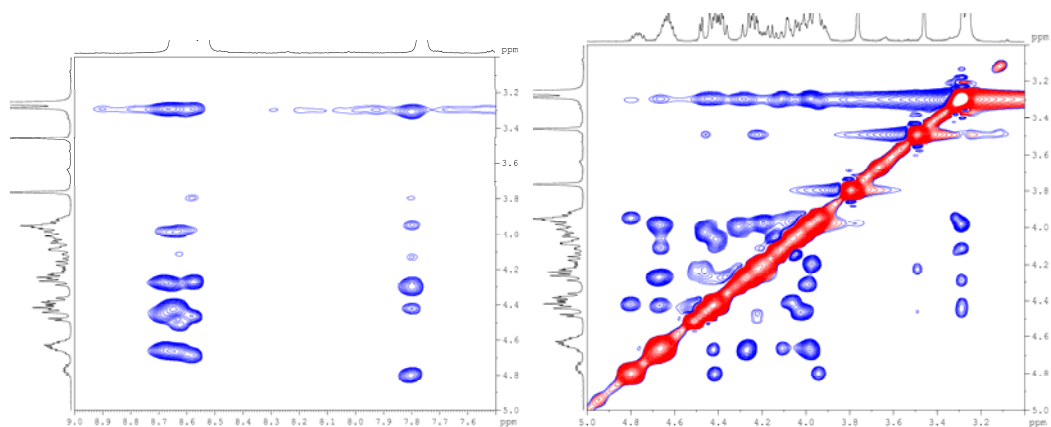
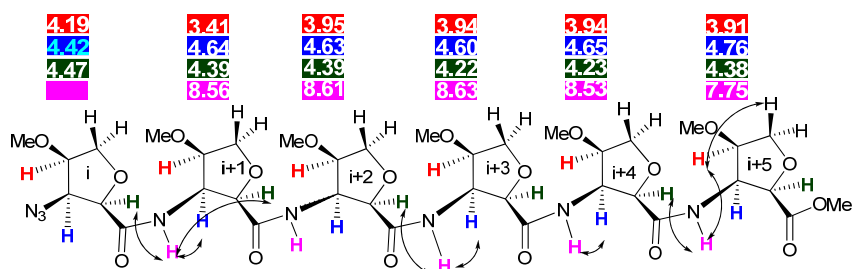


Figure 87: skeletal presentation of the hexamer **61** obtained from nOe experiment



The hexamer **61** shows $nOes$ of, $C_{\gamma}H_{(i+5)}/C_{\delta}H_{(i+5)}$, $C_{\gamma}H_{(i+5)}/NH_{(i+5)}$, $NH_{(i+5)}/C_{\alpha}H_{(i+4)}$, $C_{\alpha}H_{(i)}/NH_{(i+1)}$, $C_{\beta}H_{(i+1)}/NH_{(i+1)}$, $NH_{(i+4)}/C_{\beta}H_{(i+4)}$, $NH_{(i+3)}/C_{\beta}H_{(i+3)}$, $NH_{(i+3)}/C_{\alpha}H_{(i+2)}$, and $NH_{(i+1)}/C_{\alpha}H_{(i+1)}$ are the $nOes$ of hexamer.

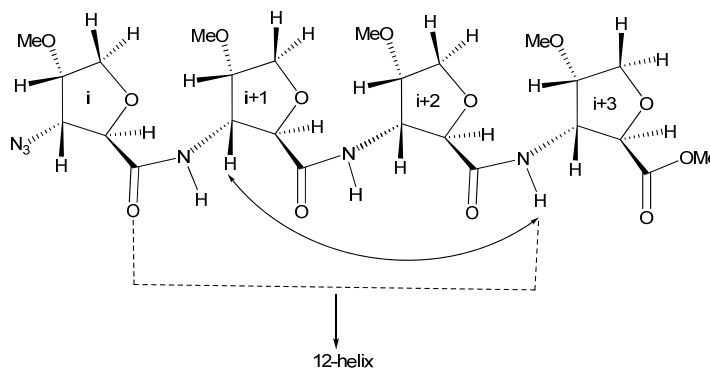
Table 9: ^1H NMR chemical shift (δ in ppm) are in CDCl_3 for hexamer **61**

Monomer \rightarrow Proton \downarrow	(i)	(i+1)	(i+2)	(i+3)	(i+4)	(i+5)
NH		8.56	8.61	8.63	8.53	7.75
α	4.47	4.39	4.39	4.22	4.23	4.38
β	4.42	4.64	4.63	4.60	4.65	4.76
γ	4.19	3.92	3.95	3.94	3.94	3.91
δ	4.12	4.38	4.33	4.24	3.98	3.99
δ'	3.92	3.95	3.98	3.96	3.99	3.28
-OMe	3.43	3.23	3.23	3.23	3.24	4.08

Discussion and Conclusion

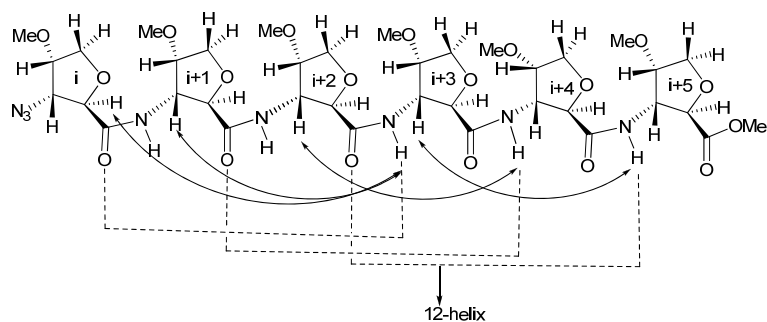
The secondary structure of *trans*- β -FAA tetramer **56** was assigned with the help of the inter-residue nOes noticed. Amongst the various nOes observed in the NOESY of the **56**, $\text{C}_\beta\text{H}_{(i+1)}/\text{NH}_{(i+3)}$ (Figure 88) indicates the presence of a single 12-helix pitch. However, the CD-ellipticity of this tetramer is substantially weak.

Figure 88: Characteristic nOes supporting a 12-helix



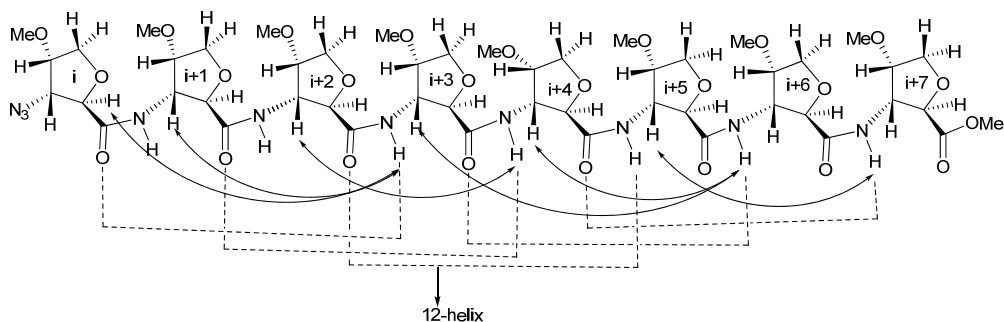
Next, we analyzed the various inter-residue nOes observed in the NOESY of the *trans*-hexamer **57** (Figure 89). The interpretation of some of the observed long-range nOes is complicated by the overlapping of two of the five NH protons. Four characteristic nOes $\text{C}_\beta\text{H}_{(i+1)}/\text{NH}_{(i+3)}$, $\text{C}_\alpha\text{H}_{(i)}/\text{NH}_{(i+3)}$, $\text{C}_\beta\text{H}_{(i+2)}/\text{NH}_{(i+4)}$ and $\text{C}_\beta\text{H}_{(i+3)}/\text{NH}_{(i+5)}$ found indicated the presence of a left-handed 12-helix, which was further supported by the concentration independent CD maxima and minima recorded for this hexamer.

Figure 89: Characteristic *nOes* supporting a 12-helix



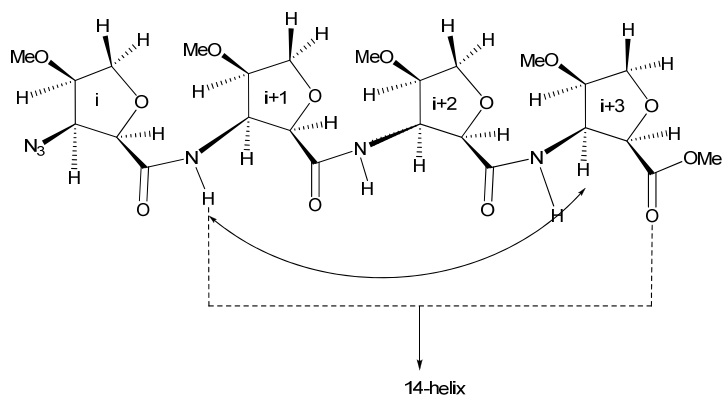
Some of the important inter-residue *nOes* observed in the NOESY of the *trans*-octamer **58** are given in Figure 90. Due to the well separation of all the NH signal, many of the inter-residue *nOes* could be assigned which indeed strongly indicated hydrogen bonding pattern leading to a left-handed 12-helix. Some of the important inter-residue *nOes* - $C_{\alpha}H(i)/NH(i+3)$, $C_{\beta}H(i+1)/NH(i+3)$, $C_{\beta}H(i+2)/NH(i+4)$, $C_{\beta}H(i+4)/NH(i+6)$, $C_{\beta}H(i+5)/NH(i+7)$ and $C_{\beta}H(i+3)/NH(i+6)$ are illustrated in the Figure 90.

Figure 90: Characteristic *nOes* supporting a 12-helix



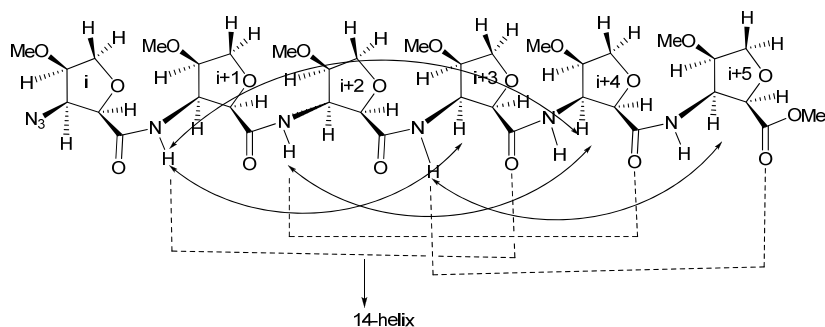
The secondary structure of *cis*- β -AHA tetramer **60** was assigned with the help of inter-residue *nOes* noticed. All protons at NH and C_{β} of each residue were well separated in $CDCl_3$ solvent. Amongst the various *nOes* observed in the NOESY of the **60**, one characteristic *nOes* *i.e.* $NH(i+1)/C_{\beta}H(i+3)$ found indicated the presence of a left-handed 14-helix (Figure 91).

Figure 91: Characteristic *nOes* supporting a 14-helix



The important inter-residue *nOes* observed in the NOESY of the *cis*-hexamer **61** are given in Figure 92. Due to the well separation of all the NH signals and the C_{β} of each residue, four characteristic *nOes* $NH_{(i+1)}/C_{\beta}H_{(i+3)}$, $NH_{(i+1)}/C_{\beta}H_{(i+4)}$, $NH_{(i+2)}/C_{\beta}H_{(i+4)}$ and $NH_{(i+3)}/C_{\beta}H_{(i+5)}$ found indicated the presence of a left-handed 14-helix (Figure 92).

Figure 92: Characteristic *nOes* supporting a 14-helix



There are several important issues which we addressed from these investigations. These are:

- a) Flexible Template – presence and the stability of a secondary structure

In the case of the *cis*- β -FAA homo-oligomers, earlier Chandrasekhar's group¹⁴ has reported that unlike the *cis*-ACPC homo-oligomers, the *cis*- β -FAA homo-oligomers present a 14-membered helix and this has been attributed to the rigidity of the furan ring that they had employed. The present investigations on *cis*- β -FAA homo-oligomers having a flexible furan template also indicate that

these homo-oligomers present a stable secondary structure involving a 14-membered helix, despite the flexibility.

- b) *Cis*- and *trans*- diastereomeric furan- β -amino acids are employed – influence of the relative orientation of amine and acids groups on the nature of the secondary structure and how they are comparable with the ACPC-homo oligomers.

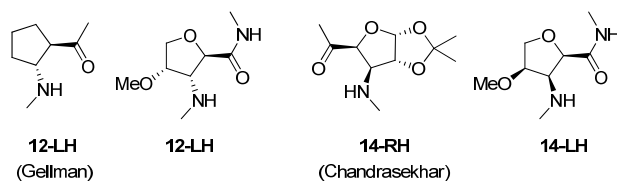
The secondary structural analysis of homo-oligomers of *trans*- β -FAA has been carried out which does indicate the presence of a 12-helical conformation in the solution. This was in agreement with the *trans*-ACPC-homo oligomers¹⁹ and other 5-membered heterocyclic- β -amino acids which also present a 12-helical conformation.²⁰ Interestingly, the *cis*-ACPC-homo oligomers were seen to adopt a sheet like structure,²⁷ while the *cis*- β -FAA homo-oligomers were found to be adopting a 14-helix structure. This can be attributed to the conformational rigidity of the furan ring over the cyclopentane ring. However, to provide a comprehensive answer to whether the attributed rigidity was due to the other substituents present on the furan ring or due to the ring oxygen alone needs to be addressed by synthesizing the homo-oligomers of unsubstituted *cis*- β -FAA.

- c) A methoxy substituent *syn*- to the amine group – the influence adjacent hydrogen-bond acceptors on the N–H... O=C– hydrogen bonding.

The results from our investigations show that the *cis*-oriented methoxy group does not interfere with the secondary structure preference by virtue of the relative orientation of the acid and amine groups. It was quite interesting to note that, in *trans*- β -ACPC oligomers, the substituents at β^4 carbon seem to disturb the 12-helix. Indeed it has been recently shown that the *trans*- β -FAA oligomers having a thymine unit at β^4 carbon were shown to form an 8-helix³⁵, instead of a 12-helix. This has been attributed to the steric factors imposed by the thymine nucleobase.

- d) The relation between the helicity and the absolute stereochemistry of β^1 -carbon: Our systems have the same orientation as the Gellman *trans*-ACPC

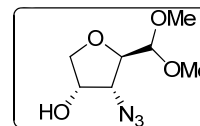
(shows LH-helix)¹⁹ and opposite orientation to the reported *cis*-furan- β -amino acids (shows RH-helix) by Chandrasekhar's group.



In the case of the *cis*- β -FAA homo-oligomers, earlier Chandrasekhar's group has reported that unlike the *cis*-ACPC homo-oligomers, the *cis*- β -FAA homo-oligomers present a 14-membered helix and this has been attributed to the rigidity of the furan ring that they employ. The present investigations on *cis*- β -FAA homo-oligomers having a flexible furan template also indicate that these homo-oligomers present a stable secondary structure involving a 14-membered helix, despite the flexibility.

Experimental

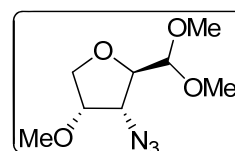
Synthesis of azido alcohol 47



To a solution of tosylate **48** (30 g, 90.4 mmol), in dry DMF (150 mL) was added sodium azide (8.8 g, 135.5 mol) and the reaction mixture was heated at 80 °C for 70 h (**precaution: protected with a safety shield**). The reaction mixture was partitioned between water and EtOAc and the aqueous phase was extracted with EtOAc (2 X 200 mL). The combined organic layer was washed with water, dried (Na₂SO₄), and concentrated. Purification of the crude residue by silica gel column chromatography (10→25 % EtOAc in petroleum ether) gave **47** (14 g, 76%).

Mol. Formula: C₇H₁₃N₃O₄. $[\alpha]_D^{25} = +18.3$ (c 0.4, CHCl₃). **IR (CHCl₃)** ν : 3445, 2934, 2105, 1375, 1256, 1083, 732 cm⁻¹. **¹H NMR (200 MHz, CDCl₃):** δ 2.03 (br. s, 1H), 3.45 (s, 3H), 3.49 (s, 3H), 3.75 (dd, $J = 2.9, 9.7$ Hz, 1H), 3.97 (dd, $J = 1.1, 5.6$ Hz, 1H), 4.01 (dd, $J = 4.1, 5.7$ Hz, 1H), 4.06 (dd, $J = 4.7, 6.5$ Hz, 1H), 4.32 (ddd, $J = 3.1, 4.3, 7.3$ Hz, 1H), 4.37 (d, $J = 4.04$ Hz, 1H). **¹³C NMR (50 MHz, CDCl₃):** δ 54.9 (q), 56.7 (q), 63.9 (d), 72.0 (d), 73.1 (t), 80.7 (d), 104.6 (d) ppm. **ESI-MS m/z :** 226.6 (100%, [M+Na]⁺). **Anal. Calcd :** C, 41.37; H, 6.4; N, 20.68%; Found: C, 41.13; H, 6.57; N, 20.29%.

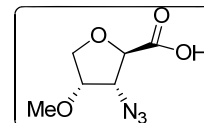
Synthesis of compound 46



At 0 °C, to a solution of azido alcohol **47** (4.5 g, 22.1 mmol) in dry DMF (35 mL), NaH (60% dispersion in mineral oil, 980 mg, 24.3 mmol) was added slowly and stirred for 10 min. To this, methyl iodide (1.5 mL, 24.3 mmol) was added at 0 °C slowly and stirring was continued at room temperature for 4 h. The reaction mixture was partitioned between water and EtOAc. Aqueous layer was extracted with EtOAc (2 X 100 mL). The combined organic layer was washed with 10% HCl, dried (Na₂SO₄) and concentrated. Purification of crude product by column chromatography (8→15% EtOAc in petroleum ether) furnished **46** (4.1 g, 84%) as a colorless oil.

Mol. Formula: C₈H₁₅N₃O₄. [α]_D²⁵ = -23.1 (*c* 2, CHCl₃). **IR (CHCl₃)** ν : 3014, 2936, 2098, 1353, 1216, 1083, 788, 757 cm⁻¹. **¹H NMR (200 MHz, CDCl₃):** δ 3.46 (s, 3H), 3.47 (s, 3H), 3.49 (s, 3H), 3.82 (dd, *J* = 5.8, 10.9 Hz, 1H), 3.96–4.05 (m, 4H), 4.34 (d, 1H, *J* = 3.8 Hz). **¹³C NMR (50 MHz, CDCl₃):** δ 54.9 (q), 56.3 (q), 58.1 (q), 61.3 (d), 70.1 (t), 81.1, (d), 81.2 (d), 104.9 (d) ppm. **ESI-MS *m/z*:** 218.1 (18.2%, [M+H]⁺), 235.2 (66.4%, [M+NH₄]⁺), 240.1 (100%, [M+Na]⁺), 256.2 (24.1%, [M+K]⁺). **Anal. Calcd :** C, 44.23; H, 6.96; N, 19.34; Found: C, 44.68; H, 7.23; N, 19.40%.

Synthesis of *trans*- β -FAA azido acid **42**

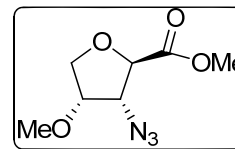


A suspension of acetal **46** (8 g, 36.8 mmol) in sulphuric acid (2N, 40 mL) and 50% acetic acid (40 mL) was heated at 80 °C for 2 h. The reaction mixture was cooled to rt, neutralized with sodium bicarbonate and extracted with CH₂Cl₂ (2 X 150 mL). The combined organic layer was washed with brine, dried (Na₂SO₄) and concentrated. The resulting crude aldehyde (5.2 g) was used directly for the next step without any further purification.

To a cooled solution of above aldehyde (5.2 g) in DMSO (15 mL) NaH₂PO₄·2H₂O (3 g dissolved in 5 mL water, pH 7) was added. Then a solution of sodium chlorite (8 g, 84.6 mmol) in water (10 mL) was added slowly and the resulting mixture was stirred at rt for 10 h. After completion of reaction, solid NaHCO₃ was added and the reaction contents were washed CH₂Cl₂ (100 mL). The aqueous layer was neutralized with con. HCl and extracted with CH₂Cl₂ (2 x 150 mL) and the combined organic layer was dried (Na₂SO₄) and concentrated. The resulting residue was purified by column chromatography (silica gel 20→40% EtOAc in petroleum ether) to afford azido acid **42** (4.6 g, 65%) as a colorless oil.

Mol. Formula: C₆H₉N₃O₄. [α]_D²⁵ = -142.6 (*c* 1, CHCl₃). **IR (CHCl₃)** ν : 3357, 3020, 2939, 2114, 1731, 1216 cm⁻¹. **¹H NMR (400 MHz, CDCl₃):** δ 3.46 (s, 3H), 3.94 (dd, *J* = 3.4, 9.4 Hz, 1H), 3.99 (br. t, *J* = 5.2 Hz, 1H), 4.05 (dd, *J* = 4.7, 9.2 Hz, 1H), 4.13 (dd, *J* = 4.9, 8.6 Hz, 1H), 4.45 (d, *J* = 5.5 Hz, 1H), 9.60 (br. s, 1H). **¹³C NMR (50 MHz, CDCl₃ + CCl₄):** δ 58.3 (d), 63.9 (q), 71.0 (t), 78.8 (d), 80.9 (d), 174.8 (s) ppm. **ESI-MS *m/z*:** 210.2 (100%, [M+Na]⁺). **Anal. Calcd:** C, 38.51; H, 4.85; N, 22.45; Found: C, 38.74 ; H, 4.57; N, 22.69%.

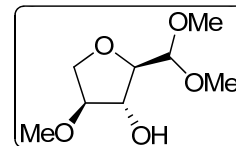
Synthesis of azido ester 42-Me



At 0 °C, to a solution of acid **42** (2 g, 10.6 mmol) in CH₂Cl₂, diazomethane in ether (30 mL) was added and stirred for additional 30 min. Solvent was removed under reduced pressure and the crude product was purified by silica gel column chromatography (15→25% EtOAc in petroleum ether) to obtain **42-Me** (2 g, 93%) as colorless oil.

Mol. Formula: C₇H₁₁N₃O₄. $[\alpha]_D^{25} = -123.7$ (*c* 1, CHCl₃). **IR (CHCl₃)** ν : 2955, 2837, 2110, 1753, 1207, 1078 cm⁻¹. **¹H NMR (200 MHz, CDCl₃)**: δ 3.45 (s, 3H), 3.79 (s, 3H), 3.92 (dd, *J* = 3.4, 6.6 Hz, 1H), 3.96 (br. d, 5.11 Hz, 1H), 4.04 (dd, *J* = 4.6, 8.2 Hz, 1H), 4.11 (ddd, *J* = 4.4, 5.1, 8.6 Hz, 1H), 4.43 (d, *J* = 5.9 Hz, 1H). **¹³C NMR (50 MHz, CDCl₃)**: δ 52.3 (d), 58.0 (d), 63.7 (d), 70.8 (t), 78.8 (q), 80.7 (q), 170 (s) ppm. **ESI-MS *m/z***: 224.6 (100% [M+H]⁺), 240.7 (16 %, [M+Na]⁺). **Anal. Calcd:** C, 41.79; H, 5.51; N, 20.89; Found: C, 41.62; H, 5.25; N, 20.71%.

Synthesis of compound 54

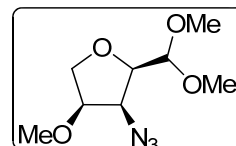


A solution of compound **50** (10 g, 30.1 mmol) in methanol (200 mL) was cooled to 0 °C and treated slowly with sodium (4.3 g, 187.5 mmol) and the reaction mixture was refluxed for 40 h. After completion, methanol was removed under reduced pressure and the residue was partitioned between water and CH₂Cl₂. The aqueous layer was extracted with CH₂Cl₂ and combined organic layer was dried (Na₂SO₄) and concentrated. The residue was purified by silica gel column chromatography (40→50% EtOAc in petroleum ether) to procure **54** (4.6 g, 71%) as light yellow oil.

Mol. Formula: C₈H₁₅N₃O₄. $[\alpha]_D^{25} = +15.3$ (*c* 1, CHCl₃). **IR (CHCl₃)** ν : 3414, 3019, 1215 cm⁻¹. **¹H NMR (200 MHz, CDCl₃)**: δ 3.35 (s, 3H), 3.4 (s, 3H), 3.43 (s, 3H), 3.67 (dd, *J* = 4.9, 6.8 Hz, 1H), 3.81 (ddd, *J* = 2.8, 4.7, 10.2 Hz, 1H), 3.89 (d, *J* = 2.9 Hz, 1H), 3.96 (dd, *J* = 5.3, 9.9 Hz, 1H), 4.11 (dd, *J* = 2.7, 5.1 Hz, 1H), 4.35 (d, *J* = 6.9 Hz, 1H). **¹³C NMR (100**

MHz, CDCl₃+CCl₄): δ 53.3 (q), 55.0 (q), 56.8 (q), 70.9 (t), 77.1 (d), 84.2 (d), 86.5 (d), 104.1 (d) ppm. **ESI-MS *m/z*:** 215.8 (100%, [M+Na]⁺). **Anal. Calcd:** C, 49.99; H, 8.39; Found: C, 49.73 ; H, 8.25%.

Synthesis of acetal **49**

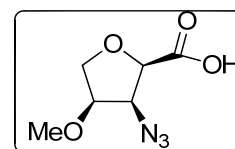


At -20 °C, a solution of **54** (2 g, 10.4 mmol) and pyridine (1.7 mL, 22 mmol) in CH₂Cl₂ (15 mL) was treated with triflic anhydride (3.4 mL, 41.6 mmol) and reaction was stirred for 30 min at 0 °C. The reaction mixture was diluted with CH₂Cl₂ (50 mL) and washed with cold 1N HCl and saturated NaHCO₃, brine and water. The organic layer was dried (Na₂SO₄) and concentrated under reduced pressure to afford crude triflate (3.1 g).

A solution of above triflate in DMSO (10 mL) was cooled to 0 °C and treated with sodium azide (2.4 g, 52.7 mmol) and the contents were stirred at room temperature for 12 h. The reaction mixture was diluted with EtOAc (100 mL), washed with water (3 X 20 mL), dried (Na₂SO₄) and concentrated under reduced pressure. The crude product was purified by silica gel column chromatography (5→15% EtOAc in petroleum ether) to obtain **54** (1.2 g, 54%) as a colorless oil.

Mol. Formula: C₈H₁₅N₃O₄. [α]_D²⁵ = +8.5 (*c* 1, CHCl₃). **IR (CHCl₃) ν :** 3017, 2108, 1215, 1088 cm⁻¹. **¹H NMR (200 MHz, CDCl₃) δ :** 3.42 (s, 3H), 3.44 (s, 3H), 3.45 (s, 3H), 3.72 (br. t, *J* = 8.2 Hz, 1H), 3.83 (dd, *J* = 3.6, 7.5 Hz, 1H), 3.97–4.06 (m, 2H), 4.15 (ddd, *J* = 4.3, 7.8, 12.3 Hz, 1H), 4.49 (d, *J* = 7.5 Hz, 1H). **¹³C NMR (100 MHz, CDCl₃):** 53.5 (q), 55.0 (q), 58.1 (q), 61.6 (d), 68.9 (t), 78.9 (d), 81.5 (d), 102.9 (d) ppm. **ESI-MS *m/z*:** 240.2 (100%, [M+Na]⁺). **Anal. Calcd:** C, 44.23; H, 6.96; N, 19.34; Found: C, 44.313; H, 6.83; N, 19.14%.

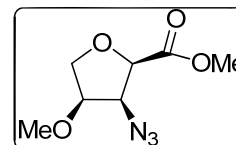
Synthesis of *cis*- β -FAA azido acid **43**



The same procedure as in the preparation of **42** was employed with the acetal **49** (7.5 g, 34.5 mmol) to prepare the *cis*-azido acid **43** (4.3 g, 67%) as colorless oil.

Mol. Formula: C₆H₉N₃O₄. $[\alpha]_D^{25} = +36.4$ (*c* 1, CHCl₃). **IR (CHCl₃)** ν : 3374, 3018, 2934, 2110, 1735, 1216 cm⁻¹. **¹H NMR (200 MHz, CDCl₃):** δ 3.46 (s, 3H), 3.88 (dd, *J* = 8.1, 16.2 Hz, 1H), 4.06–4.27 (m, 2H), 4.37 (br. t, *J* = 4.7 Hz, 1H), 4.55 (d, *J* = 4.7 Hz, 1H), 7.31 (br. s, 1H). **¹³C NMR (100 MHz, CDCl₃):** δ 58.5 (q), 61.8 (d), 69.5 (t), 78.38 (d), 81.1 (d), 171.3 (d) ppm. **ESI-MS *m/z*:** 210.2 (100%, [M+Na]⁺). **Anal. Calcd:** C, 38.51; H, 4.85; N, 22.45; Found: C, 38.69; H, 4.62; N, 22.64%.

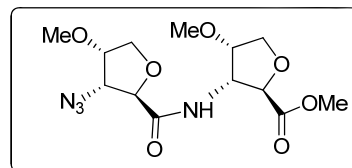
Synthesis of azido ester **43-Me**



By following the procedure used in the preparation of **42-Me**, the acid **43** (2 g, 10.6 mmol) was converted to the corresponding methyl ester **43-Me** (1.9 g, 90%, colorless oil).

Mol. Formula: C₇H₁₁N₃O₄. $[\alpha]_D^{25} = +5.2$ (*c* 1, CHCl₃). **IR (CHCl₃)** ν : 3020, 2116, 1762, 1215 cm⁻¹. **¹H NMR (200 MHz, CDCl₃):** δ 3.44 (s, 3H), 3.78 (s, 3H), 3.87 (dd, *J* = 7.8, 7.9 Hz, 1H), 4.08 (dd, *J* = 6.8, 6.9 Hz, 1H), 4.13–4.23 (m, 1H), 4.28 (br. t, *J* = 4.8 Hz, 1H), 4.52 (d, *J* = 4.5 Hz, 1H). **¹³C NMR (50 MHz, CDCl₃):** δ 51.4 (d), 57.9 (d), 61.5 (d), 69.1 (t), 78.2 (q), 80.6 (q), 168.2 (s) ppm. **ESI-MS *m/z*:** 224.3 (100%, [M+Na]⁺); **Anal. Calcd:** C, 41.79; H, 5.51; N, 20.89; Found: C, 41.54; H, 5.32; N, 20.74%.

Synthesis of *trans*-dimer **55**



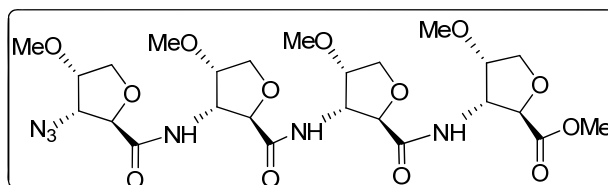
A suspension of ester **42-Me** (900 mg, 4.5 mmol), Raney nickel (500 mg) in THF (20 mL) was flushed with hydrogen gas and stirred under an atmosphere of hydrogen for 2 h. The reaction mixture was filtered through celite and the solvent removed under reduced pressure to yield the crude dimer-amine.

To a solution of acid **42** (800 mg, 4.3 mmol) in dry dichloromethane (15 mL) at 0 °C, 1-hydroxybenzotriazole (870 mg, 6.4 mmol) and diisopropylethylamine (1.1 mL, 6.4 mmol) were added and after 5 min EDCI (1.2 g, 6.4 mmol) was introduced and stirred for 30 min. To this, a solution of the above crude dimer-amine in dichloromethane (5 mL) was added at 0 °C and stirred further at rt for additional 35 h.

The reaction mixture was diluted with dichloromethane (60 mL) and washed with 2N HCl (2 x 25 mL). The organic phase was dried (Na₂SO₄) and concentrated. The crude product was purified over a silica gel column chromatography (35→50% EtoAc in petroleum ether) to afford dimer **55** (838 mg, 57%) as colorless oil.

Mol. Formula: C₁₃H₂₀N₄O₇. [α]_D²⁵ = -64.9 (*c* 0.7, CHCl₃). **IR (CHCl₃)** ν : 3315, 2854, 2107, 1747, 1660, 1544 cm⁻¹. **¹H NMR (400 MHz, CDCl₃)**: δ 3.34 (s, 3H), 3.43 (s, 3H), 3.71 (s, 3H), 3.86–4.06 (m, 5H), 4.09 (d, *J* = 3.4 Hz, 1H), 4.10 (dd, *J* = 2.0, 6.4 Hz, 1H), 4.17 (d, *J* = 7.6 Hz, 1H), 4.35 (d, *J* = 4.7 Hz, 1H), 4.59 (ddd, *J* = 5.3, 7.5, 12.8 Hz, 1H), 7.13 (d, *J* = 8.4 Hz, 1H). **¹³C NMR (100 MHz, CDCl₃)**: δ 52.3 (q), 54.4 (d), 57.2 (q), 58.3 (q), 63.6 (d), 70.3 (t), 71.0 (t), 79.2 (d), 79.4 (d), 80.4 (d), 80.5 (d), 169.9 (s), 171.2 (s) ppm. **ESI-MS *m/z***: 345.0 (100%, [M+H]⁺), 362.0 (32.5%, [M+NH₄]⁺), 367.0 (49.4%, [M+Na]⁺).

Synthesis of tetramer **56**



To a stirred solution of dimer **55** (360 mg, 1.0 mmol) in dioxane water 9:1 (10 mL), aqueous sodium hydroxide (1.1 mL, 1M) was added at rt and stirred for 1 h. The reaction mixture was neutralized with 2N HCl and solvent was removed under reduced pressure. Resulting residue was extracted with CH₂Cl₂ (2 x 40 mL). The combined organic layer was dried (Na₂SO₄), concentrated and the resulting crude dimer-acid was used immediately for the coupling.

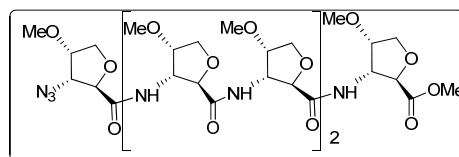
A suspension dimer **55** (360 mg, 1.0 mmol) and Raney nickel (200 mg) in THF (10 mL) was stirred under an atmosphere of hydrogen for 2 h at rt. The reaction mixture was filtered through celite and the solvent removed under reduced pressure to afford crude dimer-amine and was used immediately.

At 0 °C, a solution of dimer-acid, 1-hydroxybenzotriazole (210 mg, 1.5 mmol) and diisopropylethylamine (0.2 mL, 1.5 mmol) in dry dichloromethane (10 mL) was treated with EDCI (300 mg, 1.5 mmol) and stirred for 30 min. To this, a solution of crude dimer-amine in dichloromethane (5 mL) was introduced and stirred at rt for 35 h. The reaction mixture was diluted with dichloromethane (60 mL) and washed with 2N HCl (2 x 25 mL). The organic phase was dried (Na₂SO₄) and concentrated. The resulting crude product was purified over a silica gel column chromatography

(35→50% EtoAc in petroleum ether) furnished the tetramer **56** (350 mg, 53%) as colorless oil.

Mol. Formula: C₂₅H₃₈N₆O₁₃. [α]_D²⁵ = -73.9 (*c* 1.2 CHCl₃). **IR (CHCl₃)** ν : 3411, 3018, 2112, 1747, 1685 cm⁻¹. **¹H NMR (400 MHz, CDCl₃)**: δ 3.36 (2 x s, 6H), 3.37 (s, 3H), 3.45 (s, 3H), 3.71 (s, 3H), 3.90 (dd, *J* = 5.5, 9.0 Hz, 1H), 3.91–4.07 (m, 10H), 4.11 (dd, *J* = 3.9, 10.2 Hz, 1H), 4.14 (br. t, *J* = 4.8 Hz, 1H), 4.18 (d, *J* = 2.2 Hz, 1H), 4.19 (d, *J* = 4.2 Hz, 1H), 4.23 (d, *J* = 7.2 Hz, 1H), 4.39 (d, *J* = 4.4 Hz, 1H), 4.43–4.49 (m, 2H), 4.64 (ddd, *J* = 5.3, 7.6, 12.8 Hz, 1H), 7.21 (d, *J* = 8.4 Hz, 1H), 7.23 (d, *J* = 6.6 Hz, 1H), 7.37 (d, *J* = 8.1 Hz, 1H). **¹³C NMR (100 MHz, CDCl₃)**: δ 52.4 (q), 54.4 (d), 55.3 (d), 55.4 (d), 57.6 (q), 57.6 (q), 57.7 (q), 58.5 (q), 63.7 (d), 70.3 (t), 71.0 (t), 71.3 (t), 71.3 (t), 79.2 (d), 79.3 (d), 79.4 (d), 79.6 (d), 79.7 (d), 80.1 (d), 80.5 (d), 80.9 (d), 170.39 (s), 170.41 (s), 170.44 (s), 171.50 (s) ppm. **ESI-MS *m/z***: 631.1 (100%, [M+H]⁺), 653.2 (50%, [M+Na]⁺), 669.4 (36.6%, [M+K]⁺).

Synthesis of *trans*-hexamer **57**



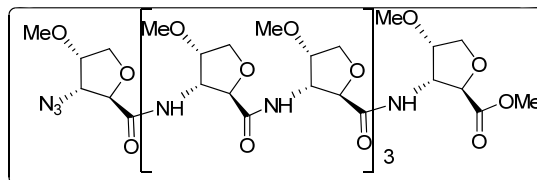
A solution of tetramer **56** (95 mg, 0.15 mmol) in THF (10 mL) was treated with Raney nickel (100 mg) and stirred under hydrogen atmosphere for 2 h and worked up as mentioned earlier to afford the tetramer-amine which was used immediately.

At 0 °C, a solution of crude dimer-acid [prepared from dimer-ester **55** (50 mg, 0.14 mmol)] 1-hydroxybenzotriazole (29 mg, 0.21 mmol) and diisopropylethylamine (0.04 mL, 0.21 mmol) in dichloromethane (8 mL) was treated with EDCI (41 mg, 0.21 mmol) and stirred for 30 min. To this solution, above tetramer-amine in dichloromethane (2 mL) was introduced and stirring was continued for 38 h at rt. Usual work followed purification by silica gel column chromatography (2→4% methanol in chloroform) gave hexamer **57** as colorless amorphous solid (65 mg, 49%).

Mol. Formula: C₃₇H₅₆N₈O₁₉. [α]_D²⁵ = -123.8 (*c* 1 CHCl₃). **IR (CHCl₃)** ν : 3410, 3018, 2936, 2112, 1746, 1682, 1216 cm⁻¹. **¹H NMR (400 MHz, CDCl₃)**: δ 3.35 (2 x s, 6H), δ 3.36 (2 x s, 6H), 3.37 (s, 3H), 3.45 (s, 3H), 3.70 (s, 3H), 3.88–3.96 (m, 6H), 3.98–4.02 (m, 5H), 4.03–4.07 (m, 5H), 4.08–4.16 (m, 2H), 4.14 (dd, *J* = 5.4, 10.2 Hz, 1H), 4.18–4.22 (m, 3H), 4.19 (d, *J* = 7.1 Hz, 1H), 4.19 (d, *J* = 5.5 Hz, 1H), 4.21 (d, *J* = 4.3 Hz, 1H), 4.23 (d, *J* = 7.4 Hz, 1H),

4.39 (d, $J = 4.7$ Hz, 1H), 4.46–4.57 (m, 2H), 4.64 (ddd, $J = 5.3, 7.6, 12.7$ Hz, 1H), 7.26 (d, $J = 8.3$ Hz, 2H), 7.34 (d, $J = 7.8$ Hz, 1H), 7.36 (d, $J = 8.2$ Hz, 1H), 7.39 (d, $J = 8.4$ Hz, 1H), 7.39 (d, $J = 8.4$ Hz, 1H). ^{13}C NMR (100 MHz, CDCl_3): δ 52.4 (q), 52.4 (d), 54.4 (d), 55.2 (2C, d), 55.4 (d), 57.5 (q), 57.6 (3C, q), 57.7 (q), 58.5 (q), 63.7 (d), 70.3 (t), 71.0 (t), 71.2 (4C, t), 79.3 (d), 79.4 (d), 79.7 (7C, d), 80.2 (d), 80.5 (d), 80.8 (d), 170.38 (s), 170.49 (s), 170.58 (s), 171.90 (2C=O, s), 171.65 (s) ppm. ESI-MS m/z : 917.2 (33.8%, $[\text{M}+\text{H}]^+$), 939.5 (100%, $[\text{M}+\text{Na}]^+$), 956.4 (25%, $[\text{M}+\text{K}]^+$).

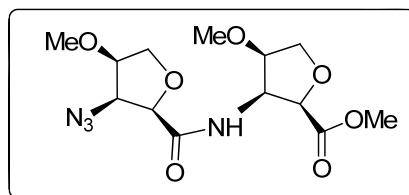
Synthesis of *trans*-octamer **58**



At 0 °C, a solution of crude tetramer-acid [prepared from **56** (80 mg, 0.11 mmol)], HOBT (29 mg, 0.21 mmol) and diisopropylethylamine (40 μL , 0.21 mmol) in dry dichloromethane (8 mL) was treated with EDCI (41 mg, 0.21 mmol) and stirred for 30 min. To this, a solution of crude tetramer-amine [prepared from **56** (80 mg, 0.11 mmol)] in dichloromethane (2 mL) was introduced and the contents were stirred at rt for 42 h. Usual workup followed by purification using silica gel column chromatography (2→4 % methanol in chloroform) afforded *trans*-octamer **58** (70 mg, 46%) as colorless amorphous solid.

Mol. Formula: $\text{C}_{49}\text{H}_{74}\text{N}_{10}\text{O}_{25}$. $[\alpha]_{\text{D}}^{25} = -140.8$ (c 1 CHCl_3). IR (CHCl_3) ν : 3314, 2925, 2855, 2110, 1744, 1676 cm^{-1} . ^1H NMR (400 MHz, CDCl_3): δ 3.33 (s, 3H), 3.34 (sx3, 9H), 3.36 (sx2, 6H), 3.37 (s, 3H), 3.45 (s, 3H), 3.71 (s, 3H), 3.90–3.94 (m, 7H), 3.96–4.13 (m, 18H), 4.18 (d, $J = 7.9$ Hz, 1H), 4.19 (d, $J = 6.9$ Hz, 1H), 4.19 (d, $J = 6.5$ Hz, 1H), 4.23 (d, $J = 7.6$ Hz, 1H), 4.25 (d, $J = 7.6$ Hz, 1H), 4.26 (d, $J = 7.6$ Hz, 1H), 4.29 (d, $J = 7.3$ Hz, 1H), 4.38 (d, $J = 4.7$ Hz, 1H), 4.44–4.69 (m, 7H), 7.27 (d, $J = 7.2$ Hz, 1H), 7.28 (d, $J = 7.8$ Hz, 1H), 7.38 (d, $J = 8.2$ Hz, 1H), 7.48 (d, $J = 8.1$ Hz, 1H), 7.55 (d, $J = 8.7$ Hz, 1H), 7.65 (d, $J = 7.8$ Hz, 1H), 7.66 (d, $J = 7.8$ Hz, 1H). ^{13}C NMR (100 MHz, CDCl_3): δ 52.4 (q), 54.4 (d), 54.4 (3C, d), 55.5 (3C, d), 57.5 (2C, d), 57.6 (q), 57.6 (2C, q), 57.7 (q), 57.7 (q), 58.5 (q), 63.8 (d), 70.4 (t), 71.1 (t), 71.3 (t), 71.3 (t), 71.4 (4C, t), 79.4 (d), 79.5 (d), 79.7 (6C, d), 79.9 (3C, d), 80.0 (2C, d), 80.2 (d), 80.6 (d), 80.7 (d), 170.38 (s), 170.48 (s), 170.86 (s), 171.05 (s), 171.27 (s), 171.29 (s), 171.42 (s), 171.73 (d) ppm. ESI-MS m/z : 1204 (100%, $[\text{M}+\text{H}]^+$).

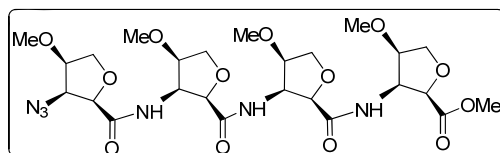
Synthesis of *cis*-dimer **59**



The same procedure as in the preparation of **55** was used to couple the acid **43** (1.9 g, 10.1 mmol) and crude amine (prepared from the ester **43**-Me (2.1 g, 10.4 mmol) and purified by column chromatography (50→60% ethyl acetate in petroleum ether) to obtain the dimer **59** (2.1 g, 61%) as yellow color solid.

Mol. Formula: C₁₃H₂₀N₄O₇. $[\alpha]_D^{25} = -38.8$ (*c* 1 CHCl₃). **IR (CHCl₃)** ν : 3399, 3019, 2117, 1751, 1681, 1216 cm⁻¹. **¹H NMR (200 MHz, CDCl₃):** δ 3.28 (s, 3H), 3.45 (s, 3H), 3.75 (s, 3H), 3.94 (dd, *J* = 7.8, 9.1 Hz, 1H), 3.94 (dt, *J* = 3.2, 5.2 Hz, 1H), 4.00 (dd, *J* = 5.0, 10.1 Hz, 1H), 4.05 (d, *J* = 3.2 Hz, 1H), 4.11 (d, *J* = 7.7 Hz, 1H), 4.14 (ddd, *J* = 4.2, 8.3, 11.6 Hz, 1H), 4.42 (br. t, *J* = 4.2 Hz, 1H), 4.45 (d, *J* = 4.1 Hz, 1H), 4.52 (d, *J* = 7.2 Hz, 1H), 4.79 (ddd, *J* = 5.5, 7.1, 12.6 Hz, 1H), 7.39 (d, *J* = 8.9 Hz, 1H). **¹³C NMR (100 MHz, CDCl₃):** δ 52.0 (q), 52.2 (d), 57.8 (q), 58.6 (q), 61.8 (d), 69.3 (t), 71.0 (t), 76.4 (d), 78.8 (d), 80.1 (d), 81.3 (d), 168.0 (s), 170.2 (s) ppm. **ESI-MS *m/z*:** 345.1 (95.6%, [M+H]⁺), 362.2 (19%, [M+NH₄]⁺), 367.1 (100%, [M+Na]⁺), 383.1 (10.2%, [M+K]⁺).

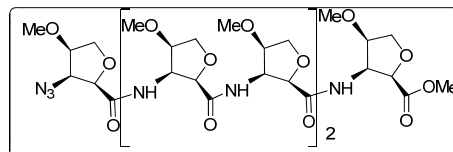
Synthesis of *cis*-tetramer **60**



The same procedure as in the preparation of **56** was used with the *cis*-dimer **59** [1.2 g, 3.4 mmol each for making dimer-acid and dimer-amine] to prepared *cis*-tetramer **60** (94 mg, 43%) as colorless amorphous solid.

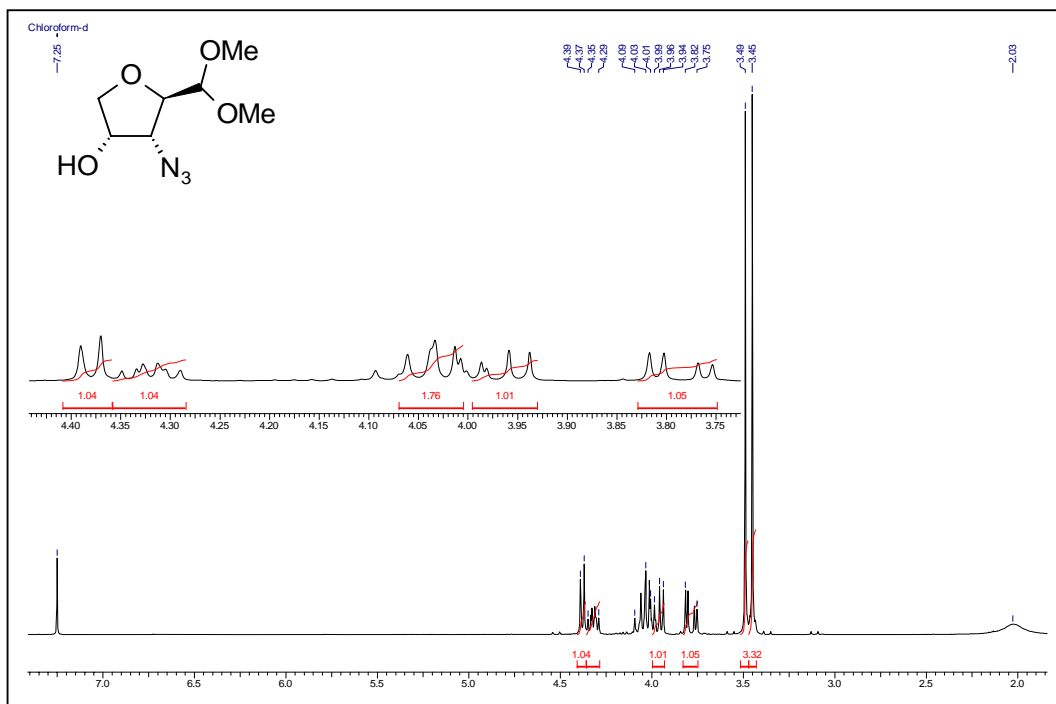
Mol. Formula: C₂₅H₃₈N₆O₁₃. $[\alpha]_D^{25} = -1.8$ (*c* 1.0, CHCl₃). **IR (CHCl₃)** ν : 3400, 3020, 2118, 1751, 1682 cm⁻¹. **¹H NMR (200 MHz, CDCl₃):** 3.25 (s, 3H), 3.26 (s, 3H), 3.28 (s, 3H), 3.46 (s, 3H), 3.76 (s, 3H), 3.88–4.01 (m, 5H), 4.03–4.10 (m, 3H), 4.12–4.30 (m, 4H), 4.34–4.52 (m, 5H), 4.59–4.71 (m, 2H), 4.78 (ddd, *J* = 2.5, 7.6, 9.2 Hz, 1H), 7.76 (d, *J* = 9.3 Hz, 1H), 8.46 (d, 7.7 Hz, 1H), 8.56 (d, 7.1 Hz, 1H). **¹³C NMR (100 MHz, CDCl₃):** δ 52.1 (q), 52.5 (d), 53.7 (d), 54.1 (d), 57.2 (q), 57.3 (q), 57.6 (q), 58.6 (q), 62.0 (d), 69.6 (t), 71.2 (2C, t), 71.5 (t), 74.0 (d), 74.4 (d), 75.4 (d), 78.1 (d), 78.4 (d), 78.7 (d), 80.3 (d), 81.5 (d), 168.30 (s), 170.83 (s), 171.83 (2C=O, s). **ESI-MS *m/z*:** 631.3 (55.3%, [M+H]⁺), 653.3 (100%, [M+Na]⁺).

Synthesis of *cis*-hexamer **61**

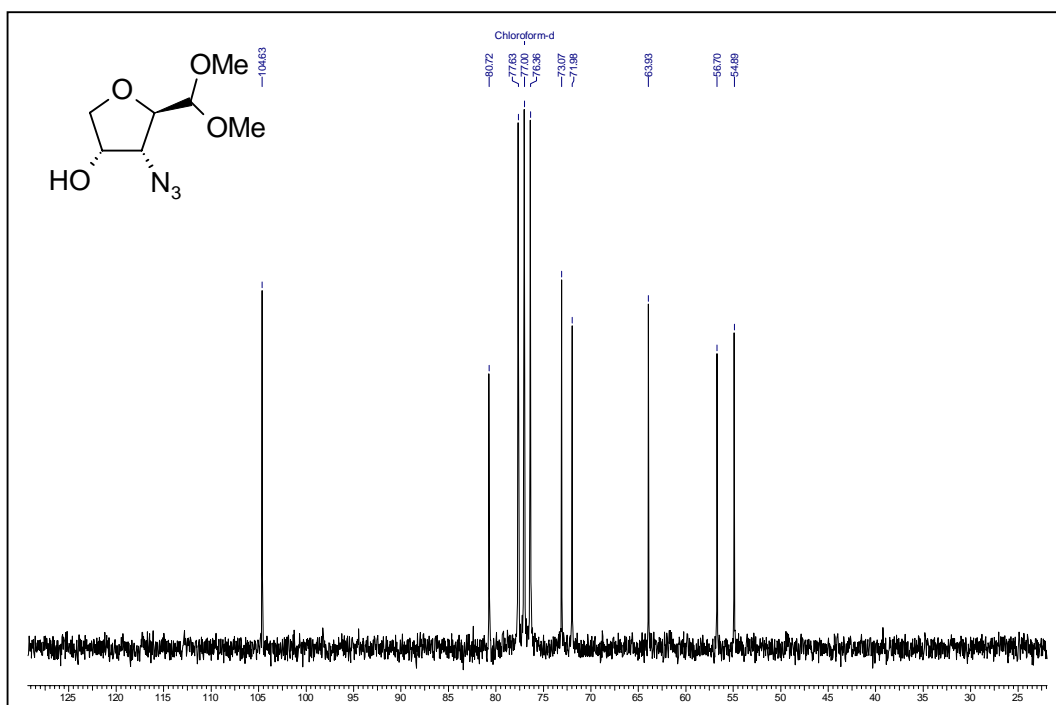


Following the general procedure, the crude dimer-acid [prepared from **59** (300 mg, 0.8 mmol)] and tetramer-amine [prepared from **60** (550 mg, 0.8 mmol)] are coupled to procure the *cis*-hexamer **61** as colorless amorphous solid (334 mg, 42%).

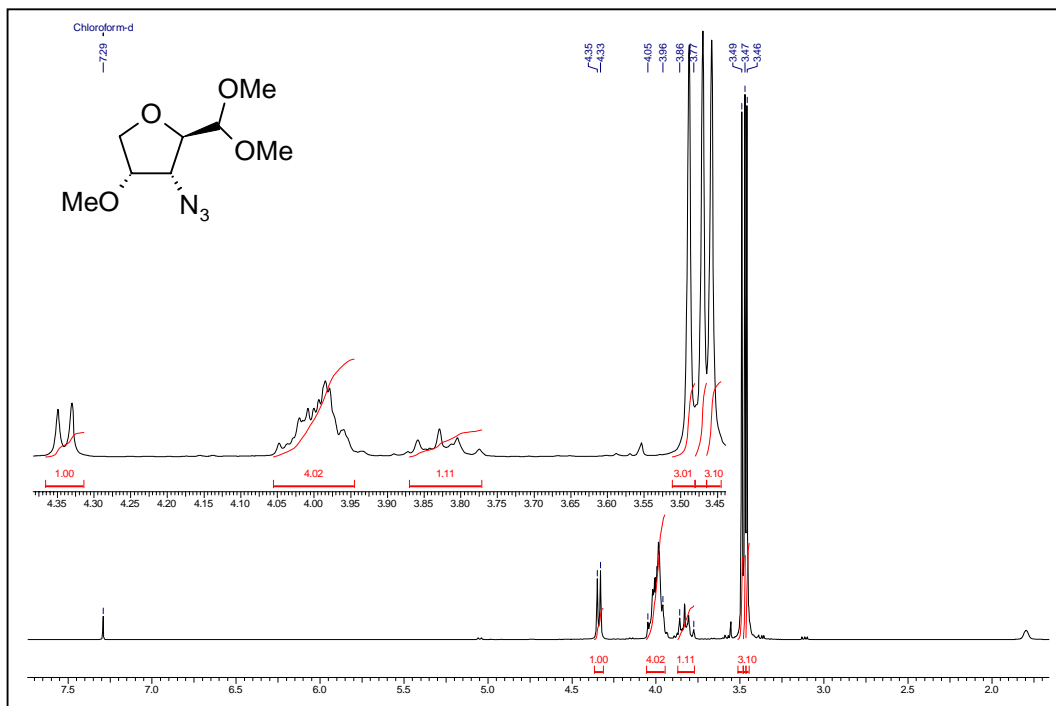
Mol. Formula: C₃₇H₅₆N₈O₁₉. $[\alpha]_D^{25} = +11.2$ (*c* 1.0, CHCl₃). **IR (CHCl₃)** ν : 3394, 3020, 2118, 1663, 1508, 1216 cm⁻¹. **¹H NMR (200 MHz, CDCl₃)**: δ 3.25 (2 x s, 6H), 3.26 (2 x s, 6H), 3.28 (s, 3H), 3.46 (s, 3H), 3.76 (s, 3H), 3.88–4.89 (m, 25H), 4.57–4.68 (m, 4H), 4.78 (ddd, *J* = 4.9, 7.4, 12.5 Hz, 1H), 7.76 (d, *J* = 9.3 Hz, 1H), 8.54 (d, *J* = 7.6 Hz, 1H), 8.59 (d, *J* = 7.1 Hz, 1H), 8.62 (d, *J* = 7.4 Hz, 1H), 8.65 (d, *J* = 7.5 Hz, 1H). **¹³C NMR (100 MHz, CDCl₃)**: δ 52.4 (q), 52.6 (d), 53.8 (d), 53.9 (d), 54.0 (d), 54.1 (d), 57.1 (q), 57.2 (q), 57.3 x 2 (q), 57.6 (q), 58.6 (q), 62.0 (d), 69.6 (t), 71.2 (t), 71.3 (t), 71.3 (t), 71.4 (t), 71.5 (t), 73.8 (d), 73.9 (d), 74.4 (2C, d), 75.4 (d), 77.2 (d), 78.2 (d), 78.4 (d), 78.5 (d), 78.8 (d), 80.3 (d), 81.6 (d), 168.3 (s), 170.9 (s), 171.9 (2C=O, s), 172.2 (s), 172.3 (s). **ESI-MS *m/z***: 917.4 (11.3%, [M+H]⁺), 939.4 (100%, [M+Na]⁺).



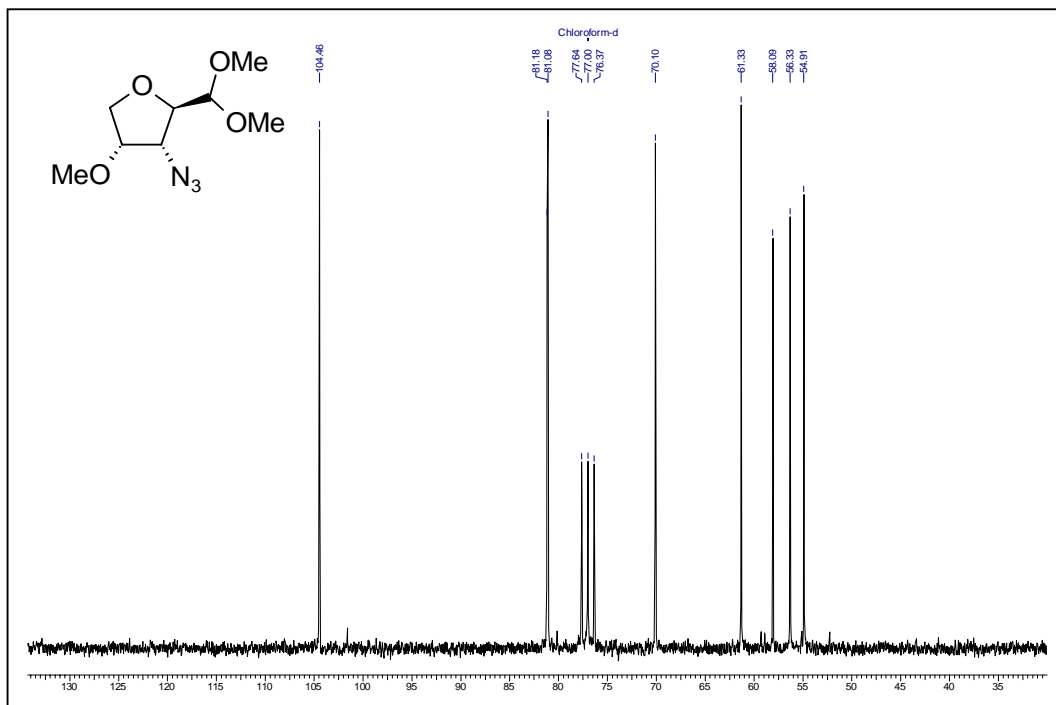
^1H NMR Spectrum of 47 in CDCl_3



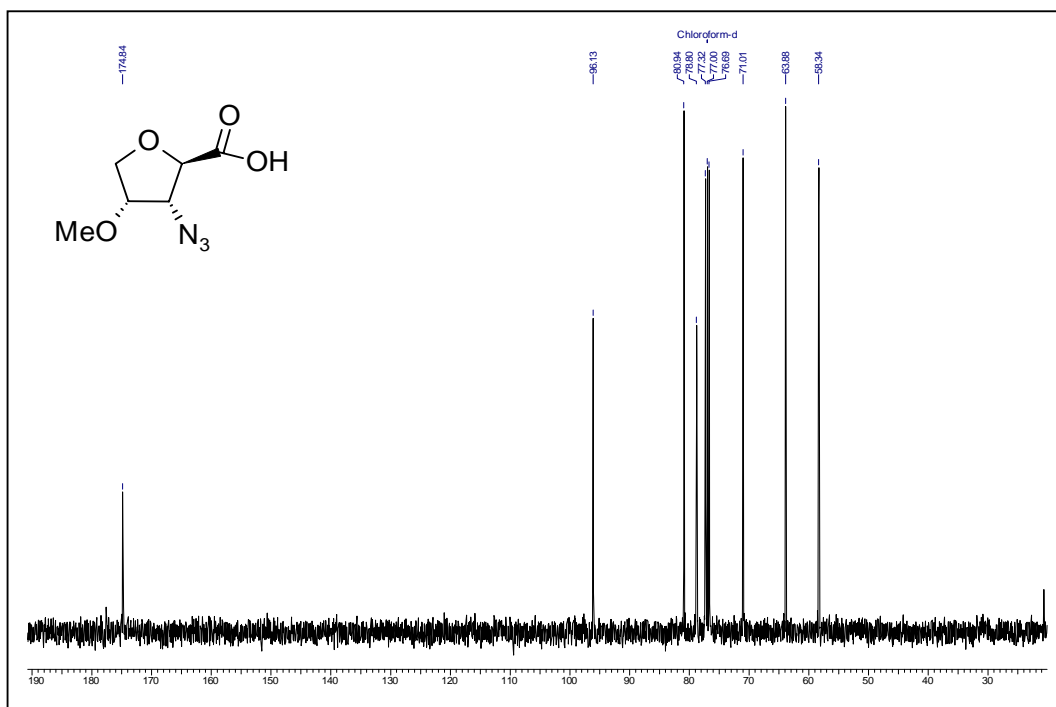
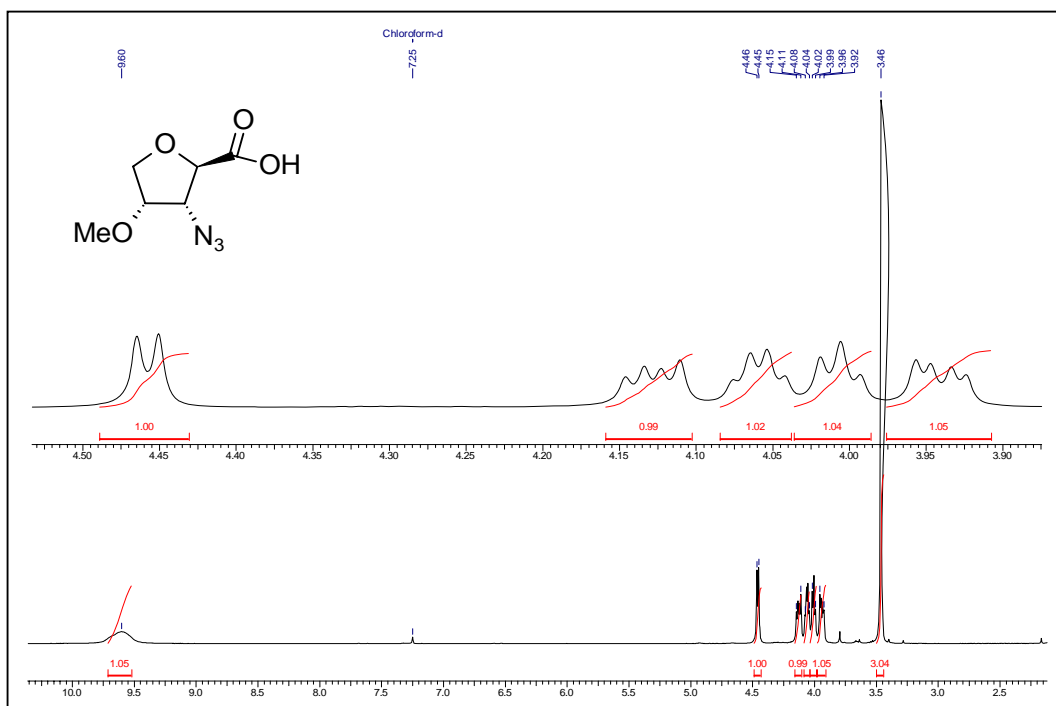
^{13}C NMR Spectrum of 47 in CDCl_3

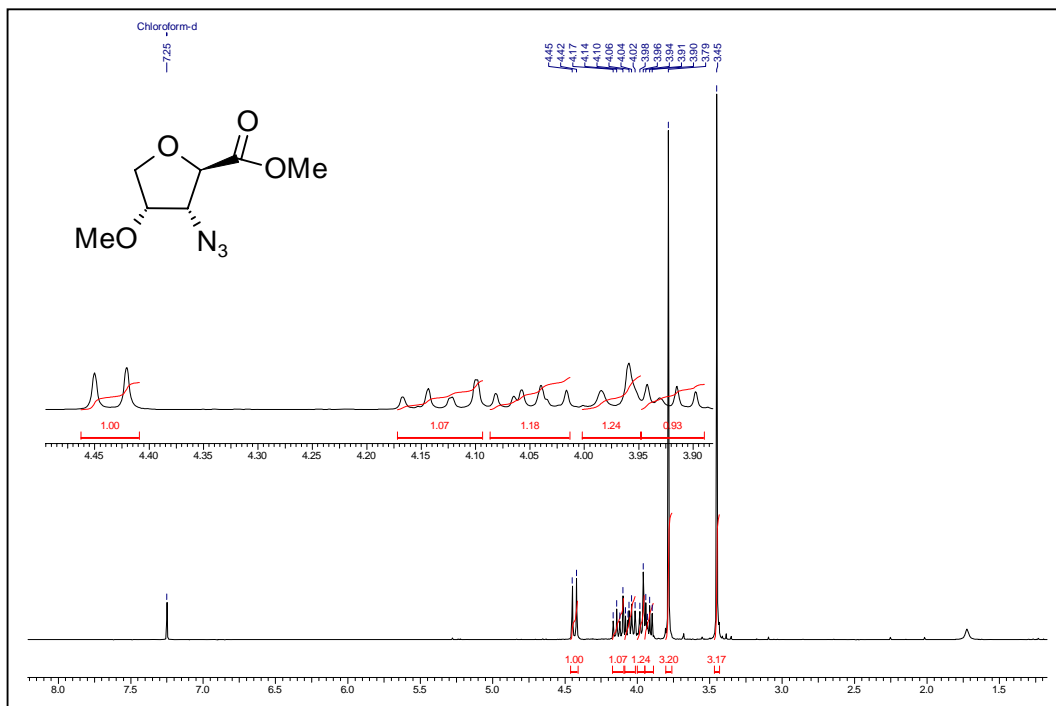


¹H NMR Spectrum of 46 in CDCl₃

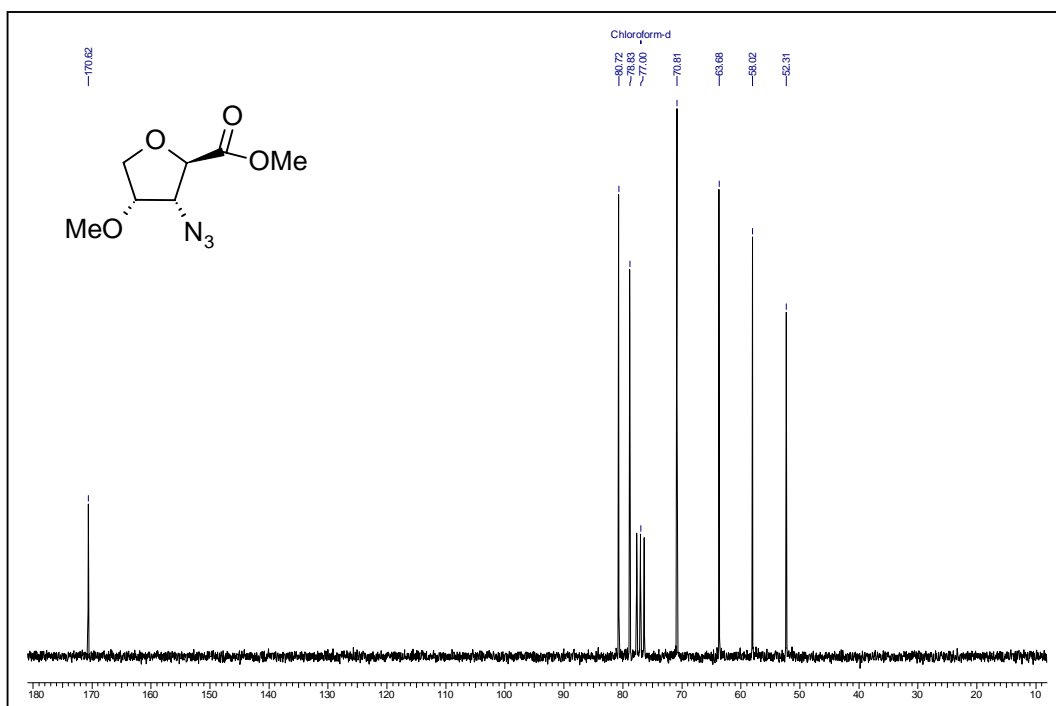


¹³C NMR Spectrum of 46 in CDCl₃

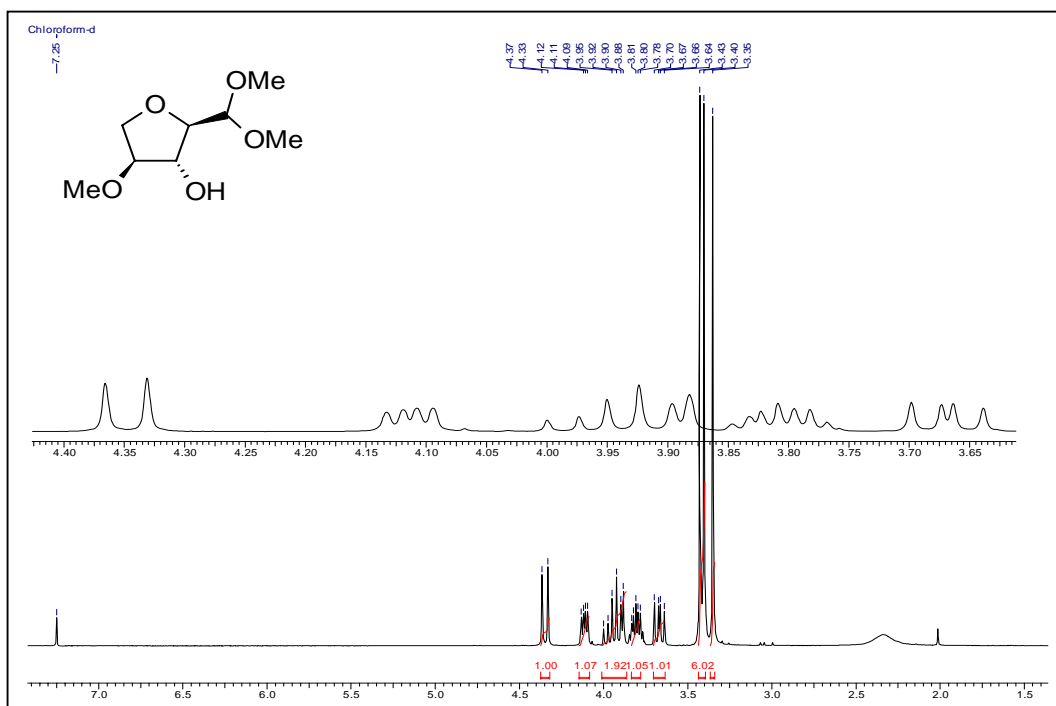




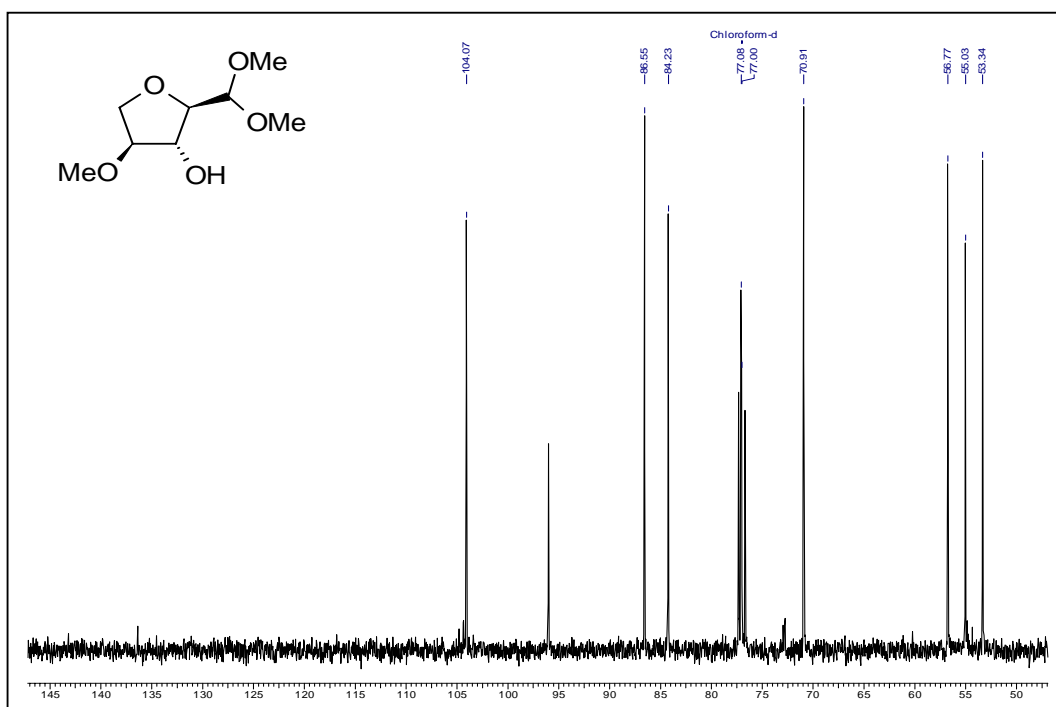
¹H NMR Spectrum of 42-Me in CDCl₃



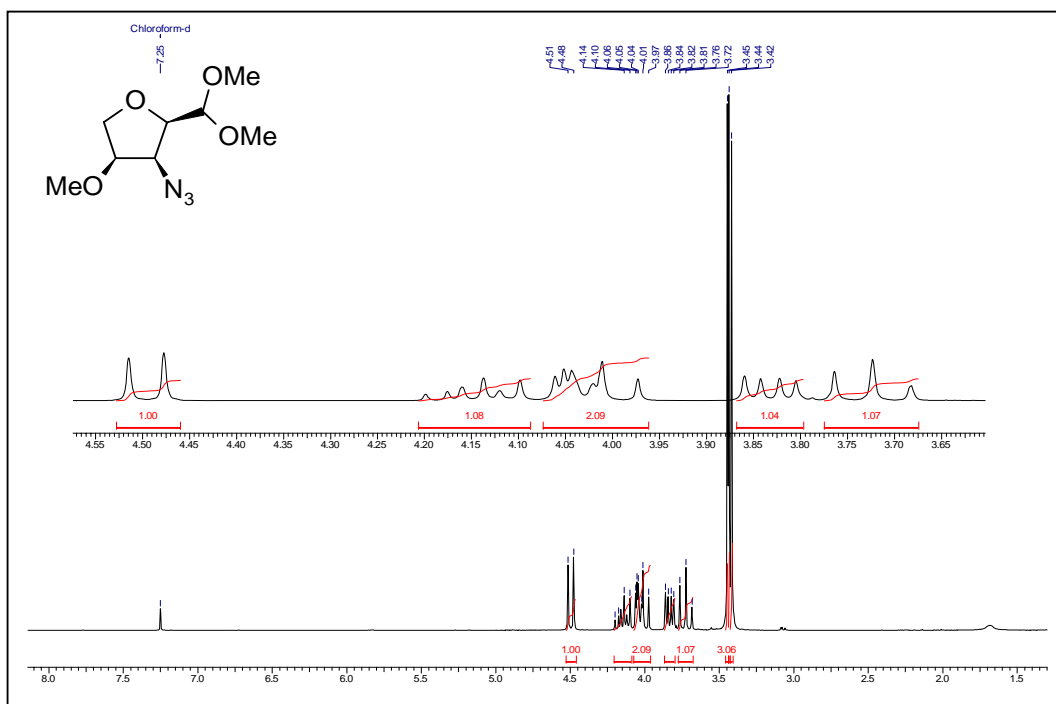
¹³C NMR Spectrum of 42-Me in CDCl₃



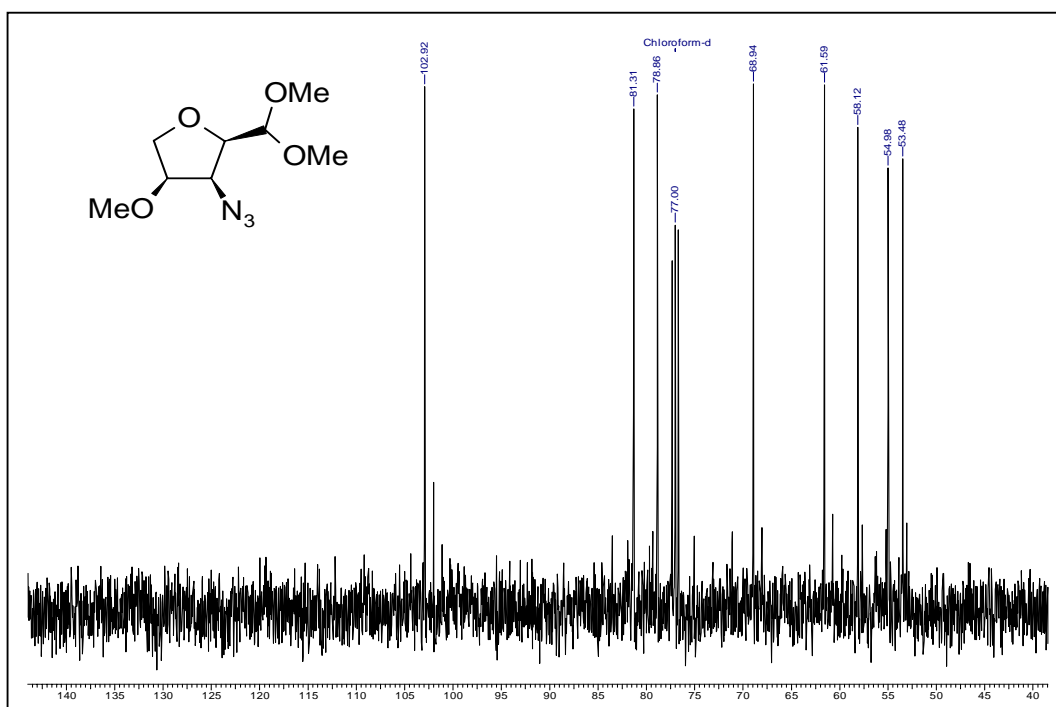
^1H NMR Spectrum of 54 in CDCl_3



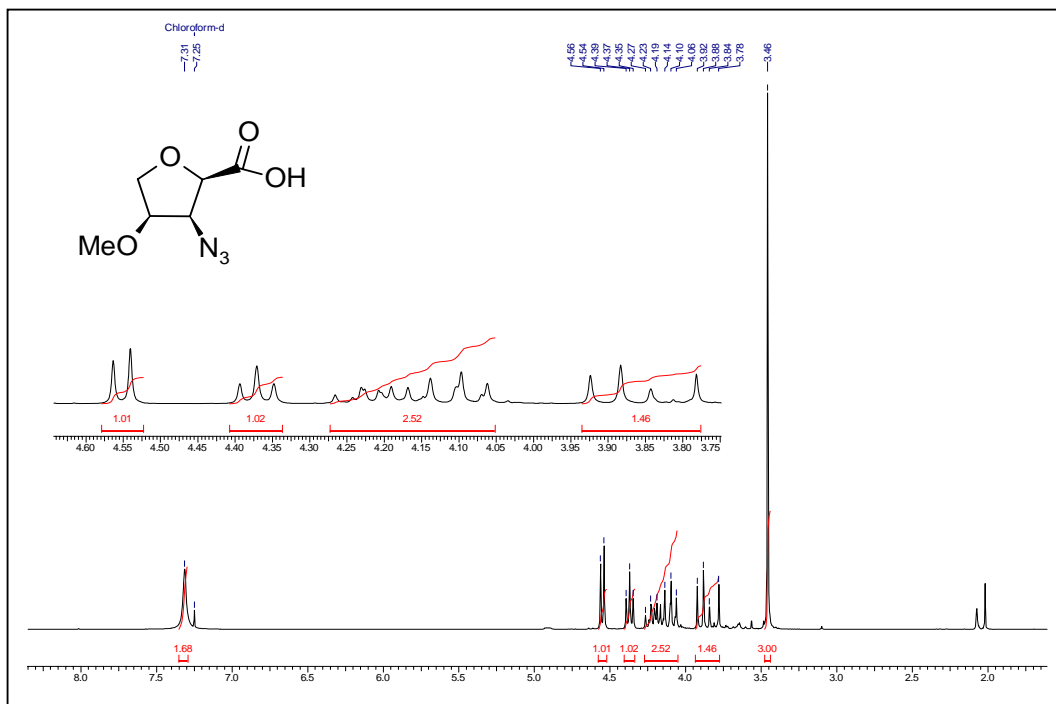
^{13}C NMR Spectrum of 54 in $\text{CDCl}_3 + \text{CCl}_4$



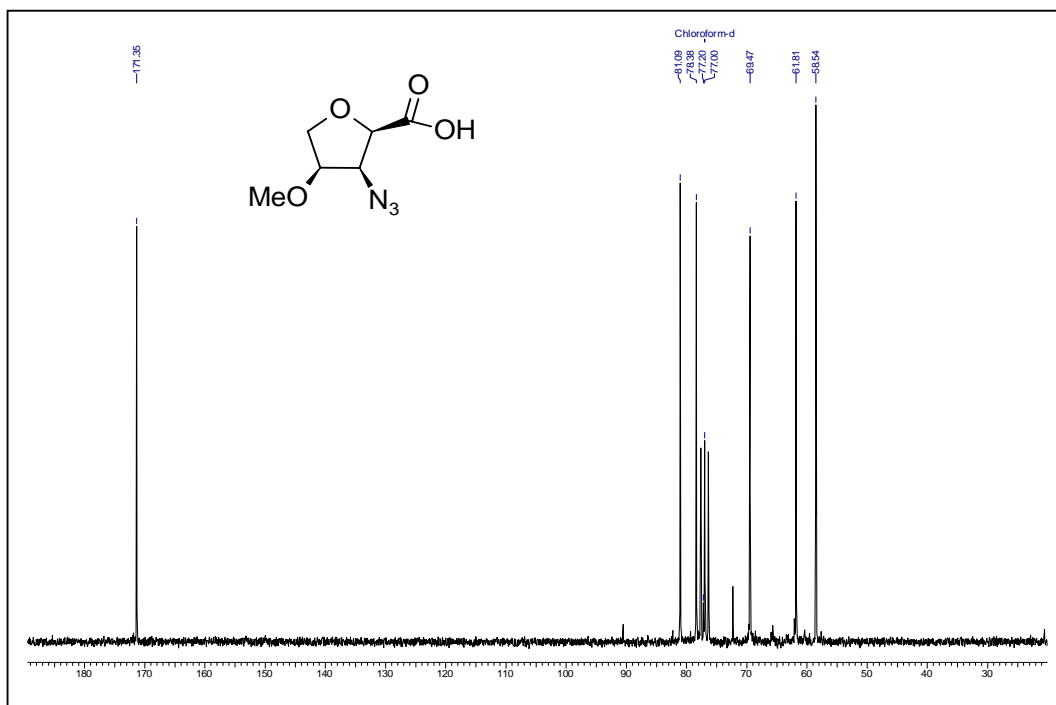
^1H NMR Spectrum of 49 in CDCl_3



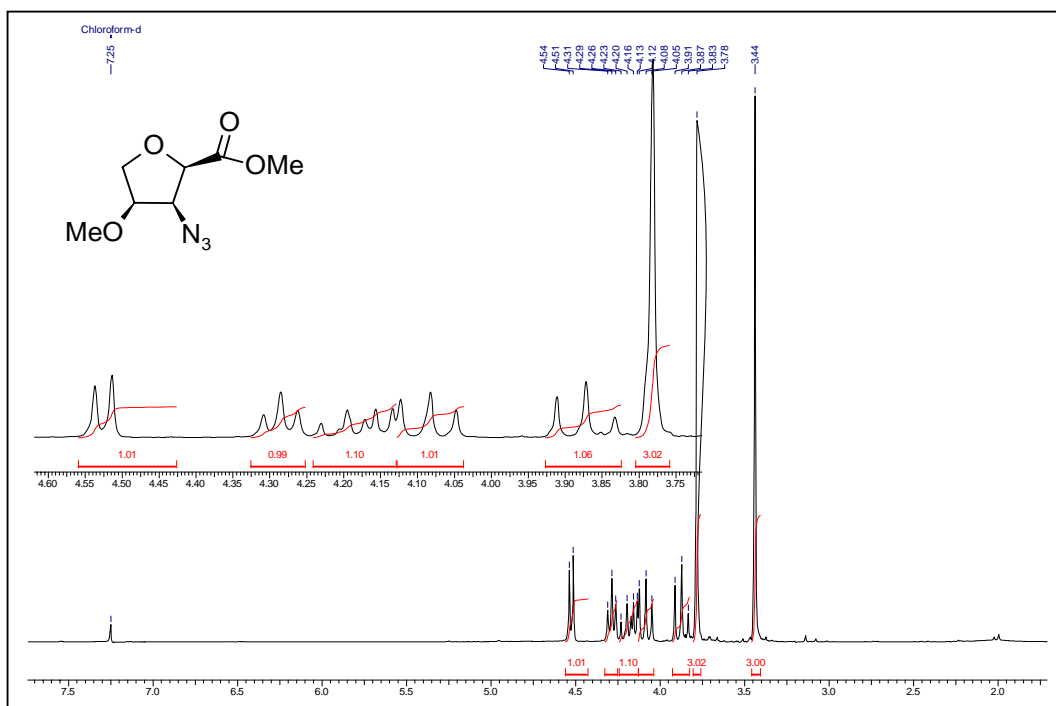
^{13}C NMR Spectrum of 49 in CDCl_3



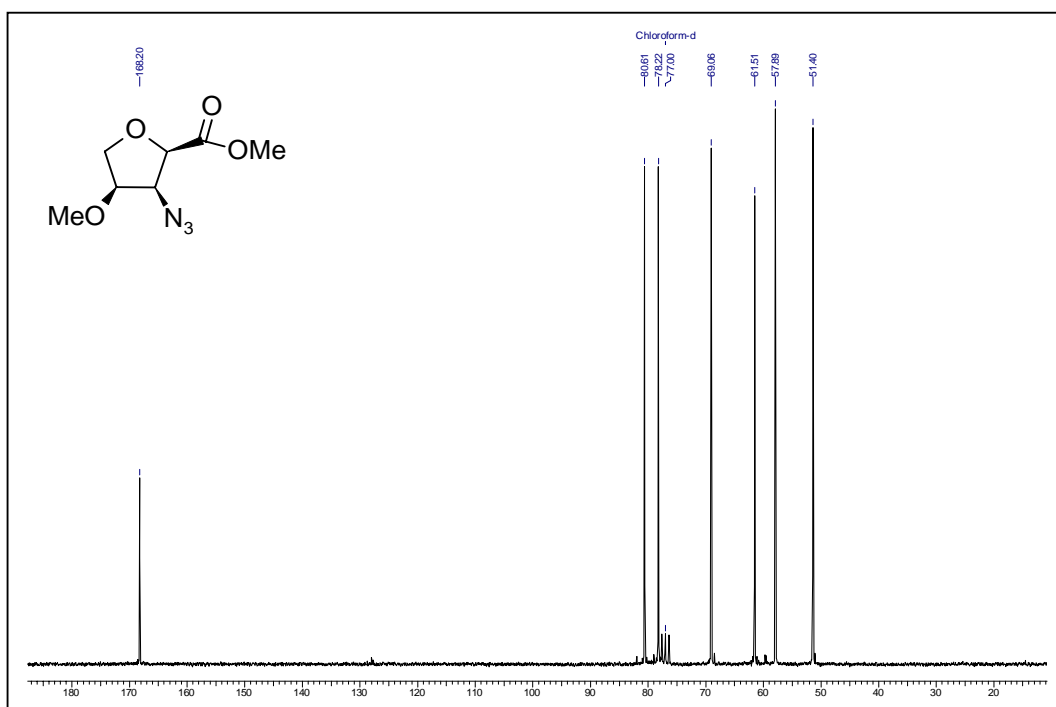
^1H NMR Spectrum of 43 in CDCl_3



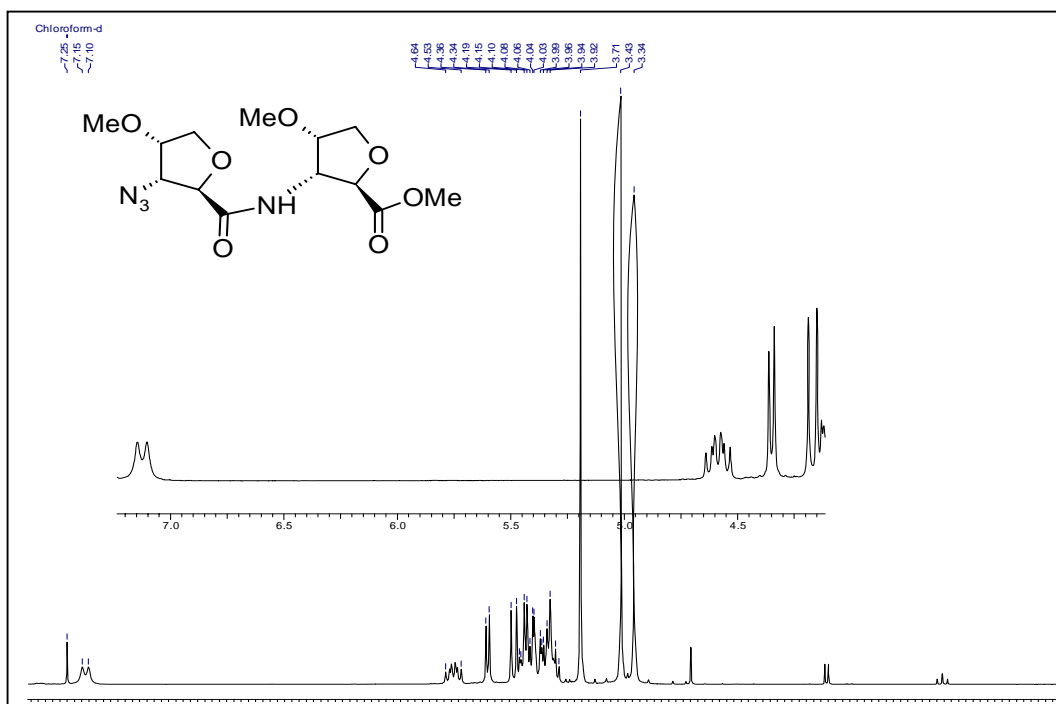
^{13}C NMR Spectrum of 43 in CDCl_3



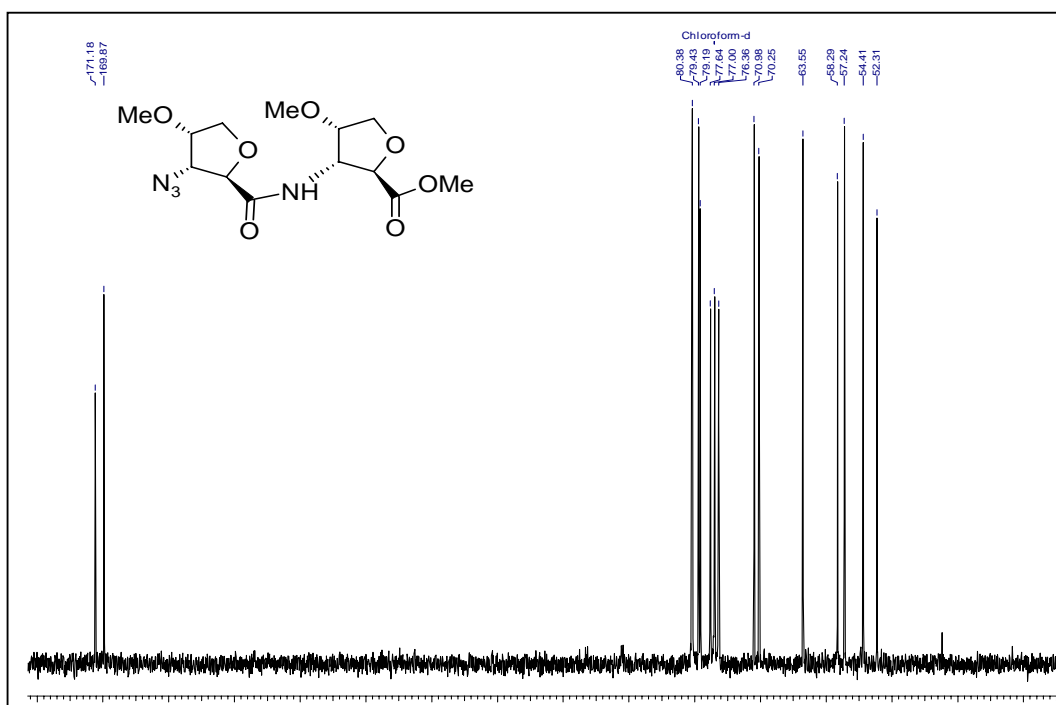
¹H NMR Spectrum of 43-Me in CDCl₃



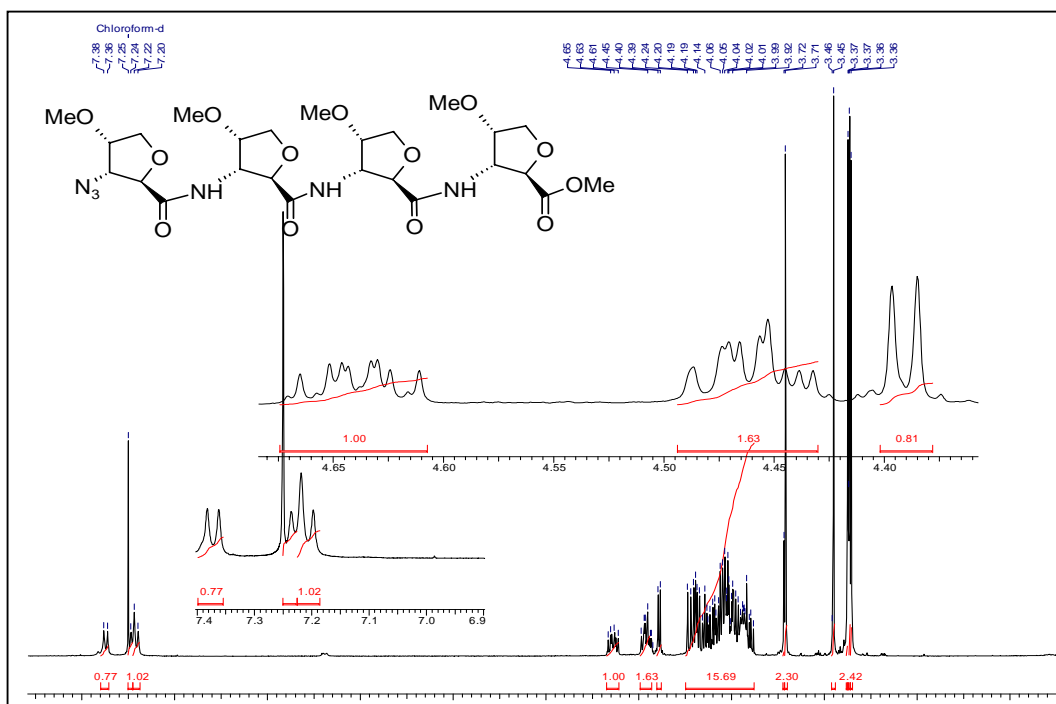
¹³C NMR Spectrum of 43-Me in CDCl₃



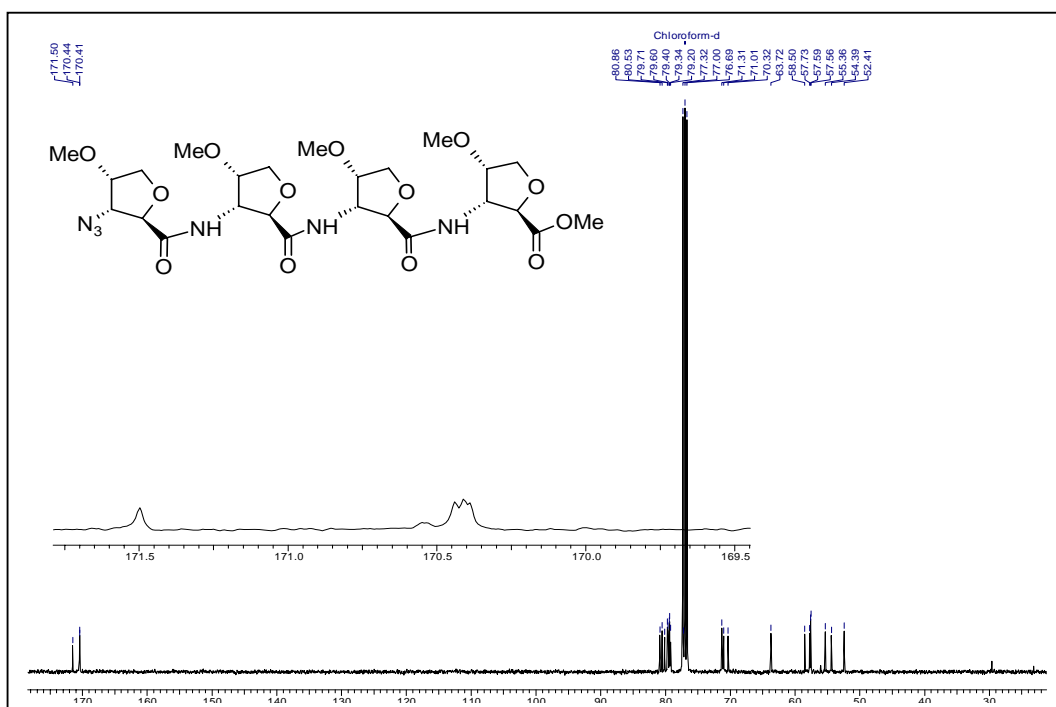
¹H NMR Spectrum of 55 in CDCl₃



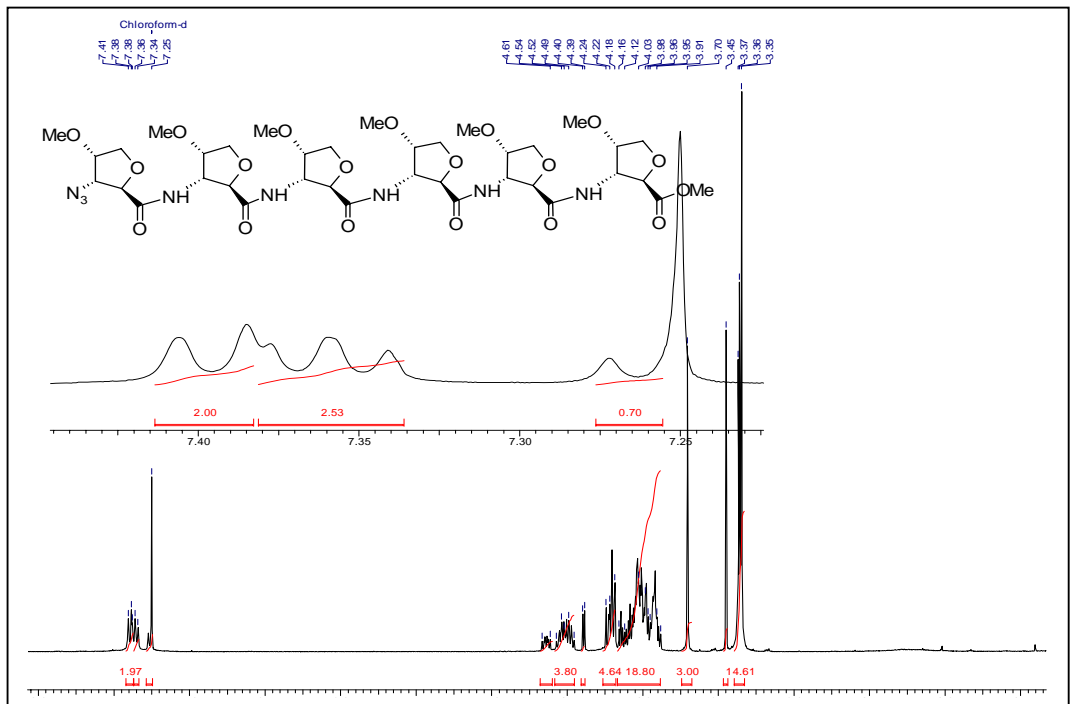
¹³C NMR Spectrum of 55 in CDCl₃



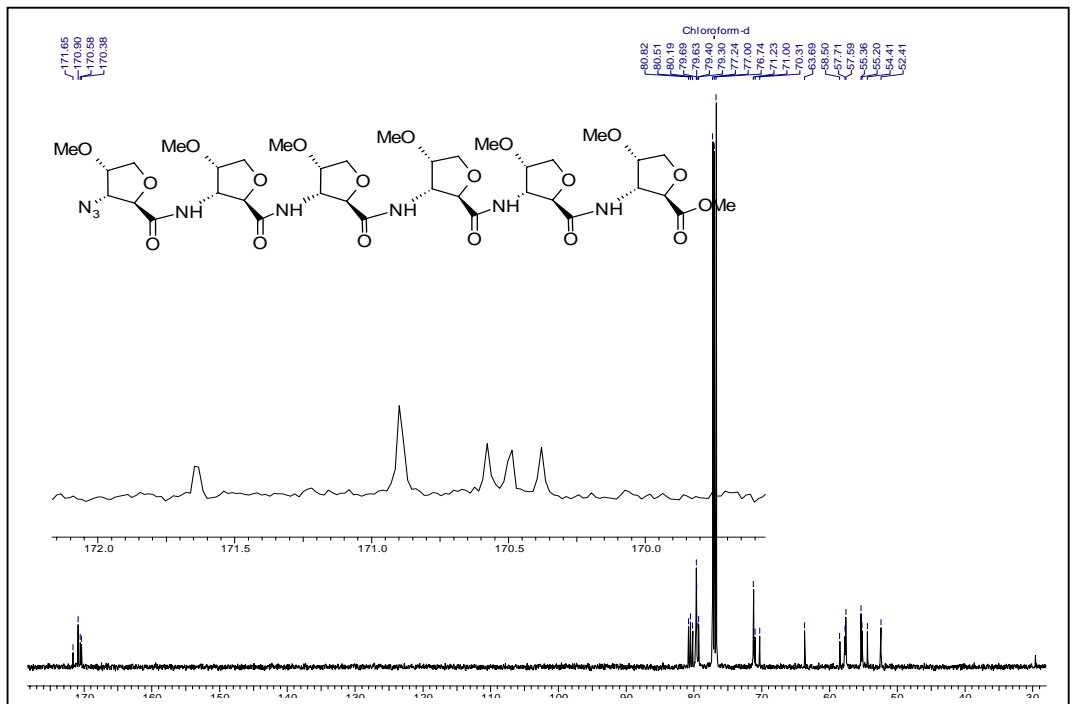
^1H NMR Spectrum of 56 in CDCl_3



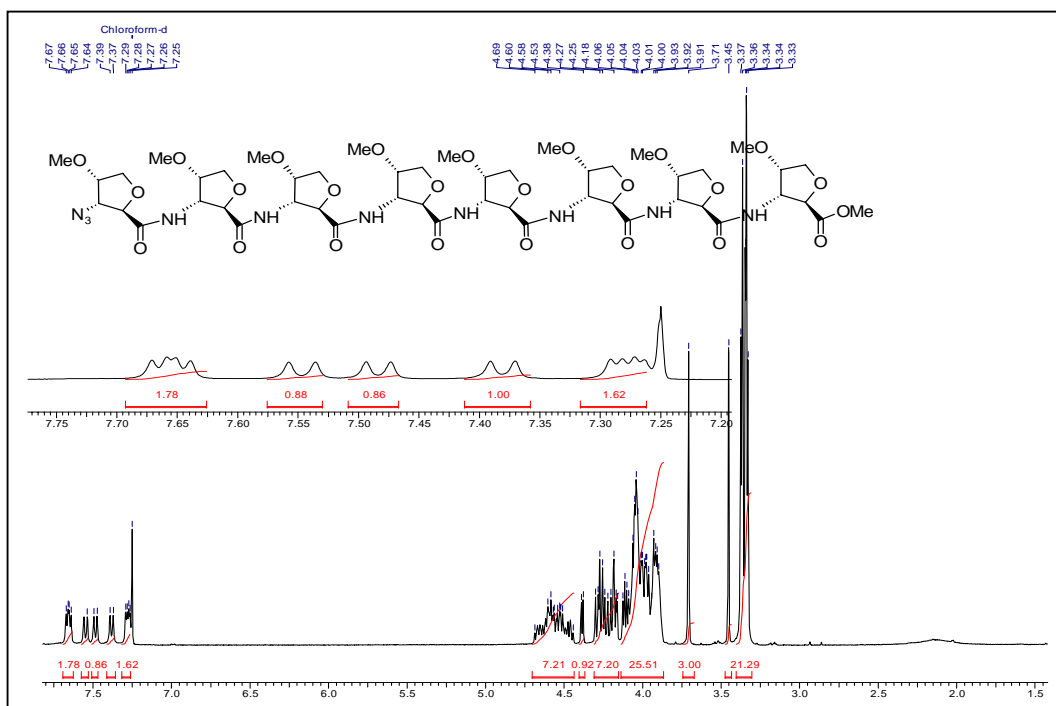
^{13}C NMR Spectrum of 56 in CDCl_3



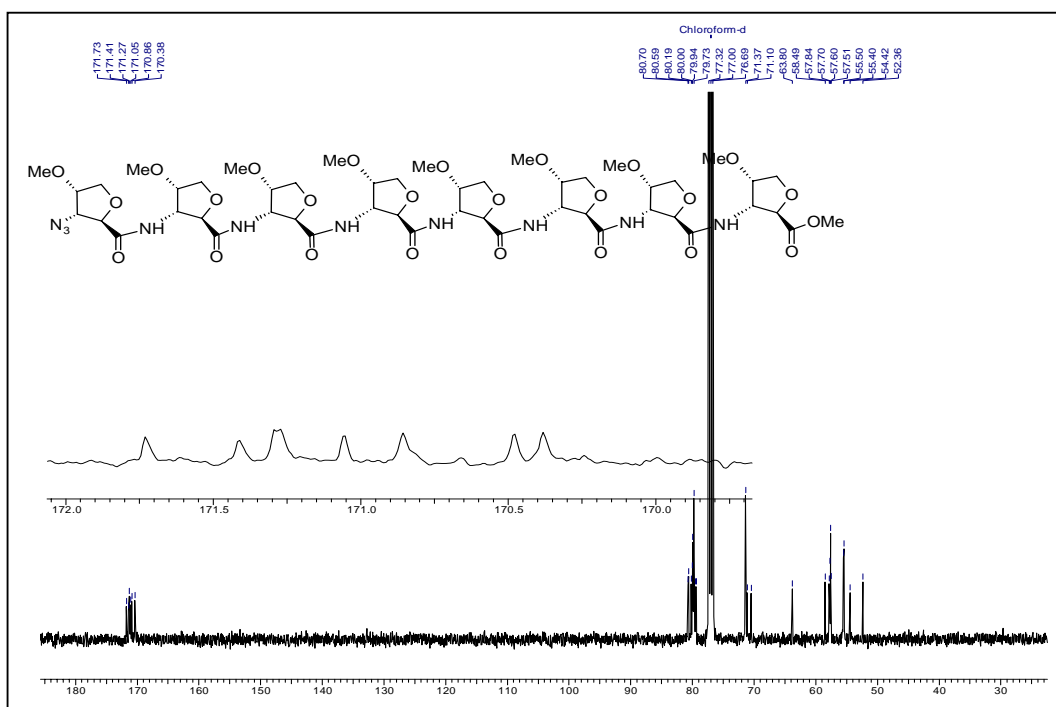
^1H NMR Spectrum of 57 in CDCl_3



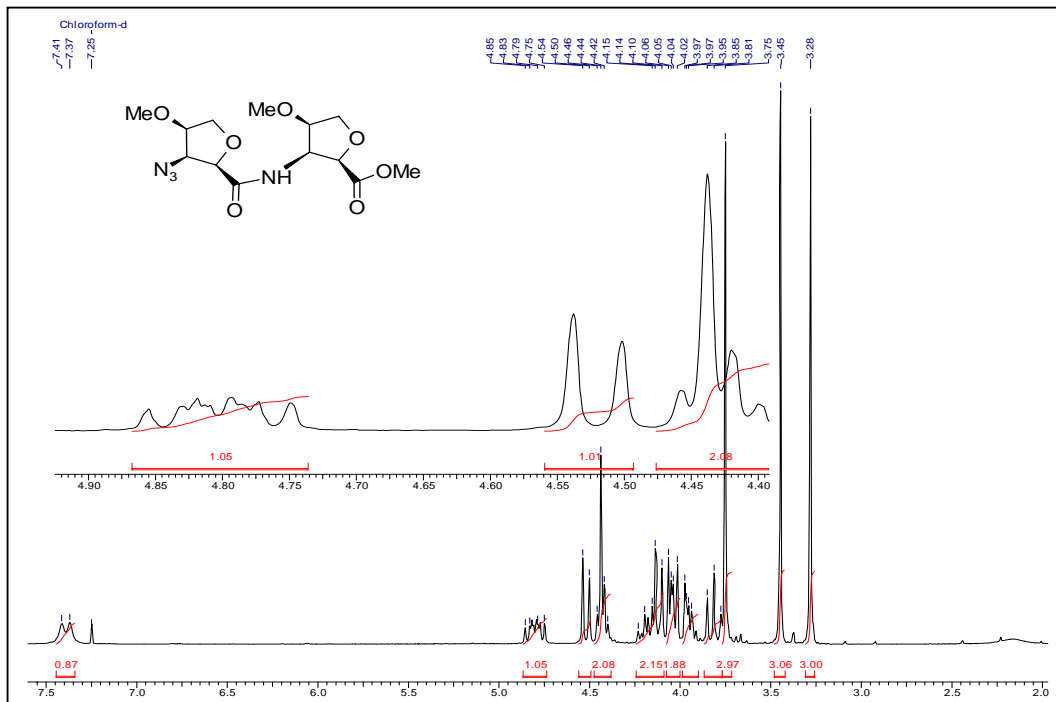
^{13}C NMR Spectrum of 57 in CDCl_3



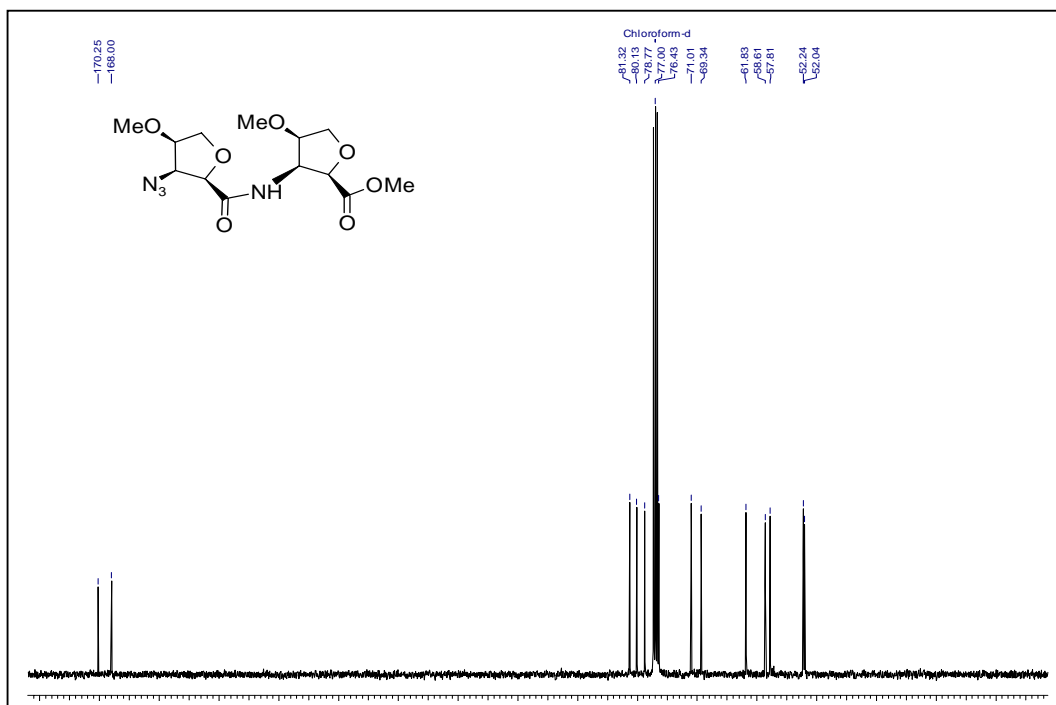
¹H NMR Spectrum of 58 in CDCl₃



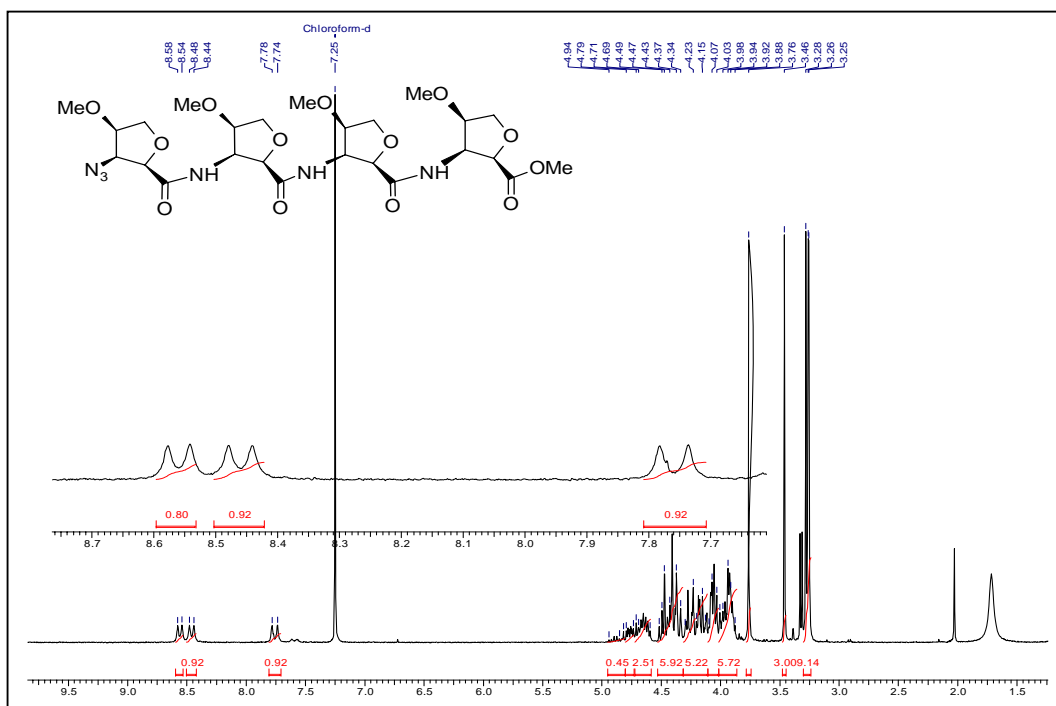
¹³C NMR Spectrum of 58 in CDCl₃



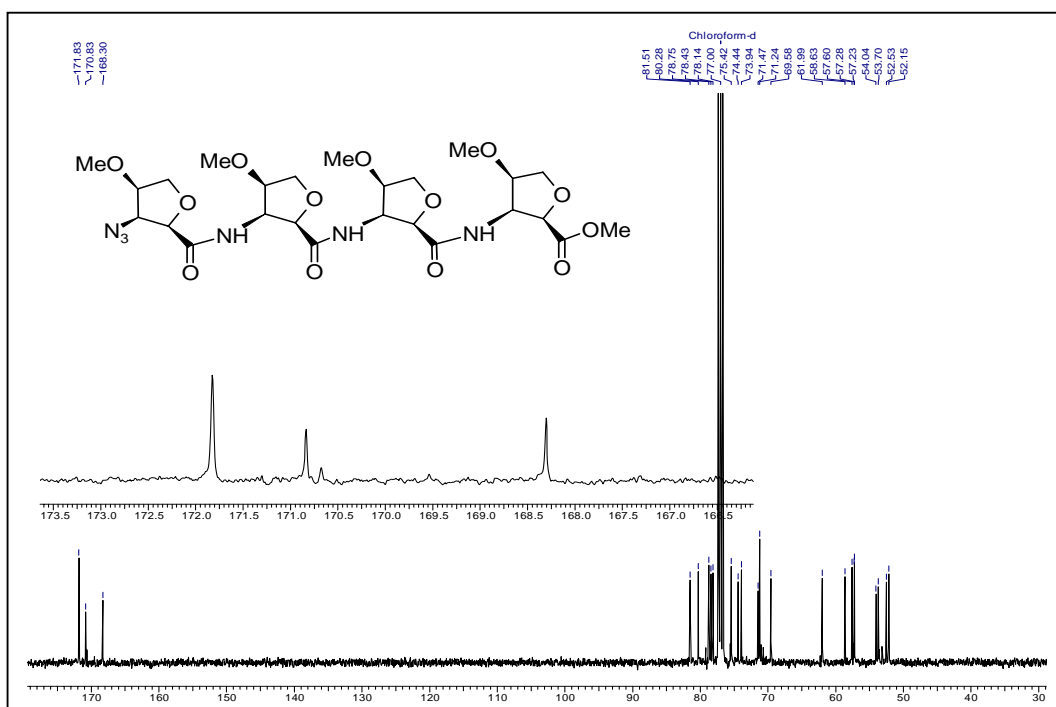
^1H NMR Spectrum of 59 in CDCl_3



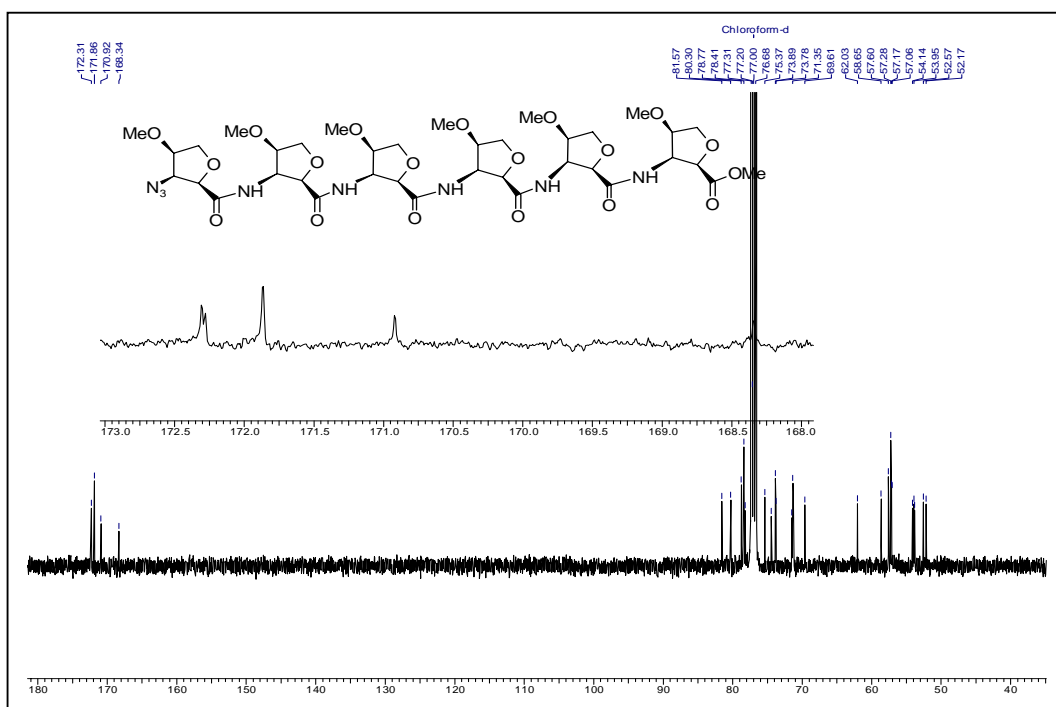
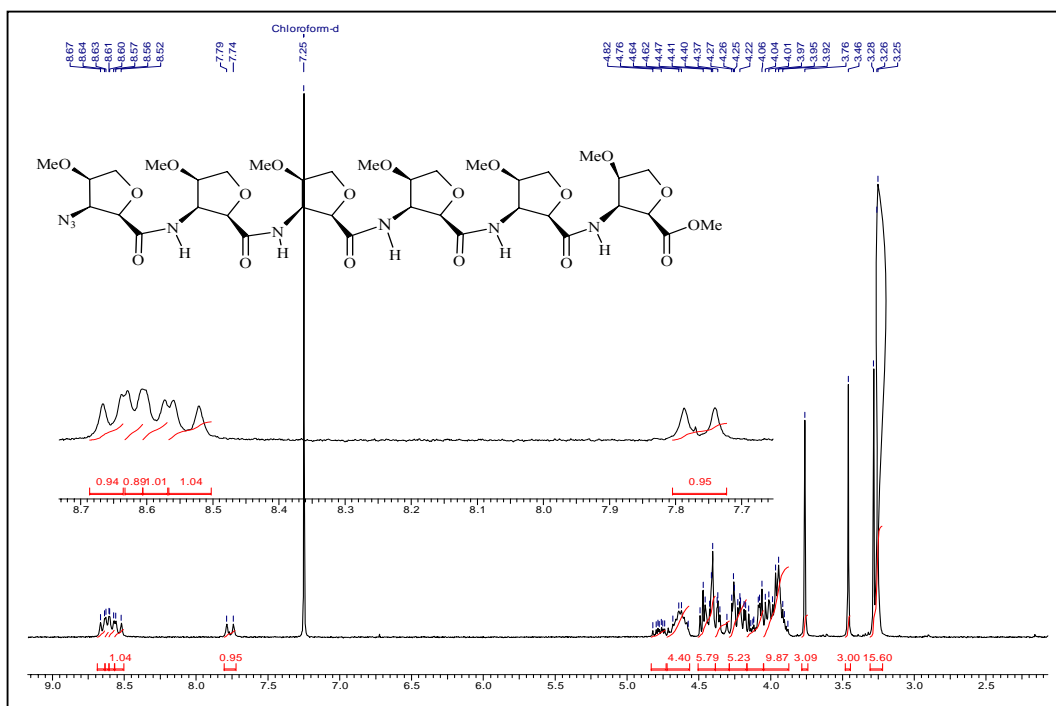
^{13}C NMR Spectrum of 59 in CDCl_3



¹H NMR Spectrum of 60 in CDCl₃



¹³C NMR Spectrum of 60 in CDCl₃



References

1. a) Porter, E. A.; Wang, X. F.; Lee, H. S.; Weisblum, B.; Gellman, S. H. *Nature* **2000**, *404*, 565. b) Porter, E. A.; Weisblum, B.; Gellman, S. H. *J. Am. Chem. Soc.* **2002**, *124*, 7324. c) Mowery, B. P.; Lee, S. E.; Kissounko, D. A.; Epand, R. F.; Epand, R. M.; Weisblum, B.; Stahl, S. S.; Gellman, S. H. *J. Am. Chem. Soc.* **2007**, *129*, 15474.
2. a) Gademann, K.; Seebach, D. *Helv. Chim. Acta.* **2001**, *84*, 2924. b) Kritzer, J.; Lear, J. D.; Hodsdon, M. E.; Schepartz, A. *J. Am. Chem. Soc.* **2004**, *126*, 9468. c) Kritzer, J. A.; Hodsdon, M. E.; Schepartz, A. *J. Am. Chem. Soc.* **2005**, *127*, 4118.
3. a) Stephens, O.; Kim, S.; Welch, B. D.; Hodsdon, M. E.; Kay, M. S.; Schepartz, A. *J. Am. Chem. Soc.* **2005**, *127*, 13126. b) Kritzer, J. S.; Stephens, O. M.; Guarracino, D. A.; Reznik, S. K.; Schepartz, A. *Bioorg. Med. Chem.* **2005**, *13*, 11.
4. a) Kimmerlin, T.; Namoto, K.; Seebach, D. *Helv. Chim. Acta.* **2003**, *6*, 2104. b) Namoto, K.; Gardiner, J.; Kimmerlin, T.; Seebach, D. *Helv. Chim. Acta.* **2006**, *89*, 3087.
5. Gellman, M. A.; Richter, S.; Cao, H.; Umezawa, N.; Gellman, S. H.; Rana, T. M. *Org. Lett.* **2003**, *5*, 3563.
6. Shimanouchi, T.; Walde, P.; Gardiner, J.; Mahajan, Y. R.; Seebach, D.; Thomae, A.; Kramer, S. D.; Voser, M.; Kuboi, R. *Biochim. Biophys. Acta: Biomembr.* **2007**, *17*, 2726.
7. Banerjee, A.; Balaram, P. *Curr. Sci. India*, **1997**, *73*, 1067.
8. a) Seebach, D.; Abele, S.; Gademann, K.; Guichard, G.; Hintermann, T.; Jaun, B.; Matthews, J. L.; Schreiber, J. V.; Oberer, L.; Hommel, U.;

- Widmer, H. *Helv. Chim. Acta* **1998**, *81*, 932. b) Appella, D. H.; Christianson, L. A.; Karle, I. L.; Powell, D. R.; Gellman, S. H. *J. Am. Chem. Soc.* **1999**, *121*, 6206. c) Appella, D. H.; LePlae, P. R.; Raguse, T. L.; Gellman, S. H. *J. Org. Chem.* **2000**, *65*, 4766. d) Appella, D. H.; Barchi, J. J.; Durell, S. R.; Gellman, S. H. *J. Am. Chem. Soc.* **1999**, *121*, 2309.
9. a) Seebach, D.; Abele, S.; Gademann, K.; Jaun, B. *Angew. Chem. Int. Ed.* **1999**, *38*, 1595. b) Krauthauser, S.; Christianson, L. A.; Powell, D. R.; Gellman, S. H. *J. Am. Chem. Soc.* **1997**, *119*, 11719.
10. a) Wu, Y.-D.; Wang, D.-P. *J. Am. Chem. Soc.* **1998**, *120*, 13485. b) Wu, Y.-D.; Wang, D.-P. *J. Am. Chem. Soc.* **1999**, *121*, 9352.
11. a) Seebach, D.; Abele, S.; Gademann, K.; Guichard, G.; Hintermann, T.; Jaun, B.; Matthews, J. L.; Schreiber, J. V.; Oberer, L.; Hommel, U.; Widmer, H. *Helv. Chim. Acta.* **1998**, *1*, 932. b) Seebach, D.; Schreiber, J. V.; Abele, S.; Daura, X.; van Gunsteren, W. F. *Helv. Chim. Acta.* **2000**, *83*, 34. c) Seebach, D.; Ciceri, P. E.; Overhand, M.; Jaun, B.; Rigo, D. *Helv. Chim. Acta.* **1996**, *79*, 2043. d) Seebach, D.; Overhand, M.; Kuhnle, F. N. M.; Martinoni, B.; Oberer, L.; Hommel, U.; Widmer, H. *Helv. Chim. Acta.* **1996**, *79*, 913.
12. Seebach, D.; Jacobi, A.; Rueping, M.; Gademann, K.; Ernst, M.; Jaun, B. *Helv. Chim. Acta.* **2000**, *83*, 2115.
13. a) Appella, D. H.; Christianson, L. A.; Karle, I. L.; Powell, D. R.; Gellman, S. H. *J. Am. Chem. Soc.* **1996**, *118*, 13071. b) Appella, D. H.; Barchi, J. J.; Durell, S. R.; Gellman, S. H. *J. Am. Chem. Soc.* **1999**, *121*, 2309.
14. Chandrasekhar, S.; Reddy, M. S.; Bharatam, J.; Prabhakar, A.; Ramana Rao, M. H. V.; Jagannadh, B. *J. Am. Chem. Soc.* **2004**, *126*, 13586.

15. Arvidsson, P. I.; Rueping, M.; Seebach, D. *Chem. Commun.*, **2001**, 649.
16. Richard, P. C.; DeGrado, W. F. *J. Am. Chem. Soc.* **2001**, *123*, 5162.
17. Scott, A. H.; Adilah, B. F.; Bahadoor, E. E.; Matthews, X. J. Q.; Alanna S. *J. Am. Chem. Soc.* **2003**, *125*, 4022.
18. a) Tami, L. R.; Jonathan, R. L.; Gellman, S. H. *J. Am. Chem. Soc.* **2003**, *125*, 5592. b) Daniel H. A.; Paul R. L.; Tami L. R.; Gellman S. H. *J. Org. Chem.* **2000**, *65*, 4766. c) Marina S.; Justin K. M.; Joseph M. L.; Gellman S. H.; *Eur. J. Org. Chem.* **2003**, 721.
19. a) Appella, D. H.; Christianson, L. A.; Klein, A.; Powell, D. R.; Huang, X.; Barchi, J. J.; Gellman, S. H. *Nature* **1997**, *387*, 381. b) Daniel H. A.; Christianson, L. A.; Daniel, A. K.; Michele, R. R.; Douglas, R. P.; Gellman, S. H. *J. Am. Chem. Soc.* **1999**, *121*, 7574.
20. Xifang, W.; Juan, F. E.; Gellman, S. H. *J. Am. Chem. Soc.* **2000**, *122*, 4821.
21. Emilie A. P.; Xifang W.; Margaret A. S.; Gellman, S. H. *Org. Lett.*, **2002**, *4*, 3317.
22. Matthew G. W.; John D. F.; Paul R. L.; Gellman S. H. *J. Am. Chem. Soc.* **2002**, *124*, 12447.
23. Seebach, D.; Abele, S.; Gademann, K.; Guichard, G.; Hintermann, T.; Jann, B.; Matthews, J. L.; Schreiber, J. V.; Oberer, L.; Hommel, U.; Widmer, H.; *Helv Chim. Acta.* **1998**, *81*, 932.
24. Sharma G. V. M.; Reddy K. R.; Krishna P. R.; Sankar A. R.; Jayaprakash P.; Jagannadh B.; Kunwar . A. C. *Angew. Chem. Int. Ed.* **2004**, *43*, 3961.

25. Claridge, T. D. W.; Goodman, J. M.; Moreno, A.; Angus, D.; Barker, S. F.; Taillefumier, C.; Watterson, M. P.; Fleet, G. W. J. *Tetrahedron Lett.* **2001**, *42*, 4251.
26. Abele, S.; Seebach, D. *Helv. Chim. Acta* **1999**, *82*, 1559.
27. Martinek, T. A.; To' th, G. K.; Vass, E.; Hollo'si, M.; Fülöp, F. *Angew. Chem. Int. Ed.* **2002**, *41*, 1718.
28. Applequist, J.; Bode, K. A.; Appella, D. H.; Christianson, L. A.; Gellman, S. A. *J. Am. Chem. Soc.* **1998**, *120*, 4891.
29. Graf v. R.; Kessler, H. *Angew. Chem. Int. Ed.* **1994**, *33*, 687.
30. Mark, P. W.; Lea, P.; Martin, D. S.; Sarah J. H.; Paul, R. M.; Jacqueline, E. M.; David, J. W.; Christopher, J. N.; Fleet, G. W. J. *Tetrahedron: Asymmetry* **1999**, *10*, 1855.
31. Yu, H.-W.; Zhang, L.-R.; Zhou, J.-C.; Ma, L.-T.; Zhang, L.-H. *Bioorg. Med. Chem.* **1996**, *4*, 609.
32. Defaye, D. H.; Muesser, M. *Carbohydr. Res.* **1971**, *20*, 305.
33. Enrico, D. *J. Org. Chem.* **1986**, *51*, 567.
34. Claridge T. D. W.; Long D. D.; Baker C. M.; Odell B.; Grant G. H.; Edwards A. A.; Tranter G.E.; Fleet G. W. J.; Smith M. D. *J. Org. Chem.* **2005**, *70*, 2082.
35. Richard T.; Andrew D.; Nicola M. H.; Julie F.; Richard C. *Chem. Commun.* **2008**, 585.

LIST OF PUBLICATIONS

1. “Total synthesis of pachastrissamine (jaspine B) enantiomers from D-glucose”
C. V. Ramana, **Awadut G. Giri**, Sharad B. Suryawanshi and Rajesh G. Gonnade. *Tetrahedron Letters* **2007**, *48*, 265.
2. “Effect of The Allylic Substituents on Ring Closing Metathesis: The Total Synthesis of Stagonolide B and 4-*epi*-Stagonolide B ” **Awadut. G. Giri**, M. A. Mondal, V. G. Puranik and C. V. Ramana, *Org. Biomol. Chem.*, **2010**, *8*, 398.

POSTER PRESENTATIONS

1. Total synthesis of Jaspine B (pachastrissamine) from D-glucose (*National Science Day* celebration at NCL – **2007**).
2. Effect of The Allylic Substituents on Ring Closing Metathesis: The Total Synthesis of Stagonolide B and 4-*epi*-Stagonolide B (*National Science Day* celebration at NCL – **2010**).

Erratum
